Tumor Response under Treatment with the Microtubule Stabilizing Agent Patupilone and Ionizing Radiation

---

Dissertation

zur

Erlangung der naturwissenschaftlichen Doktorwürde

(Dr. sc. nat.)

vorgelegt der

Mathematisch-naturwissenschaftlichen Fakultät

der

Universität Zürich

von

Katrin Orlowski

aus

der Bundesrepublik Deutschland

Promotionskomitee

Prof. Dr. Martin Pruschy (Vorsitz, Leitung der Dissertation)

Prof. Dr. Roland Wenger

Prof. Dr. Stephan Bodis

Zürich, 2012

Abstract

Radiotherapy is one of the most potent treatment modalities among anti-cancer therapies and is used in the treatment of as many as 50% of all cancer patients worldwide. Ionizing radiation (IR) is often combined with chemotherapeutic agents and/or surgery, leading to further improved tumor growth control. Patupilone (epothilone B) is a clinically relevant microtubule stabilizing agent, which impairs the dynamic instability of the microtubule network important for cell division, migration and invasion. Furthermore, patupilone has the potential to accumulate cells in the radiosensitive G2/M-phase of the cell cycle and also possesses anti-vascular and anti-angiogenic properties. Our laboratory has previously demonstrated an additive effect of combined IR and patupilone treatment *in vitro* and even a supra-additive tumor growth delay effect *in vivo*.

In this work, we investigated mechanistic and efficacy-oriented aspects of the combined treatment modality of patupilone in combination with IR on xenografts derived from several genetically defined human tumor cell lines. A specific focus was set on the analysis of the tumor microenvironment, especially treatment-induced tumor hypoxia.

The human non-small cell lung carcinoma cell line A549 and its patupilone-resistant counterpart A549.EpoB40 were used to investigate the role of patupilone in the radiosensitization of both the tumor cell compartment and the tumor microenvironment. A549.EpoB40 cells harbor a genetically defined mutation in β-tubulin, which impairs the binding of patupilone leading to patupilone resistance. Combined IR and patupilone treatment of the two different cell lines *in vitro* and *in vivo* showed an additive anti-proliferative effect for sensitive A549 cells but not for their resistant counterparts. Analysis of microvessel density and the hypoxic marker pimonidazole revealed a decrease in microvessel density and a consequent increase in pimonidazole-positive areas after patupilone treatment in the A549-derived xenografts, while no difference was observed in the xenografts derived from the resistant cell line. These results indicated a tumor cell-mediated effect on tumor hypoxia in response to microtubule interference by patupilone.

Hypoxia inducible factor 1 (HIF-1) is the major transcription factor specifically activated under hypoxia. HIF-1 is responsible for the transcription of various pro-angiogenic cytokines, such as VEGF, which is the most prominent HIF-1 target gene regulating endothelial cell growth and protection. We therefore analyzed the effect of patupilone and IR on the HIF-1α protein level and its activity. HIF-1α protein and activity levels both decreased in the A549 cell line but not in the resistant A549.EpoB40 cell line in response to patupilone treatment.

VEGF expression and secretion were analyzed *in vitro* under the different treatment conditions. Patupilone treatment of the A549 cell line resulted in decreased levels of both VEGF mRNA and secreted protein. No difference was observed under treatment with patupilone or irradiation in the resistant A549.EpoB40 cell line.

An increase in tumor hypoxia was observed in the patupilone-sensitive tumor xenografts after treatment with patupilone alone or when combined with IR. This increase in tumor hypoxia is most likely mediated by the decrease in secreted VEGF from patupilone-sensitive tumor cells, leading to a more fragile or damaged tumor microvasculature. Hypoxic tumors are 2-3 times more radiation resistant than normoxic tumors. Furthermore, hypoxia increases the aggressiveness and also chemoresistance of tumors. Therefore, we were interested in monitoring the development of tumor hypoxia under treatment over a prolonged time period in the A549-derived xenografts. For this purpose we developed a luciferase-based reporter system, in which part of the oxygen-dependent degradation domain of HIF-1α was fused to the luciferase reporter gene. In this hypoxia reporter system, the luciferase gene is stabilized under hypoxia and degraded under normoxia independently of the transcriptional activity of HIF-1. Tumor xenografts derived from A549 cells, stably expressing this luciferase construct, revealed a prolonged, transient increase in luciferase activity after patupilone treatment in comparison to untreated control tumor xenografts. Interestingly, luciferase activity did not increase in tumor xenografts of mice that did not respond to patupilone treatment at the level of tumor growth. These results suggest that an increase in tumor hypoxia might be used as a surrogate marker for the antitumoral treatment response to patupilone. Irradiation in combination with patupilone was investigated as part of both concomitant and adjuvant treatment modalities in A549 xenografts. Importantly, despite patupilone-induced hypoxia, the potency of IR was not reduced in either treatment scheme.

As part of our efficacy-oriented studies, we investigated the combined treatment of patupilone and IR on medulloblastoma cell lines *in vitro* and *in vivo*. Medulloblastoma is the most common malignant brain tumor in children with poor prognosis and is typically treated with surgery followed by IR and adjuvant chemotherapy. Patients suffer severe side effects after therapy with the microtubule destabilizing agent vincristine, a part of many chemotherapy regimens. Analysis of the effect of the microtubule stabilizing agent patupilone on medulloblastoma cell lines *in vitro* revealed cellular accumulation in the radiosensitive G2/M phase of the cell cycle, a decrease in proliferation and an induction of apoptosis or autophagy. The combined treatment with IR led to a reduction in clonogenicity in an at least additive manner. Interestingly, combined treatment of medulloblastoma-derived xenografts revealed a

strong supra-additive tumor growth control with complete tumor regression *in vivo*. These results indicate that patupilone might be a promising replacement for vincristine as part of a combined treatment strategy with IR.

This study demonstrates that the combined treatment modality of patupilone and IR is an effective and attractive strategy for anti-cancer treatment. The sensitizing effect of patupilone for IR treatment acts at multiple layers: patupilone has the potential to accumulate cells in the most radiosensitive phase of the cell cycle and to sensitize endothelial cells to IR by the inhibition of paracrine signals provided by tumor cells. Furthermore, patupilone exhibits anti-proliferative activity under normoxic and hypoxic conditions, and patupilone-induced tumor hypoxia does not hamper the radiation response of tumor xenografts, as demonstrated at the level of tumor growth delay. These results demonstrate that the combined treatment of patupilone and IR might be of great benefit for cancer therapy but still needs to be evaluated in clinical trials.

Zusammenfassung

Die Radiotherapie ist eine der potentesten Krebstherapieformen, die bei der Behandlung von 50% aller Krebspatienten eingesetzt wird. Die ionisierende Bestrahlung wird oft mit Chemotherapie und/oder Chirurgie kombiniert, um schlussendlich zu einer besseren Tumorkontrolle zu führen. Patupilone ist ein klinisch relevanter Wirkstoff, der zu einer Stabilisierung der Mikrotubuli führt. Patupilone beeinträchtigt somit die dynamische Instabilität des Mikrotubulinetzwerkes, die wichtig für die Zellteilung, Migration und Invasion ist. Des Weiteren führt Patupilone zu einer Ansammlung der Zellen in der radiosensitiven G2/M-Phase des Zellzyklus und zu einer negativen Beeinflussung der Tumorvaskulatur. Studien unseres Labors zeigten einen additiven Effekt der kombinierten Therapie von Patupilone und ionisierender Bestrahlung auf die Hemmung des Tumorzellwachstum *in vitro* und eine noch stärkere Hemmung des Tumorwachstums *in vivo*.

In dieser Arbeit wurden verschiedene mechanistische und auf Effizienz ausgerichtete Aspekte der kombinierten Therapie von Patupilone und Bestrahlung, in verschiedenen Tumormodellen definierter humaner Tumorzelllinien untersucht. Ein besonderer Fokus lag dabei auf der Untersuchung der Tumorumgebung. Insbesondere wurde der durch Behandlung induzierte Sauerstoffmangel (Hypoxie) innerhalb des Tumors analysiert.

Die humane Lungenkrebszelllinie A549, sowie ihr Patupilone resistentes Pendant A549.EpoB40, wurden für die Untersuchung der Rolle von Patupilone in der Sensibilisierung für die Bestrahlung, auf der Ebene der Tumorzellen und der Tumorumgebung verwendet. Die A549.EpoB40 Zelllinie besitzt eine genetisch definierte Mutation innerhalb des β-Tubulin, welche die Bindung von Patupilone verhindert und somit zu einer Resistenz gegen den Wirkstoff führt. Die Behandlung der zwei verschiedenen Zelllinien mit der kombinierten Therapie von Patupilone und Bestrahlung, *in vitro* und *in vivo*, zeigten einen additiven Effekt auf die Hemmung des Tumorzellwachstums der sensitiven A549 Zelllinie, nicht aber für ihr resistentes Pendant. Untersuchungen der Dichte kleinster Blutgefässe, sowie der Bindung des Hypoxie Markers Pimonidazole, ergaben eine Verringerung der Blutgefässdichte mit gleichzeitiger Zunahme der Bindung von Pimonidazole nach Behandlung mit Patupilone in den Tumoren der A549 Tumorzelllinie, nicht aber in Tumoren der resistenten Zelllinie. Diese Resultate weisen darauf hin, dass die Tumorhypoxie als Antwort auf die Beeinträchtigung der Mikrotubulifunktion der Tumorzellen durch die Behandlung mit Patupilone beeinflusst wird.

Der Hypoxie-induzierte Faktor 1 (HIF-1) ist der wichtigste Transkriptionsfaktor der unter Hypoxie aktiviert wird. HIF-1 ist für die Transkription verschiedener Angiogenese fördernde Zytokine, wie dem vascular endothelial growth factor (VEGF) verantwortlich. VEGF ist das wichtigste Zielgen von HIF-1, das das Wachstum und den Schutz von Endothelzellen reguliert. Aus diesem Grund wurde der Effekt von Patupilone und Bestrahlung auf die HIF-1α Proteinmenge, der sauerstoffsensitiven Untereinheit von HIF-1, und die HIF-1 Aktivität untersucht. Die Proteinmenge von HIF-1α, sowie die HIF-1 Aktivität, verringerten sich in der A549 Zelllinie als Antwort auf die Behandlung mit Patupilone, nicht aber in den resistenten A549.EpoB40 Zellen.

Die VEGF Expression und Sekretion wurde *in vitro* unter den verschiedenen Therapieformen analysiert. Die Behandlung mit Patupilone in der sensitiven Zelllinie führte zu einer Abnahme von VEGF mRNA, sowie in der Menge des sekretierten Proteins. Stattdessen konnte in den resistenten A549.EpoB40 Zellen nach Behandlung mit Patupilone oder Bestrahlung kein Unterschied bezüglich der VEGF mRNA und Proteinmenge festgestellt werden.

Tumorxenografts der Patupilone sensitiven Zelllinie zeigten einen Anstieg in der Tumorhypoxie nach Behandlung mit Patupilone, oder Patupilone in Kombination mit Bestrahlung. Dieser Anstieg der Tumorhypoxie wird vermutlich durch die Abnahme an sekretiertem VEGF der Patupilone sensitiven Zelllinie verursacht, der zu einer schwachen oder geschädigten Tumorvaskulatur führt. Hypoxische Tumore sind 2-3mal strahlenresistenter als normoxische Tumore. Des Weiteren führt Hypoxie zu einer verstärkten Aggressivität und Chemoresistenz von Tumoren. Aus diesem Grund waren wir daran interessiert, die Entwicklung der Tumorhypoxie, während der Behandlung mit verschiedenen Therapieformen, über eine verlängerte Zeitspanne in A549-Xenografts zu verfolgen. Wir entwickelten ein, auf das Enzym Luciferase basierendes, Reporter System. In diesem System wurde ein Teil der sauerstoffabhängigen Domäne von HIF-1α, die für den Abbau des Proteins unter Normoxie verantwortlich ist, an das Luciferase Gen kloniert. Hypoxie führt in diesem Reporter System zu einer Stabilisierung des Luciferase Proteins, unabhängig von der HIF-1 Aktivität, und zu einem Abbau unter Normoxie.

Tumorxenografts der A549 Zelllinie, die das Luciferase Konstrukt stabil exprimierten, zeigten einen verlängerten transienten Anstieg der Luciferase Aktivität nach Behandlung mit Patupilone im Vergleich zu unbehandelten Kontrolltumoren. Interessanterweise stieg die Luciferase Aktivität in Mäusen, die hinsichtlich des Tumorvolumens nicht auf die Behandlung mit Patupilone ansprachen, nicht an. Diese Resultate deuten darauf hin, dass eine Zunahme in der Tumorhypoxie als Surrogat für das Tumoransprechen auf die Behandlung mit

Patupilone verwendet werden könnte. Die Bestrahlung in Kombination mit Patupilone wurde als Teil einer adjuvanten und konkomitierenden Behandlungsmethode in A549 Xenografts untersucht. Trotz einer durch Patupilone induzierten Hypoxie wurde die Wirksamkeit der ionisierenden Bestrahlung weder in der konkomitierenden noch in der adjuvanten Behandlungsmethode reduziert.

Als Teil unserer Effizienz orientierten Studie wurde der Einfluss der kombinierten Behandlung mit Bestrahlung und Patupilone auf Medulloblastoma Zelllinien *in vitro* und *in vivo* untersucht. Medulloblastoma ist der häufigste bösartige Gehirntumor mit schlechter Prognose und massiven Nebenwirkungen nach der Therapie, zum Beispiel nach dem Mikrotubuli destabilisieren Wirkstoff Vincristine, in Kindern. Untersuchungen von dem Mikrotubuli stabilisierenden Wirkstoff Patupilone auf Medulloblastoma Zelllinien zeigten eine Anhäufung der Zellen in der radiosensitiven G2/M Phase des Zellzyklus, eine Verringerung der Proliferation sowie eine Induktion von Apoptose oder Autophagie. Die kombinierte Behandlung mit Bestrahlung führte zu einer mindestens additiven Verringerung der Klonogenität der Zellen. Interessanterweise führte die kombinierte Behandlung von Xenografts einer Medulloblastoma Zelllinie zu einer sehr starken Tumorkontrolle mit teilweise kompletter Tumorremission. Diese Resultate weisen darauf hin, dass Patupilone eine vielversprechende Alternative zu Vincristine in der kombinierten Therapieform mit Bestrahlung sein könnte.

Diese Studie zeigt, dass die kombinierte Behandlungsmethode von Patupilone und Bestrahlung eine effektive und attraktive Strategie in der Krebsbehandlung ist. Zusammenfassend wirkt der strahlensensibilisierende Effekt von Patupilone auf verschiedenen Ebenen. Patupilone hat einerseits das Potential Zellen in der radiosensitiven Phase des Zellzyklus anzuhäufen, andererseits sensibilisiert Patupilone die Endothelzellen, durch eine Inhibierung parakriner Signale der Tumorzellen, auch für die Bestrahlung. Des Weiteren kann Patupilone seine wachstumsinhibierende Wirkung sowohl unter Hypoxie als auch unter Normoxie entfalten. Ausserdem wird die Strahlenwirksamkeit in einer kombinierten Therapie nicht von der Patupilone induzierten Hypoxie beeinflusst, wie auf der Ebene der Tumorwachstumshemmung gezeigt werden konnte. Diese Resultate weisen darauf hin, dass die kombinierte Behandlung von Patupilone und Bestrahlung einen grossen Nutzen für die Krebstherapie haben könnte, nachdem sie in klinischen Studien validiert worden ist.

Contents

Abstract i
Zusammenfassung v
List of Abbreviations xi
1. Introduction 1
1.1. Cancer and Cancer treatment 1
1.1.1. Cancer distribution and incidence 1
1.1.2. Tumor biology 3
1.1.3. Microenvironment of the tumor 7
1.2. Tumor oxygenation 8
1.2.1. Tumor hypoxia 8
1.2.2. Methods to measure tumor hypoxia 11
1.2.2.1. Invasive imaging of tumor hypoxia 11
1.2.2.2. Non-invasive imaging of tumor hypoxia 12
1.2.2.3. Hypoxia measurements using in vivo bioluminescence 14
1.3. Radiotherapy 15
1.3.1. R's of radiotherapy 15
1.3.2. Tumor hypoxia in radiotherapy 17
1.4. Microtubules as target for cancer therapy 19
1.4.1. The microtubule network 19
1.4.2. The cellular functions of microtubule 21
1.4.3. Microtubule interfering agents 22
1.5. Combined treatment modalities 24
2. Aims of the study 27
3. Results 35
3.1. Dynamics of tumor hypoxia in response to patupilone and ionizing radiation 35
3.2. Role of the microenvironment for radiosensitization by Patupilone 59
3.3. Regulation of VEGF-expression by patupilone and ionizing radiation in lung adenocarcinoma cells 69
3.4. The microtubule stabilizer Patupilone (Epothilone B) is a potent radiosensitizer in medulloblastoma cells 79

3.5. Microtubule Stabilizing Agents and Ionizing Radiation: Multiple Exploitable Mechanisms for Combined Treatment 91
4. Discussion 109
4.1. Combined treatment modality of patupilone and ionizing irradiation 109
4.2. The importance of monitoring tumor hypoxia in anti-cancer treatment 112
4.3. Translational importance 116
5. Outlook 118
Curriculum vitae 123
Acknowledgments 127

List of Abbreviations

AVO	acidic vesicular organelles
CA IX	carbonic anhydrase 9
DMOG	Dimethyloxalylglycine (PHD inhibitor)
EF5	2-nitroimidazole agent: 2-(2-nitro-1-*H*-imidazol-1-yl)-*N*-(2,2,3,3,3-pentafluoropropyl) acetamide
EGFR	epidermal growth factor receptor
EMT	epithelial to mesenchymal transition
FMISO	18F-fluoromisonidazole
HIF-1	Hypoxia inducible factor 1
HR	homologous recombination
HRE	hypoxia response element
IFP	intratumoral fluid pressure
IR	ionizing radiation
IVIS	in vivo imaging system
MB	Medulloblastoma
MMP	matrix metalloproteinase
MSA	microtubule stabilizing agent
MTOC	microtubule-organizing center
MVD	microvessel density
NHEJ	non-homologous end joining
ODD	oxygen dependent degradation domain (of HIF-1α)
PET	positron emission tomography
PHD	prolyl hydroxylase domain proteins
pO2	partial oxygen pressure
ROS	reactive oxygen species
VEGF	vascular endothelial growth factor
VHL	von Hippel Lindau protein

1. Introduction

1.1. Cancer and Cancer treatment

1.1.1. Cancer distribution and incidence

Cancer is a disease caused by uncontrolled proliferation of cells that can subsequently invade the organ of origin and spread to more distant parts of the body. The uncontrolled proliferation of cancer cells impairs the function of healthy cells in the affected organ. In cases where the growing tumor disrupts essential organs and tissues, the disease becomes lethal. Often, more aggressive tumor cells metastasize to different organs within the whole body complicating the treatment and therefore treatment outcome.

Cancer is the leading cause of death in economically developed countries and the second leading cause of death in developing countries after cardiovascular diseases (Global cancer, Facts and Figures, 2011). The incidence of cancer is continuously rising due to longer life expectancies and the increase in cancer-promoting behaviors like smoking, unhealthy diets and physical inactivity, especially in economically developing countries. Worldwide, in 2008 the cancer incidence rate was estimated to be 12.7 million , with 7.6 million cancer deaths [1]. The cancer type with the highest death rate in the U.S is lung cancer, responsible for 26-28% of cancer deaths for both sexes, followed by prostate and breast cancer and colon cancer [2]. The highest cancer incidence worldwide, however, remains breast cancer for women and lung and bronchus followed by prostate cancer for men [1]. Studies on cancer epidemiology show a higher trend for certain cancer types in specific countries, such as melanoma in Australia, cervical cancer in eastern Africa or liver cancer in middle Africa (see Figure 1.1.). The high numbers of cervical and liver cancers are mainly caused by chronic infections from hepatitis B virus (HBV), hepatitis C virus (HCV) and some types of Human Papilloma Virus (HPV). Besides the cancers caused by virus infections, a high percentage of cancers like lung or head and neck cancer, could be prevented by reducing tobacco and alcohol use. In addition, prevention of melanoma can be improved by the use of sun cream, huts, tight fitting sunglasses and minimizing sun exposure during the hours with high UV alert. Although the cancer incidence rate in developing countries is lower than in economically developed countries, the death rate remains the same, which is mainly due to late detection of the disease, poor cancer prevention and limited access to basic cancer treatments in developing countries [1].

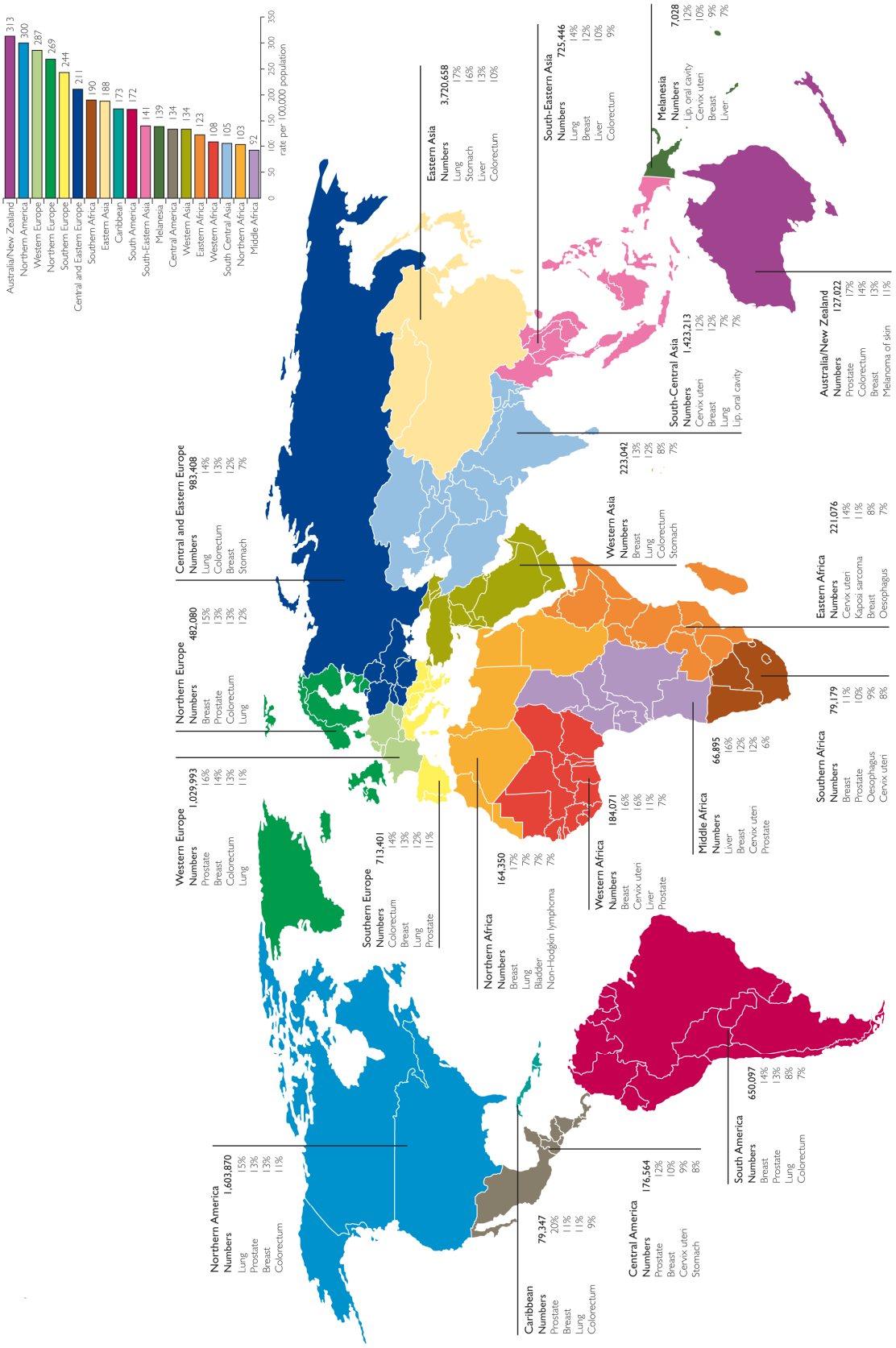

Figure 1.1. Cancer Incidence Worldwide 2008, adapted from Cancer Research UK, source GLOBOCAN 2008, http://globocan.iarc.fr

Standard cancer therapy is composed of three different approaches: surgery, radiotherapy and chemotherapy. Surgery and radiotherapy are used for the local treatment of the disease, whereas chemotherapy can also be used for systemic treatment, e.g. for lymphoma or metastatic disease. Surgery aims to excise the malignant tumor or part of affected organs in order to eliminate or reduce the tumor burden and to prevent further spreading. Surgery is used in about 60% of cancer patients. Radiotherapy is also used for local treatment of tumors, where precise planning allows application of high-dose radiation to malignant tissue while minimizing radiation to the surrounding healthy tissue. Radiotherapy affects all cells, malignant as well as benign. Malignant cancer cells are highly proliferative cells that often harbor defects in cell cycle checkpoints. Therefore, damage induced by ionizing radiation (IR) is often not repaired properly, and triggered by mitotic catastrophe eventually leads to cell death in these cells compared to benign ones. Radiotherapy is applied in around 50% of all cancer patients [3]. Chemotherapy uses agents that prevent proliferation of rapidly dividing cells and thus targets malignant cells but also healthy epithelial and bone marrow cells. It is applied as adjuvant treatment after radiotherapy or surgery to prevent recurrence, as well as neo-adjuvant therapy for surgery or in case of high risk for metastatic spread. The different approaches are often combined during treatment to achieve a better survival rate or shorter treatment time.

1.1.2. Tumor biology

Cancer can be caused by various external (infections, tobacco, chemicals, etc.) as well as internal (inherited or spontaneous mutations, immune conditions etc.) factors. Hanahan and Weinberg describe eight distinct hallmarks that enable tumor growth and metastatic dissemination of malignant cells [4]. The first hallmark is *sustained proliferative signaling*: cancer cells evade the normal regulation of the cell cycle which is controlled by growth-factor signaling. Tumor cells can release factors like the transforming growth factor β (TGFβ), that in turn increase production of the growth factor hepatocyte growth factor (HGF) by surrounding fibroblasts [5]. Tumor cells can also upregulate growth factor receptors on their surface, allowing proliferation even at a low level of surrounding growth factors. Alternatively, they can express ligands leading to an autocrine activation of their own surface receptors. A very high percentage of cancer cells express constitutively activate components of the signaling pathways downstream of growth factor receptors like mutated K-ras in order to proliferate in the absence of growth factors [6].

The second hallmark of cancer is *evasion from growth suppression*. The proliferation of normal cells is usually impaired by different factors such as shortage of space, a lack of nutrients or internal damage. The proliferation under these non-favorable circumstances is tightly regulated by different growth suppressors. The most prominent growth or tumor suppressors are p53 and the retinoblastoma-associated (Rb) protein. Rb primarily regulates extracellular signals and determines whether cells can proceed in the cell cycle. p53 instead receives signals from within the cell indicating damage to the genome or lack or shortage of nucleotides, glucose or oxygenation and acts as gatekeeper for cell cycle progression. In case of severe DNA damage, p53 can also induce apoptosis. Mutations in these tumor suppressors lead to uncontrolled proliferation of tumor cells. The high importance of p53 in the regulation of growth suppression is supported by the fact that more than 50% of all human cancer display different mutations in the TP53 gene [7].

The third hallmark of cancer is *resistance to cell death*. Programmed cell death or apoptosis serves as natural defense against cancer development or uncontrolled proliferation. Apoptosis can be induced by extrinsic factors via Fas binding to the death receptor FasR, or by intrinsic factors in response to multiple intracellular stress conditions via activation of the caspase cascade. However, cancer cells often evade apoptosis by overexpression of anti-apoptotic Bcl-2 family regulatory proteins or downregulation of pro-apoptotic proteins like Bax, Bim or Puma. Caspase-independent intrinsic apoptosis is mediated by the apoptosis-inducing factor (AIF) and endonuclease G (ENDOG), which relocate to the nucleus and induce large scale DNA fragmentation [8]. A further mode of cell death that gains more and more interest is mitotic catastrophe. Mitotic catastrophe is triggered by aberrant mitosis and executed during mitosis or in the subsequent interphase by caspase-2 activation. It has been proposed that mitotic catastrophe is an oncosuppressive pathway that precedes apoptosis, necrosis or senescence [9]. Another pathway to avoid cell death is the induction of autophagy or senescence. This latter dormant-like, reversible state allows the recovery of cancer cells from treatment, which eventually leads to a more persistent tumor or to tumor regrowth after end of treatment.

The fourth hallmark of cancer is *enabling replicative immortality*. Cells pass only a limited number of cell cycle divisions before entering senescence or cell death. The block in cell division is caused by shortening of telomeres, which are hexanucleotide repeats at the end of chromosomes protecting the chromosome ends. However, tumor cells often overexpress the enzyme telomerase which adds additional telomere repeats to the end of telomeric DNA and therefore prevents cells from undergoing senescence or cell death.

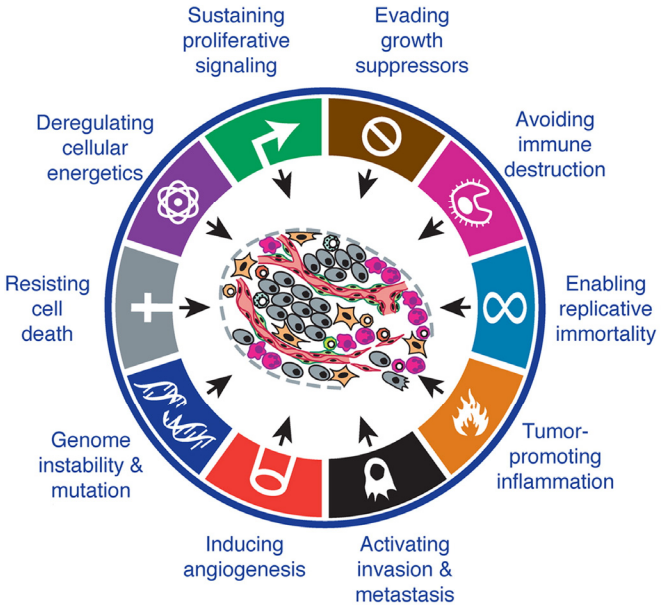

Figure 1.2. The Hallmarks and Enabling characteristics of Cancer. Research conducted in the past years led to the description of two new hallmarks of cancer: avoidance of immune destruction and deregulation of cellular energetics. Enabling characteristics include tumor promoting inflammation and genome instability and mutation. (Hanahan et al, 2011)

The fifth hallmark of cancer is the ability to *induce angiogenesis*. In adult tissues, angiogenesis is either in a quiescent state or transiently active. Tumor cells, however, induce an angiogenic switch which leads to a constant sprouting of new vessels to supply the growing tumor with nutrients and oxygen [10]. The upregulation of angiogenesis is initiated by the expression and secretion of pro-angiogenic factors like vascular endothelial growth factor (VEGF) or fibroblast growth factor (FGF). The expression of these proteins can either be triggered by oncogene signaling or by tumor hypoxia.

The sixth hallmark of cancer is *activation of invasion and metastasis*. In order to progress to higher pathological stages, cancer cells develop different alterations in cell shape and express pro-metastatic genes promoting the consecutive steps in metastasis formation. The different steps in the malignant progression are: First, the invasion of cancer cells into the local tissue followed by the intravasation into nearby blood or lymphatic vessels and transition within the vascular network. The next step is the extravasation out of the vasculature into the new tissue and the establishment of micrometastases. Finally, tumor cells have to adapt to the new microenvironment in order to form macrometastases. The first step of invasion is often accompanied by the loss of E-cadherin, a cell-to-cell adhesion molecule expressed in epithelial cells that normally keeps cells in a quiescent state. The high frequency of this mutation indicates that E-cadherin is a key suppressor for invasion. An adhesion molecule frequently upregulated in cancer cells is N-cadherin, which is important for migration of neurons and mesenchymal cells during organogenesis. The specific changes within the expression of the adhesion molecules are part of a process called epithelial to mesenchymal

transition (EMT), which is activated in most malignant tumor cells. EMT changes the morphology of cells into a more fibroblastic shape, decreases E-cadherin expression and increases N-cadherin expression, increases the expression of matrix-degrading enzymes and consequently increases the invasive capacities of the cells [11].

Invasion of tumor cells is also influenced by crosstalk with the neoplastic stroma, which contains cancer associated fibroblasts, endothelial cells, extracellular matrix, pericytes and also inflammatory cells. Inflammatory cells contribute to the invasive capacities of a tumor by secretion of matrix-degrading enzymes. Therefore, a new enabling characteristic of cancer is *tumor promoting inflammation* that contributes to several steps in tumor progression. Inflammatory cells, mainly from the innate immune system, can provide tumor cells with growth and survival factors to promote tumor cell proliferation. Further, they can provide pro-angiogenic factors, induce EMT or even lead to a higher mutation rate in tumor cells by secretion of reactive oxygen species (ROS).

However, the immune system is also involved in the prevention of tumor initiation, and thus, an additional emerging hallmark of cancer is the *evasion of immune destruction*. Cancer cells may paralyze infiltrating natural killer cells (NK) and cytotoxic T-cells (CTL) cells by transforming growth factor β (TGF-β) secretion or attract immunosuppressive cells like regulatory T-cells to avoid immune destruction. Nevertheless, only rudimentary evidence demonstrates that the immune system protects from cancer formation. Pages and colleagues demonstrated that human ovarian and colon carcinoma with a very high number of infiltrating CTL and NK cells results in a better prognosis than tumors with fewer CTL and NK cells [12,13].

A further emerging hallmark for cancer is the *deregulation of cellular energetics* allowing tumor cells to perform anaerobic glycolysis even under aerobic conditions. Thereby tumor cells are limiting their metabolism to glycolysis, which allows them to redirect glycolytic intermediates into other biosynthetic pathways to generate nucleosides or amino acids used for cell growth and proliferation. Glycolysis yields 18 times less ATP which is the reason why tumor cells frequently increase their glucose uptake by overexpressing the Glut-1 transporter [14,15]. Interestingly, some tumors contain two different subpopulations regarding their energy generating pathways. The hypoxic subpopulation uses glucose as main energy source, thereby producing lactate which in turn is consumed by the better oxygenated subpopulation to generate energy by feeding lactate into the citric acid cycle [16,17].

In addition to tumor promoting inflammation described above, Hanahan and Weinberg suggest a second enabling characteristic for cancer, *genome instability and mutation*. They

propose that the loss of important components of the DNA repair machinery or increased sensitivity to mutagenic agents can further lead to increased rates of mutation and hence facilitate tumor progression. However, the loss or inactivation of a tumor suppressor can also be acquired by epigenetic mechanisms such as DNA methylation or histone modification and consequently inherited by the daughter cells [18].

In conclusion, several mutations and changes in different regulatory systems must occur within benign cells in order to promote cancer development. Further research will improve our understanding of the important features of invasion and metastasis formation and will shed light on the importance and role of immune cells in cancer progression or prevention.
In the present work we were focusing on one specific hallmark of cancer, "angiogenesis". Therefore I would like to describe in more detail factors influencing angiogenesis and tumor hypoxia, which results from damaged or non-functional angiogenesis.

1.1.3. Microenvironment of the tumor

Tumors are composed not only of malignant tumor cells, but also consist of other cell types forming the tumor microenvironment. Tumor stroma, which is an important element of the microenvironment, is composed of extracellular matrix, endothelial cells, mural cells and fibroblasts. Endothelial cells forming the blood vessels supply the tumor with nutrients and oxygen and may also play an important role in modulating the aggressiveness of a tumor. Endothelial cells are often activated by angiogenic and growth factors secreted by the tumor cells, which then induces the so-called angiogenic switch promoting the growth and development of new vessels. Depending on the pathways activated in the endothelial cells, tumor cell invasion can be facilitated. Loss of HIF-1α, the oxygen-sensitive subunit of the transcription factor hypoxia inducible factor 1 (HIF-1), in endothelial cells leads e.g. to a reduction in NO synthesis and retards tumor cell migration. The loss of HIF-2α, the oxygen-sensitive subunit of the transcription factor HIF-2, instead has the opposite effect [19]. Endothelial cells are associated with supporting pericytes or vascular smooth muscle cells which help building the vascular basement membrane and fortify the vessels. A lack of pericytes often results in leakage of the vessels and increased tumor cell intravasation [20]. Indeed, deficient pericyte coverage of the tumor vasculature in human colon carcinoma was associated with an increase in metastasis [21].
Cancer-associated fibroblasts are another group of cells found within tumors. Myofibroblasts are usually present in wounds and at sites of chronic inflammation and can be identified by

the expression of α-smooth muscle actin. They may derive from locally proliferating stromal cells but can also descend from bone marrow-derived stem and progenitor cells [22]. Cancer-associated fibroblasts are involved in promoting cancer cell proliferation, angiogenesis, invasion and migration [23,24]. Loss of HIF-1α and VEGF-A, a pro-angiogenic target gene of HIF-1, in cancer-associated fibroblasts accelerates tumor growth in a murine mammary tumor model. This loss also leads to a decrease in vascular density and myeloid cell infiltration correlating with improved perfusion of the tumor [25].

Finally, the immune inflammatory cells found in tumors can play varying roles in tumor promotion as well as in tumor suppression functions as discussed above. Recent work suggests a very complex role that needs to be further explored: deletion of VEGF secreted from tumor myeloid cells leads to normalization of tumor vessels and unexpectedly accelerates tumor growth [26].

A complex signaling network connects the different cells forming the whole tumor complex, and the diverse interactions are only starting to be understood. The fact that blockage of VEGF secreted by cancer-associated fibroblasts and myeloid cells leads to enhanced tumor growth might explain the modest objective responses in clinical trials after single treatment with anti-angiogenic drugs [27]. Therapies should therefore be developed not only to target tumor cells but also further components of the tumor microenvironment to optimize an antitumor response.

1.2. Tumor oxygenation

1.2.1. Tumor hypoxia

Normal atmospheric air contains 21% oxygen which corresponds to 190 mmHg partial oxygen pressure (pO_2) in dry air at sea level. Oxygen of inspired air has already fallen to a pO_2 of about 100 mmHg upon reaching the alveoli. In most adult tissues pO_2 pressure exceeds 20 mmHg [28]. However, hypoxic zones can be found in different organs in the body, for example the inner medulla of the kidneys, with partial oxygen pressures ranging from 10–15 mmHg [29]. Clinically relevant tumor hypoxia is reached at a pO_2 below values of 5-10 mmHg [30].

Tumor hypoxia is mainly caused by insufficient angiogenesis or can be induced after treatment affecting the tumor vasculature. Abnormal angiogenesis in tumors compared to normal tissue was already observed in the mid-1800s by contrast agents. Later, functional angiogenesis was proposed to be essential for the growth of tumors by supplying enough

nutrients and oxygen. However, tumor vasculature is often not sufficient or functional, consequently leading to tumor hypoxia. Dewhirst and colleagues summarize seven features in tumor vasculature that influence tumor oxygenation and lead to tumor hypoxia (as displayed in figure 1.3.) [28].

However, one of the most important features of tumor hypoxia is its high instability and cycling character. There is evidence that cycling hypoxia appears in two dominant timescales. The first timescale has a frequency of a few cycles per hour, whereas the second timescale has a period of hours or days. The cycling hypoxia with the higher frequency is mainly caused by changes in blood flow. The amount of circulating red blood cells can decrease in small networks, causing an increase of hypoxia within a period of 3 hours. Another possibility for fast hypoxia changes is vasodilatation of another vessel, leading to higher blood flow in the direction of the dilated vessel and lower flow in the parallel vessel, increasing hypoxia. This phenomenon might especially play a role during ongoing angiogenesis. Vasculature remodeling instead is responsible for the slower cycling hypoxia in which blood flow adapts to new vessels or intersections.

The second form of tumor hypoxia, besides the hypoxia caused by abnormal vasculature, is chronic hypoxia starting at a distance of 70-100 µm from tumor blood vessels [31].

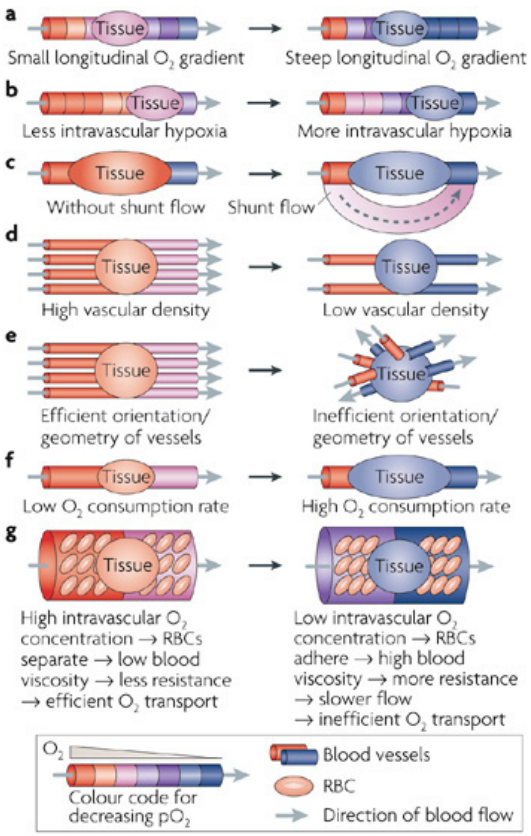

Figure 1.3. Regulation of tumor oxygenation by seven features contributing to hypoxia. (a) Intravascular pO_2 can drop with increasing distance from feeding arterioles. (b) At the end of a long vessel, red blood cells have already lost all oxygen and cannot provide further oxygen to the tumor tissue. (c) Shunt flows redirect oxygen and nutrients away from the tumor. (d) Low vascular density leads to hypoxia due to the limitations in the diffusion distance. (e) Inefficient orientation of vessels leads to insufficient supply within the tumor. (f) Oxygen consumption of a tumor can increase, leading to insufficient supply and consequent increase in hypoxia. (g) Intravascular hypoxia reduces red blood cell deformability, increasing blood viscosity which in turn reduces flow rate. [28]

Hypoxia-inducible factor (HIF)-1 is a transcription factor composed of two subunits, the constitutively expressed β-subunit and the oxygen-sensitive α-subunit. Under hypoxic conditions, HIF-1 binds together with the transcriptional cofactors p300 and CBP to the promoter regions of target genes like VEGF, leading to their transcription [32]. Cycling hypoxia leads to increased activity of HIF-1 that supersedes the level of activity under chronic hypoxia. In particular, repeated cycles of hypoxia can lead to a total higher expression of HIF-1 in comparison to chronic hypoxia and thus alter angiogenesis [33].

The oxygen-sensitive α-subunit (HIF-1α) of HIF-1 is mainly regulated by the oxygen status of the cell, but also by different hypoxia independent mechanisms. Under normoxic conditions, HIF-1α is hydroxylated by prolylhydroxylases on proline402 and proline564 within the oxygen-dependent degradation (ODD) domain. Hydroxylation leads to recognition by the von Hippel Lindau (VHL) protein, ubiquitination and subsequent degradation [34]. HIF-1α can also be degraded by binding to the RACK1 protein. RACK1 binds HIF-1α in competition with the heat shock protein Hsp90, which normally stabilizes HIF-1α. Under normoxic conditions, the activity of HIF-1α is inhibited by hydroxylation of asparagine803 by the factor inhibiting HIF-1 (FIH-1). This hydroxylation prevents interaction with the transcriptional cofactors p300 and CBP.

However, stabilization of HIF-1α can also occur under normoxic conditions. The Akt-mTOR pathway stimulates translation of HIF-1α in response to different growth factors, signaling molecules or cytokines such as epidermal growth factor (EGF), fibroblast growth factor (FGF-2), insulin-like growth factor (IGF-1 and IGF-2) and interleukin 1β (IL1β).

HIF-1α is the major regulator in the hypoxic adaptive response and leads to the expression of several pro-angiogenic factors such as VEGF or angiopoietins (ANG-1 and -2), thereby promoting angiogenesis. HIF-1α is, however, also involved in several other mechanisms, including the blockage of proliferation by inhibiting c-myc through the Max interactor 1 (Mxi1) and interference in the balance of pro- and anti-apoptotic proteins by regulating Bcl2/adenovirus EIB interacting protein 3 (BNIP3) or BCL-xL [35].

1.2.2. Methods to measure tumor hypoxia

1.2.2.1. Invasive imaging of tumor hypoxia

Hypoxia is one of the most important parameters determining treatment response, and different methods have been developed to measure tumor hypoxia in an invasive and non-invasive manner. The main invasive measurement is obtained by using the *pO_2 electrode*.

Invasive polarographic electrodes have been used extensively in human and animal tumors and are considered gold standard. The main advantage of pO_2 electrodes is the exact determination of the partial oxygen pressure in a tissue, in particular pressures below 10 mmHg. Determination of tumor hypoxia with this technique allowed prediction of treatment outcome and metastatic potential depending on the hypoxic status of the tumor. It has been shown that low oxygen pressures under 2.5 mmHg determined by the pO_2 electrode in head and neck cancer is prognostic for poor loco-regional control after radiotherapy [36,37]. Similarly, tumor hypoxia under 5 mmHg leads to a poor prognosis in both non-small cell lung carcinoma [38] and uterine cervix carcinoma [39]. However, the use of the electrodes requires localised easily accessible tumors like head and neck tumors or cervical tumors and great expertise. The disadvantages of this technique are its invasiveness, causing disruption of the tissue, and the challenge to distinguish between already necrotic tissue and hypoxic tissue.

Indirect hypoxia measurement

Tumor hypoxia can also be determined by detection of endogenous markers through immunohistochemistry. The most common endogenous markers are HIF-1 or HIF-1 target genes like Glut-1 or carbonic anhydrase 9 (CA IX). Glut-1 is a membrane-associated glucose transporter that is mainly expressed in erythrocytes and endothelial cells. It is upregulated at low glucose concentrations and under hypoxia through the transcriptional regulation of HIF-1. CA IX is a membrane-associated enzyme involved in respiration and acid-base balance. It shows only limited distribution in normal tissue like gastric mucosa, small intestine and muscle but is overexpressed in many tumors.

Both markers are widely used for hypoxia detection in tissue samples. Due to the various factors regulating HIF-1 independently of hypoxia, these markers often do not correspond with other hypoxia measurements like F-MISO PET or the pO_2 electrode [40,41].

The described invasive measurements give only a partial view of the hypoxic status of a tumor. Therefore, non-invasive measurements of tumor hypoxia were developed which allow monitoring oxygenation status of the whole tumor.

1.2.2.2. Non-invasive imaging of tumor hypoxia

PET imaging

The most common non-invasive measurement of tumor hypoxia is positron emission tomography (PET) using specific imaging agents. Organic molecular markers are labeled with positron-emitting radioisotopes, mainly ^{18}F, ^{124}I and $^{60/64}Cu$, to measure tumor hypoxia (figure 1.4.). Under severe hypoxic conditions, the different markers form stable adducts that can be measured with the PET scanner. Under normoxic conditions, they are rapidly reoxidized and removed from cells, thereby providing a good difference between normoxic and hypoxic cells for imaging.

Fluoromisonidazole (F-MISO) belongs to the first generation of nitroimidazole markers used in PET imaging and requires hypoxic levels of less than 10 mmHg to accumulate in hypoxic cells. It is used in a broad range of tumors for the detection of hypoxia [42,43]. However, its accumulation shows a vide variation between different cancer types and patients. Studies using F-MISO revealed controversial data in correlating an increase in F-MISO with an increase in hypoxia and with prognosis [44,45].

Therefore, the second generation of nitroimidazoles – fluoroetanidazole (FETA), EF5 [2-(2-nitro-1-*H*-imidazol-1-yl)-*N*-(2,2,3,3,3-pentafluoropropyl) acetamide] and ^{18}F-fluoroerythronitroimidazole (FETNIM) - was developed. These nitroimidazoles have the advantages of being more water soluble and degraded under most of the oxidizing mechanisms in the body. EF5, the most stable of these derivates, showed a high specificity for hypoxic areas. The main disadvantage of EF5 is its complex labeling chemistry.

Iodinated analogs, developed as hypoxic radiotracers, had low resolution and long half-lives requiring longer patient exposure to irradiation and are therefore not used in the clinics.

Cu-labeled organic markers are mainly dithiosemicarbazones, especially diacetyl-bis(-methylthiosemicarbazone) (ATSM), labeled with ^{60}Cu-^{64}Cu. They are reduced in living aerobic cells but trapped in hypoxic cells. They have shown to be effective tracers especially in situations were blood flow is limited. Furthermore, they revealed good correlation with hypoxia measurements using the pO_2 electrode, and the imaging results are comparable to F-MISO when measured at a later time point after injection [46]. Radiation emitted by ^{64}Cu can cause DNA damage and induces apoptosis in hypoxic cells, ^{64}Cu-ATSM could therefore be used as both an imaging and therapeutic agent [47]. However its efficacy varies between different tumor types.

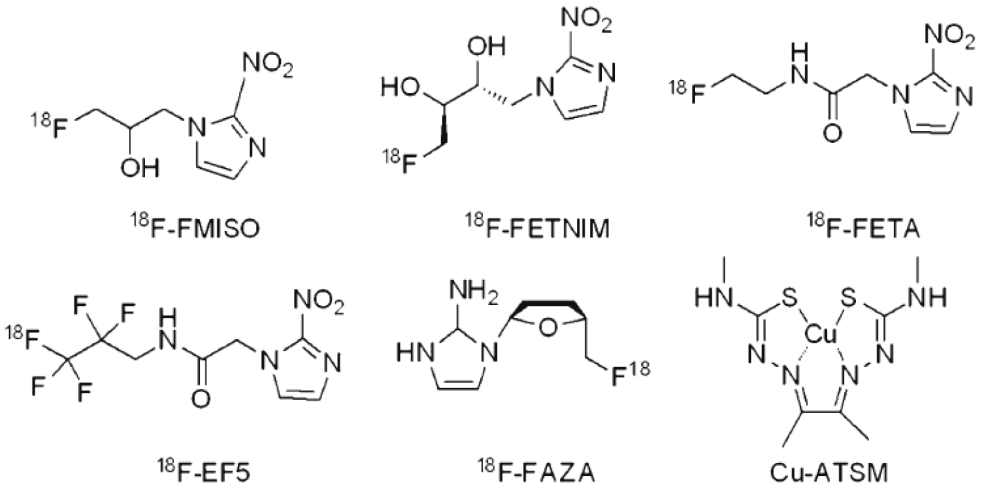

Fig. 1.4. Chemical structures of hypoxia PET imaging agents [47]

BOLD magnetic resonance imaging

BOLD magnetic resonance imaging (MRI) uses the differences between oxyhemoglobin and deoxyhemoglobin to directly estimate pO_2 by differences in the relaxation rates of the surrounding protons [48]. However, this technique allows only measurement of vessel oxygenation and not tissue oxygenation and can be easily disturbed by others factors like changes in blood flow, hematocrit, pH or temperature [47].

^{19}F Magnetic resonance imaging

F-MRI uses different types of markers, perfluorocarbons (PFC) or fluorinated nitroimidazoles. The F spin lattice relaxation rate of PFCs varies linearly with the oxygen concentration, allowing measurement of vascular oxygen. PFCs are used for detecting changes in oxygen after radio-sensitizing and oxygen-augmenting treatments, but measurement is disturbed by changes in dilution, pH or temperature. Other disadvantages are slow clearance and the risk of embolism after intratumoral injection. Usage of nitroimidazoles instead resulted in neuropathy or central nervous system toxicity.

Taken together, the different methods for tumor hypoxia measurement have to be considered for their advantages and disadvantages regarding the specific question. The most used non-invasive imaging measurement up to now is PET using the markers FMISO or EF5. However, the combination of specific techniques or tracers, like injection of ^{18}F-FMISO and ^{18}F-fluorodeoxyglucose (^{18}F-FDG) to determine the hypoxic as well as the glycolytic status of a tumor, might give more specific results than the use of a single tracer. Nevertheless, there is still need for a non-invasive technique to measure hypoxia allowing the discrimination of acute and cycling hypoxia, as well as low oxygen concentrations in the range of 0.1 to 1% pO_2.

1.2.2.3. Hypoxia measurements using *in vivo* bioluminescence

Different approaches have been used to measure hypoxia using bioluminescence reporter systems in mouse models. In these imaging systems, cells of interest express the enzyme luciferase in response to hypoxia. Luciferase converts the injected substrate D-luciferin into oxyluciferin, thereby producing CO_2, PPi, AMP and light. The light output can be measured and quantified with the help of an *in vivo* bioluminescence imaging apparatus. In a first approach, the promoter regions of HIF target genes were cloned in front of the luciferase gene. They often contained different numbers of the hypoxia response element (HRE) as shown in figure 1.4. These constructs were used to create stably expressing single clones or pools to follow the activity of HIF-1 *in vitro* and *in vivo* [40,49]. However, different factors influencing HIF-1 levels led to a hypoxia-independent increase or decrease of the luciferase signal [50]. These HRE-luciferase constructs were therefore not feasible to measure tumor hypoxia *in vivo*, showing no significant correlation between HIF-1 activity and PET measurement [40]. Harada and colleagues designed a new construct that displayed HIF-1 activity even more stringently by including a part of the ODD domain fused to the luciferase gene. This HRE-ODD-luciferase construct is induced under HIF-1 activity and degraded in the same fashion as HIF-1α itself, allowing real time imaging of HIF-1 activity [51]. Tumor xenografts expressing the HRE-ODD-luciferase construct were used to follow HIF-1 activity after treatment with a HIF-1 inhibitor in combination with ionizing radiation. The data showed that irradiation followed by treatment with the HIF-1 inhibitor YC-1 delayed tumor growth, whereas the opposite order of treatment led to a suppression of the growth delay induced by radiotherapy [52].

Finally, a construct was developed to follow the dynamics of the HIF-prolylhydroxylases *in vivo*. Safran and colleagues developed a mouse model expressing luciferase, fused to a part of the ODD domain (530 to 652 aa of HIF-1α), ubiquitously. They observed emitted light after D-luciferin injection in the kidney, known to by slightly hypoxic, in mice breathing normal air. The signal increased 5-10-fold when mice were placed in a low oxygen environment (8% oxygen). Finally, they showed that the prolylhydroxylase inhibitor FG-4383 led to an increase of luciferase signal mainly in the kidney and the liver as well as an increase in the circulating erythropoietin (EPO) level [53]. The same ODD-luciferase construct was used in 2010 by Lu and colleagues to investigate the influence of hypoxia on a metastatic organotropic breast cancer model. They showed that hypoxia has distinct functions in the regulation of angiogenesis and metastases in different organ microenvironments [54]. Viola and colleagues used a similar ODD-luciferase construct, containing the full-length ODD domain, to measure

HIF-1 levels in a xenograft mouse model. They observed an increase in luciferase signal after treatment with chemotherapy. However, the increased signal was caused by the stabilization of the construct through NO-dependent nitrosylation at Cys530 caused by infiltrating macrophages rather than an increase in hypoxia [55]. Taking the different properties of the described constructs into account, the short version of the ODD-luciferase construct can be used for longitudinal *in vivo* measurement of tumor hypoxia, whereas the luciferase constructs containing HRE-elements are indicated for the detection of HIF-1 activity.

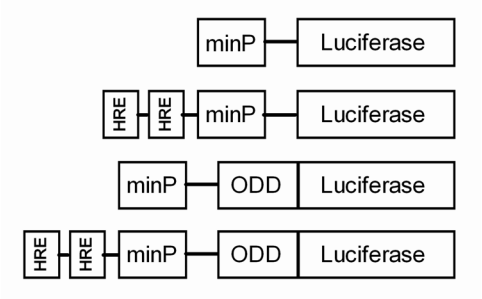

Figure 1.5. Luciferase constructs. Luciferase control construct with a minimal promoter, HRE-Luciferase construct with HRE elements 5' of the minimal promoter (minP), ODD-luciferase construct with a part of the ODD domain of HIF-1α fused 5' to the luciferase gene, HRE-ODD-luciferase construct combining the HRE and the ODD-domain of the described constructs.

1.3. Radiotherapy

1.3.1. R's of radiotherapy

The discovery of X-rays in 1895 by Wilhelm Conrad Röntgen opened the door for radiation therapy, with which 50% of all cancer patients are treated nowadays. Fast accelerated secondary electrons – induced by the interaction of photons with matter - lead to the generation of reactive oxygen species (ROS) which induce permanent damage of cellular components like membranes, proteins or DNA [56]. The damage to DNA is, however, the most relevant for the intended killing of the cells [57]. DNA damage can occur in different forms, including the formation of intra- and inter-strand crosslinks, oxidative base damage, dimer formation or single and double strand breaks (DSB). In order to repair such lesions, the cell uses different DNA damage sensing and repair mechanisms. The most complex lesions for the cells to repair in order to maintain genomic integrity are DSBs, which can be repaired by the two most prominent repair mechanisms, non-homologous end joining (NHEJ) and homologous recombination (HR). NHEJ is an error-prone repair mechanism that rejoins free ends of DSBs without requiring homologous bases at the end of the breaks. Therefore, NHEJ is often accompanied with deletion and loss of genetic information. Since NHEJ does not use homologous sister chromatids for repair, it is the most prominent repair mechanism in the G_1 and early S phases of the cell cycle. HR instead is an error-free repair mechanism. This repair

mechanism uses the homologous sister chromatid as a template for repair and therefore operates in the late S and G_2 phases of the cell cycle [58]. The main DNA damage in normal tissue is repaired within 6 hours after irradiation, therefore fractionated irradiation could be applied in a smaller window than the conventional 1 fraction/day. Different studies compared hyperfractionated irradiation with 2 smaller fractions/day with the conventional irradiation schedule of 1 fraction/day. Hyperfractionated irradiation achieved in cancer cases of advanced stages a better local control than the conventional irradiation regimen [59,60].

Radiobiologists have defined a set of specific factors that comprise cellular and tissue response to irradiation. Considering these biological response mechanism factors, radiotherapists can minimize the normal tissue toxicity while increasing the radiation response of a tumor. The first of the so-called 4 R's of radiotherapy is the above-described *Repair,* which leads to the restoration of the damaged macromolecules and especially DNA. The second R of radiotherapy is *Redistribution/Reassortment,* describing the cellular response on the level of the cell cycle. The cellular sensitivity towards ionizing radiation differs depending on the cell cycle. The most sensitive phase of the cell cycle is the M phase. The obtained DNA damage is passed over to daughter cells, leading to mitotic catastrophe and cell death. The G_2 phase is considered as a radiosensitive phase as well, whereas G_1 and especially late S phase are the most radioresistant phases. IR induces cell death in the radiosensitive cell cycle phases, whereas cells in the radioresistent phases will consequently progress to a more sensitive phase after DNA repair. Fractionated irradiation therefore leads to synchronization of the surviving cells sensitizing them to the next treatment fraction.

The *Repopulation* of the surviving fraction of tumor cells after IR is one of the major challenges in radiotherapy. Tumor cells might repopulate even after a fractionated treatment regime, starting to reform the tumor. Therefore, a fractionated treatment regimen should be conducted without unnecessary interruptions. Treatment with IR can lead to an increase in cell proliferation in some tumors like head and neck squamous cell carcinoma [61]. Therefore, molecular-targeted agents are used to reduce repopulation during radiotherapy. The most prominent target is the epidermal growth factor receptor (EGFR) which is often overexpressed in tumors. The use of specific therapies targeting EGFR in a combined treatment modality with IR will be described later in the introduction. Another example is the aurora kinase B inhibitor AZD1152-HQPA, which inhibited the repopulation of two different non small cell lung carcinoma cell lines *in vitro* when combined with fractionated irradiation. The aurora kinases control the cellular mitotic progression and their activity is frequently

upregulated in cancer cells [62]. Aurora inhibitors might therefore be a promising agent for the control of repopulation in a concomitant treatment regimen with IR.

The last R of radiotherapy is the *Reoxygenation* of the surviving tumor cells after treatment. Radiosensitivity decrease with increasing hypoxia, leading to a two to three times higher radiation resistance of hypoxia cells compared to well-oxygenated tumor cells. Irradiation induces cell death in oxygenated tumor cells, subsequently leading to improved oxygenation of the hypoxic surviving tumor cells. The reoxygenated cells are afterwards more radiosensitive to the next dose of irradiation in a fractionated radiation set-up. Reoxygenation and Reassortment are therefore beneficial for radiotherapy, whereas Repair and Repopulation hamper radiotherapy [63].

Of major concern in the field of radiotherapy are the cancer stem cells, which exhibit high levels of radioresistance. Cancer stem cells escape the damage by irradiation by various mechanisms. They are in a quiescent state of the cell cycle and therefore not cycling into a radiosensitive phase. Cancer stem cells further exhibit an enhanced repair of DNA by increased activation of the NHEJ repair mechanism through ATM signaling compared to non-tumoral stem cells. Additionally, cell cycle control mechanism to arrest the cell cycle in order to allow DNA repair are upregulated. Furthermore, cancer stem cells contain a higher activity of ROS-scavenging enzymes therefore minimizing the induced DNA damage [64]. Different strategies to overcome these radiation mechanisms are currently under investigation. Targeting specific signaling pathways of the cancer stem cells [65] or the use of radiation therapy with heavy particles like carbon ions might be more indicated for cancer stem cells than classic irradiation with photons [66].

Both, the R's of radiotherapy as well as the hallmarks of cancer describe factors related to the phenotype and the treatment response of a tumor. While the R's of radiotherapy derive from perspectives of "Clinical Radiation Biology and Radiotherapy", the Hallmarks of Cancer derive from "Molecular Oncology". It is a challenge to "reconcile" these two different worlds, but eventually a chance to identify novel treatment regimens and molecular processes as targets for a combined treatment modality of ionizing radiation with antisignaling agents.

1.3.2. Tumor hypoxia in radiotherapy

Tumor hypoxia hinders effective radiotherapy in several ways. Radiotherapy induces free radicals, including ones in close proximity to DNA. Oxygen fixes the damage by oxidizing DNA radicals, therefore inducing a permanent damage. Under hypoxic conditions, DNA radicals are reduced by components containing SH groups, which repair the DNA damage to

its original form [31]. Therefore, radiosensitivity is progressively reduced when the pO_2 in a tumor is below 15-20 mmHg resulting in a two to three fold higher radioresistance of hypoxic tumors. A low partial pressure (< 5-10 mmHg) determined with invasive pO_2 electrodes prior treatment revealed a strong correlation with poor locoregional control in non-small cell lung and uterine cervix carcinoma [38,39]. Therefore, tumor hypoxia can in some cases be used as surrogate marker or treatment outcome after radiotherapy.

The cellular radioresistance under hypoxia is mediated by the HIF-1 protein and is described as follows. Radiation of a solid tumor activates HIF-1, which in turn leads to the expression of VEGF. VEGF protects endothelial cells from further damage by radiation, allowing vessels to continue providing tumor cells with nutrients and oxygen. This model is supported by the fact that the supernatant of irradiated tumor cells protects endothelial cells from irradiation [31,67]. Moreover, data by Harada et al. demonstrated that the concomitant treatment modality of IR with the HIF-1 inhibitor YC-1 impaired the post-irradiation induced upregulation of HIF-1α, consequently leading to a decrease in microvessel density in a xenograft model. The concomitant treatment regimen further resulted in a stronger tumor growth delay when compared to the treatment with IR alone [52].

After irradiation, HIF-1α distribution changes dramatically due to the induced changes in the microenvironment. Oxygenation of hypoxic regions in the tumor improves due to death of the well-oxygenated tumor cells. It was shown that HIF-1α activity decreases in the first hours after IR and increases again afterwards [52]. The later increase in HIF-1α can be explained by an increase in secreted nitric oxide (NO) of tumor-associated macrophages caused by the reoxygenation of tumor cells after IR. NO in turn leads to S-nitrosylation of HIF-1α at cysteine520 in the ODD domain, consequently stabilizing the protein [68]. Furthermore, HIF-1α stabilization after reoxygenation occurs due to the release of HIF-1α transcripts from stress granules, consequent translation of the protein and nuclear accumulation of HIF-1α in response to ROS formation [69].

Therefore, different approaches have been tried to overcome the treatment resistance caused by hypoxia. To overcome the lack of oxygen, investigators tried increasing the level of oxygen in the breathing air of patients or increasing the amount of red blood cells [70,71]. While these approaches showed promising results in preclinical studies, they did not made it into the clinics due to controversial results in clinical trials. To address radioresistance caused by HIF-1α, the use of specific HIF-1 inhibitors like YC-1 or the regulation of key factors that control the expression of HIF-1α was employed [52]. The radiosensitizing properties of PI3K-Akt-mTOR pathway inhibitors are related, in part, to the inhibition of HIF-1α. The

specific mTOR inhibitor RAD001 showed a downregulation of the HIF-1α protein and its downstream products in a mouse model for prostate cancer [72]. Nevertheless, HIF-1α inhibitors are still mainly in preclinical studies.

1.4. Microtubules as target for cancer therapy

1.4.1. The microtubule network

The cytoskeleton is a cytoplasmic system of fibers, which is critical for different cell functions like motility, organization of cell contents and cell shape. The different fibers forming the cytoskeleton are microfilaments, intermediate filaments and microtubule, which are all built up of small protein subunits. Microfilaments and intermediate filaments are attached to plasma membrane proteins thereby supporting the shape of the plasma membrane. Microfilaments, built up of G-actin monomers to form F-actin polymers, and microtubule are responsible for cell movements and cell shape. Motor proteins from the kinesin and dynein families are moving along the microtubule or microfilaments to ferry organelles or vessels. Many cell movements require, however, cytoskeleton rearrangement, which is reached by assembly and reassembly of the cytoskeleton fibers.

Microtubules are dynamic polymers, which form rope like structures that can grow as long as 25 micrometers. The α/β tubulin heterodimer are arranged head-to-tail to form linear protofilaments that associate laterally to a hollow like tube with a diameter of 25nm. Microtubules are usually formed by 13 protofilaments. Every tubulin heterodimer binds two guanosine triphosphates (GTP). The GTP bound to the α-subunit is not exchangeable and trapped between the α-tubulin and the β-tubulin. The β-tubulin instead binds the GTP reversible and hydrolyses it to GDP during polymerization. The GDP bound to the β-tubulin is not exchanged while the β-tubulin remains in the polymer. However, β-tubulin exposing GDP at the end of a microtubule leads to depolymerisation of the microtubule. The GTP cap model describes a layer of β-tubulin containing unhydrolyzed GTP, which stabilizes the microtubule structure. Microtubules contain a dynamic plus end with an exposed β-tubulin and a less dynamic minus end characterized by an exposed α-tubulin. Microtubule form a well organized network in which the minus end is usually anchored at the microtubule-organizing center (MTOC) like the centrosome whereas the plus pole grows towards specific targets [73,74].

β-tubulin exists in 7 isotypes that are expressed in a tissue specific manner. The βI- and βIV-tubulins are expressed constitutively in all main cell types, whereas βII- and βIII-tubulins are

mainly expressed in neurons. βIII-tubulins have also been found in different tumors and have been associated with aggressiveness and invasiveness. The βV-tubulin is mainly expressed in the uterus and endometrium, but has also been found in adenocarcinomas. βVI-tubulin can be found in hepatopoesis-specific cells.

Further members of the tubulin superfamily include γ, δ, ε, ζ and η-tubulin. The γ-tubulin plays an important role in the microtubule nuclearisation, whereas the function and the interactions of the other tubulins have been associated with the centrosome or other MTOCs [75].

Different microtubule-associated proteins organize microtubules and affect their stability. Microtubule stabilizing proteins found in most cells are the microtubule associated protein 4 (MAP4) which is regulating microtubule stability in mitosis and cytoplasmic linker protein of 170 kDa (CLIP170), which cross-links microtubules to chromosomes. Further proteins stabilizing microtubules are MAP1, MAP2 and Tau which are mainly found in dendrites and axons. The microtubule binding domain of these proteins contains several repeats of a conserved positively charged amino-acid-sequence binding to the negatively charged C-terminal of tubulin. Due to this binding the charge repulsion of tubulin subunits in a microtubule is reduced. Binding of MAPs to the outer wall of a microtubule hinders the dissociation of tubulin subunits from the microtubule. MAPs are regulated by reversible phosphorylation of MAP kinases or cyclin-dependent kinases (CDKs). Phosphorylation of the MAPs impairs binding to microtubule consequently promoting microtubule disassembly [73].

Microtubule destabilizing proteins are for example katanin and stathmin. Katanin leads to breakage of the internal bonds between tubulin subunits causing the fragmentation of microtubules or dissociation from the MTOC. Stathmin instead binds tubulin dimers thereby reducing the amount of dimers needed for polymerization [76].

Microtubules are modified by diverse reversible post-translational modifications such as phosphorylation, tyrosination, acetylation, polyglutamylation or polyglycylation. Acetylation and deacetylation are involved in the regulation of cell motility by influencing the binding of MAPs to microtubule. Polyglutamylation is as well involved in the interaction of microtubule and MAPs, but leads further to centriole maturation and stability. However, most of the biological functions of these modifications are not yet fully understood [77].

1.4.2. The cellular functions of microtubule

Generation of movements by assembly and disassembly of the microtubule, as well as the interaction with motor proteins are highly important to execute the different functions of the microtubule network such as the separation of chromosomes during mitosis, organelle trafficking or cell motility. Motor proteins of the kinesin and dynein families were found to interact with microtubules. Motor proteins utilize the energy of ATP hydrolysis to move unidirectly along the microtubule. Most of the kinesins move towards the plus end of a microtubule whereas dyneins move in the direction of the minus end. The motor proteins usually contain two motor subunits which bind to the microtubule and hydrolyze ATP, and regulatory subunits. The cargo is bound to either of the subunits. Cargo of motor proteins consists of endosomes moving towards lysosomes, trans-Golgi network-derived vesicles or mitochondria. However, motor proteins also transport non-vesicular cargo such as cytoplasmic protein complexes, RNA-protein complexes, ribosomes or cytoskeletal polymers. Besides their function in cargo transport, motor proteins also play a role in cell signalling. Kinesin-1, one of the most prominent motor proteins for anterograde transport in the cell, acts also as a scaffolding protein which recruits active kinase complexes to vesicle-associated kinesin-1 linkers. Kinesin-4 (KIF4A) instead regulates neuronal survival by the suppression of the enzymatic activity of poly (ADP-ribose) polymerase-1 (PARP-1) [78].

Another highly important role of microtubules and the associated motor proteins lies in the separation of chromosomes during mitosis. Aster microtubules are forming the asters around the centrosomes whereas the polar and kinetochore microtubules form the spindle. Kinetochore microtubules attach at the kinetochore of the chromosome and transport them by forces generated by spindle kinesins as well as by shortening of the microtubule to the metaphase plane. Dyneins instead walk along astral microtubules which are attached to the plasma membrane thereby pulling the poles outward. The correct attachment of the microtubule originated from the two different centromeres to the kinetochore is monitored by different proteins. The key regulator ensuring the accuracy of the correct attachment is the Aurora B kinase [79]. Aurora B kinase is therefore one of the targets of anti-cancer drugs aimed to interfere with cell division.

Furthermore, microtubules play an important role in cell motility. In order to initiate migration the microtubule network gets first polarized with detyrosinated microtubules aligning in the direction of the front-rear axis of cells. The microtubule network restricts actin polymerization, regulates focal adhesions in cells and locally regulates the activity of Rho GTPases which are known to regulate actin cytoskeleton. A good coordination between

microtubule, actin and focal adhesions are therefore essential for cell migration. Indanocine, a microtubule destabilizing agent led to an increased acetylation of microtubules, defects in cell polarization and defects in adhesion disassembly consequently reducing cell migration [80].
The dynamic instability of the microtubule network is crucial for its proper function in cell division, cell shape maintenance, motility and intracellular organelle trafficking, which makes microtubules an attractive target in anti-cancer treatment.

1.4.3. Microtubule interfering agents

Microtubules are one of the most successful targets of anticancer drugs, the so-called microtubule interfering agents [81]. Microtubule interfering agents can be divided in two classes, microtubule destabilizing and microtubule stabilizing agents. Microtubule destabilizing agents inhibit the assembly of tubulin heterodimers into microtubules. Most of the microtubule destabilizing agents bind at two distinct domains to the tubulin, the vinca domain or the colchicine domain. Substrates binding to the vinca domain are vinca-alkaloids (vincristine, vinblastine), dolastatins (eribulin, spongistatin) or cryptophycins. Substrates binding to the colchicine domain include colchicine, steganacins and curacins. Vinca alkaloids bind mostly to the microtubule ends whereas colchicine binds to soluble dimers which are incorporated into the microtubules [74]. The most well-known members of this group are vincristine and vinblastine, which have been used in anticancer treatments since the 1960s.
Microtubule stabilizing agents (MSA) promote the polymerization of tubulin heterodimers into microtubules and stabilize preformed microtubules. Most of the MSAs bind to the same or to an overlapping taxoid binding site on the β-tubulin located on the inside surface of the microtubule. MSAs impair the dynamic instability of the microtubule network, leading to defective mitotic spindle formation [82,83] or at lower concentrations to G1-arrest [84] followed by apoptosis [85]. The altered microtubule network also leads to a reduction of cell invasion and migration [86,87]. MSAs include taxanes, epothilones, discodermolide, cyclostreptin, laulimalide, rhazinilam and further substrates. The first FDA approved agent in the group of taxanes was taxol (paclitaxel) in 1992 followed by its related analogue docetaxel in 1996. However, treatment with taxanes is often limited by the development of resistance towards the drug and taxane-related toxicities [88].
Therefore, epothilones, a non-taxoid group of MSAs, are gaining more and more interest because of their tolerable toxicity profile [89], activity against P-glycoprotein-mediated multidrug resistance and better water solubility in comparison to taxanes.

Epothilones were initially discovered for their anti-fungal properties in a screen using extracts of the myxobacterium *Sorangium cellulosum Soce90* [90], and shortly afterwards their ability to inhibit tumor cell proliferation was described. Epothilones share the same binding site on β-tubulin with taxanes, which is in close proximity to residue Thr274 on β–tubulin [91]. At least seven epothilone-derived agents are in clinical trials for cancer treatment, with the two most promising compounds being Ixabepilone and Patupilone (EPO906). Ixabepilone is the first FDA approved agent in this group for treatment of metastatic breast cancer [92]. Patupilone was tested as a phase III monotherapy agent against ovarian cancer and has passed a phase I trial for CNS malignancies with concurrent radiotherapy [93].

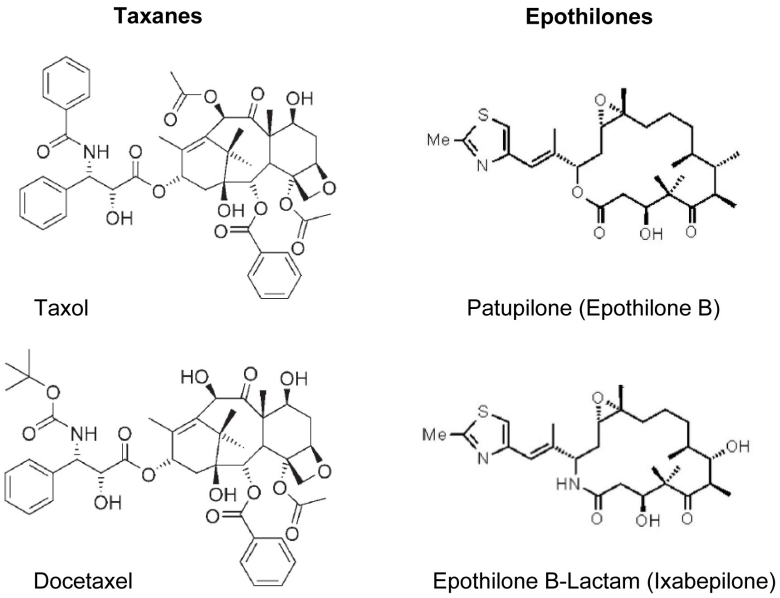

Figure 1.6. Chemical structures of MSA agents [94]

1.5. Combined treatment modalities

Besides technical improvements in the field of radiotherapy, radiobiologists aim to enhance the tumor growth control of cancer treatment by sensitizing cells to radiotherapy using different chemotherapeutic agents. The rationale behind the combined treatment is the use of drugs that influence the different features induced by radiotherapy (R's of radiotherapy) to generate a better treatment response. As discussed above, IR results in the strongest inhibition of proliferation in cells in specific phases of the cell cycle. It has been shown that the MSA Patupilone accumulates cells in the radiosensitive G2/M phase. The combined treatment modality of IR and Patupilone led consequently to an additive tumor growth delay in xenograft mouse models [95]. A further approach in the combined treatment modality is the blockage of repopulation, especially by inhibition of EGFR. Overexpression of EGFR is a common feature of head and neck cancer leading to accelerated tumor growth. Activation of EGFR by EGF or transforming growth factor α (TGFα) triggers the downstream pathways of PI3K, Ras/MAP kinase and STAT-3, leading to increased proliferation. It has been shown that IR leads to dimerization and therefore activation of EGFR [96]. Combination of IR with the clinically relevant anti-EGFR monoclonal antibody C225 (Cetuximab) in a phase III trial demonstrated significant locoregional tumor control, minimal tissue toxicity and an increased overall survival [97,98]. This overall strong tumor growth control results not only from inhibition of repopulation but also from inhibition of DNA damage repair and blockage of VEGF and therefore inhibition of angiogenesis by EGFR inhibition [99,100].

Modulation of the microenvironment, especially the tumor vasculature, is another target for anticancer agents. Blockage of the vasculature will lead to decreased delivery of nutrients, growth factors and oxygen and therefore impair tumor growth. Anti-angiogenic agents are thought to also decrease metastatic spreading, and the risk of treatment resistance of endothelial cells is lower than for tumor cells that have already acquired several mutations. Anti-angiogenic agents directly block pro-angiogenic growth factors or their respective receptors on endothelial cells, or decrease the secretion of pro-angiogenic factors by tumor cells. Another aspect of anti-angiogenic agents, however, is the so-called normalization of the tumor vasculature. This phenomenon is caused by destruction of immature vessels and the recruitment of pericytes and therefore fortification of intact vessels after treatment with anti-angiogenic agents [101,102]. Interestingly, the combined treatment of anti-angiogenic agents and cytotoxic agents provided improved results over the single treatments alone [103]. The concept of the normalization of blood vessels under treatment with anti-angiogenic agents renders the combination with ionizing irradiation an attractive strategy for cancer treatment.

The oxygenation of tumor cells improves due to vessel normalization leading to a higher responsiveness to IR. The combination of anti-VEGFR2 antibodies and IR has been shown to significantly enhance the tumor growth retarding properties of IR [104,105]. The same holds true for the combined treatment of an anti-VEGF antibody in combination with IR [67,106].
However, there are still concerns about this combined treatment modality due to the fact that both treatments can also induce tumor hypoxia. IR, in fact, possesses both angiogenesis promoting and anti-angiogenic properties. The anti-angiogenic effect is caused by the high radiosensitivity of endothelial cells, consequently leading to endothelial cell death and an increase in hypoxia. The angiogenesis promoting effect is caused by a growth factor-independent activation of the VEGF receptor on endothelial cells and increased VEGF secretion of tumor cells as a stress response towards IR [67]. An approach to overcome these restrictions might lie in the scheduling of the different treatments. Treatment schedules with an adjuvant application of the anti-angiogenic agent resulted in a prolonged tumor growth delay [107], while simultaneous application of the anti-angiogenic agent and IR in a study with murine mammary carcinoma also resulted in a prolonged tumor growth delay [105]. These results indicate that the combination of IR with anti-angiogenic agents can be considered a promising strategy and that further investigations on scheduling could result in even better tumor control, paving the way for clinical trials.

2. Aims of the study

The combined treatment of ionizing irradiation (IR) and microtubule stabilizing agents (MSA) has been shown to be an effective strategy for cancer treatment in preclinical models [95,108]. Our group previously demonstrated that the microtubule stabilizing agent patupilone combined with IR inhibited tumor cell proliferation *in vitro* in an additive manner, whereas the combined treatment revealed an even supra-additive tumor growth delay effect [95]. MSAs sensitize tumor cells towards IR by the accumulation of the cells in a radiosensitive cell phase. However, MSAs can also lead to a decrease in the HIF-1 protein level, the major transcription factor under hypoxia, in cells treated with high dosages of MSA [109]. MSAs might therefore also affect the tumor microenvironment, especially the tumor vasculature, by interfering with secretion of pro-angiogenic factors, mostly HIF-1 target genes.
The first aim of this study was to investigate the effect of patupilone and IR, alone and as part of a combined treatment modality, on different tumor cell lines *in vitro* and on tumor xenografts, with a specific focus on the tumor microenvironment. A genetically defined tumor cell system was used, which consists of the non-small cell lung carcinoma cell line A549 and its patupilone-resistant counterpart A549.EpoB40. This cell pair was used to investigate the effect of the combined treatment modality on the tumor cell level as well as on the level of the tumor microenvironment. The *in vitro* studies of different cell lines included the analysis of tumor cell proliferation, clonogenicity and cell cycle distribution in response to the different treatment modalities. Furthermore, the expression and secretion of HIF-1 target genes were analyzed under the different treatment modalities. *In vivo* experiments of tumor xenografts derived from different cell lines aimed to analyze the tumor growth delay induced by the different treatment modalities and the impact of the treatments on the tumor vasculature by analyzing microvessel density.

DNA-damage is the most relevant damage induced by ionizing radiation. The damage is caused by the formation of intracellular reactive oxygen species (ROS) and their interaction with the DNA. The reduced oxygen content in hypoxic tumor cells is therefore a major reason for a two to three fold increase in radiation resistance. Hypoxic conditions can be caused by insufficient angiogenesis due to rapid tumor growth or limited oxygen diffusion or perfusion. Furthermore, the oxygen content in a tumor can also be shifted in response to different treatment modalities such as inhibitors of angiogenesis. Thus, combined treatment of ionizing radiation with compounds affecting the tumor vasculature could create an additional risk for

an effective radiotherapy due to treatment-induced hypoxia. Detailed insights into the dynamics of tumor hypoxia might contribute to the improvement and adaptation of existing therapies to changes in the tumor microenvironment.

The second aim of this study was therefore to investigate changes of hypoxia, during and in response to different treatment modalities *in vivo*. For this purpose, a bioluminescence-based system, leading to the expression of the reporter gene luciferase in response to increasing hypoxia, was first developed and validated *in vitro*. Major requirements were a stable signal induction under hypoxia and luciferase expression, which is not perturbed by chemotherapeutic agents altering the HIF-1 activity. The *in vivo* research part was performed using a murine xenograft tumor model expressing the developed reporter construct, which allowed serial determination of tumor hypoxia. The main focus was to probe the dynamics of tumor hypoxia in response to IR, patupilone and the combined treatment modality. This system allowed us to evaluate the dynamics of tumor hypoxia as surrogate marker for the respective treatment modalities.

References

1. Jemal A, Bray F, Center MM, Ferlay J, Ward E, et al. Global cancer statistics. CA Cancer J Clin 61: 69-90.
2. Siegel R, Ward E, Brawley O, Jemal A Cancer statistics, 2011: the impact of eliminating socioeconomic and racial disparities on premature cancer deaths. CA Cancer J Clin 61: 212-236.
3. Delaney G, Jacob S, Featherstone C, Barton M (2005) The role of radiotherapy in cancer treatment: estimating optimal utilization from a review of evidence-based clinical guidelines. Cancer 104: 1129-1137.
4. Hanahan D, Weinberg RA Hallmarks of cancer: the next generation. Cell 144: 646-674.
5. Cheng N, Chytil A, Shyr Y, Joly A, Moses HL (2008) Transforming growth factor-beta signaling-deficient fibroblasts enhance hepatocyte growth factor signaling in mammary carcinoma cells to promote scattering and invasion. Mol Cancer Res 6: 1521-1533.
6. Cejas P, Lopez-Gomez M, Aguayo C, Madero R, de Castro Carpeno J, et al. (2009) KRAS mutations in primary colorectal cancer tumors and related metastases: a potential role in prediction of lung metastasis. PLoS One 4: e8199.
7. Hollstein M, Sidransky D, Vogelstein B, Harris CC (1991) p53 mutations in human cancers. Science 253: 49-53.
8. Galluzzi L, Vitale I, Abrams JM, Alnemri ES, Baehrecke EH, et al. (2012) Molecular definitions of cell death subroutines: recommendations of the Nomenclature Committee on Cell Death 2012. Cell Death Differ 19: 107-120.
9. Vitale I, Galluzzi L, Castedo M, Kroemer G (2011) Mitotic catastrophe: a mechanism for avoiding genomic instability. Nat Rev Mol Cell Biol 12: 385-392.
10. Hanahan D, Folkman J (1996) Patterns and emerging mechanisms of the angiogenic switch during tumorigenesis. Cell 86: 353-364.
11. Thiery JP, Sleeman JP (2006) Complex networks orchestrate epithelial-mesenchymal transitions. Nat Rev Mol Cell Biol 7: 131-142.
12. Pages F, Galon J, Dieu-Nosjean MC, Tartour E, Sautes-Fridman C, et al. Immune infiltration in human tumors: a prognostic factor that should not be ignored. Oncogene 29: 1093-1102.
13. Nelson BH (2008) The impact of T-cell immunity on ovarian cancer outcomes. Immunol Rev 222: 101-116.
14. Jones RG, Thompson CB (2009) Tumor suppressors and cell metabolism: a recipe for cancer growth. Genes Dev 23: 537-548.
15. Hsu PP, Sabatini DM (2008) Cancer cell metabolism: Warburg and beyond. Cell 134: 703-707.
16. Feron O (2009) Pyruvate into lactate and back: from the Warburg effect to symbiotic energy fuel exchange in cancer cells. Radiother Oncol 92: 329-333.
17. Semenza GL (2008) Tumor metabolism: cancer cells give and take lactate. J Clin Invest 118: 3835-3837.
18. Berdasco M, Esteller M (2010) Aberrant epigenetic landscape in cancer: how cellular identity goes awry. Dev Cell 19: 698-711.
19. Branco-Price C, Zhang N, Schnelle M, Evans C, Katschinski DM, et al. Endothelial cell HIF-1alpha and HIF-2alpha differentially regulate metastatic success. Cancer Cell 21: 52-65.
20. Raza A, Franklin MJ, Dudek AZ (2010) Pericytes and vessel maturation during tumor angiogenesis and metastasis. Am J Hematol 85: 593-598.
21. Yonenaga Y, Mori A, Onodera H, Yasuda S, Oe H, et al. (2005) Absence of smooth muscle actin-positive pericyte coverage of tumor vessels correlates with

hematogenous metastasis and prognosis of colorectal cancer patients. Oncology 69: 159-166.
22. Giaccia AJ, Schipani E (2010) Role of carcinoma-associated fibroblasts and hypoxia in tumor progression. Curr Top Microbiol Immunol 345: 31-45.
23. Rasanen K, Vaheri A (2010) Activation of fibroblasts in cancer stroma. Exp Cell Res 316: 2713-2722.
24. Pietras K, Ostman A (2010) Hallmarks of cancer: interactions with the tumor stroma. Exp Cell Res 316: 1324-1331.
25. Kim JW, Evans C, Weidemann A, Takeda N, Lee YS, et al. (2012) Loss of fibroblast HIF-1alpha accelerates tumorigenesis. Cancer Res.
26. Stockmann C, Doedens A, Weidemann A, Zhang N, Takeda N, et al. (2008) Deletion of vascular endothelial growth factor in myeloid cells accelerates tumorigenesis. Nature 456: 814-818.
27. Mayer EL, Lin NU, Burstein HJ (2007) Novel approaches to advanced breast cancer: bevacizumab and lapatinib. J Natl Compr Canc Netw 5: 314-323.
28. Dewhirst MW, Cao Y, Moeller B (2008) Cycling hypoxia and free radicals regulate angiogenesis and radiotherapy response. Nat Rev Cancer 8: 425-437.
29. Palm F, Nordquist L (2011) Renal oxidative stress, oxygenation, and hypertension. Am J Physiol Regul Integr Comp Physiol 301: R1229-1241.
30. Mortensen LS, Buus S, Nordsmark M, Bentzen L, Munk OL, et al. (2010) Identifying hypoxia in human tumors: A correlation study between 18F-FMISO PET and the Eppendorf oxygen-sensitive electrode. Acta Oncol 49: 934-940.
31. Harada H How can we overcome tumor hypoxia in radiation therapy? J Radiat Res (Tokyo) 52: 545-556.
32. Wenger RH, Stiehl DP, Camenisch G (2005) Integration of oxygen signaling at the consensus HRE. Sci STKE 2005: re12.
33. Peng YJ, Yuan G, Ramakrishnan D, Sharma SD, Bosch-Marce M, et al. (2006) Heterozygous HIF-1alpha deficiency impairs carotid body-mediated systemic responses and reactive oxygen species generation in mice exposed to intermittent hypoxia. J Physiol 577: 705-716.
34. Wenger RH (2002) Cellular adaptation to hypoxia: O2-sensing protein hydroxylases, hypoxia-inducible transcription factors, and O2-regulated gene expression. FASEB J 16: 1151-1162.
35. Hansen AE, Kristensen AT, Law I, Jorgensen JT, Engelholm SA Hypoxia-inducible factors--regulation, role and comparative aspects in tumourigenesis. Vet Comp Oncol 9: 16-37.
36. Nordsmark M, Overgaard J (2000) A confirmatory prognostic study on oxygenation status and loco-regional control in advanced head and neck squamous cell carcinoma treated by radiation therapy. Radiother Oncol 57: 39-43.
37. Nordsmark M, Overgaard J (2004) Tumor hypoxia is independent of hemoglobin and prognostic for loco-regional tumor control after primary radiotherapy in advanced head and neck cancer. Acta Oncol 43: 396-403.
38. Le QT, Chen E, Salim A, Cao H, Kong CS, et al. (2006) An evaluation of tumor oxygenation and gene expression in patients with early stage non-small cell lung cancers. Clin Cancer Res 12: 1507-1514.
39. Knocke TH, Weitmann HD, Feldmann HJ, Selzer E, Potter R (1999) Intratumoral pO2-measurements as predictive assay in the treatment of carcinoma of the uterine cervix. Radiother Oncol 53: 99-104.
40. Lehmann S, Stiehl DP, Honer M, Dominietto M, Keist R, et al. (2009) Longitudinal and multimodal in vivo imaging of tumor hypoxia and its downstream molecular events. Proc Natl Acad Sci U S A 106: 14004-14009.

41. Mayer A, Wree A, Hockel M, Leo C, Pilch H, et al. (2004) Lack of correlation between expression of HIF-1alpha protein and oxygenation status in identical tissue areas of squamous cell carcinomas of the uterine cervix. Cancer Res 64: 5876-5881.
42. Eschmann SM, Paulsen F, Reimold M, Dittmann H, Welz S, et al. (2005) Prognostic impact of hypoxia imaging with 18F-misonidazole PET in non-small cell lung cancer and head and neck cancer before radiotherapy. J Nucl Med 46: 253-260.
43. Gagel B, Reinartz P, Demirel C, Kaiser HJ, Zimny M, et al. (2006) [18F] fluoromisonidazole and [18F] fluorodeoxyglucose positron emission tomography in response evaluation after chemo-/radiotherapy of non-small-cell lung cancer: a feasibility study. BMC Cancer 6: 51.
44. Koh WJ, Bergman KS, Rasey JS, Peterson LM, Evans ML, et al. (1995) Evaluation of oxygenation status during fractionated radiotherapy in human nonsmall cell lung cancers using [F-18]fluoromisonidazole positron emission tomography. Int J Radiat Oncol Biol Phys 33: 391-398.
45. Gillham C, Zips D, Ponisch F, Evers C, Enghardt W, et al. (2008) Additional PET/CT in week 5-6 of radiotherapy for patients with stage III non-small cell lung cancer as a means of dose escalation planning? Radiother Oncol 88: 335-341.
46. O'Donoghue JA, Zanzonico P, Pugachev A, Wen B, Smith-Jones P, et al. (2005) Assessment of regional tumor hypoxia using 18F-fluoromisonidazole and 64Cu(II)-diacetyl-bis(N4-methylthiosemicarbazone) positron emission tomography: Comparative study featuring microPET imaging, Po2 probe measurement, autoradiography, and fluorescent microscopy in the R3327-AT and FaDu rat tumor models. Int J Radiat Oncol Biol Phys 61: 1493-1502.
47. Sun X, Niu G, Chan N, Shen B, Chen X (2011) Tumor hypoxia imaging. Mol Imaging Biol 13: 399-410.
48. Howe FA, Robinson SP, McIntyre DJ, Stubbs M, Griffiths JR (2001) Issues in flow and oxygenation dependent contrast (FLOOD) imaging of tumours. NMR Biomed 14: 497-506.
49. Harada H, Kizaka-Kondoh S, Hiraoka M (2005) Optical imaging of tumor hypoxia and evaluation of efficacy of a hypoxia-targeting drug in living animals. Mol Imaging 4: 182-193.
50. Ou G, Itasaka S, Zeng L, Shibuya K, Yi J, et al. (2009) Usefulness of HIF-1 imaging for determining optimal timing of combining bevacizumab and radiotherapy. Int J Radiat Oncol Biol Phys 75: 463-467.
51. Harada H, Kizaka-Kondoh S, Itasaka S, Shibuya K, Morinibu A, et al. (2007) The combination of hypoxia-response enhancers and an oxygen-dependent proteolytic motif enables real-time imaging of absolute HIF-1 activity in tumor xenografts. Biochem Biophys Res Commun 360: 791-796.
52. Harada H, Itasaka S, Zhu Y, Zeng L, Xie X, et al. (2009) Treatment regimen determines whether an HIF-1 inhibitor enhances or inhibits the effect of radiation therapy. Br J Cancer 100: 747-757.
53. Safran M, Kim WY, O'Connell F, Flippin L, Gunzler V, et al. (2006) Mouse model for noninvasive imaging of HIF prolyl hydroxylase activity: assessment of an oral agent that stimulates erythropoietin production. Proc Natl Acad Sci U S A 103: 105-110.
54. Lu X, Yan CH, Yuan M, Wei Y, Hu G, et al. In vivo dynamics and distinct functions of hypoxia in primary tumor growth and organotropic metastasis of breast cancer. Cancer Res 70: 3905-3914.
55. Viola RJ, Provenzale JM, Li F, Li CY, Yuan H, et al. (2008) In vivo bioluminescence imaging monitoring of hypoxia-inducible factor 1alpha, a promoter that protects cells, in response to chemotherapy. AJR Am J Roentgenol 191: 1779-1784.

56. Stadtman ER (1993) Oxidation of free amino acids and amino acid residues in proteins by radiolysis and by metal-catalyzed reactions. Annu Rev Biochem 62: 797-821.
57. Bernier J, Hall EJ, Giaccia A (2004) Radiation oncology: a century of achievements. Nat Rev Cancer 4: 737-747.
58. Wilson GD (2004) Radiation and the cell cycle, revisited. Cancer Metastasis Rev 23: 209-225.
59. Pan ZQ, He XY, Guo XM, Ye M, Zhang Z, et al. (2011) A Phase III Study of Late Course Accelerated Hyperfractionated Radiotherapy Versus Conventionally Fractionated Radiotherapy in Patients With Nasopharyngeal Carcinoma. Am J Clin Oncol.
60. Baumann M, Herrmann T, Koch R, Matthiessen W, Appold S, et al. (2011) Final results of the randomized phase III CHARTWEL-trial (ARO 97-1) comparing hyperfractionated-accelerated versus conventionally fractionated radiotherapy in non-small cell lung cancer (NSCLC). Radiother Oncol 100: 76-85.
61. Withers HR, Taylor JM, Maciejewski B (1988) The hazard of accelerated tumor clonogen repopulation during radiotherapy. Acta Oncol 27: 131-146.
62. Sak A, Stuschke M, Groneberg M, Kubler D, Pottgen C, et al. (2012) Inhibiting the Aurora B Kinase Potently Suppresses Repopulation During Fractionated Irradiation of Human Lung Cancer Cell Lines. Int J Radiat Oncol Biol Phys.
63. Oehler C, Dickinson DJ, Broggini-Tenzer A, Hofstetter B, Hollenstein A, et al. (2007) Current concepts for the combined treatment modality of ionizing radiation with anticancer agents. Curr Pharm Des 13: 519-535.
64. Moncharmont C, Levy A, Gilormini M, Bertrand G, Chargari C, et al. (2012) Targeting a cornerstone of radiation resistance: Cancer stem cell. Cancer Lett.
65. Kendziorra E, Ahlborn K, Spitzner M, Rave-Frank M, Emons G, et al. (2011) Silencing of the Wnt transcription factor TCF4 sensitizes colorectal cancer cells to (chemo-) radiotherapy. Carcinogenesis 32: 1824-1831.
66. Cui X, Oonishi K, Tsujii H, Yasuda T, Matsumoto Y, et al. (2011) Effects of carbon ion beam on putative colon cancer stem cells and its comparison with X-rays. Cancer Res 71: 3676-3687.
67. Gorski DH, Beckett MA, Jaskowiak NT, Calvin DP, Mauceri HJ, et al. (1999) Blockage of the vascular endothelial growth factor stress response increases the antitumor effects of ionizing radiation. Cancer Res 59: 3374-3378.
68. Li F, Sonveaux P, Rabbani ZN, Liu S, Yan B, et al. (2007) Regulation of HIF-1alpha stability through S-nitrosylation. Mol Cell 26: 63-74.
69. Moeller BJ, Cao Y, Li CY, Dewhirst MW (2004) Radiation activates HIF-1 to regulate vascular radiosensitivity in tumors: role of reoxygenation, free radicals, and stress granules. Cancer Cell 5: 429-441.
70. Hirst DG (1986) Oxygen delivery to tumors. Int J Radiat Oncol Biol Phys 12: 1271-1277.
71. Poskitt TR (1987) Radiation therapy and the role of red blood cell transfusion. Cancer Invest 5: 231-236.
72. Majumder PK, Febbo PG, Bikoff R, Berger R, Xue Q, et al. (2004) mTOR inhibition reverses Akt-dependent prostate intraepithelial neoplasia through regulation of apoptotic and HIF-1-dependent pathways. Nat Med 10: 594-601.
73. Honore S, Pasquier E, Braguer D (2005) Understanding microtubule dynamics for improved cancer therapy. Cell Mol Life Sci 62: 3039-3056.
74. Dumontet C, Jordan MA (2010) Microtubule-binding agents: a dynamic field of cancer therapeutics. Nat Rev Drug Discov 9: 790-803.
75. McKean PG, Vaughan S, Gull K (2001) The extended tubulin superfamily. J Cell Sci 114: 2723-2733.

76. Howell B, Larsson N, Gullberg M, Cassimeris L (1999) Dissociation of the tubulin-sequestering and microtubule catastrophe-promoting activities of oncoprotein 18/stathmin. Mol Biol Cell 10: 105-118.
77. Westermann S, Weber K (2003) Post-translational modifications regulate microtubule function. Nat Rev Mol Cell Biol 4: 938-947.
78. Muresan V, Muresan Z Unconventional functions of microtubule motors. Arch Biochem Biophys 520: 17-29.
79. Ricke RM, van Deursen JM Correction of microtubule-kinetochore attachment errors: mechanisms and role in tumor suppression. Semin Cell Dev Biol 22: 559-565.
80. Kapoor S, Panda D Kinetic stabilization of microtubule dynamics by indanocine perturbs EB1 localization, induces defects in cell polarity and inhibits migration of MDA-MB-231 cells. Biochem Pharmacol 83: 1495-1506.
81. Altmann KH, Wartmann M, O'Reilly T (2000) Epothilones and related structures--a new class of microtubule inhibitors with potent in vivo antitumor activity. Biochim Biophys Acta 1470: M79-91.
82. Bollag DM, McQueney PA, Zhu J, Hensens O, Koupal L, et al. (1995) Epothilones, a new class of microtubule-stabilizing agents with a taxol-like mechanism of action. Cancer Res 55: 2325-2333.
83. Kamath K, Okouneva T, Larson G, Panda D, Wilson L, et al. (2006) 2-Methoxyestradiol suppresses microtubule dynamics and arrests mitosis without depolymerizing microtubules. Mol Cancer Ther 5: 2225-2233.
84. Chen JG, Yang CP, Cammer M, Horwitz SB (2003) Gene expression and mitotic exit induced by microtubule-stabilizing drugs. Cancer Res 63: 7891-7899.
85. Jordan MA, Wendell K, Gardiner S, Derry WB, Copp H, et al. (1996) Mitotic block induced in HeLa cells by low concentrations of paclitaxel (Taxol) results in abnormal mitotic exit and apoptotic cell death. Cancer Res 56: 816-825.
86. Ogasawara M, Matsubara T, Suzuki H (2001) Screening of natural compounds for inhibitory activity on colon cancer cell migration. Biol Pharm Bull 24: 720-723.
87. Westerlund A, Hujanen E, Hoyhtya M, Puistola U, Turpeenniemi-Hujanen T (1997) Ovarian cancer cell invasion is inhibited by paclitaxel. Clin Exp Metastasis 15: 318-328.
88. Rowinsky EK, Eisenhauer EA, Chaudhry V, Arbuck SG, Donehower RC (1993) Clinical toxicities encountered with paclitaxel (Taxol). Semin Oncol 20: 1-15.
89. Rubin EH, Rothermel J, Tesfaye F, Chen T, Hubert M, et al. (2005) Phase I dose-finding study of weekly single-agent patupilone in patients with advanced solid tumors. J Clin Oncol 23: 9120-9129.
90. Gerth K, Bedorf N, Hofle G, Irschik H, Reichenbach H (1996) Epothilons A and B: antifungal and cytotoxic compounds from Sorangium cellulosum (Myxobacteria). Production, physico-chemical and biological properties. J Antibiot (Tokyo) 49: 560-563.
91. Nettles JH, Li H, Cornett B, Krahn JM, Snyder JP, et al. (2004) The binding mode of epothilone A on alpha,beta-tubulin by electron crystallography. Science 305: 866-869.
92. Gradishar W (2009) Management of advanced breast cancer with the epothilone B analog, ixabepilone. Drug Des Devel Ther 3: 163-171.
93. Fogh S, Machtay M, Werner-Wasik M, Curran WJ, Jr., Bonanni R, et al. (2010) Phase I trial using patupilone (epothilone B) and concurrent radiotherapy for central nervous system malignancies. Int J Radiat Oncol Biol Phys 77: 1009-1016.
94. Altmann KH, Pfeiffer B, Arseniyadis S, Pratt BA, Nicolaou KC (2007) The chemistry and biology of epothilones--the wheel keeps turning. ChemMedChem 2: 396-423.

95. Hofstetter B, Vuong V, Broggini-Tenzer A, Bodis S, Ciernik IF, et al. (2005) Patupilone acts as radiosensitizing agent in multidrug-resistant cancer cells in vitro and in vivo. Clin Cancer Res 11: 1588-1596.
96. Goldkorn T, Balaban N, Shannon M, Matsukuma K (1997) EGF receptor phosphorylation is affected by ionizing radiation. Biochim Biophys Acta 1358: 289-299.
97. Raben D, Helfrich B, Chan DC, Ciardiello F, Zhao L, et al. (2005) The effects of cetuximab alone and in combination with radiation and/or chemotherapy in lung cancer. Clin Cancer Res 11: 795-805.
98. Milas L, Mason K, Hunter N, Petersen S, Yamakawa M, et al. (2000) In vivo enhancement of tumor radioresponse by C225 antiepidermal growth factor receptor antibody. Clin Cancer Res 6: 701-708.
99. Huang SM, Harari PM (2000) Modulation of radiation response after epidermal growth factor receptor blockade in squamous cell carcinomas: inhibition of damage repair, cell cycle kinetics, and tumor angiogenesis. Clin Cancer Res 6: 2166-2174.
100. Krause M, Ostermann G, Petersen C, Yaromina A, Hessel F, et al. (2005) Decreased repopulation as well as increased reoxygenation contribute to the improvement in local control after targeting of the EGFR by C225 during fractionated irradiation. Radiother Oncol 76: 162-167.
101. Jain RK (2005) Normalization of tumor vasculature: an emerging concept in antiangiogenic therapy. Science 307: 58-62.
102. Winkler F, Kozin SV, Tong RT, Chae SS, Booth MF, et al. (2004) Kinetics of vascular normalization by VEGFR2 blockade governs brain tumor response to radiation: role of oxygenation, angiopoietin-1, and matrix metalloproteinases. Cancer Cell 6: 553-563.
103. Teicher BA, Holden SA, Ara G, Dupuis NP, Liu F, et al. (1995) Influence of an anti-angiogenic treatment on 9L gliosarcoma: oxygenation and response to cytotoxic therapy. Int J Cancer 61: 732-737.
104. Kozin SV, Boucher Y, Hicklin DJ, Bohlen P, Jain RK, et al. (2001) Vascular endothelial growth factor receptor-2-blocking antibody potentiates radiation-induced long-term control of human tumor xenografts. Cancer Res 61: 39-44.
105. Fenton BM, Paoni SF, Ding I (2004) Pathophysiological effects of vascular endothelial growth factor receptor-2-blocking antibody plus fractionated radiotherapy on murine mammary tumors. Cancer Res 64: 5712-5719.
106. Lee CG, Heijn M, di Tomaso E, Griffon-Etienne G, Ancukiewicz M, et al. (2000) Anti-Vascular endothelial growth factor treatment augments tumor radiation response under normoxic or hypoxic conditions. Cancer Res 60: 5565-5570.
107. Zips D, Hessel F, Krause M, Schiefer Y, Hoinkis C, et al. (2005) Impact of adjuvant inhibition of vascular endothelial growth factor receptor tyrosine kinases on tumor growth delay and local tumor control after fractionated irradiation in human squamous cell carcinomas in nude mice. Int J Radiat Oncol Biol Phys 61: 908-914.
108. Kim JC, Kim JS, Saha D, Cao Q, Shyr Y, et al. (2003) Potential radiation-sensitizing effect of semisynthetic epothilone B in human lung cancer cells. Radiother Oncol 68: 305-313.
109. Escuin D, Kline ER, Giannakakou P (2005) Both microtubule-stabilizing and microtubule-destabilizing drugs inhibit hypoxia-inducible factor-1alpha accumulation and activity by disrupting microtubule function. Cancer Res 65: 9021-9028.

3. Results

3.1. Dynamics of tumor hypoxia in response to patupilone and ionizing radiation

Katrin Orlowski[1], Carla Rohrer Bley[2], Martina Zimmermann[1], Van Vuong[1], Daniel Hug[1], Alex Soltermann[3], Angela Broggini-Tenzer[1], Martin Pruschy[1]

[1]Department of Radiation Oncology, University Hospital Zurich, Zurich, Switzerland
[2]Division of Radiation Oncology, Vetsuisse Faculty, University of Zurich, Zurich, Switzerland
[3]Department of Pathology, University Hospital Zurich, Zurich, Switzerland

Status of the manuscript: in revision for PLoS One

Author contribution K. Orlowski:
Planning, data acquisition, analysis and interpretation of all experiments, except for the performance of the experiment leading to figure 1D. Manuscript drafting, revision and editing.

Competing Interests: The authors have declared that no competing interest exist.

Financial Disclosure: This work was supported by the Swiss Cancer League, the Swiss National Science Foundation and the Vontobel-Stiftung (all to M.P.). The funders had no role in study design, data collection and analysis, decision to publish, or preparation of the manuscript.

Abstract

Tumor hypoxia is one of the most important parameters that determines treatment sensitivity, and is mainly due to insufficient tumor angiogenesis. However, the local oxygen concentration in a tumor can also be shifted in response to different treatment modalities such as cytotoxic agents or ionizing radiation. Thus, combined treatment modalities including microtubule stabilizing agents could create an additional challenge for an effective treatment response due to treatment-induced shifts in tumor oxygenation. Tumor hypoxia was probed over a prolonged observation period in response to treatment with different cytotoxic agents, using a non-invasive bioluminescent ODD-Luc reporter system, in which part of the oxygen-dependent degradation (ODD) domain of HIF-1α is fused to luciferase. As demonstrated *in vitro*, this system not only detects hypoxia at an ambient oxygen concentration of 1% O_2, but also discriminates low oxygen concentrations in the range from 0.2 to 1% O_2. Treatment of A549 lung adenocarcinoma-derived tumor xenografts with the microtubule stabilizing agent patupilone resulted in a prolonged increase in tumor hypoxia, which could be used as marker for its antitumoral treatment response, while irradiation did not induce detectable changes in tumor hypoxia. Importantly, despite patupilone-induced hypoxia, the potency of ionizing radiation (IR) was not reduced as part of a concomitant or adjuvant combined treatment modality.

Introduction

Hypoxia is one of the most important parameters that cause enhanced tumor aggressiveness and treatment resistance, and hypoxia is now considered to be an independent prognostic indicator of poor outcome for different tumor entities. Alternating periods of hypoxia and normoxia in the tumor support the selection of tumor cells with elevated mutation frequency with a more stress resistant and aggressive phenotype. Independent of the cellular genotype, hypoxic cells are more treatment resistant than normoxic cells, in particular towards ionizing radiation (IR). Irradiation of cells leads to the formation of reactive oxygen species (ROS), which induce cytotoxic DNA damage. Furthermore the oxygenation fixation theory implies that radiation-induced free radical sites in the DNA are chemically derivatized ("fixed") in the presence of oxygen so that they can not be repaired and accumulate, leading to an enhanced rate of cell death. Thereby normoxic cells are two- to three-fold more radiation sensitive than cells under hypoxia [1,2].

Tumor hypoxia is mainly caused by insufficient tumor angiogenesis and oxygen supply during tumor growth, however, the oxygen content in a tumor can also be shifted in response to different treatment modalities such as cytotoxic agents acting on the tumor vasculature. Therefore, the combination of cytotoxic agents, provoking an increase in tumor hypoxia, with ionizing irradiation may impact treatment efficiency. We previously investigated various combined treatment modalities with regard to changes in tumor hypoxia, e.g. VEGF-receptor tyrosine kinase inhibitors in combination with IR [3,4]. Furthermore the tumor- and tumor vasculature targeting, clinically relevant microtubule stabilizing agent (MSA) patupilone (epothilone B) induced an at least additive antitumoral effect when combined with IR [5,6] raising the question on the dynamics of patupilone-induced hypoxia and the combination scheduling with IR.

MSAs belong to the most important classes of anti-cancer agents with taxanes being approved for a broad range of indications including single treatment for non-small cell lung carcinoma or advanced breast cancer [7,8]. The epothilones are nontaxoid macrolide MSAs of bacterial origin, which share the same binding site on β-tubulin (in close proximity to residue Thr274) with taxanes [9,10,11]. Clinically different epothilone derivatives are currently in various stages of development as antitumor compounds [12]. Ixabepilone (Ixempra®) is the first approved compound in this class and indicated as monotherapy or in combination with capecitabine for the treatment of patients with metastatic breast cancer. Apart from a manageable safety profile, ixabepilone demonstrates anti-tumor activity after failure and resistance towards anthracycline and taxane standard therapy [13].

Epothilone B (patupilone) was tested as a phase III monotherapy agent against ovarian cancer and other epothilones are undergoing a wide spectrum of single and combined treatment modality in phase II studies (e.g. for recurrent glioblastoma, CNS metastases from breast cancer, prostate, cervical, renal cell, gastric and lung tumors, as well as non-Hodgkin's Lymphoma (www.cancer.gov) [13,14,15,16,17].

MSAs impair the dynamics of the microtubule network, leading to defective mitotic spindle formation and accumulation of cells in the G2/M-phase of the cell cycle [11,18] or at low concentrations to transient G1-and S-phase arrest [5,19], followed by apoptosis-induction [20]. An MSA-altered microtubule network also reduces the cellular migration and invasion capacity [21,22]. Furthermore the potential of MSAs to accumulate cells in the radiosensitive G2/M phase renders them potent sensitizers [23] for the combined treatment with ionizing radiation [5,6,24].

The hypoxia-inducible transcription factor HIF-1 is a heterodimer composed of an oxygen-sensitive alpha subunit and a constitutively expressed beta subunit. HIF-1 binds to the hypoxia response element (HRE) in the promoter region of diverse target genes such as VEGF and induces their expression [25]. Under normoxic conditions the alpha subunit is hydroxylated on proline402 and proline564 in the oxygen dependent degradation (ODD)-domain of HIF-1α by prolyl hydroxylase domain (PHD) proteins. Proline hydroxylation leads to the recognition by the von Hippel-Lindau tumor suppressor and subsequent ubiquitination and proteasomal degradation [26].

Tumor hypoxia has previously been probed using different luciferase-based bioimaging reporter constructs, which are either based on luciferase expression under the control of an HRE-based promoter system or on the fusion of extended or shorter ODD-domains to the reporter gene [27,28,29]. The HRE-based approach depends on intact HIF-signaling, however, several classes of antisignaling agents including microtubule stabilizing agents interfere with the activity of HIF-1-upstream elements or the direct expression of HIF-1, independent of the pO_2 [6,30,31,32,33,34]. We therefore did not use an HRE-based but a minimal ODD-based *in vivo*-bioimaging reporter approach, which demonstrated high sensitivity even in the range of low pO_2-levels, to serially probe the dynamics of tumor hypoxia in response and in relation to the antitumor effect of the microtubule stabilizing agent patupilone and ionizing radiation, alone and as part of the combined treatment modality.

Materials and Methods

Cell culture

The human colon carcinoma cell line HCT116 was obtained from Bert Vogelstein [35] and the lung adenocarcinoma cell line A549 from Susan Band Horwitz [36]. All cell lines were kept at 37ºC in 5% CO_2. The cell line HCT116 was grown in McCoy medium containing 10% (v/v) fetal bovine serum, 100 U/ml penicillin and 100 µg/ml streptomycin. The cell line A549 was grown in RPMI 1640 containing 10% (v/v) fetal bovine serum, 100 U/ml penicillin, 100 µg/ml streptomycin and 2 mM L-glutamine. Patupilone (epothilone B, EPO906) was provided by the chemistry department of Novartis Pharma AG (Basel, Switzerland).

Vector construction

The plasmid SV40-pGl4.27 was obtained by inserting the SV40 promoter of pGl3control (Promega Corporation, Madison, WI, USA), cut with the restriction enzymes KpnI and HindIII, into the pGl4.27 vector (Promega Corporation) containing the luciferase gene including a 3'PEST sequence for rapid degradation and turnover of the luciferase protein. An additional NarI restriction site was inserted in the pGL4.27 plasmid at position 174 by site directed mutagenesis. The ODD-domain of HIF-1α was amplified by PCR from the pcDHIF plasmid (kindly provided by R.Wenger) as described in Safran et al, 2005 [37]. The product was cloned into the pGL3 basic vector (by HindIII and NarI) and finally inserted into the SV40-pGl4.27 vector, containing the additional NarI-site, to obtain the vector construct SV40-ODD-pGl4.27. To obtain the plasmids SV40-pGL4.26 and SV40-ODD-pGL4.26, the SV40 promoter or the SV40-ODD sequence was subcloned from the respective pGL4.27 plasmids cut by KpnI and BsrG1 into the pGL4.26 backbone (Promega Corporation).

Stable transfection, reporter gene assay and Western blot analysis

HCT116 cells were stably transfected with the SV40-ODD-pGL4.27 plasmid and the A549 cells were stably transfected with the SV40-ODD-pGL4.26 or the SV40-pGL4.26 plasmid by lipofection (Lipofectamine™ 2000 system; Invitrogen, Carlsbad, CA, USA) following the manufacturer's instruction. Stable single clones of hygromycin selected pools were selected for the highest induction of luciferase activity after 8 hours of hypoxic conditions. The reporter gene assay was performed as described by Rohrer Bley et al, 2009 [6]. Hypoxic conditions were mimicked by the prolyl hydroxylase inhibitor dimethyloxalylglycine (DMOG) (Biomol GmbH, Hamburg, Germany) at a concentration of 0.25 mM or $CoCl_2$ (0.25 mM). Alternatively, cells were incubated under different pO_2 in the hypoxic chamber

(Invivo2 400 hypoxia workstation, Biotrace International, Bridgend, UK). Cells were allowed to attach for 8-10 hours before addition of patupilone. Hypoxic conditions were applied 24 hours after patupilone treatment and luciferase activity was determined 8 hours thereafter. Western blot analyses were performed as described by Rohrer Bley et al, 2011 [38].

Hypoxyprobe-1 immunofluorescence

A549 cells were seeded on glass cover slips and allowed to attach overnight. Medium was exchanged and cells were incubated with 150 µM hypoxyprobe-1 (HPI, Burlington, MA, USA) for 3.5 hours under normoxic or hypoxic conditions. Culture slides were washed with phosphate buffered saline (PBS), fixed in 4% formaldehyde for 10 minutes at RT. Cells were washed and permeabilized with 0.2% Triton X-100 buffer on ice for 10 minutes. Cells were washed and autofluorescence was quenched with 0.3 M glycin for 5 minutes. After preincubation with 3% BSA in PBS at RT for 30 minutes, cells were incubated with the fluorescein isothiocyanate (FITC)-labeled monoclonal antiHypoxyprobe-1 monoclonal antibody (mAb1) in 3% BSA/PBS, (HPI), at RT in the dark for 1 hour. DNA was counterstained with DAPI (1:2500 DAPI stock solution (1 mg/ml) in PBS Sigma) for 15 minutes at RT. Cells were finally washed with PBS. Images were captured by fluorescence microscopy using a CCD camera (Leica DM6000B equipped with Leica CTR6000).

Tumor xenograft in nude mice and application of treatment regimes

Stably transfected HCT116 cells (4 x 10^6) and A549 cells (7 x 10^6) were subcutaneously injected on the back of 4- to 8-week old athymic nude mice. Tumors were allowed to expand to a volume of 300 mm^3 (± 10%) or 200 mm^3 (± 10%) before treatment start. Tumor volumes were determined as described elsewhere [6]. The group sizes ranged from n = 7-12 for the HCT116-xenograft experiments, from n = 3-5 for the A549-Luc only and $CoCl_2$-control experiments, and n = 5-16 for all other experiments. Patupilone (dissolved in 30% PEG-300 / 70% saline) was applied i.v. at a concentration of 2 mg/kg and $CoCl_2$ (45 mg/kg, dissolved in saline) i.p after the first IVIS measurement (day 0). Control mice were treated i.v. or i.p. with saline. IVIS measurements were performed daily at the indicated time points. Fractionated irradiation (3 x 1 Gy on 3 consecutive days) was applied locally using a customized led shielding device with a Gulmay 200 kV X-ray unit at 1 Gy/min.

Statement of ethical approval

This study was performed in strict accordance with the recommendations in the Guide for the Care and Use of Laboratory Animals of the Swiss Cantonal Veterinary Authorities. The protocol was approved by the Committee of the Swiss Cantonal Veterinary Authorities (Permit Number: 136/2008 and 154/2011). All procedures and measurements were performed under isoflurane anesthesia, and every effort was made to minimize suffering.

In vivo bioluminescence imaging and analysis

Mice were i.p. injected with 150 mg/kg D-luciferin (CaliperLife Sciences, Hopkinton, MA, USA) (10 µl/g of a 15 mg/ml stock solution) prior to anesthesia. Sequential measurements of light emission were taken approx. 5 minutes after D-luciferin injection with the IVIS200 (CaliperLife Sciences). The measurement with the highest total flux in the respective region of interest (ROI) was used for the longitudinal survey.

Results

Establishment and evaluation of a highly sensitive *in vitro* and *in vivo* tumor hypoxia reporter system

To monitor changes in tumor hypoxia *in vivo*, a reporter gene system was constructed, which consists of an oxygen-dependent degradation (ODD)-domain fused 5' to the luciferase reporter gene (ODD-Luc). This construct is constantly expressed in cells under control of a minimal, hypoxia-independent, SV40-promoter to be rapidly degraded under normoxic conditions, and slightly differs from previously used ODD-based constructs [29,39]. The ODD-sequence derives from the originally-identified human oxygen-dependent degradation domain (ODD) of HIF-1α but includes only the sequence coding for aa530 to aa652. This shorter ODD includes proline564, which is hydroxylated under normoxia and thereby marked for ubiquitin-dependent degradation by the VHL-proteasome-pathway, but excludes the NO-sensitive Cys-residue at amino acid position 520 (corresponding to mouse HIF-1α aa533), which could lead to a hypoxia-independent stabilization of the reporter construct in the presence of tumor associated macrophages [39]. A luciferase reporter construct without an ODD and under control of the same SV40 promoter served as control system (Figure 1A).

Hypoxia-sensitivity of the ODD-luciferase reporter construct was probed in stably-transfected A549 non-small cell lung cancer cells under hypoxia and hypoxia-mimicking conditions using the specific prolyl hydroxylase domain (PHD) inhibitor dimethyloxalylglycine (DMOG) at non-toxic conditions. Western blot analysis of cell lysates derived from cells

incubated under normoxic and hypoxic conditions (0.2% O_2) or with DMOG (0.25 mM) revealed high hypoxia- and DMOG-dependent protein levels of the ODD-luciferase construct. Prolonged expression level of the construct was observed under permanent hypoxic conditions but the ODD-luciferase expression level decreased over time in DMOG-treated cells (Figure 1B). This might be due to a reduced potency of DMOG to constantly inhibit related PHDs. HIF-1α protein stability paralleled ODD-luciferase protein levels under these conditions but also decreased over time, most probably due to a previously described regulatory feedback mechanism [40]. An *in vitro* luciferase activity assay also clearly demonstrated a strong hypoxia and DMOG-dependent increase in luciferase activity in this stably transfected tumor cell line (Fig 1C).

The kinetics of ODD-luciferase activity was further investigated after cellular treatment with DMOG during a 22-hours time course experiment and demonstrated the highest fold-increase in ODD-luciferase activity 8-10 hours after PHD-inhibition, with a subsequent slow decrease of luciferase activity over time (Figure 1D). Keeping cells under hypoxia for 8 hours followed by full reoxygenation to aerated conditions resulted in a rapid decrease of luciferase activity within the first 20 minutes, to reach 50% of its activity under hypoxic conditions already 90 minutes after reoxygenation (Figure 1E).

To validate this non-invasive ODD-luciferase reporter system *in vivo*, we used cobalt salt $CoCl_2$, which also inhibits PHDs. $CoCl_2$ (0.25 mM) induced a time-dependent increase in HIF-1α and ODD-luciferase protein levels *in vitro* (Figure 2B), and cellular luciferase activity peaked 14 hours after addition of $CoCl_2$ (Figure 2A). Mice carrying tumor xenografts, which derived from ODD-Luc stably transfected A549 cells, were treated with $CoCl_2$ (45 mg/kg, i.p.), and luciferase activity in the tumor xenograft was determined 14, 22 and 38 hours after $CoCl_2$-treatment by *in vivo* bioimaging. Luciferase activity in the tumor xenografts reached a maximum of 2.5-fold induction at the 14 hour time point after treatment and returned to basal levels 38 hours after treatment start. In comparison, luciferase activity in placebo-treated control mice did not change over this 38 hour period (Figure 2C and D).

To determine the sensitivity of the luciferase reporter system towards different levels of hypoxia, stably-transfected A549 cells were incubated for 8 hours at 0.2, 0.5, 1 and 2% O_2. Interestingly, the luciferase activity constantly increased with cellular incubation at lower pO_2-levels. An 8-fold increase in luciferase activity from normoxia to 1% O_2 and a 2.8-fold increase in luciferase activity from 1% to 0.2% O_2 was observed, which indicate a high sensitivity towards different levels of hypoxia (Figure 3A).

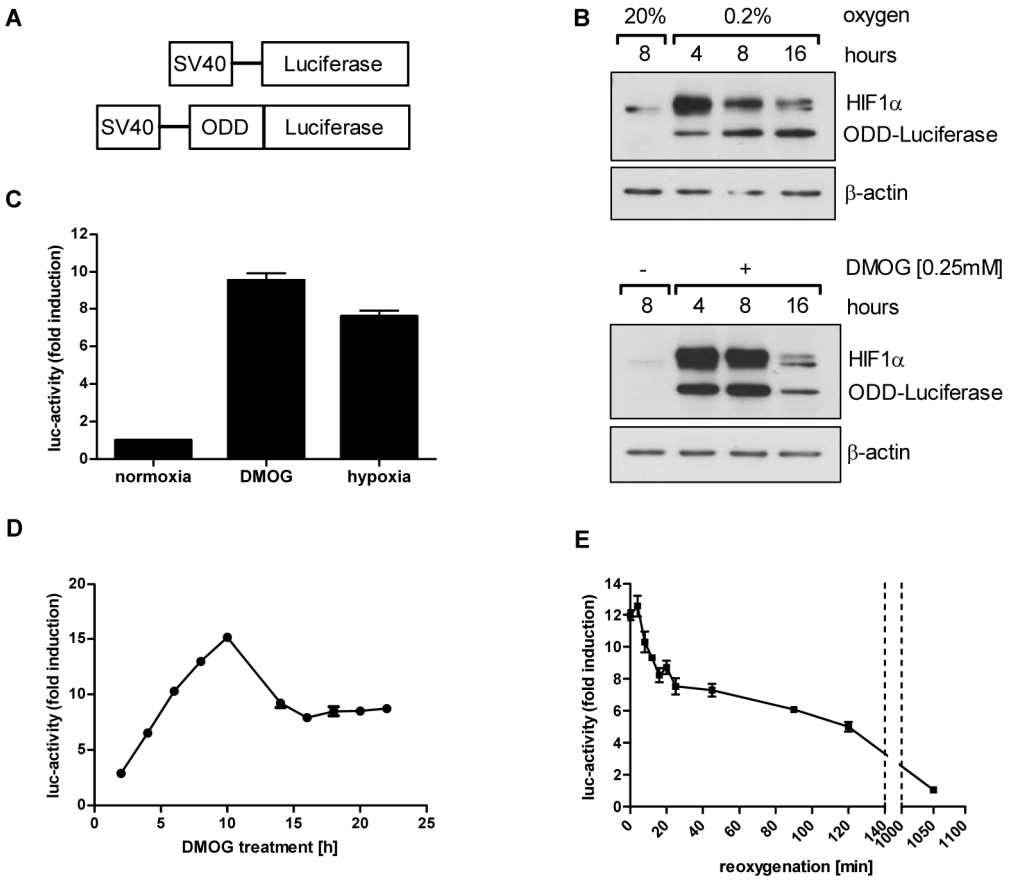

Figure 1. Oxygen-sensitive luciferase reporter system. (A) Scheme of luciferase constructs for constitutive (Luc) and oxygen-sensitive luciferase expression (ODD-Luc), containing a part of the oxygen-dependent degradation (ODD) domain of HIF-1α. Both constructs are under the control of a minimal SV40 promoter. (B) Protein levels of HIF-1α and ODD-luciferase in cellular extracts of stably transfected A549 cells, incubated for different time periods under normoxia, 0.2% O_2 or DMOG. (C) Luciferase activity in stably transfected ODD-Luc A549 cells. Cells were incubated for 8 hours under normoxia, DMOG or hypoxia. (D) Luciferase activity in DMOG-treated, stably transfected ODD-Luc A549 cells over a 22 hour period. (E) Luciferase activity in stably transfected ODD-Luc A549 cells kept for 8 hours under hypoxia and reoxygenated (time point 0 minutes) thereafter.

The bioreductive hypoxia marker pimonidazole forms stable adducts with thiol (sulphydryl) groups in proteins below the threshold of 10 mmHg pO_2, corresponding to approx. 1.5-2% O_2. To analyze whether different low levels of pO_2 can be distinguished from each other by an increased cellular accumulation of pimonidazole, A549 cells were incubated with pimonidazole (150 μM) under normoxia and various concentrations of pO_2 (0.2, 0.5, 1, 2 and 5% O_2) for 3.5 hours and stained with an FITC-labelled anti-pimonidazole antibody. The staining intensity of pimonidazole increased in a dose dependent way from normoxia to 2%

O_2, however no difference in the staining intensity could be detected below 1% O_2 (Figure 3B).

Overall these *in vitro* and *in vivo* results obtained with the non-invasive ODD-Luc-reporter approach demonstrate the high practicability and sensitivity to monitor dynamic changes in tumor hypoxia *in vitro* and *in vivo*.

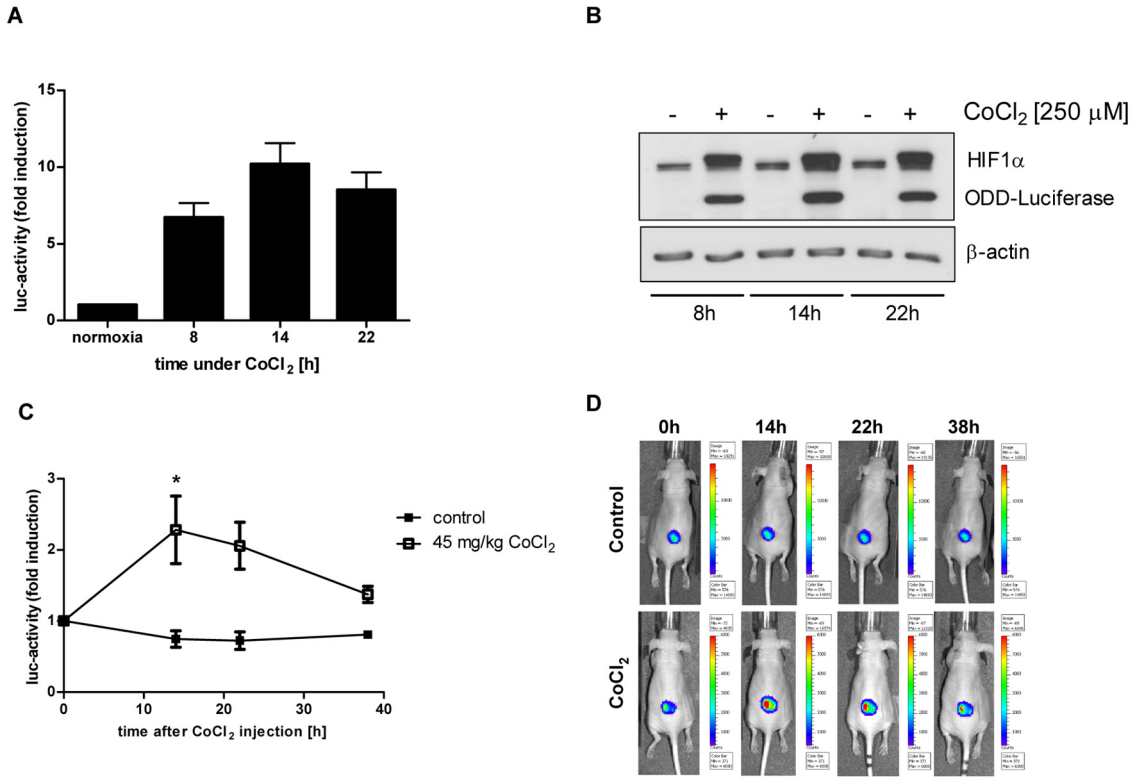

Figure 2. $CoCl_2$ increases luciferase activity in A549 ODD-Luc cells *in vitro* and *in vivo*. (A,B) Luciferase-activity (A) and HIF-1α, and ODD-luciferase protein levels (B) of $CoCl_2$ (0.25 mM)-treated, stably transfected ODD-Luc A549 cells, determined at the indicated time points. (C) Luciferase activity of A549 ODD-Luc-derived tumor xenografts in mice injected with $CoCl_2$ (45 mg/kg) at time point 0 hour and at the indicated time points thereafter. (D) Representative *in vivo* bioimages of untreated and $CoCl_2$-treated mice.

Changes in tumor hypoxia as marker for treatment response to cytotoxic agents

Using logistically-demanding non-invasive small animal positron emission tomography and classic invasive immunohistochemical approaches, we previously demonstrated that cytotoxic, anti-signaling and anti-angiogenic agents affect the tumor microenvironment and thereby tumor hypoxia [3]. In the intracellular signaling-based bioluminescence reporter system used in this report, which has been designed to investigate the dynamics of tumor hypoxia under different treatment modalities, the level of reporter gene expression and activity must be virtually independent of direct interference with the agent of interest (see

introduction). To control for such a putative, detrimental interference, luciferase activity in the human A549 lung adenocarcinoma and the human HCT116 colon adenocarcinoma cell line, both stably transfected with the ODD-Luc-construct, was determined *in vitro* on treatment with increasing concentrations of patupilone under normoxic and hypoxic conditions. Hypoxia strongly increased luciferase activity in both cells lines but cellular treatment with increasing concentrations of patupilone did not perturb luciferase activity significantly neither under normoxic nor hypoxic conditions (Figure 4A).

Having in hand a sensitive system to probe tumor hypoxia *in vivo,* the dynamics of tumor hypoxia in response to patupilone treatment was monitored over a prolonged observation period. Stably-transfected A549 ODD-Luc cells were subcutaneously injected on the back of nude mice and tumors were allowed to grow until a volume of 200 mm^3 +/-10 %. Mice were then treated with patupilone as a single dose (2 mg/kg, i.v.) and luciferase activity in control and patupilone-treated mice was determined over 10 days by *in vivo* bioimaging. The basal level of luciferase activity in A549 ODD-Luc xenografts was measured prior to patupilone injection and treatment-dependent changes in luciferase activity were further corrected for treatment-dependent changes in the tumor volume (see Material and Methods). A significant increase in luciferase activity already occurred on day 4 in tumor xenografts of mice treated with patupilone in comparison to placebo-treated mice and reached a maximal induction of luciferase activity at day 10 after treatment (5.2-fold versus 0.8-fold in control tumors) (Figure 4B). Patupilone-treatment also significantly inhibited tumor growth during this observation period (Figure 4B). Relative luciferase activity declined approximately 20 days after treatment, in mice probed over a prolonged time period (data not shown).

No substantial patupilone-induced tumor growth delay was observed in three patupilone-treated xenografted mice, and likewise, luciferase activity did not increase in these tumor xenografts. We could not explain the lack of responsiveness in these three mice, but more importantly they illustrate the correlation between the anti-tumoral effect of patupilone and the increase in intratumoral hypoxia in response to patupilone treatment (Figure 4C). Thus, increase in tumor hypoxia in response to patupilone treatment might serve as immediate surrogate marker for treatment sensitivity.

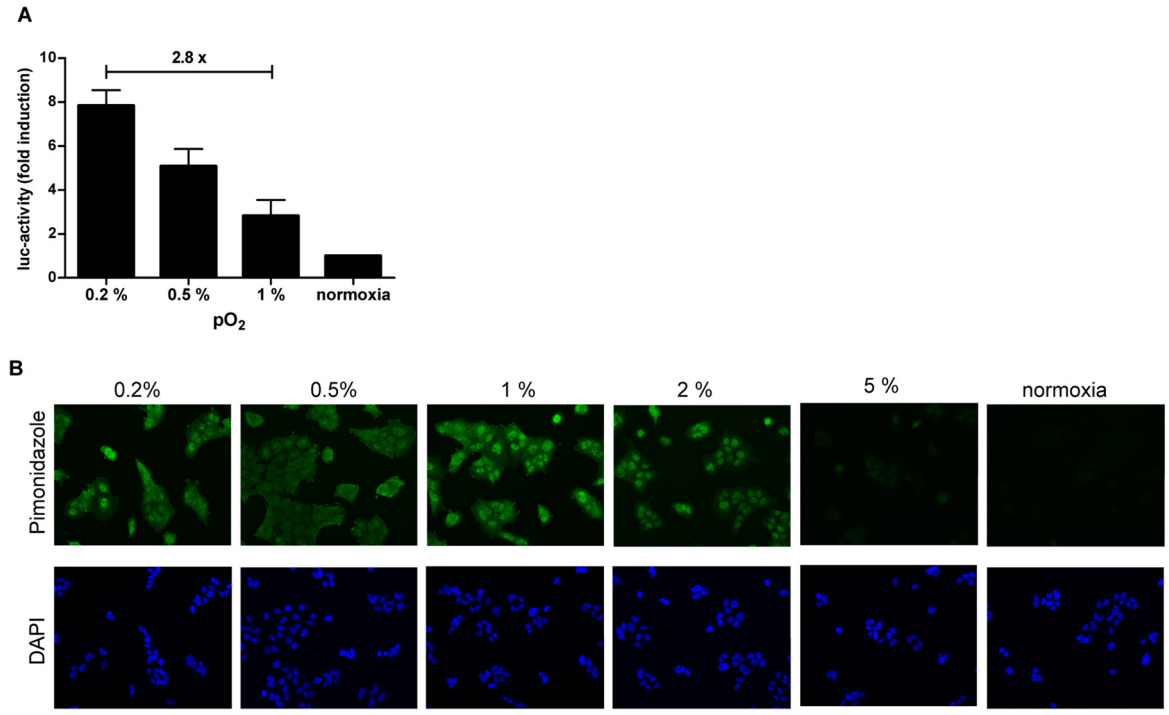

Figure 3. Differential sensitivity for low levels of pO_2 by ODD-luciferase and pimonidazole. (A) Luciferase activity in A549 ODD-Luc cells was determined after cellular incubation for 8 hours at different levels of hypoxia and normoxia. (B) Detection of pimonidazole accumulation in A549 cells incubated at different levels of hypoxia and normoxia. Images display immunocytochemistry staining of pimonidazole and DAPI for nuclear staining (magnification, x 300).

Control experiments were performed with tumor xenografts derived from A549 cells, which were stably-transfected with intact ODD-luciferase construct or a luciferase construct lacking an ODD-domain (Luc-only). With the latter construct, interference of patupilone with the SV40 promoter or with D-luciferin uptake and diffusion could be excluded. Tumors were allowed to grow until a volume of 200 mm^3 +/-10%, and mice were treated with either placebo or patupilone (2 mg/kg). Growth rate was similar for both A549 ODD-Luc and A549 Luc-only-derived tumor xenografts, and patupilone induced a comparable tumor growth delay for both tumor types. In contrast luciferase activity only increased after patupilone treatment in tumors derived from the ODD-Luc expressing A549 cells. These results further corroborate the specificity of the hypoxia-reporter construct to monitor treatment-related changes *in vivo* (Figure 4D).

To test for patupilone-increased tumor hypoxia in other tumor cell systems, the human colorectal adenocarcinoma cell line HCT116 was stably transfected with the ODD-Luc-construct and xenotransplanted in nude mice. HCT116 ODD-Luc derived tumors were allowed to grow to a volume of 300 mm^3, and mice were treated with placebo or a single dose

of patupilone (2 mg/kg). Tumor growth was strongly inhibited and luciferase activity also increased in this tumor model in response to patupilone treatment. However increase in luciferase activity already peaked on day 7 after patupilone treatment, though to a lesser extent in comparison to the A549-derived tumor system (Figure 4E). Histologic-morphologic analysis revealed a high percentage of necrosis (> 50%) in this tumor model, thus complicating tumor volume standardization. Therefore, further experiments were only performed with the A549-derived tumor model with a low level of tumor necrosis.

Tumor hypoxia is an important parameter for tumor radiosensitivity, and fluctuation of tumor hypoxia may influence the treatment response to radiotherapy. Short-term fractionated irradiation was therefore used as a second cytotoxic treatment modality to probe the dynamics of tumor hypoxia under treatment (Figure 5). A549 ODD-Luc-derived tumor xenografts with a small or a large tumor volume (200 mm^3 and 400 mm^3, respectively) were irradiated with a minimally fractionated treatment regimen of 3 x 1 Gy on 3 consecutive days and luciferase activity was determined during treatment and seven follow-up days. In the two control groups covering small and large tumor volumes, tumors steadily increased in size and volume-corrected luciferase activity did not change over time (Figure 5B and D). The minimal irradiation regimen suppressed tumor growth until day 8 after treatment start in the group of small tumors, and during the entire observation period in the group with large tumors (Figure 5A and C). Irradiation induced a slight increase in luciferase activity in both groups (1.5 to 1.7-fold), which remained stable in the group of large tumors but again decreased to basal level in the group of small tumors towards the end of the observation period. Interestingly, this drop of volume-corrected luciferase activity coincided with resumed tumor growth and remained at basal levels during subsequent tumor growth (data not shown).

A

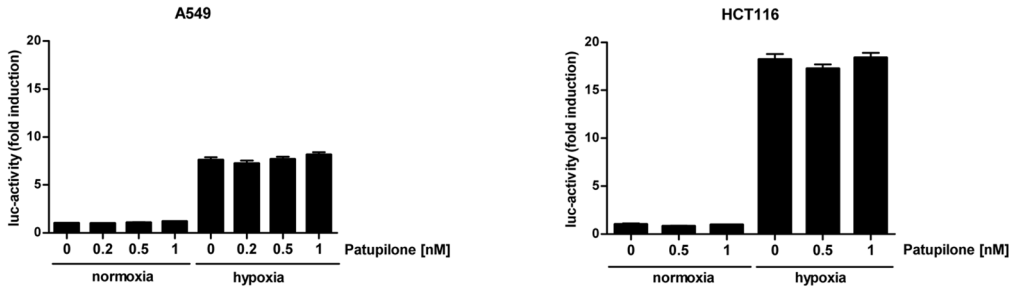
A549
HCT116
luc-activity (fold induction)
0 0.2 0.5 1 0 0.2 0.5 1
0 0.5 1 0 0.5 1
Patupilone [nM]
normoxia
hypoxia

B

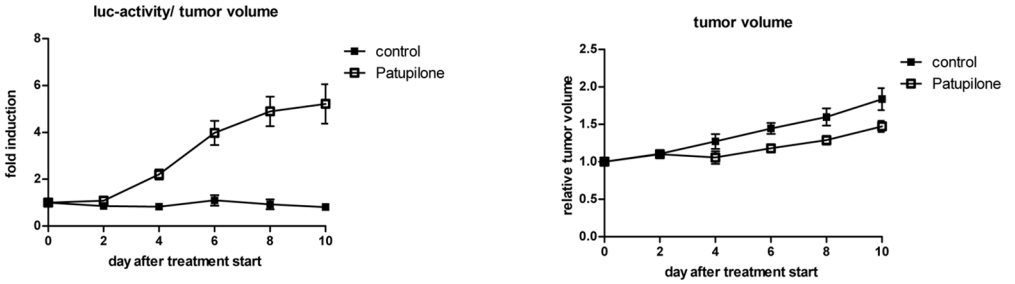
luc-activity/ tumor volume
tumor volume
fold induction
relative tumor volume
day after treatment start
control
Patupilone

C

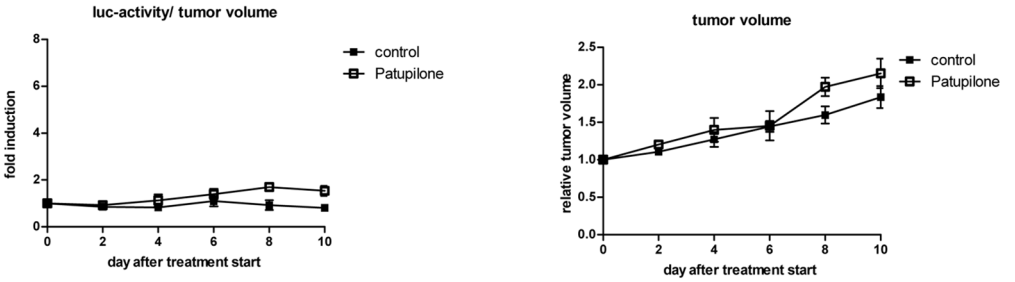
luc-activity/ tumor volume
tumor volume
fold induction
relative tumor volume
day after treatment start
control
Patupilone

D

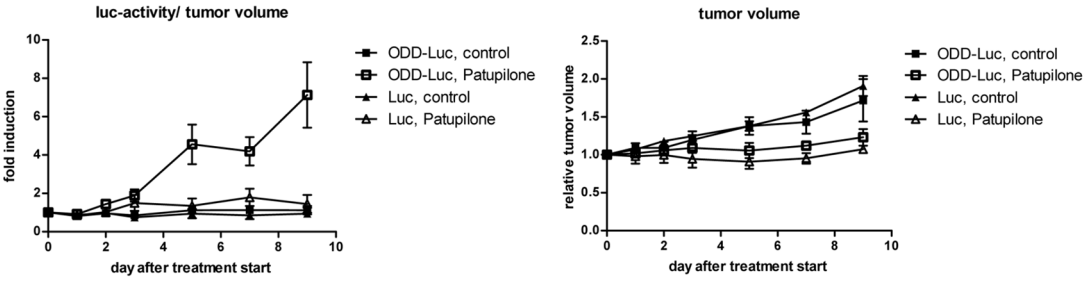
luc-activity/ tumor volume
tumor volume
fold induction
relative tumor volume
day after treatment start
ODD-Luc, control
ODD-Luc, Patupilone
Luc, control
Luc, Patupilone

E

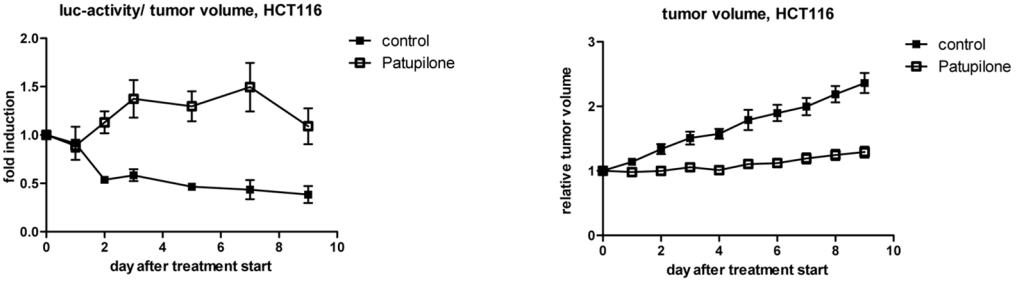
luc-activity/ tumor volume, HCT116
tumor volume, HCT116
fold induction
relative tumor volume
day after treatment start
control
Patupilone

Figure 4. Patupilone-dependent increase in tumor hypoxia *in vivo*. (A) Stably-transfected A549 ODD-Luc and HCT116 ODD-Luc cells were treated with increasing concentrations of patupilone for 24 hours before incubation under normoxia and hypoxia (0.2% O_2). Luciferase activity was determined after 8 hours of hypoxia. (B) Luciferase activity (left side) and tumor growth (right side) of A549 ODD-Luc-derived tumor xenografts in mice treated with patupilone (2 mg/kg). (C) Equal treatment as in (B) of mice not responding to patupilone treatment. (D) Luciferase activity and tumor growth of A549 ODD-Luc and A549 Luc-only-derived xenografts in mice treated with patupilone (2 mg/kg). (E) Luciferase activity and tumor growth of HCT116 ODD-Luc-derived xenografts in mice treated with patupilone (2 mg/kg).

Patupilone-induced hypoxia does not impair the radiation response

We previously investigated the combined treatment modality of patupilone and ionizing radiation and determined an at least additive treatment response on concurrent treatment on A549, SW480 colon carcinoma and D425Med medulloblastoma xenografts [5,6,41]. We now aimed to investigate the dynamics of tumor hypoxia, as indicated by changes in luciferase activity, in response to this combined treatment modality and to determine a putative counteractive effect of patupilone-induced tumor hypoxia on the radiation response. Therefore, A549 ODD-Luc-derived tumor xenografts were treated with different treatment schedules and luciferase-activity was monitored.

First, A549 ODD-Luc xenotransplanted mice at a small tumor volume (200 m^3) were treated with patupilone (2 mg/kg) and ionizing radiation (3 x 1 Gy) as part of a concomitant treatment regimen. In comparison to the intermediate treatment response to IR and patupilone alone (see above), the combined, concomitant treatment modality induced an additive tumor growth delay over the entire observation period. Interestingly, induction of luciferase activity in response to the combined treatment modality was similar to the increase in luciferase activity after patupilone-treatment alone and thus dominated over the effect on luciferase activity after irradiation (Figure 6A).

Next, A549-ODD-Luc xenotransplants were treated with placebo or patupilone alone (2 mg/kg) at a small tumor volume (200 mm^3) and were adjuvantly irradiated once the tumors reached a volume of 400 mm^3 +/- 10% (in control and patupilone-pretreated mice, which corresponds to the day of highest patupilone-induced luciferase activity). Irradiation of placebo-treated mice only resulted in a slight induction of luciferase-activity, while irradiation of patupilone-pretreated mice further enhanced the already elevated luciferase-activity twofold. Interestingly though, the IR-induced tumor growth delay was similar in the placebo- and the patupilone-pretreated mice, despite the elevated hypoxic status in the patupilone-pretreated tumors at the time point of irradiation (Figure 6B).

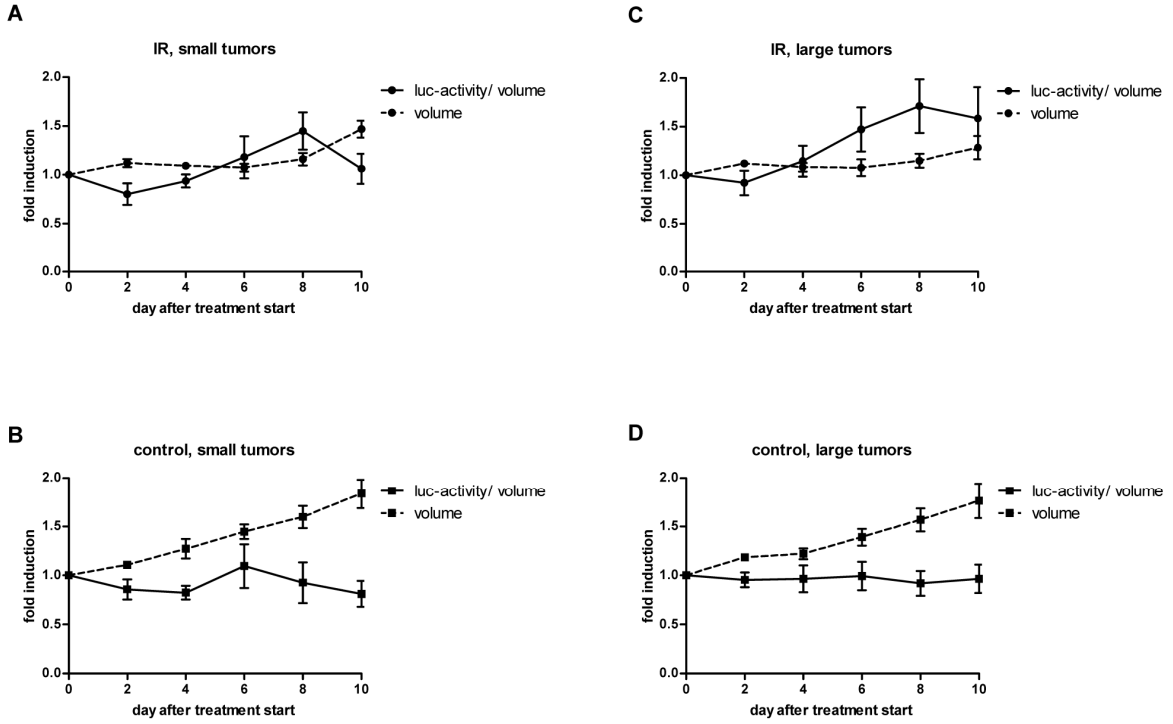

Figure 5. Minimal effect of ionizing irradiation on tumor hypoxia. Luciferase activity and tumor volume of A549 ODD-Luc-derived xenografts in control (B, D) and irradiated mice (A, C, 3 x 1 Gy) at a small (A, B, 200 mm^3) and at a large (C, D 400 mm^3) tumor volume at the day of treatment start. Fold induction of luciferase activity per tumor volume (solid line) and relative tumor volume (dotted line) were set to 1 at day 0.

Discussion

Radiosensitivity is progressively reduced when the pO_2 in a tumor is below 15-20 mmHg. pO_2 determination with invasive pO_2 electrodes revealed a strong correlation between low pO_2 (< 5-10 mmHg) prior treatment and locoregional control after radiotherapy in squamous cell cancer of the head and neck, uterine cervix and non-small cell lung carcinoma [42,43,44,45,46]. However, the dynamics of tumor microenvironmental parameters like hypoxia during treatment might even represent the better prognostic factor with regard to clinical outcome [47]. Furthermore tumor microenvironment-interfering agents might also negatively change tumor oxygenation and the hypoxic tumor fraction by itself, thereby affecting the treatment response to irradiation. Thus, a combined treatment modality might be challenged by new potential hazards created by the combination itself [3,6]. To address and investigate these processes and endpoints, non-invasive methods are required that allow serial determination of tumor hypoxia.

Here we established a non-invasive luciferase-based reporter system to serially probe tumor hypoxia, and determined the course of treatment-induced changes in tumor hypoxia in response to ionizing radiation and the clinically relevant microtubule stabilizing agent patupilone. The fusion construct luciferase linked to a minimal ODD-domain was stably expressed in tumor cells but rapidly degraded under normoxic conditions by the oxygen-sensing prolyl hydroxylases. This hypoxia-sensing approach was previously developed in mouse models, which express this fusion protein ubiquitously and even as an ODD-luciferase transgene in a spontaneous murine mammary carcinoma model [37,48]. Here we demonstrate that this approach could also be easily adapted to tumor xenografts in order to probe the effect of clinically relevant antitumor treatment modalities on tumor hypoxia. In contrast to HRE-based-luciferase hypoxia-reporting systems, the ODD-luciferase system with a minimal ODD-domain has the advantage to be robust against putative interference of agents of interest with the signaling cascade upstream of HIF-1, thereby avoiding false positive or negative readouts. Control experiments on the expression level of prolyl hydroxylase 2 and 3 in the A549 tumor cell line and in histological A549 ODD-Luc cell-derived tumor sections did not reveal treatment-induced changes, which might have influenced the reporter system (data not shown).

Our *in vitro* experiments revealed that the ODD-luciferase hypoxia reporter systems can be used to sense and differentiate decreasing pO_2-levels even as low as 0.2% O_2. Thus, this approach is more sensitive than pO_2-measurements with the hypoxia marker pimonidazole, which did not discriminate hypoxic milieus below 1.5% O_2, corresponding to 10 mmHg, or more sensitive than 18F-fluoromisonidazole (FMISO), which is used as hypoxia tracer for positron emission tomography in experimental tumor models and which has similar chemical properties as pimonidazole [49]. While the ODD-luciferase reporter system is highly sensitive to detect tumor hypoxia, unfortunately, the resolution of the *in vivo* bioimaging system is rather low. Therefore, only collective luminescence derived from the luciferase activity in the whole tumor could be determined, representing the mean tumor oxygenation status in the whole tumor. Thus, we could not distinguish between tumor areas with high or low tumor hypoxia and could not identify tumor-sections that are specifically prone to treatment-induced changes in tumor hypoxia. Future *in vivo* bioimaging approaches with improved resolution are required to overcome these drawbacks.

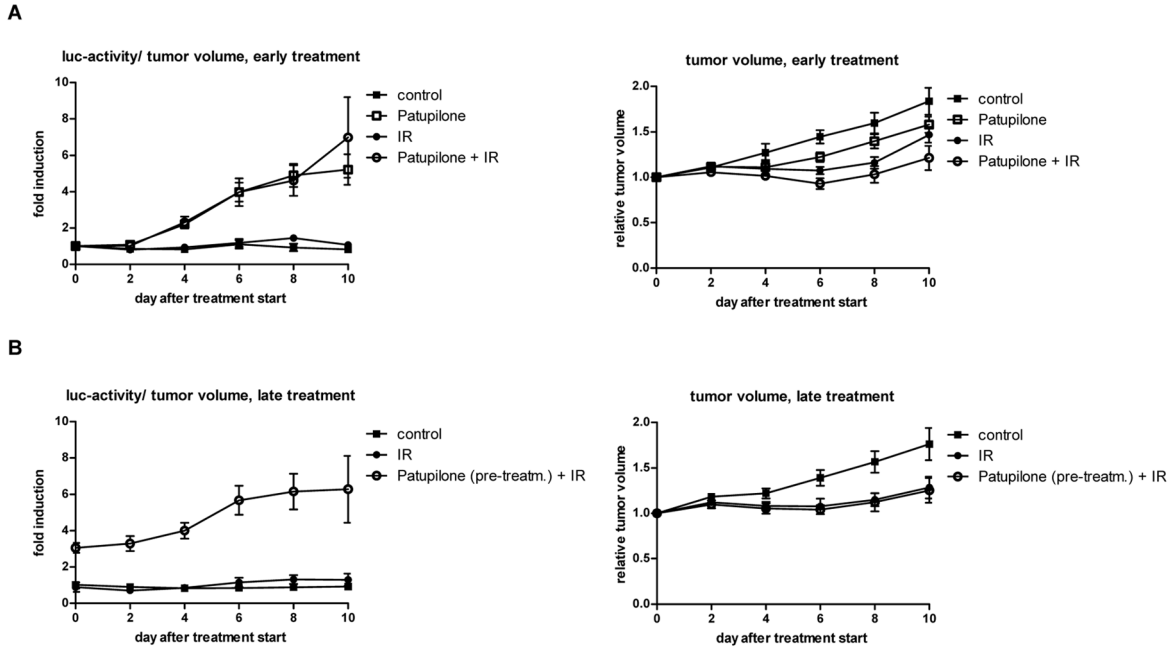

Figure 6. Tumor hypoxia in response to the combination of patupilone and ionizing radiation. (A) Luciferase activity and tumor growth of A549 ODD-Luc-derived xenografts in response to patupilone (2 mg/kg) and ionizing radiation (3 x 1 Gy) alone and in combination, treated at a tumor volume of 200 mm^3. (B) Luciferase activity and tumor growth of A549 ODD-Luc-derived xenografts in control and patupilone-pretreated mice irradiated at a tumor volume of 400 mm^3 (control) or 10 days after patupilone-pretreatment.

The dynamics of tumor hypoxia in tumor xenografts were probed in response to minimal fractionated irradiation and the microtubule stabilizing agent patupilone. Independent of the initial tumor volume, irradiation resulted in a transient tumor growth arrest with a slight increase in the hypoxic fraction (volume-corrected luciferase activity). A drop in the hypoxic tumor fraction 5 days after treatment end in tumors treated at a small tumor volume coincided with resumed tumor growth, which could be due to the recovery or normalization of the tumor vasculature. We previously demonstrated that the hypoxic fraction in response to low dose, fractionated irradiation changes only minimally, but that the tumor vasculature nevertheless may undergo structural changes (e.g. switch to intussusceptive angiogenesis) with full recovery only after extended tumor regrowth [3,50].

Single treatment with patupilone resulted in extended tumor growth arrest in both tumor models (A549, HCT116) and a strong, prolonged increase in the hypoxic tumor fraction. This correlation was accidentally confirmed in patupilone-non-responding animals on the level of tumor growth and tumor hypoxia. Thus, an increase in tumor hypoxia could represent an early surrogate marker for treatment sensitivity towards patupilone and likewise towards other microtubule stabilizing agents. However, we have only limited mechanistic insights how

patupilone affects tumor hypoxia. Patupilone has anti-angiogenic and vascular disruptive activity leading to reduced tumor blood volume, which finally could translate into enhanced tumor hypoxia [51]. Patupilone directly interferes with HIF-signaling, which eventually results in a diminished tumor hypoxia stress response. Using a genetically defined patupilone-sensitive and -resistant tumor model, we previously demonstrated that the major cytotoxic insult occurs on the tumor cell level, and that the anti-angiogenic effect of patupilone required patupilone-dependent blockage of pro-angiogenic cytokine expression and secretion from the targeted, patupilone-sensitive tumor cell, such as VEGF [6,38]. Here, histologic analysis of patupilone-treated tumors did not reveal a significant additional increase in pimonidazole-staining in comparison to the already intense pimonidazole-level for the A549 control tumors. This might be due to lack of correlation between HRE- or ODD-based bioimaging readouts and pimonidazole-staining, as already observed by others [27,52], or the already low pO_2-levels present in the control tumors, which does not allow anymore the use of pimonidazole to differentiate between treatment-dependent changes in pO_2-levels (see above).

Own studies revealed a supra-additive antitumoral effect of patupilone in combination with ionizing radiation, against tumor xenografts derived from different tumor cell lines [5,6,41]. We previously demonstrated that ionizing radiation counteracted an inhibitor-of-angiogenesis-induced increase in tumor hypoxia in tumor xenografts when used as part of a combined treatment modality and thereby counteracted the potential risk of enhanced radiation resistance by the inhibitor of angiogenesis [3]. Concomitant treatment of patupilone with ionizing radiation did not reduce the patupilone-dependent increase in tumor hypoxia. Nevertheless, combined treatment resulted in an enhanced tumor growth delay, which could be due to a synergistic insult to the tumor cell compartment and tumor vasculature. Interestingly, the hypoxic fraction in the patupilone-pretreated xenografts even increased after adjuvant irradiation, which might derive from persistent fragility of the tumor vasculature in patupilone-pretreated xenografts and subsequent further damage on irradiation. Nevertheless and despite the presence of an enhanced hypoxic tumor fraction in the patupilone pretreated xenografts, irradiation still induced a similar antitumoral effect in patupilone-pretreated xenografts as in naive xenografts with a lower hypoxic tumor fraction. However, we cannot rule out that a low, radiosensitizing level of patupilone might still be present at the timepoint of irradiation.

Overall, our results obtained with the two anticancer agents patupilone and ionizing radiation demonstrate, that the ODD-luciferase reporter system is a highly convenient, non-invasive approach to serially probe the dynamics of tumor hypoxia in murine tumor xenograft models.

Patupilone-induced increase in tumor hypoxia might be used as marker for patupilone sensitivity. Furthermore, scheduling-experiments of the treatment modality of patupilone in combination with ionizing radiation reveal that patupilone-induced tumor hypoxia does not enhance radiation resistance as part of a concomitant or neo-adjuvant treatment regimen.

Acknowledgments

We thank Roland Wenger for the pcDHIF plasmid, Silvia Behnke for excellent technical support and the Biologisches Zentrallabor of the University Hospital of Zurich for animal housing. We thank Susan Band Horwitz for the A549 cells and Bert Vogelstein for the HCT116 cells.

References

1. Chapman JD, Dugle DL, Reuvers AP, Meeker BE, Borsa J (1974) Letter: Studies on the radiosensitizing effect of oxygen in Chinese hamster cells. Int J Radiat Biol Relat Stud Phys Chem Med 26: 383-389.
2. Wachsberger P, Burd R, Dicker AP (2003) Tumor response to ionizing radiation combined with antiangiogenesis or vascular targeting agents: exploring mechanisms of interaction. Clin Cancer Res 9: 1957-1971.
3. Riesterer O, Honer M, Jochum W, Oehler C, Ametamey S, et al. (2006) Ionizing radiation antagonizes tumor hypoxia induced by antiangiogenic treatment. Clin Cancer Res 12: 3518-3524.
4. Oehler-Janne C, Jochum W, Riesterer O, Broggini-Tenzer A, Caravatti G, et al. (2007) Hypoxia modulation and radiosensitization by the novel dual EGFR and VEGFR inhibitor AEE788 in spontaneous and related allograft tumor models. Mol Cancer Ther 6: 2496-2504.
5. Hofstetter B, Vuong V, Broggini-Tenzer A, Bodis S, Ciernik IF, et al. (2005) Patupilone acts as radiosensitizing agent in multidrug-resistant cancer cells in vitro and in vivo. Clin Cancer Res 11: 1588-1596.
6. Bley CR, Jochum W, Orlowski K, Furmanova P, Vuong V, et al. (2009) Role of the microenvironment for radiosensitization by patupilone. Clin Cancer Res 15: 1335-1342.
7. Bonomi P, Kim K, Fairclough D, Cella D, Kugler J, et al. (2000) Comparison of survival and quality of life in advanced non-small-cell lung cancer patients treated with two dose levels of paclitaxel combined with cisplatin versus etoposide with cisplatin: results of an Eastern Cooperative Oncology Group trial. J Clin Oncol 18: 623-631.
8. Sparano JA (2000) Taxanes for breast cancer: an evidence-based review of randomized phase II and phase III trials. Clin Breast Cancer 1: 32-40; discussion 41-32.
9. Nettles JH, Li H, Cornett B, Krahn JM, Snyder JP, et al. (2004) The binding mode of epothilone A on alpha,beta-tubulin by electron crystallography. Science 305: 866-869.
10. Altmann KH, Pfeiffer B, Arseniyadis S, Pratt BA, Nicolaou KC (2007) The chemistry and biology of epothilones--the wheel keeps turning. ChemMedChem 2: 396-423.
11. Bollag DM, McQueney PA, Zhu J, Hensens O, Koupal L, et al. (1995) Epothilones, a new class of microtubule-stabilizing agents with a taxol-like mechanism of action. Cancer Res 55: 2325-2333.
12. Altmann KH, Wartmann M, O'Reilly T (2000) Epothilones and related structures--a new class of microtubule inhibitors with potent in vivo antitumor activity. Biochim Biophys Acta 1470: M79-91.
13. Gradishar W (2009) Management of advanced breast cancer with the epothilone B analog, ixabepilone. Drug Des Devel Ther 3: 163-171.
14. Fogh S, Machtay M, Werner-Wasik M, Curran WJ, Jr., Bonanni R, et al. Phase I trial using patupilone (epothilone B) and concurrent radiotherapy for central nervous system malignancies. Int J Radiat Oncol Biol Phys 77: 1009-1016.
15. Stupp R, Tosoni A, Bromberg JE, Hau P, Campone M, et al. Sagopilone (ZK-EPO, ZK 219477) for recurrent glioblastoma. A phase II multicenter trial by the European Organisation for Research and Treatment of Cancer (EORTC) Brain Tumor Group. Ann Oncol 22: 2144-2149.
16. Dumontet C, Jordan MA Microtubule-binding agents: a dynamic field of cancer therapeutics. Nat Rev Drug Discov 9: 790-803.
17. Melichar B, Casado E, Bridgewater J, Bennouna J, Campone M, et al. Clinical activity of patupilone in patients with pretreated advanced/metastatic colon cancer: results of a phase I dose escalation trial. Br J Cancer 105: 1646-1653.

18. Kamath K, Okouneva T, Larson G, Panda D, Wilson L, et al. (2006) 2-Methoxyestradiol suppresses microtubule dynamics and arrests mitosis without depolymerizing microtubules. Mol Cancer Ther 5: 2225-2233.
19. Chen JG, Yang CP, Cammer M, Horwitz SB (2003) Gene expression and mitotic exit induced by microtubule-stabilizing drugs. Cancer Res 63: 7891-7899.
20. Jordan MA, Wendell K, Gardiner S, Derry WB, Copp H, et al. (1996) Mitotic block induced in HeLa cells by low concentrations of paclitaxel (Taxol) results in abnormal mitotic exit and apoptotic cell death. Cancer Res 56: 816-825.
21. Ogasawara M, Matsubara T, Suzuki H (2001) Screening of natural compounds for inhibitory activity on colon cancer cell migration. Biol Pharm Bull 24: 720-723.
22. Westerlund A, Hujanen E, Hoyhtya M, Puistola U, Turpeenniemi-Hujanen T (1997) Ovarian cancer cell invasion is inhibited by paclitaxel. Clin Exp Metastasis 15: 318-328.
23. Pawlik TM, Keyomarsi K (2004) Role of cell cycle in mediating sensitivity to radiotherapy. Int J Radiat Oncol Biol Phys 59: 928-942.
24. Milas L, Saito Y, Hunter N, Milross CG, Mason KA (1996) Therapeutic potential of paclitaxel-radiation treatment of a murine ovarian carcinoma. Radiother Oncol 40: 163-170.
25. Wenger RH, Stiehl DP, Camenisch G (2005) Integration of oxygen signaling at the consensus HRE. Sci STKE 2005: re12.
26. Wenger RH (2002) Cellular adaptation to hypoxia: O2-sensing protein hydroxylases, hypoxia-inducible transcription factors, and O2-regulated gene expression. FASEB J 16: 1151-1162.
27. Lehmann S, Stiehl DP, Honer M, Dominietto M, Keist R, et al. (2009) Longitudinal and multimodal in vivo imaging of tumor hypoxia and its downstream molecular events. Proc Natl Acad Sci U S A 106: 14004-14009.
28. Harada H, Kizaka-Kondoh S, Itasaka S, Shibuya K, Morinibu A, et al. (2007) The combination of hypoxia-response enhancers and an oxygen-dependent proteolytic motif enables real-time imaging of absolute HIF-1 activity in tumor xenografts. Biochem Biophys Res Commun 360: 791-796.
29. Kim HA, Kim K, Kim SW, Lee M (2007) Transcriptional and post-translational regulatory system for hypoxia specific gene expression using the erythropoietin enhancer and the oxygen-dependent degradation domain. J Control Release 121: 218-224.
30. Escuin D, Kline ER, Giannakakou P (2005) Both microtubule-stabilizing and microtubule-destabilizing drugs inhibit hypoxia-inducible factor-1alpha accumulation and activity by disrupting microtubule function. Cancer Res 65: 9021-9028.
31. Lu Y, Liang K, Li X, Fan Z (2007) Responses of cancer cells with wild-type or tyrosine kinase domain-mutated epidermal growth factor receptor (EGFR) to EGFR-targeted therapy are linked to downregulation of hypoxia-inducible factor-1alpha. Mol Cancer 6: 63.
32. Harada H, Kizaka-Kondoh S, Li G, Itasaka S, Shibuya K, et al. (2007) Significance of HIF-1-active cells in angiogenesis and radioresistance. Oncogene 26: 7508-7516.
33. Carbonaro M, O'Brate A, Giannakakou P Microtubule disruption targets HIF-1alpha mRNA to cytoplasmic P-bodies for translational repression. J Cell Biol 192: 83-99.
34. Moeller BJ, Cao Y, Li CY, Dewhirst MW (2004) Radiation activates HIF-1 to regulate vascular radiosensitivity in tumors: role of reoxygenation, free radicals, and stress granules. Cancer Cell 5: 429-441.
35. Waldman T, Kinzler KW, Vogelstein B (1995) p21 is necessary for the p53-mediated G1 arrest in human cancer cells. Cancer Res 55: 5187-5190.

36. Chao SK, Lin J, Brouwer-Visser J, Smith AB, 3rd, Horwitz SB, et al. Resistance to discodermolide, a microtubule-stabilizing agent and senescence inducer, is 4E-BP1-dependent. Proc Natl Acad Sci U S A 108: 391-396.
37. Safran M, Kim WY, O'Connell F, Flippin L, Gunzler V, et al. (2006) Mouse model for noninvasive imaging of HIF prolyl hydroxylase activity: assessment of an oral agent that stimulates erythropoietin production. Proc Natl Acad Sci U S A 103: 105-110.
38. Rohrer Bley C, Orlowski K, Furmanova P, McSheehy PM, Pruschy M Regulation of VEGF-expression by patupilone and ionizing radiation in lung adenocarcinoma cells. Lung Cancer 73: 294-301.
39. Li F, Sonveaux P, Rabbani ZN, Liu S, Yan B, et al. (2007) Regulation of HIF-1alpha stability through S-nitrosylation. Mol Cell 26: 63-74.
40. Stiehl DP, Wirthner R, Koditz J, Spielmann P, Camenisch G, et al. (2006) Increased prolyl 4-hydroxylase domain proteins compensate for decreased oxygen levels. Evidence for an autoregulatory oxygen-sensing system. J Biol Chem 281: 23482-23491.
41. Oehler C, von Bueren AO, Furmanova P, Broggini-Tenzer A, Orlowski K, et al. The microtubule stabilizer patupilone (epothilone B) is a potent radiosensitizer in medulloblastoma cells. Neuro Oncol 13: 1000-1010.
42. Nordsmark M, Overgaard J (2004) Tumor hypoxia is independent of hemoglobin and prognostic for loco-regional tumor control after primary radiotherapy in advanced head and neck cancer. Acta Oncol 43: 396-403.
43. Brizel DM, Sibley GS, Prosnitz LR, Scher RL, Dewhirst MW (1997) Tumor hypoxia adversely affects the prognosis of carcinoma of the head and neck. Int J Radiat Oncol Biol Phys 38: 285-289.
44. Gatenby RA, Kessler HB, Rosenblum JS, Coia LR, Moldofsky PJ, et al. (1988) Oxygen distribution in squamous cell carcinoma metastases and its relationship to outcome of radiation therapy. Int J Radiat Oncol Biol Phys 14: 831-838.
45. Knocke TH, Weitmann HD, Feldmann HJ, Selzer E, Potter R (1999) Intratumoral pO2-measurements as predictive assay in the treatment of carcinoma of the uterine cervix. Radiother Oncol 53: 99-104.
46. Le QT, Chen E, Salim A, Cao H, Kong CS, et al. (2006) An evaluation of tumor oxygenation and gene expression in patients with early stage non-small cell lung cancers. Clin Cancer Res 12: 1507-1514.
47. Yaromina A, Kroeber T, Meinzer A, Boeke S, Thames H, et al. Exploratory study of the prognostic value of microenvironmental parameters during fractionated irradiation in human squamous cell carcinoma xenografts. Int J Radiat Oncol Biol Phys 80: 1205-1213.
48. Goldman SJ, Chen E, Taylor R, Zhang S, Petrosky W, et al. Use of the ODD-luciferase transgene for the non-invasive imaging of spontaneous tumors in mice. PLoS One 6: e18269.
49. Dubois L, Landuyt W, Haustermans K, Dupont P, Bormans G, et al. (2004) Evaluation of hypoxia in an experimental rat tumour model by [(18)F]fluoromisonidazole PET and immunohistochemistry. Br J Cancer 91: 1947-1954.
50. Hlushchuk R, Riesterer O, Baum O, Wood J, Gruber G, et al. (2008) Tumor recovery by angiogenic switch from sprouting to intussusceptive angiogenesis after treatment with PTK787/ZK222584 or ionizing radiation. Am J Pathol 173: 1173-1185.
51. Ferretti S, Allegrini PR, O'Reilly T, Schnell C, Stumm M, et al. (2005) Patupilone induced vascular disruption in orthotopic rodent tumor models detected by magnetic resonance imaging and interstitial fluid pressure. Clin Cancer Res 11: 7773-7784.

52. Viola RJ, Provenzale JM, Li F, Li CY, Yuan H, et al. (2008) In vivo bioluminescence imaging monitoring of hypoxia-inducible factor 1alpha, a promoter that protects cells, in response to chemotherapy. AJR Am J Roentgenol 191: 1779-1784.

3.2. Role of the Microenvironment for Radiosensitization by Patupilone

Carla Rohrer Bley,[1,2] Wolfram Jochum,[3] Katrin Orlowski,[1] Polina Furmanova,[1] Van Vuong,[1] Paul MJ. McSheehy,[4] Martin Pruschy[1]

[1]Department of Radiation Oncology, University Hospital Zurich, Zurich, Switzerland
[2]Section of Diagnostic Imaging and Radio-Oncology, Vetsuisse Faculty, University of Zurich, Zurich, Switzerland
[3]Department of Pathology, University Hospital Zurich, Zurich, Switzerland
[4]Novartis Institutes for BioMedical Research, Novartis Pharma AG, Basel, Switzerland

Status of the manuscript: published in Clin Cancer Res. 2009 Feb 15;15(4):1335-42.

Author contribution K. Orlowski:
Cloning of the luciferase vector used for the analysis of the HIF-transcriptome. Planning and data analysis of the luciferase assay leading to figure 5. Involved in proof-reading of the manuscript.

Running title: Patupilone and the tumor microenvironment

Key words: Patupilone, Ionizing Radiation, Angiogenesis, Hypoxia, Microtubules

DOI:10.1158/1078-0432.CCR-08-0969

Clinical Cancer Research

Role of the Microenvironment for Radiosensitization by Patupilone

Carla Rohrer Bley, Wolfram Jochum, Katrin Orlowski, et al.

Clin Cancer Res 2009;15:1335-1342. Published online February 19, 2009.

DOI:10.1158/1078-0432.CCR-08-0969

Role of the Microenvironment for Radiosensitization by Patupilone

Carla Rohrer Bley,[1,3] Wolfram Jochum,[2] Katrin Orlowski,[1] Polina Furmanova,[1] Van Vuong,[1] Paul M.J. McSheehy,[4] and Martin Pruschy[1]

Abstract

Purpose: The combined treatment modality of ionizing radiation (IR) and the clinically relevant microtubule-stabilizing compound patupilone (epothilone B, EPO906) is a promising approach for anticancer therapy. Here, we investigated the role of the tumor microenvironment for the supra-additive *in vivo* response in tumor xenografts derived from patupilone-sensitive and patupilone-resistant non-small cell lung cancer cells.

Experimental Design: The treatment response to a combined regimen of patupilone and IR was investigated *in vitro* and in tumor xenografts derived from wild-type A549 and A549.EpoB40 cells, which are resistant to patupilone due to a β-tubulin mutation.

Results: In both A549 and A549.EpoB40 cells, proliferative activity and clonogenicity were reduced in response to IR, whereas patupilone, as expected, inhibited proliferation of the mutant cell line with reduced potency. Combined treatment with patupilone and IR induced a cytotoxic effect *in vitro* in an additive way in A549 cells but not in the tubulin-mutated, patupilone-resistant A549.EpoB40 cells. A supra-additive tumor growth delay was induced by combined treatment in xenografts derived from A549 cells but not in xenografts derived from A549.EpoB40 cells. Histologic analysis revealed a significant decrease in tumor cell proliferation (Ki-67) and microvessel density and a treatment-dependent change of tumor hypoxia in A549 but not A549.EpoB40 xenografts.

Conclusions: Using a genetically defined patupilone-sensitive and patupilone-resistant tumor model, we here showed that the major cytotoxic effect of the combined treatment modality of IR and patupilone is directed against the tumor cell compartment. The induced antiangiogenic effect derives indirectly from the tumor cell.

Interference with microtubule function is a promising strategy for anticancer therapy (1). This approach has been extensively validated by the use of taxanes (microtubule stabilizers) for the treatment of a wide variety of human malignancies. The suppression of microtubule dynamics interferes with mitotic spindle formation, leading to cell cycle arrest in M phase and eventually to apoptosis or postmitotic cell death. The primary mechanism of microtubule-stabilizing agents (MSA) at the biochemical level is well investigated, but the signaling consequences relevant for their cytotoxic effect are far from clear. Furthermore, treatment with taxanes (paclitaxel and docetaxel) is limited by taxane-related toxicities and the development of multidrug resistance. This has prompted an ongoing worldwide search for novel microtubule-targeting compounds. One new class of MSAs are the epothilones, which are structurally distinct from the taxanes and may overcome some of their limitations, suggesting a promising new treatment approach for cancer (2–4).

Epothilones are nontaxoid MSA of bacterial origin, which share the same binding site on β-tubulin with taxanes (5, 6). One of the epothilones, patupilone (epothilone B, EPO906), is currently in phase II clinical development in several different solid tumors and is in phase III clinical trials for ovarian cancers in patients refractory to carboplatin-taxane treatment. Patupilone retains activity against P-glycoprotein-expressing multidrug-resistant cells both *in vitro* and *in vivo* (5) and shows different clinical toxicities to the taxanes (6, 7). Apart from the direct tumor-cytotoxic action, patupilone has also shown antivascular (8) and antiangiogenic (9) effects. The antiangiogenic effect might be linked to different mechanisms either directly targeting endothelial cells (10) or indirectly interfering with the secretion of proangiogenic agents from tumor cells (11, 12).

The accumulation of cells in the most radiosensitive G_2-M phase of the cell cycle represents the current rationale to combine MSAs with ionizing radiation (IR) and promises a strong radiosensitizing effect in combination with IR (2, 13, 14). Our own previous *in vitro* and *in vivo* experiments done with patupilone in combination with IR showed an at least additive cytotoxic effect in various cancer cell types *in vitro* and strong supra-additivity of the combined treatment regimen against tumor xenografts *in vivo*. Interestingly, also a S-phase

Authors' Affiliations: Departments of [1]Radiation Oncology and [2]Pathology, University Hospital Zurich; [3]Section of Radio-Oncology, Vetsuisse Faculty, University of Zurich, Zurich, Switzerland; and [4]Novartis Institutes for BioMedical Research, Novartis Pharma AG, Basel, Switzerland

Received 4/14/08; revised 10/23/08; accepted 11/14/08.

Grant support: Oncosuisse, Sassella, Novartis, and Swiss National Science Foundations (M. Pruschy).

The costs of publication of this article were defrayed in part by the payment of page charges. This article must therefore be hereby marked *advertisement* in accordance with 18 U.S.C. Section 1734 solely to indicate this fact.

Requests for reprints: Martin Pruschy, Department of Radiation Oncology, University Hospital Zurich, Raemistr. 100, CH-8091 Zurich, Switzerland. Phone: 41-44-255-8549; Fax: 41-44-255-4435; E-mail: martin.pruschy@usz.ch.

doi:10.1158/1078-0432.CCR-08-0969

DOI:10.1158/1078-0432.CCR-08-0969

Translational Relevance

Patupilone is a novel microtubule inhibitor with known antitumor and antiangiogenic/vascular activity currently in phase II/III clinical trials. Herein, we present first complementary *in vitro* and *in vivo* results investigating the role of the tumor microenvironment in the treatment response to the combination of ionizing radiation (IR) and patupilone. Using a genetically defined patupilone-sensitive and patupilone-resistant human non-small cell lung cancer tumor model system, we show that the major cytotoxic effect of the combined treatment modality of IR and patupilone is directed against the tumor cell compartment and that the induced antiangiogenic effect, which contributes to the synergistic treatment response of this combined treatment modality, derives indirectly from the tumor cell. These preclinical experiments are of relevance for clinical strategies that target the microtubule cytoskeleton and hypoxia-inducible factor dysregulation in combination with IR.

progression-related mechanism for radiosensitization was observed (15).

The observed *in vivo* supra-additive response to patupilone in combination with IR points to an additional mechanism of sensitization, which is not limited to the tumor cell but may also be due to effects on the microenvironment within the solid tumor (15).

Here, we investigated the different treatment modalities of patupilone and IR alone and in combination *in vitro* and *in vivo* using a patupilone-sensitive A549 cell line and the mutant derivative cell line (A549.EpoB40), which is strongly resistant to patupilone *in vitro* because it contains a defined β-tubulin mutation (3, 11, 16, 17). In this manner, we aimed to distinguish between a tumor cell and/or tumor microenvironment-directed effect of the different treatment modalities. Our results show a major tumor cell-directed effect with a subsequent indirect antiangiogenic effect especially by the combined treatment modality of patupilone in combination with IR.

Materials and Methods

Patupilone (epothilone B, EPO906) was provided by the Chemistry Department of Novartis Pharma. The human cell line pair A549 and A549.EpoB40 was obtained from the laboratory of Dr. Susan Band Horwitz.

Cell cultures, drug preparation, and irradiation. The human non-small cell lung cancer lines A549 and A549.EpoB40 were grown in RPMI 1640 containing 10% (v/v) fetal bovine serum, 1% (v/v) penicillin-streptomycin, and 1% (v/v) L-glutamine at 37°C in 5% CO_2. A549.EpoB40 is derived from A549 by stepwise selection with patupilone and contains a point mutation in class 1 β-tubulin (β292 from Gln to Glu), which is associated with ~95-fold resistance to patupilone (3). The A549.EpoB40 cell line was grown and maintained in medium containing 10 nmol/L patupilone. For *in vitro* experiments, patupilone was dissolved in DMSO (1 mmol/L stock solution) and further diluted with medium containing 10% FCS.

Irradiation of cell cultures was carried out using a Pantak Therapax 300 kV X-ray unit at 70 cGy/min at room temperature. For combined treatment, the cells were pretreated with patupilone 18 h before irradiation.

Cell proliferation and clonogenic survival assays. The proliferative activity of tumor cells was assessed in 96-well plates with the colorimetric alamarBlue assay, which is based on detection of metabolite activity according to the protocol of the manufacturer (Biosource International). Absorption was measured at 570 and 630 nm using a Tecan GENios spectrophotometer. Experiments were carried out under normoxic as well as hypoxic conditions. To render cells hypoxic, cells were grown in a hypoxic incubator at 1% pO_2. Clonogenic survival was determined by the ability of single cells to form colonies *in vitro*. The number of plated cells was adjusted to obtain ~100 colonies per cell culture dish with a given treatment. After treatment with different regimes, the dishes were maintained at 37°C in 5% CO_2 and allowed to grow for 12 days before fixation in methanol/acetic acid (3:1) and staining with crystal violet. Colonies with >50 cells/colony were counted manually. All assays were repeated as independent experiments at least thrice.

Tumor xenograft in nude mice and application of treatment regimes. A549 or A549.EpoB40 cells (4×10^6) were injected subcutaneously on the back of 4- to 8-week-old athymic nude mice. Tumor volumes were determined from caliper measurements of tumor length (L) and width (l) according to the formula: $(L \times l^2) / 2$. Tumors were allowed to expand to a volume of 200 mm^3 (±10%) before treatment start. Using a customized shielding device, mice were given a strictly locoregional radiotherapy of 4×3 or 3×1 Gy at 4 or 3 consecutive days using a Pantak Therapax 300 kV X-ray unit at 0.7 Gy/min. Patupilone (dissolved in 30% PEG-300/70% saline) was applied intravenously 24 h before the first treatment with IR (at day 0 of the treatment). Tumor growth was monitored at least thrice and body weight once weekly.

Histology and immunohistochemistry. Tissues were immersion fixed in 4% PBS-buffered formalin and embedded in paraffin. Sections (3 μm thick) were mounted on glass slides (SuperFrost Plus; Menzel), deparaffinized, rehydrated, and stained with H&E using standard histologic techniques. In addition, CC1 (antigen retrieval solution; Ventana Medical Systems)-pretreated sections were immunostained for Ki-67 (rabbit clone SP6; dilution 1:100; NeoMarkers), CD31 (rabbit polyclonal, ab28364; dilution 1:50; Abcam), and GLUT1 (rabbit polyclonal, MYM AB 1351; dilution 1:1,000; Chemicon International) using a Discovery immunohistochemistry staining system (Ventana Medical Systems). Detection of primary antibody was done with a biotinylated anti-rabbit IgG antibody (Jackson ImmunoResearch) and the iView DAB kit (Ventana Medical Systems). For hypoxia detection, pimonidazole hydrochloride (60-80 mg/kg) was applied intravenously 45 min before sacrifice. CC1-pretreated sections were incubated with Hypoxyprobe-1 MAb1 (mouse IgG1; dilution 1:300; Chemicon International) conjugated with FITC. Detection of primary antibody was done with a biotinylated mouse anti-FITC antibody (Jackson ImmunoResearch) and the iView DAB kit. All immunostains were counterstained with hematoxylin.

To determine proliferative activity, Ki-67-positive tumor cells were counted in 5 to 10 randomly chosen visual fields (magnification ×200) in each xenogaft ($n = 4$ for each group). The mean Ki-67-positive cell count from these fields was determined. Microvessel density (MVD) was determined in 5 to 10 randomly chosen visual fields (high-power fields) in each of three equally treated vital tumor tissues at ×100 magnification (0.3 mm^2 visual field size). Hypoxia staining was quantified by manual counting using a grid of 1,200 points in two photographs per tumor, which displayed the whole tumor section.

Transfections and reporter gene assay. Both cell lines were stably transfected with a vector construct containing two copies of the Transferrin promoter hypoxia response element (HRE) and SV40 promoter in front of the firefly luciferase gene. Stably transfected, hygromycin-selected A549 and A549.EpoB40 cell lines were tested for luciferase enzymatic activity with a commercial kit (Bright-Glo luciferase assay; Promega) using a GloMax 20/20 luminometer. Hypoxic conditions were mimicked using dimethyloxaloylglycine (Biomol), a prolyl-4-hydroxylase inhibitor, which prevents hypoxia-inducible

DOI:10.1158/1078-0432.CCR-08-0969

factor (HIF) degradation at prior tested nontoxic concentrations of 0.25 and 1 mmol/L, respectively. To discriminate between treatment-induced cell death and treatment-interfered HIF signaling, cells were transiently cotransfected with a *Renilla* luciferase-expressing control vector. Patupilone was applied 24 h after transient transfection. Dimethyloxaloylglycine treatment was started 24 h and irradiation (5 Gy) 28 h after patupilone treatment. Luciferase activity was determined 14 h after treatment with dimethyloxaloylglycine.

Statistical analysis. Statistical analysis of the *in vivo* tumor growth data was done with the Mann-Whitney *U* test. The absolute tumor growth delay was defined as the time for tumor volume in the treated groups to triplicate the initial treatment size minus the time in the untreated control group to reach the same size. Kruskal-Wallis one-way ANOVA was used to test for significant differences of Ki-67, CD31, and hypoxia following the various treatments. Treatments effects (difference between control and treatments) were analyzed using the Mann-Whitney *U* test. The level of significance was set at 0.05. The calculations were all done using the StatView program (SAS Institute) version 5.0.1.

Results

Antiproliferative effect of patupilone under normoxic and hypoxic conditions. The antiproliferative effect of patupilone was tested over 72 h in the A549 wild-type and A549.EpoB40 mutant cell lines under normoxic and hypoxic conditions. A dose-dependent decrease of the proliferative activity was observed in the A549 tumor cells (IC_{50} ~0.2 nmol/L), whereas a >100-fold higher concentration (>20 nmol/L) was required to obtain the same antiproliferative effect in the mutant A549.EpoB40 cell line. No difference with regard to the antiproliferative effect by patupilone was observed under normoxia and under hypoxia (1% pO_2; Fig. 1A and B).

Antiproliferative and clonogenic cell death-inducing effect by combined treatment with patupilone and IR. The antiproliferative effect of patupilone in combination with IR was tested using increasing concentrations of patupilone and doses of IR. In the patupilone-sensitive A549 cell line, an additive antiproliferative effect was induced with 5 Gy, a dose that shows <50% inhibition of proliferation over 72 h in response to irradiation alone (Fig. 2A and B). No radiosensitizing effect could be detected in the drug-resistant A549.EpoB40 cell line at various doses of patupilone and IR. Interestingly, these cells were also slightly more radioresistant than the wild-type counterpart cell line (Fig. 2C and D). Patupilone was also highly potent against human umbilical vein endothelial cells. Picomolar concentrations of patupilone were sufficient to inhibit endothelial cell proliferation and cell viability alone and in combination with IR (data not shown). Clonogenic survival assays were done with both cell lines and increasing concentrations of patupilone and IR. Clonogenicity was reduced in an at least additive way in the A549 cell population. In contrast, the mutant cell line A549.EpoB40 was refractory to patupilone alone up to 10 nmol/L, and patupilone did not sensitize for IR (Fig. 2E and F).

Effect of combined treatment with patupilone and IR on growth of tumor xenografts. We previously observed a supra-additive effect of a combined patupilone/IR treatment on tumor growth delay in xenografts derived from radioresistant SW480 human colon adenocarcinoma cells (15). In the tumor xenografts derived from the wild-type A549 cell line, a small growth delay was induced by 3 × 1 Gy irradiation compared with untreated control tumors. Growth was significantly inhibited by patupilone (1 × 2 mg/kg) treatment alone ($P = 0.022$). In response to the combined treatment modality, a supra-additive tumor growth delay was observed. Tumor growth in the combined treatment group was significantly inhibited compared with IR- or patupilone-treated groups ($P = 0.010$ and 0.013; Fig. 3A). The absolute growth delay to triple the initial tumor volume at the start of treatment (200 mm^2 ± 10%) was most enhanced with the combined treatment modality when compared with the absolute tumor growth delay in response to patupilone or IR alone [26 days (patupilone + IR) versus 6 days (patupilone) and 2 days (IR)], respectively (data not shown). In contrast, no tumor growth delay was induced by the same dose of patupilone in tumors derived from the drug-resistant A549.EpoB40 cells, indicating that the tumor growth suppression effect of patupilone primarily derives from tumor cell-directed cytotoxicity (Fig. 3B). The tumors derived from the mutated cell line were also more radiation-resistant than the wild-type counterparts. Nevertheless, a treatment regimen of 4 × 3 Gy alone induced a significant growth delay in tumors derived from these cells ($P = 0.004$). On the other hand, combined treatment did not further increase the antitumor effect, and even a slightly diminished absolute tumor growth delay was observed after combined treatment versus treatment

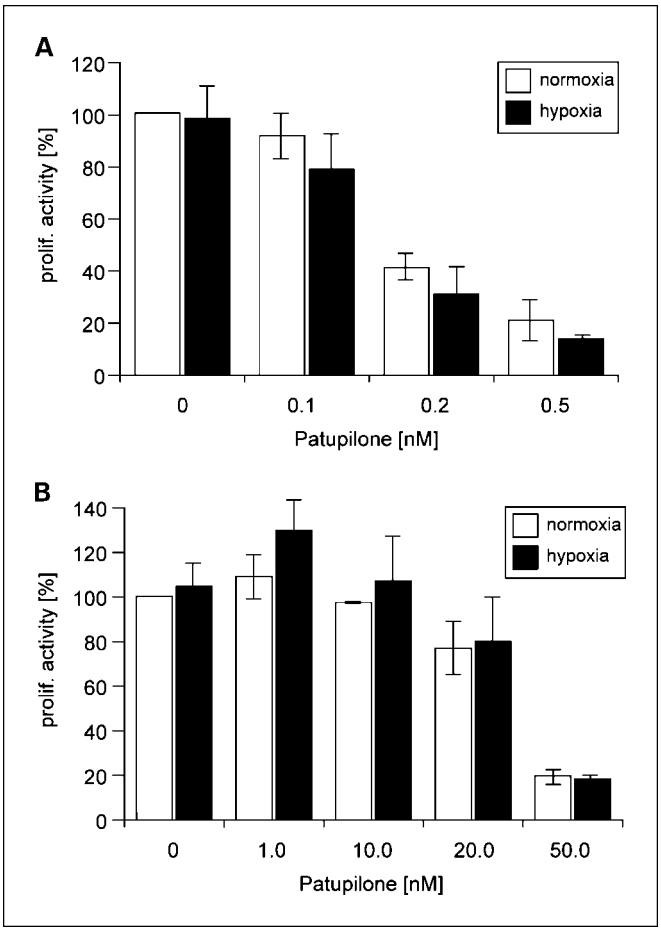

Fig. 1. Antiproliferative effect of patupilone under normoxia and hypoxia. Lung adenocarcinoma cells A549 (*A*) and mutant cells A549.EpoB40 (*B*) were exposed to increasing concentrations of patupilone and grown in normoxic or hypoxic conditions (1%) for 72 h. Data were pooled from three independent experiments. *Columns,* mean; *bars,* SE.

DOI:10.1158/1078-0432.CCR-08-0969

with IR alone [14 days (IR) versus 9 days (patupilone + IR); data not shown]. These results indicate that the major antitumor effect of the investigated treatment modality derives from tumor cell-directed cytotoxicity. A direct antiangiogenic effect of patupilone alone or in combination with irradiation is unlikely to contribute to the observed tumor growth delay. Determination of body weight changes only revealed a minor patupilone-dependent transient weight loss over 48 h after treatment

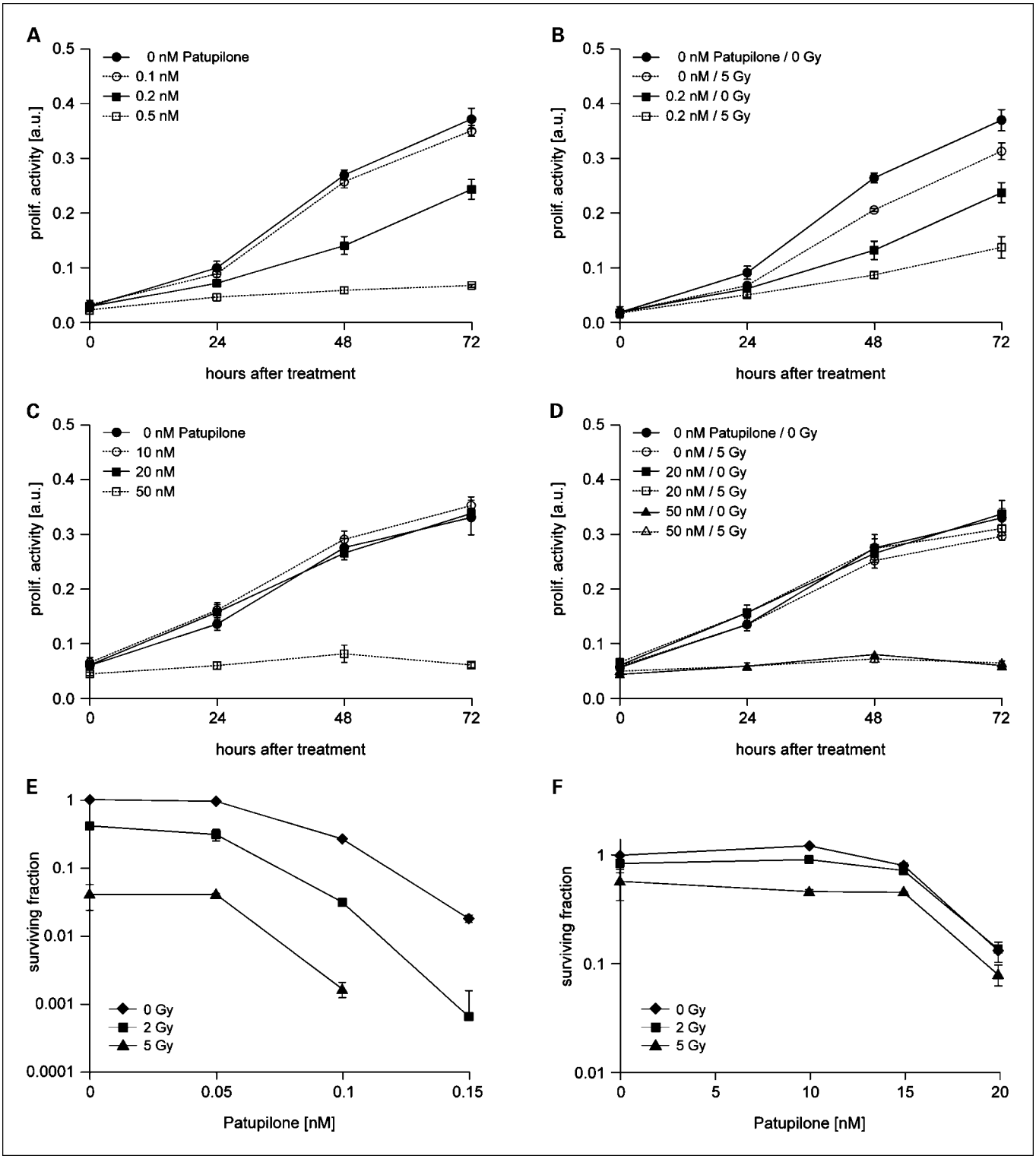

Fig. 2. Antiproliferative effect of patupilone alone and in combination with IR (5 Gy). Lung adenocarcinoma cells A549 (*A* and *B*) and mutant cells A549.EpoB40 (*C* and *D*) were exposed to increasing concentrations of patupilone and IR. Clonogenic survival after treatment with patupilone and IR was determined for A549 cells (*E*) and mutant A549.EpoB40 cells (*F*) treated with patupilone 18 h before irradiation.

DOI:10.1158/1078-0432.CCR-08-0969

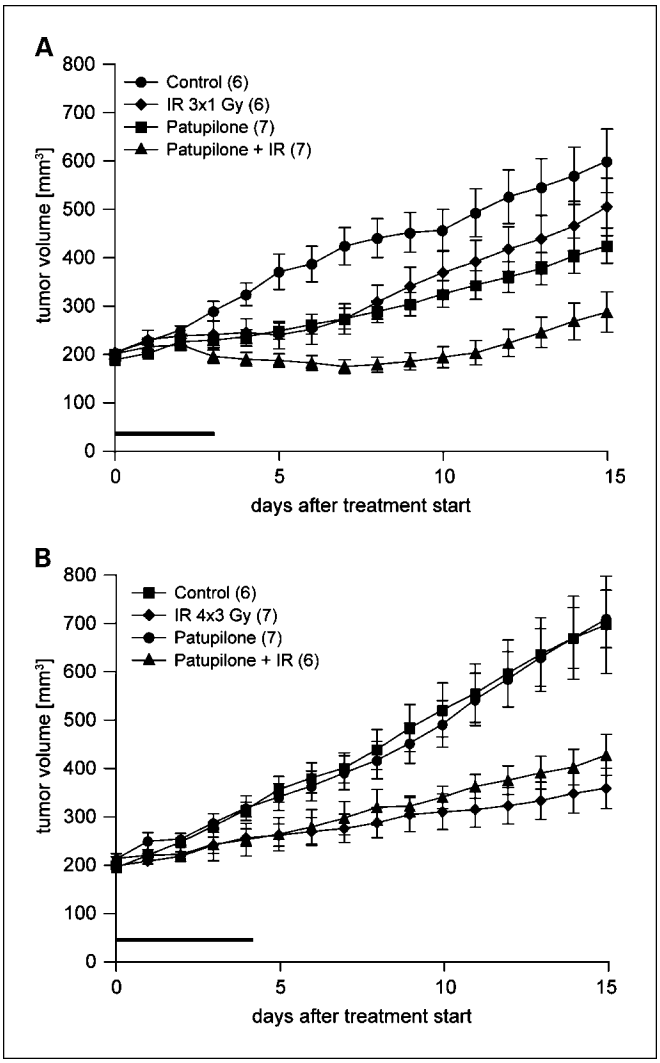

Fig. 3. Effect of patupilone and IR alone or in combination on the growth of A549-derived (*A*) and A549.EpoB40-derived (*B*) xenografts in nude mice. Mice were treated with patupilone (2 mg/kg once) and IR (3 × 1 or 4 × 3 Gy on consecutive days) alone and in combination, with administration of patupilone or the vehicle 24 h before the first fraction of IR. *Horizontal column,* days of treatment. Mean ± SE tumor volume per group.

initiation. No skin changes or tissue damage were observed in the coirradiated healthy tissue area around the tumor.

Histologic analysis of treatment-induced effects in tumor xenografts. To investigate a putative antiangiogenic effect of the different treatment modalities, MVD, tumor hypoxia, and proliferative status were determined in tumor sections of treated mice, which were collected 84 h after treatment with patupilone (2 mg/kg) or vehicle alone, after fractionated irradiation (3 × 1 or 3 × 3 Gy, respectively) or the combined treatment modality. Histologic analysis was first done on xenografts without any treatment to compare baseline characteristics of A549 and A549.EpoB40 xenografts. Xenografts of both A549 and A549.EpoB40 cells showed solid growth of carcinoma cells with areas of necrosis and thin stromal septa.

Tumor cell proliferation was determined using immunohistochemistry for the Ki-67 protein, which is expressed during all phases of the cell cycle, except G_0. In the tumors derived from the drug-sensitive A549 cell line, the proliferative activity was reduced by 32% 84 h after treatment with patupilone alone, whereas irradiation and the combined treatment reduced the proliferative activity by 54% and 71%, respectively ($P < 0.0001$). No change in the proliferative activity could be detected in A549.EpoB40-derived tumor sections after patupilone treatment. Irradiation reduced the proliferative activity by 22% ($P < 0.0001$), without any further effect in the combined treatment group (Fig. 4A and B). To examine the effect of the different treatment modalities on the tumor vasculature, MVD was determined by CD31 immunohistochemistry. Patupilone reduced the MVD in the drug-sensitive tumors by 25% at the 84 h time point when compared with control tumors ($P = 0.0003$). Irradiation and combined treatment reduced the MVD by 37% and 47%, respectively ($P < 0.0001$). In the drug-resistant tumors, a tendency in MVD reduction was only observed in the irradiated group ($P = 0.074$; Fig. 4C and D).

Treatment-induced changes of the tumor vasculature may also affect the pO_2 in the tumor tissue. We therefore determined treatment-dependent changes of tumor oxygenation by injection of the hypoxia probe pimonidazole, which specifically accumulates in hypoxic tissue areas. Treatment-dependent changes of hypoxic areas were determined in histologic sections 84 h after treatment. A significant increase of pimonidazole accumulation was determined in A549-derived tumors after treatment with patupilone ($P = 0.0019$), whereas the amount of hypoxic, pimonidazole-positive areas was reduced in the irradiated group ($P = 0.0045$). Interestingly, the amount of hypoxic areas was similar to untreated tumors after treatment with patupilone in combination with IR ($P = 0.747$). No change of pimonidazole accumulation was observed in any of the treatment groups in A549.EpoB40-derived tumor sections (Fig. 4E and F). These results indicate that changes in the tumor microenvironment in response to the different treatment modalities mainly derive from the treatment effect directed against the tumor cells (see below).

Treatment-interfered expression of hypoxia-induced gene expression. The HIF represents the major determinant in tumor cells for hypoxia-regulated expression of proangiogenic factors and patupilone reduced the level of the hypoxia-sensitive HIF-1α subunit under hypoxic conditions in the patupilone-sensitive A549 cell line as determined by Western blotting (data not shown). Using a reporter gene assay where luciferase expression is under the control of multiple HREs, the treatment response of patupilone and IR alone and in combination was quantitatively assessed in the patupilone-sensitive and patupilone-resistant cell lines. To normalize for transfection efficacy and cell numbers, cells were cotransfected with the *Renilla* luciferase-expressing vector system. To mimic hypoxic conditions, cells were incubated in dimethyloxaloylglycine, thereby up-regulating the endogenous HIF level and inducing luciferase expression 8.5-fold over control conditions (data not shown). Treatment of the patupilone-sensitive A549 cells with increasing doses of the MSA significantly reduced luciferase expression already at subnanomolar concentrations ($P = 0.010$). Of note, the A549.EpoB40 cells were resistant up to low nanomolar concentrations of patupilone (20 nmol/L), indicating a role of microtubule interference in HIF-1α-regulated gene expression (Fig. 5A). Treatment of cells with increasing doses of irradiation only minimally affected luciferase expression (data not shown). Treatment with increasing doses of patupilone in combination with IR (5 Gy) additionally

DOI:10.1158/1078-0432.CCR-08-0969

decreased luciferase expression (P = 0.018) in the A549 cell line, indicating a increased stress response on the level of hypoxia-regulated gene expression (Fig. 5B).

Discussion

Here, we investigated the treatment response of tumor xenografts derived from MSA-sensitive and MSA-resistant lung adenocarcinoma cell lines to treatment with patupilone and IR alone or in combination. We previously identified a strong treatment response to this combined treatment modality *in vivo* in the SW480 human colon xenograft model, which strongly exceeded the additive cytotoxic effect of the treatment combination *in vitro* (15). By means of this genetically defined tumor model, we now were able to differentiate between a direct tumor cell-directed and a microenvironment-directed

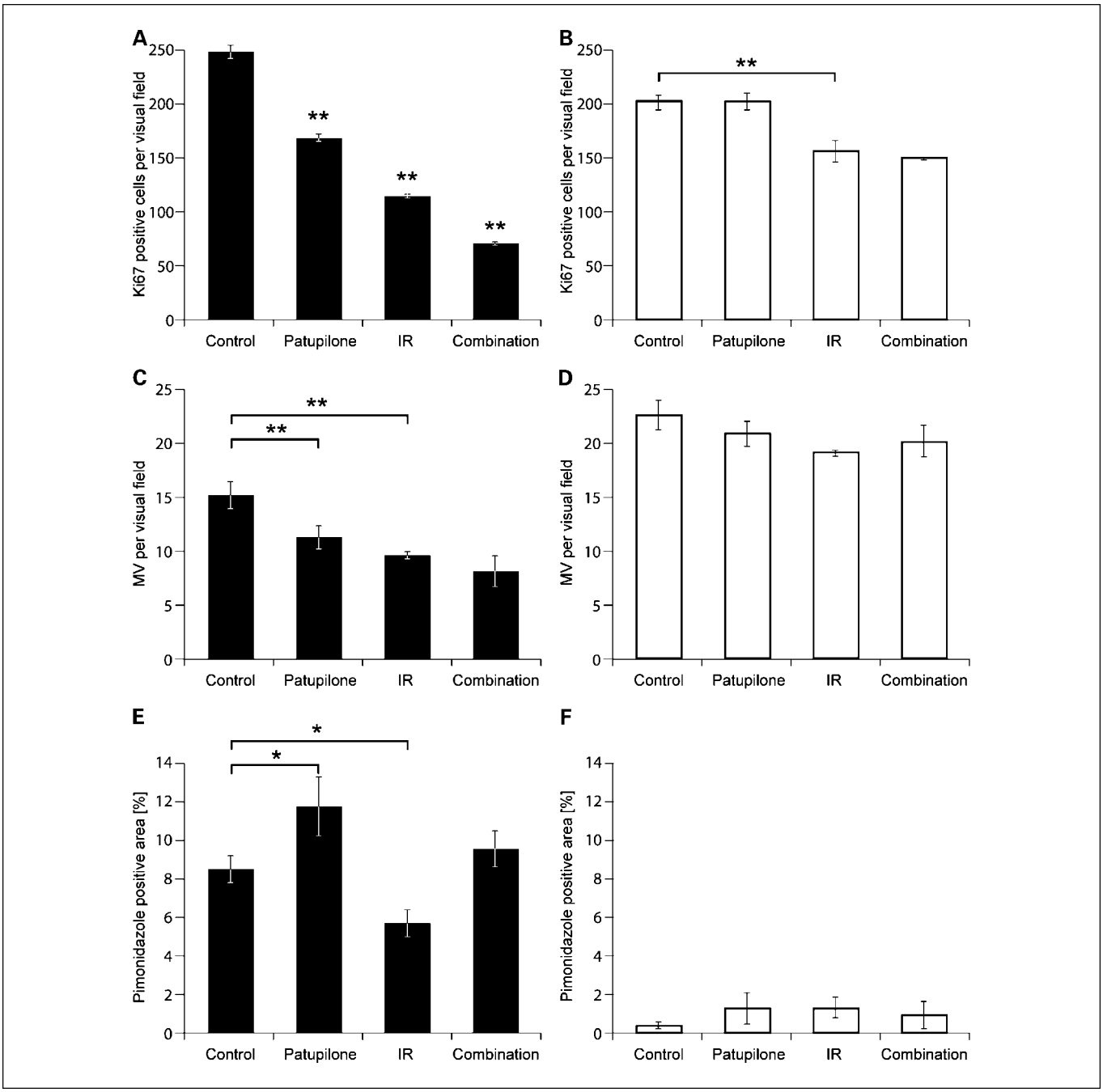

Fig. 4. Tumor cell proliferation, MVD, and changes in tumor hypoxia in response to treatment. Mice with A549-derived (*A, C*, and *E*) and A549.EpoB40-derived (*B, D*, and *F*) xenografts were treated with vehicle, patupilone (2 mg/kg), IR (3 × 1 and 3 × 3 Gy, respectively), or a combination of patupilone and IR. Mice were sacrificed 84 h after treatment and tumors were harvested, formalin fixed, and stained for the Ki-67 (*A* and *B*), CD31 as marker of tumor cell proliferation and MVD (*C* and *D*), and antibodies against the exogenous hypoxia marker pimonidazole hydrochloride for the immunohistochemical detection of tumor hypoxia (*E* and *F*), respectively. Mean ± SE value per group. *, $P < 0.01$; **, $P < 0.001$.

DOI:10.1158/1078-0432.CCR-08-0969

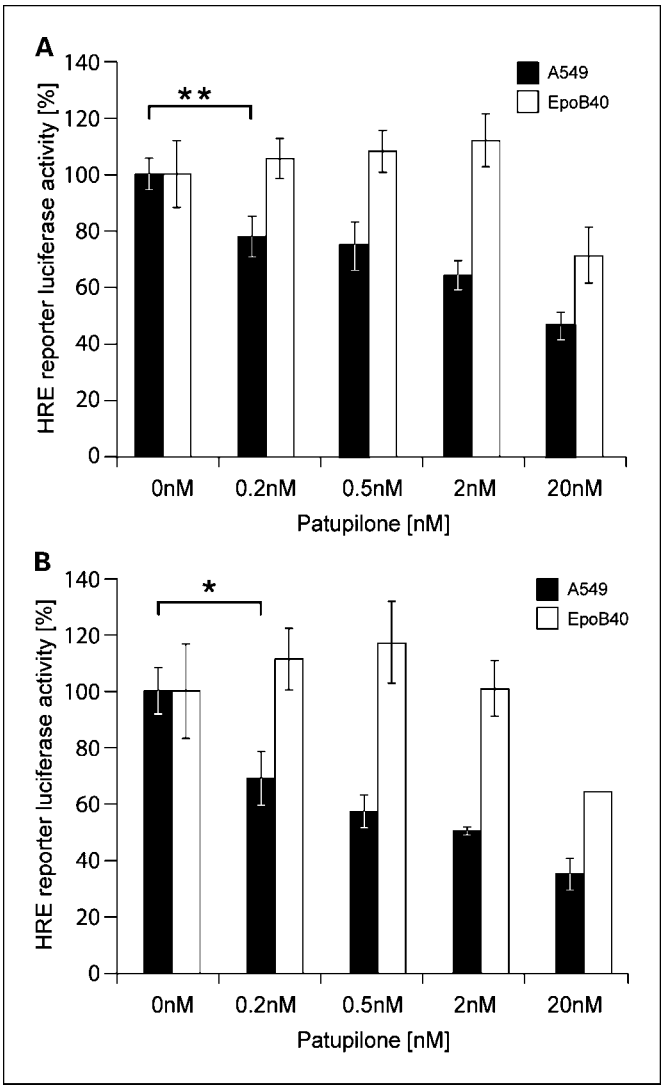

Fig. 5. Patupilone reduces HRE-dependent luciferase expression. A549 and A549.EpoB40 cells stably transfected with a pGL4.27 HRE vector (3× HRE-VEGF promoter for firefly-luciferase expression) and the pRL SV40 vector (*Renilla* luciferase) were treated with increasing doses of patupilone (*A*) and in combination with IR (5 Gy; *B*) under normal and hypoxia mimicking conditions. The cells were tested for luciferase reporter activity 24 h after patupilone treatment. Mean ± SE value per group. *, $P < 0.01$; **, $P < 0.001$.

cytotoxic *in vivo* effect in response to the different treatment modalities.

We observed a cytotoxic and tumor growth delay effect in the tumors derived from the MSA-sensitive adenocarcinoma cell line A549 in response to irradiation and patupilone alone and a supra-additive response to combined treatment. As expected, patupilone reduced the proliferative activity of the MSA-resistant cell line A549.EpoB40 *in vitro* only at >100-fold the concentration necessary for the wild-type cell line (3, 18). As determined here in this report, no tumor growth delay could be observed *in vivo* with treatment of patupilone alone and no enhancement of an IR effect was induced on combined treatment in tumors derived from the MSA-resistant cell line. Of note, patupilone induced an antiangiogenic response with reduced MVD and enhanced hypoxia in the wild-type but not MSA-resistant tumors.

The wild-type A549 cell line was also more sensitive to treatment with increasing doses of IR than A549.EpoB40 cells, which carry a specific Gln-to-Glu mutation at residue 292 in the M loop of β-tubulin and which changes the affinity of β-tubulin to the MSA (3). We cannot exclude that additional mutations are present in the patupilone-resistant cells, but most likely the known β-tubulin mutation not only reduces the affinity to patupilone but also affects microtubule dynamics, which may subsequently render the cells more radiation resistant. Importantly, the proliferative activity and growth kinetics of untreated cells or tumors derived from the two different cell lines were similar. An increased radiation resistance was present in the patupilone-resistant tumor cells and not in the sensitive ones and thus still enabled to investigate the involvement of the tumor microenvironment in response to the combined treatment modality of IR with patupilone.

The potent antiangiogenic activity of MSAs was proposed to be a major mechanism leading to the successful anticancer activity of this class of compounds (9, 11, 19, 20). Patupilone has an antiproliferative and apoptosis-inducing effect in microvascular and macrovascular endothelial cells (9) and our own *in vitro* experiments done with primary human umbilical vein endothelial cells confirmed the high potency of patupilone against this cell type (data not shown). Patupilone also induces vascular disruption leading to reduced tumor blood volume (8). We showed previously an at least additive antitumor effect by the combined treatment of IR with different inhibitors of angiogenesis, such as the VEGF receptor tyrosine kinase inhibitor PTK787 or the dual receptor tyrosine kinase inhibitor AEE788 (21, 22). Based on the putative direct antiangiogenic property of patupilone, a partial tumor growth delay effect was expected on treatment with patupilone alone or in combination with IR even in tumors derived from the patupilone-resistant tumor cells (A549.Epo40). However, treatment with neither patupilone alone nor in combination with IR reduced tumor growth or increased tumor growth delay, respectively, in A549.Epo40-derived tumors.

A strong reduction in MVD and change in tumor hypoxia on treatment with patupilone alone was only detected in tumors derived from the A549 wild-type cells and not in tumors derived from the patupilone-resistant tumor cells. Despite direct *in vitro* cytotoxicity against endothelial cells (9), our results indicate that the antiangiogenic effect of patupilone *in vivo* is indirectly induced by interference on the level of the tumor cellular stress response. Our *in vitro* experiments done with the hypoxia-regulated reporter gene assay clearly showed that patupilone reduces the expression of the HIF-1 "transcriptome" such as VEGF and other genes involved in angiogenesis and hypoxic adaptation but only in patupilone-sensitive tumor cells, thereby leading to an indirect tumor cell-mediated antiangiogenic effect of patupilone. Patupilone might also directly target the microtubule system in the tumor endothelial cell compartment but might be less cytotoxic in presence of sufficient VEGF and other survival factors secreted from the tumor cells. The radiosensitivity of the tumor vascular network codetermines the tumor response to IR (23). Therefore, pharmacologic approaches, which interfere with the survival signaling of endothelial cells, render these cells more radiosensitive and subsequently enhance the tumor response to IR.

DOI:10.1158/1078-0432.CCR-08-0969

A major obstacle for the successful tumor response to IR is tumor hypoxia, which renders tumor cells two or three times more radioresistant than under normoxic conditions. Of note, our *in vitro* experiments revealed that patupilone is as potent against tumor cells under normoxic as under hypoxic conditions. Thus, a combined treatment modality of patupilone in combination with IR also bears promise against tumors with an increased hypoxic fraction. Here, we observed an increase of tumor hypoxia induced by patupilone alone presumably through this antiangiogenic, indirect MVD-reducing effect. We investigated previously the dynamics of tumor hypoxia in response to inhibitors of angiogenesis alone and in combination with IR and observed that irradiation counteracts the risk of treatment-induced hypoxia by the inhibition of angiogenesis (21, 22). Although treatment with the VEGF receptor/tyrosine kinase inhibitor PTK787/ZK222584 also increased overall and local tumor hypoxia, combined treatment with IR resulted in extended tumor growth delay and tumor cell apoptosis but no increase in tumor hypoxia (22). As the radiosensitivity of the tumor vascular network codetermines the tumor response to IR (23), pharmacologic approaches, which interfere with the survival signaling of endothelial cells, render these cells more radiosensitive and subsequently enhance the tumor response to IR. The reduction of survival factors secreted by the tumor cells, after treatment with patupilone, leaves the endothelial cells more vulnerable to direct irradiation. Nevertheless, combined treatment of patupilone with radiation did not enhance tumor hypoxia relative to untreated tumors as if radiation antagonizes the patupilone-induced increase of tumor hypoxia. The mechanisms underlying this antagonistic effect is unclear, but it is conceivable that enhanced cell death together with reduced proliferation of tumor cells may reduce the intratumoral oxygen demand to a level that can still be met by the damaged tumor vasculature and thereby avoid a hypoxic state in the allograft (24, 25). This mechanism might be relevant for the combined treatment of irradiation with direct and indirect inhibitors of angiogenesis.

In summary, our results using *in vivo* tumor models derived from patupilone-sensitive and patupilone-resistant variants of the non-small cell lung cancer cell line A549 strongly suggest that the major antitumor effect of patupilone and a combined patupilone/IR treatment is mainly due to directed effects on the tumor cell compartment and that patupilone may induce an antiangiogenic effect in an indirect way through tumor cell targeting. Overall, these preclinical experiments are of strong relevance for a clinical strategy and further support the promising treatment modality of patupilone alone and in combination with IR.

Disclosure of Potential Conflicts of Interest

No potential conflicts of interest were disclosed.

Acknowledgments

We thank Marion Bawohl for excellent technical support, Dr. Malgorzata Roos (Section of Biostatistics, Institute of Social and Preventive Medicine, University of Zurich) for statistical assistance, Biologisches Zentrallabor of the University Hospital of Zurich for animal housing, and Dr. Susan Band Horwitz for the A549 and A549.EpoB40 cells.

References

1. Altmann KH, Gertsch J. Anticancer drugs from nature—natural products as a unique source of new microtubule-stabilizing agents. Nat Prod Rep 2007;24:327–57.
2. Altmann KH, Wartmann M, O'Reilly T. Epothilones and related structures—a new class of microtubule inhibitors with potent *in vivo* antitumor activity. Biochim Biophys Acta 2000;1470:M79–91.
3. He L, Yang CP, Horwitz SB. Mutations in β-tubulin map to domains involved in regulation of microtubule stability in epothilone-resistant cell lines. Mol Cancer Ther 2001;1:3–10.
4. Nogales E. Structural insights into microtubule function. Annu Rev Biochem 2000;69:277–302.
5. O'Reilly T, Wartmann M, Brueggen J, et al. Pharmacokinetic profile of the microtubule stabilizer patupilone in tumor-bearing rodents and comparison of anticancer activity with other MTS *in vitro* and *in vivo*. Cancer Chemother Pharmacol 2008;62:1045–54.
6. Bollag DM, McQueney PA, Zhu J, et al. Epothilones, a new class of microtubule-stabilizing agents with a Taxol-like mechanism of action. Cancer Res 1995;55:2325–33.
7. Goodin S, Kane MP, Rubin EH. Epothilones: mechanism of action and biologic activity. J Clin Oncol 2004;22:2015–25.
8. Ferretti S, Allegrini PR, O'Reilly T, et al. Patupilone induced vascular disruption in orthotopic rodent tumor models detected by magnetic resonance imaging and interstitial fluid pressure. Clin Cancer Res 2005;11:7773–84.
9. Bocci G, Nicolaou KC, Kerbel RS. Protracted low-dose effects on human endothelial cell proliferation and survival *in vitro* reveal a selective antiangiogenic window for various chemotherapeutic drugs. Cancer Res 2002;62:6938–43.
10. Thorpe PE. Vascular targeting agents as cancer therapeutics. Clin Cancer Res 2004;10:415–27.
11. Escuin D, Kline ER, Giannakakou P. Both microtubule-stabilizing and microtubule-destabilizing drugs inhibit hypoxia-inducible factor-1α accumulation and activity by disrupting microtubule function. Cancer Res 2005;65:9021–8.
12. Pasquier E, Honore S, Braguer D. Microtubule-targeting agents in angiogenesis: where do we stand? Drug Resist Updat 2006;9:74–86.
13. Pawlik TM, Keyomarsi K. Role of cell cycle in mediating sensitivity to radiotherapy. Int J Radiat Oncol Biol Phys 2004;59:928–42.
14. Sinclair WK. Cyclic X-ray responses in mammalian cells *in vitro*. Radiat Res 1968;33:620–43.
15. Hofstetter B, Vuong V, Broggini-Tenzer A, et al. Patupilone acts as radiosensitizing agent in multidrug-resistant cancer cells *in vitro* and *in vivo*. Clin Cancer Res 2005;11:1588–96.
16. Giannakakou P, Gussio R, Nogales E, et al. A common pharmacophore for epothilone and taxanes: molecular basis for drug resistance conferred by tubulin mutations in human cancer cells. Proc Natl Acad Sci U S A 2000;97:2904–9.
17. Wang Y, O'Brate A, Zhou W, Giannakakou P. Resistance to microtubule-stabilizing drugs involves two events: β-tubulin mutation in one allele followed by loss of the second allele. Cell Cycle 2005;4:1847–53.
18. Yang CP, Verdier-Pinard P, Wang F, et al. A highly epothilone B-resistant A549 cell line with mutations in tubulin that confer drug dependence. Mol Cancer Ther 2005;4:987–95.
19. Eberhard A, Kahlert S, Goede V, Hemmerlein B, Plate KH, Augustin HG. Heterogeneity of angiogenesis and blood vessel maturation in human tumors: implications for antiangiogenic tumor therapies. Cancer Res 2000;60:1388–93.
20. Pasquier E, Carre M, Pourroy B, et al. Antiangiogenic activity of paclitaxel is associated with its cytostatic effect, mediated by the initiation but not completion of a mitochondrial apoptotic signaling pathway. Mol Cancer Ther 2004;3:1301–10.
21. Oehler-Janne C, Jochum W, Riesterer O, et al. Hypoxia modulation and radiosensitization by the novel dual EGFR and VEGFR inhibitor AEE788 in spontaneous and related allograft tumor models. Mol Cancer Ther 2007;6:2496–504.
22. Riesterer O, Honer M, Jochum W, Oehler C, Ametamey S, Pruschy M. Ionizing radiation antagonizes tumor hypoxia induced by antiangiogenic treatment. Clin Cancer Res 2006;12:3518–24.
23. Garcia-Barros M, Paris F, Cordon-Cardo C, et al. Tumor response to radiotherapy regulated by endothelial cell apoptosis. Science 2003;300:1155–9.
24. Moeller BJ, Cao Y, Vujaskovic Z, Li CY, Haroon ZA, Dewhirst MW. The relationship between hypoxia and angiogenesis. Semin Radiat Oncol 2004;14:215–21.
25. Rak J, Yu JL. Oncogenes and tumor angiogenesis: the question of vascular "supply" and vascular "demand". Semin Cancer Biol 2004;14:93–104.

3.3. Regulation of VEGF-expression by patupilone and ionizing radiation in lung adenocarcinoma cells

Carla Rohrer Bley[a,b], Katrin Orlowski[a], Polina Furmanova[a], Paul MJ. McSheehy[c], Martin Pruschy [a]

[a]Department of Radiation Oncology, University Hospital Zurich, Zurich, Switzerland
[b]Section of Radiation Oncology, Vetsuisse Faculty, University of Zurich, Zurich, Switzerland
[c]Novartis Institutes for BioMedical Research, Novartis Pharma AG, Basel, Switzerland

Status of the manuscript: published in Lung Cancer. 2011 Sep;73(3):294-301.

Author contribution K. Orlowski:
Set-up and planning of the ELISA assay. Participation in data analysing of the ELISA assay leading to figure 4. Involved in proof-reading of the manuscript.

Lung Cancer 73 (2011) 294–301

Contents lists available at ScienceDirect

Lung Cancer

journal homepage: www.elsevier.com/locate/lungcan

Regulation of VEGF-expression by patupilone and ionizing radiation in lung adenocarcinoma cells

Carla Rohrer Bley[a,b], Katrin Orlowski[a], Polina Furmanova[a], Paul M.J. McSheehy[c], Martin Pruschy[a,*]

[a] Department of Radiation Oncology, University Hospital Zurich, Raemistr. 100, CH-8091 Zurich, Switzerland
[b] Section of Radiation Oncology, Vetsuisse Faculty, University of Zurich, Zurich, Switzerland
[c] Novartis Institutes for BioMedical Research, Novartis Pharma AG, Basel, Switzerland

ARTICLE INFO

Article history:
Received 2 August 2010
Received in revised form
23 December 2010
Accepted 18 January 2011

Keywords:
Patupilone
Ionizing radiation
Angiogenesis
A549 lung adenocarcinoma cells
Microtubules
VEGF
Hypoxia

ABSTRACT

The use of microtubule stabilizing agents (MSAs) is a promising strategy for anti-cancer therapy alone and as part of combined treatment modalities with ionizing radiation. However MSA-provoked molecular and cellular processes including the regulation of intercellular, paracrine signaling pathways are far from clear. Here we investigated the interference of the novel, clinically relevant MSA patupilone (epothilone B) with the tumor-cell derived vascular endothelial growth factor (VEGF), which is most relevant for tumor angiogenesis. Low-dose, sub-nanomolar concentrations of patupilone specifically reduced hypoxia-driven stabilization of the transcription factor HIF-1α in the patupilone-sensitive lung adenocarcinoma cell line A549, but not in the mutant derivative cell line A549.EpoB40. Patupilone further reduced hypoxia-induced VEGF expression and secretion but only in the A549 wildtype cell line. In the wildtype cell line, ionizing radiation alone induced hypoxia-dependent VEGF-expression but a strong dominant counteracting effect of patupilone was always observed when ionizing radiation was combined with patupilone, on the level of HIF-1α protein stability, VEGF-expression and VEGF-secretion. These results demonstrate that patupilone and ionizing radiation dysregulate hypoxia-induced stress responses, which might contribute to the potency of this promising, combined treatment modality.

1. Introduction

Interference with microtubule function leads to defective mitotic spindle formation, cell cycle arrest in M-phase, and eventually to apoptosis or post-mitotic cell death. The use of microtubule interfering agents is therefore a promising strategy for anti-cancer therapy alone and as part of combined treatment modalities with cytotoxic agents [1]. The effects of microtubule interfering agents at the biochemical level are well investigated, but additional cytotoxic effects due to signaling interference have been identified, which merit further investigation [2–5].

We previously investigated the combined treatment modality of ionizing radiation (IR) with the novel, clinically relevant microtubule stabilizing agent patupilone (Epothilone B), and interestingly, the combination of patupilone with IR resulted *in vitro* only in an additive cytotoxic effect (against various cancer cell types) but in a supra-additive tumor growth delay against tumor xenografts derived from the same tumor cells [2,4]. The accumulation of tumor cells in the most radiosensitive G2-M phase of the cell cycle represents the major rationale for the sensitization to IR [6–9], though other S-phase progression-related mechanisms have been observed as well [4]. Additional anti-vascular and anti-angiogenic effects might contribute to the supra-additive tumor growth delay observed *in vivo*, and indeed, direct targeting of endothelial cells [10–12] and indirect, anti-angiogenic interference with the secretion of pro-angiogenic factors from tumor cells have been proposed [2,13]. Microtubule stabilizing and destabilizing agents block the nuclear translocation and correct assembly of the hypoxia inducible factor (HIF) by disrupting the structural organization of the microtubule cytoskeleton. In consequence, the downstream signaling of HIF-1 target genes in response to hypoxia is compromised [2,3,5]. A reduction of pro-angiogenic (and cytoprotective) cytokine secretion by patupilone via inhibition of HIF could contribute to this mechanism [14,15]. However, such a link between microtubule-interfering agents and HIF-signaling has only been investigated at high-dose concentrations of these agents.

The group of microtubule stabilizing agents (MSAs) are amongst the most promising chemotherapeutic agents for the treatment of non-small cell lung cancer. The MSA docetaxel is the only chemotherapeutic agent currently approved for first- and second-line treatment of advanced non-small cell lung cancer. Although single agent docetaxel as well as combined treatments with platinum-based agents have led to significant progress in the treatment of lung cancer, its use often results in strong side-effects

* Corresponding author. Tel.: +41 44 255 8549; fax: +41 44 255 4435.
E-mail address: martin.pruschy@usz.ch (M. Pruschy).

0169-5002/$ – see front matter © 2011 Elsevier Ireland Ltd. All rights reserved.
doi:10.1016/j.lungcan.2011.01.010

[16–18]. In order to overcome such limitations, new MSA with fewer side-effects, superior pharmacological and anticancer activity are under investigation in order to maximize the induced benefits for lung cancer patients. At the same time and based on the immense technological improvements of current radiotherapy with regard to treatment conformality and accuracy radiotherapy is becoming standard of care for the management of lung cancer. As such, combined radiochemotherapy treatment modalities are also of high interest for this tumor entity.

Here we investigated the treatment response of low-dose, subnanomolar concentrations of patupilone alone and in combination with IR specifically on hypoxia-driven VEGF expression and secretion in the patupilone-sensitive lung adenocarcinoma cell line A549 and the mutant derivative A549.EpoB40, which is strongly resistant to patupilone due to a genetically defined β-tubulin-mutation [3,19–21]. Thereby we aim to further explore the interference of patupilone with the tumor-cell derived growth factor most relevant for tumor angiogenesis.

2. Materials and methods

2.1. Drugs and cell lines

Patupilone (epothilone B, EPO906) was provided by Novartis Pharma AG (Basel, Switzerland). The human cell line pair A549 and A549.EpoB40 was obtained from the laboratory of Dr. S.B. Horwitz.

2.2. Cell cultures, drug preparation and irradiation

The human non-small cell lung cancer lines A549 and A549.EpoB40 were grown in RPMI 1640 containing 10% (v/v) fetal bovine serum, 1% (v/v) penicillin–streptomycin and 1% (v/v) L-glutamine at 37 °C in 5% CO_2. A549.EpoB40 is derived from A549 by stepwise selection with patupilone and contains a point mutation in class 1 β-tubulin (β292 from Gln to Glu) which is associated with a ~95-fold resistance to patupilone [20]. The A549.EpoB40 cell line was grown and maintained in medium containing 10 nM patupilone. For *in vitro* experiments, patupilone was dissolved in DMSO (1 mM stock solution) and further diluted with media containing 10% FCS.

Irradiation of cell cultures was carried out using a Gulmay 200 kV X-ray unit at 100 cGy/min at room temperature. For combined treatment and hypoxia experiments, cells were pretreated with patupilone 24 h before applying hypoxia or hypoxia mimicking conditions. Cells were irradiated 4 h thereafter.

2.3. Cultivation of cells under hypoxia

Hypoxia experiments with A549 and A549.EpoB40 were performed for various time spans at 0.2% or 1% oxygen using a Invivo2 400 hypoxia workstation (Biotrace International). Cells were preincubated with patupilone for 24 h under normoxic conditions, followed by incubation in the hypoxia chamber or under hypoxia-mimicking conditions, using Dimethyloxaloylglycine (DMOG) (Biomol GmbH, Hamburg, Germany), a prolyl-4-hydroxylase inhibitor (0.25 and 1 mM, respectively) [2].

2.4. Western blot analysis

A549 and A549.EpoB40 were cultivated in 6-well dishes, washed twice with ice cold PBS, and whole cell extracts were obtained by scraping cells with 150 μl of pre-cooled hypotonic lysis buffer (Laemmli-buffer (4% SDS, 15% glycerol, 0.125 M Tris–HCl) and 2× SDS-buffer (20% glycerol, 0.100 M Tris, 0.1% bromphenol blue; 10% β-mercaptoethanol) 1:1) and immediately heated for 5 min at 95 °C on a heating block. Hypoxic probes were retrieved under hypoxic conditions. Proteins were resolved by 10% SDS–PAGE, followed by western blotting onto polyvinylidene difluoride membranes. Membranes were probed with the HIF-1α antibody (HIF-1α (H-206), Santa Cruz Biotechnology, Inc.). Antibody detection was achieved by enhanced chemoluminescence (Amersham, Piscataway, NJ) according to the protocol of the manufacturer. All experiments were carried out independently at least thrice.

2.5. Isolation and analysis of RNA

Total RNA was isolated using the Quiagen RNeasy Plus Mini Kit (Qiagen, Hombrechtikon, Switzerland). First-strand cDNA synthesis was performed with 1–5 mg total RNA using reverse transcriptase enzyme, and mRNA levels were measured by real-time quantitative PCR using a SybrGreen qPCR reagent kit (Applied Biosystems) in combination with a 7900 HT TaqMan rtPCR system (Applied Biosystems) and SDS manager 2.3, patch 3-software. Real-time PCR was carried out as recommended by the manufacturer. To verify equal input levels, β-actin was used as a housekeeping gene and the data were expressed as ratios relative to β-actin levels. The primers (Microsynth, Balgach, Switzerland) used for RT-PCR of VEGF-A mRNA were as follows: (a) forward primer, 5′-ATG AAC TTT CTG CTG TCT TGG GT-3′ and (b) reverse primer: 5′-TCA CCG CCT CGG CTT GTC AC-3′ [22]. The forward primer sequence for β-actin mRNA (internal control) quantification was 5′-GTC CTC TCC CAA GTC CTC ACA-3′; the reverse primer sequence was 5′-AAT TTA CAC GAA AGC AAT CCT ATC AC-3′.

2.6. ELISA

Supernatants of cultured cells were centrifuged at 10,000 × *g* to remove debris and stored at −80 °C. Cell numbers were manually counted after trypsination to allow correction to cell number. Total protein content of supernatant was measured with a Nanodrop spectrophotometer (Witec AG, Switzerland) at an absorbance of 280 nm. The concentration of VEGF-levels in the supernatant was determined using the commercially available Quantikine® Human VEGF Immunoassay kit (R&D Systems GmbH, Wiesbaden-Nordenstadt, Germany), following the manufacturer's description.

2.7. Statistical analysis

Experiments presented in the figures are representative of three or more different repetitions if not otherwise indicated. Statistical analysis was performed using GraphPad Prism5 software (GraphPad Software Inc.). Student's *t*-test was used to evaluate the differences between normoxic and hypoxic and between drug and IR treated samples. The level of significance was set at 0.05.

3. Results

3.1. Stabilization of microtubules leads to inhibition of the HIF pathway

The hypoxia-stabilized HIF-1α-subunit of the transcription factor HIF represents a major determinant for hypoxia-regulated expression of pro-angiogenic growth factors. To determine hypoxia-dependent HIF-1α stabilization on patupilone treatment, patupilone-sensitive lung adenocarcinoma A549 wildtype and patupilone-resistant A549.EpoB40 cells were pretreated for 24 h with increasing concentrations of patupilone (0–1 nM) followed by incubation in 0.2% pO_2 or addition of the hypoxia-mimicking agent DMOG (0.25 and 1 mM, respectively). Maximum stabilization of the HIF-1α subunit under hypoxic conditions was observed at 4 h of hypoxic exposure and in hypoxia-mimicking conditions (Fig. 1) and was reduced again to background levels at the 24 h

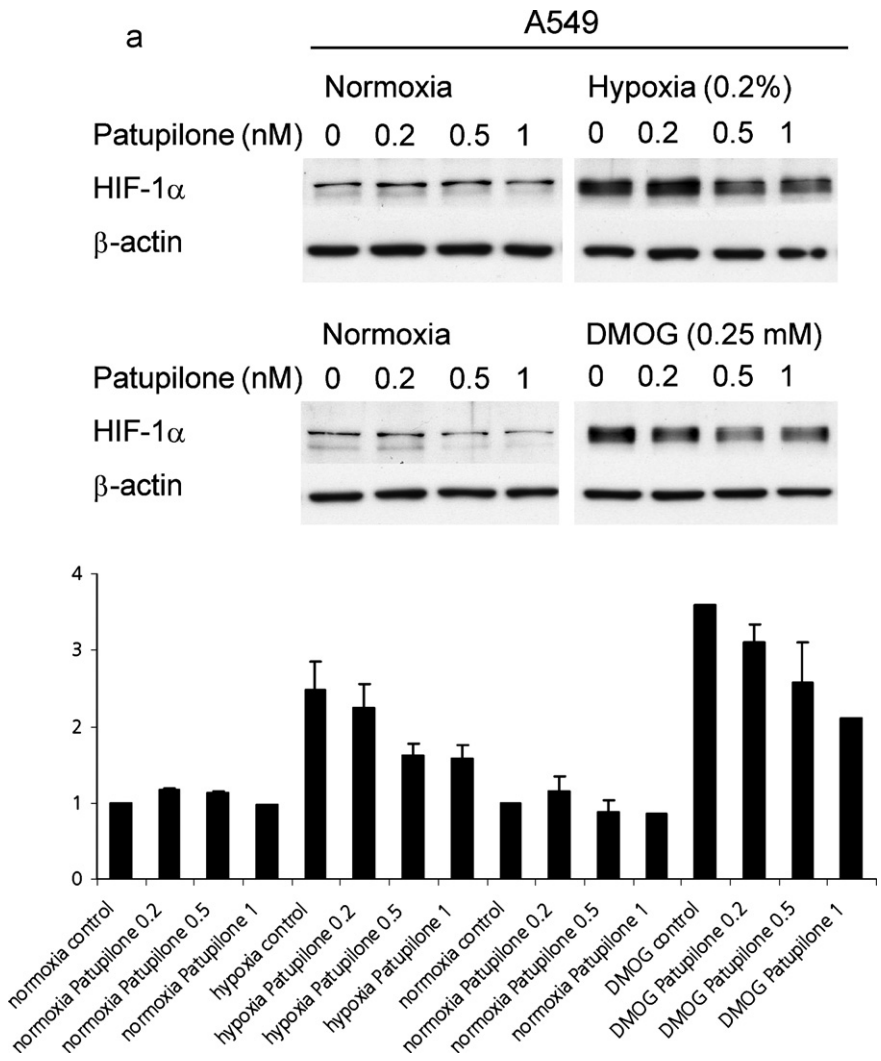

Fig. 1. Patupilone reduces HIF-1α levels under hypoxia. (a) A549 wildtype and (b) A549.EpoB40 cells were treated for 24 h with increasing concentrations of patupilone and then subjected to hypoxia or hypoxia mimicking conditions (0.2% pO_2 or DMOG, respectively), for additional 4 h. HIF-1α protein levels were determined by western blotting. Band intensities of two independent experiments were quantified, pooled and are plotted.

time point in both cell lines (data not shown). In the A549 wildtype cells HIF-1α stabilization was abrogated by patupilone in a dose-dependent way, while HIF-1α protein levels were not reduced in the A549.EpoB40 cells on patupilone treatment (Fig. 1). HIF-1α stabilization in the A549.EpoB40 cells was only affected at approximately 100-fold higher concentrations of patupilone, which correlates to the 100-fold-reduced affinity of mutant β-tubulin to patupilone in these cells (data not shown).

We previously observed an at least additive reduction of microvessel density in tumor xenografts derived from A549-adenocarcinoma tumor cells on combined treatment with patupilone and IR [2]. This might be due to a combined effect on the HIF-1α -dependent expression or secretion of pro-angiogenic factors such as the vascular endothelial growth factor (VEGF). Irradiation of cells alone did not affect HIF-1α-level but synergized with patupilone. When A549 wildtype cells were pretreated with low dose patupilone (0.2 nM and 0.5 nM; with only a minor effect on HIF-1α stability alone), followed by incubation with DMOG and irradiation 2 h thereafter, HIF-1α-protein levels were even further reduced than after treatment with patupilone alone. No downregulation of HIF-1α was observed in the β-tubulin-mutated counterpart cells after treatment with either condition (Fig. 2).

3.2. Downstream signaling of HIF at the level of VEGF mRNA is affected by treatment with patupilone

To determine the consequence of deregulated HIF-1α stability on the expression of the major pro-angiogenic factor VEGF, VEGF mRNA levels were quantified by real-time PCR. Incubation of cells for 24 h under hypoxic (0.2% pO_2) or hypoxia mimicking conditions (DMOG) resulted in a 6- and 4-fold upregulation of VEGF mRNA levels, in A549 wildtype and A549EpoB40 mutated lung adenocarcinoma cells, respectively (Fig. 3). Similar to the effect on HIF-1α-stability, pretreatment with patupilone (0.5 nM) resulted in diminished VEGF mRNA upregulation in the A549 cells by 43% ($p = 0.002$), but not in the patupilone-resistant A549.EpoB40 cells, when treated under hypoxic or hypoxia mimicking conditions.

Under hypoxia-mimicking conditions irradiation alone (4 h after start of DMOG-treatment) resulted in enhanced VEGF expression in the A549 wildtype cells but not in the A549EpoB40 cells, which are more radiation resistant [2]. The discrepancy between IR-downregulated HIF-1α-levels (see above) and IR-enhanced VEGF-mRNA levels might be due to the different time points of data collection. However and more important, the relative downregulation of VEGF mRNA levels in patupilone-pretreated cells was observed to a similar extent in irradiated as in unirradiated A549

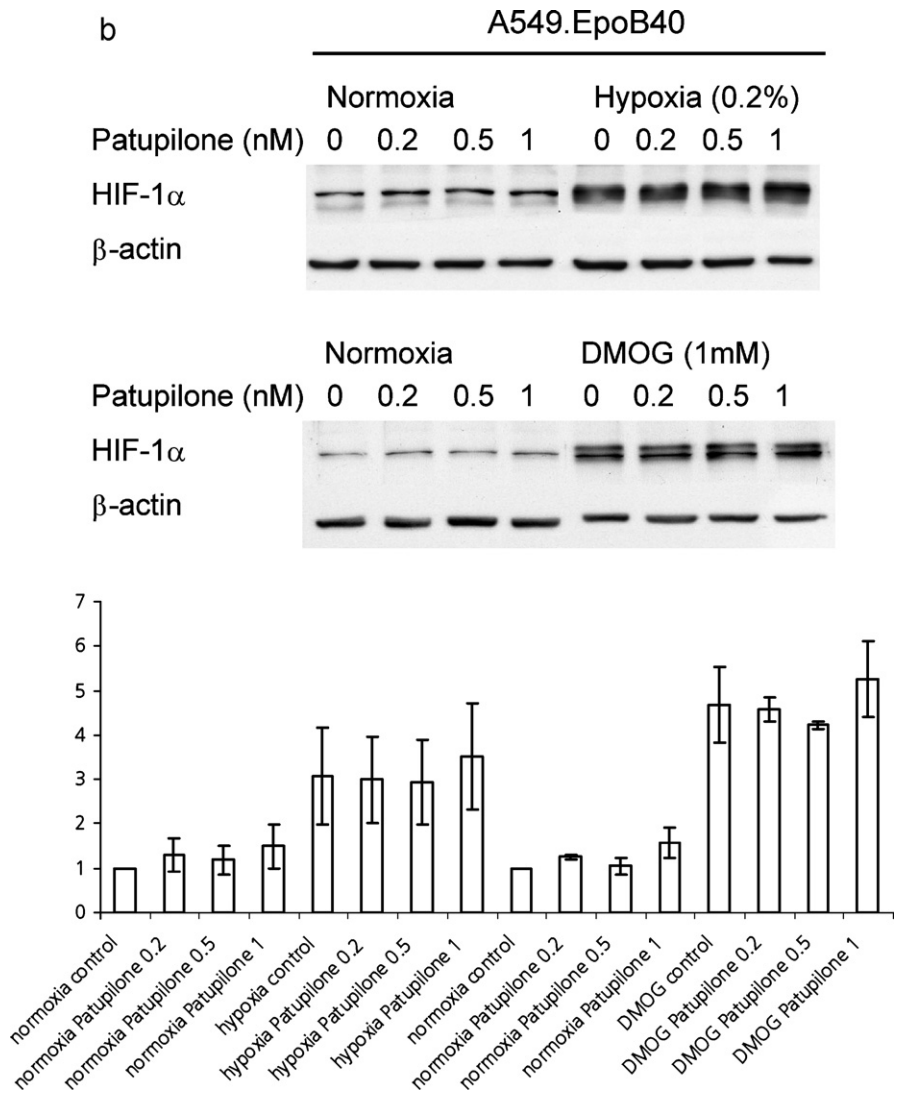

Fig. 1. (*Continued.*)

wildtype cells (reduction by 45% of initial values ($p = 0.006$)), while patupilone treatment did not downregulate VEGF expression in irradiated A549.EpoB40 cells.

3.3. VEGF protein secretion with drug pretreatment is inhibited in A549

To determine the amount of secreted VEGF in response to treatment with IR and patupilone, cells were preincubated with patupilone for 24 h, incubated under hypoxia mimicking conditions (for 30 h) and irradiated at the 4 h time point following DMOG-addition. Supernatants were collected during a 12 h interval of incubation under hypoxia-mimicking conditions (18–30 h time period) and were analyzed for VEGF protein levels by ELISA.

As expected from the real time PCR results, secreted VEGF levels in supernatants derived from DMOG-treated cells were 3–4-fold enhanced in both A549 wildtype and A549.EpoB40 mutated cells in comparison to supernatants derived from cells kept in normoxia. Of note, while irradiation enhanced VEGF mRNA levels in A549 cells kept under hypoxia-mimicking conditions (see above), no further increased VEGF protein level could be detected in supernatants derived from these cells. Interestingly, in response to patupilone treatment (0.5 nM) a significant reduction in VEGF-secretion under normoxic (31%, $p = 0.008$) as well as DMOG conditions (34%, $p < 0.001$) was determined in the patupilone-sensitive cell line A549 (Fig. 4) but not in the patupilone-resistant cell line. Similar results were determined when cells were kept under hypoxia (1%) instead of DMOG-treatment or in supernatants collected over a 48 h-interval from cells treated under the same conditions (data not shown). Of note, prior results demonstrated that the antiproliferative effect of patupilone under normoxic and hypoxic (pO_2 of 1%) conditions remains the same (data not shown [2]). Thus combined treatment modality of low doses of patupilone in combination with ionizing radiation also bears promise against tumors with an increased hypoxic fraction.

Overall our results demonstrate that low-dose treatment of tumor cells with patupilone antagonizes a major pro-angiogenic signaling axis on the level of the hypoxia-inducible factor HIF-1α, thereby reducing hypoxia-enhanced expression and subsequent secretion of the vascular endothelial growth factor VEGF.

4. Discussion

Here, we investigated the regulation of the hypoxia-inducible factor HIF-1α and its downstream target VEGF by the novel, clinically relevant microtubule stabilizing agent patupilone alone and in combination with ionizing radiation. The effect of patupilone

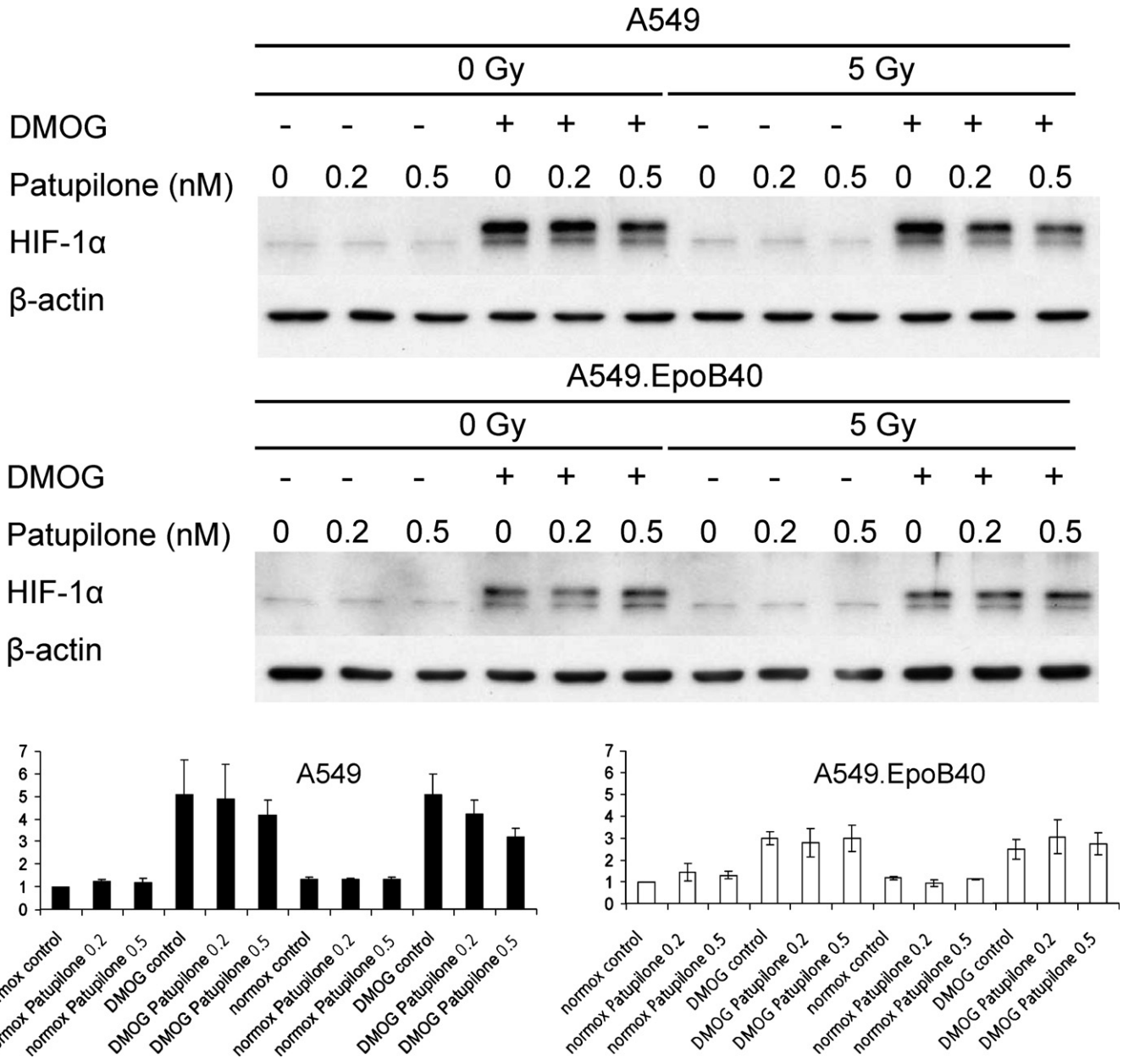

Fig. 2. Enhanced reduction of HIF-1α levels on combined treatment with patupilone and ionizing radiation: A549 wildtype and A549.EpoB40 cells were treated for 24 h with increasing concentrations of patupilone, subjected to hypoxia mimicking conditions, irradiated after 2 h and analyzed for HIF-1a protein levels 4 h after start of DMOG incubation. Band intensities of three independent experiments were quantified, pooled and are plotted: columns: mean; bars: ±SE.

was specifically tested in the lung adenocarcinoma cell line A549 at subnanomolar concentrations, which do not induce the classic MSA-dependent M-phase arrest and have only minimal cytotoxic activity. Under hypoxia HIF-1α-protein levels were reduced by low-dose treatment with patupilone. Subsequently VEGF mRNA transcription was diminished, and reduced levels of secreted VEGF-protein were detected in cell supernatants. Furthermore patupilone repressed IR-induced VEGF mRNA expression. The specificity of patupilone and the involvement of the microtubular system were evidenced by the lack of a treatment response in the mutated A549 cell line derivative harboring a specific β-tubulin mutation, which abrogates patupilone-binding.

A variety of microtubule targeting drugs has previously been described to exhibit anti-HIF properties in tumor cells exposed to hypoxia [3,5]. 2-Methoxyestradiol and classic microtubule stabilizing (taxanes) and microtubule destabilizing (vincristine, discodermolide) agents downregulated HIF-1α at the posttranscriptional level resulting in reduced HIF-1α protein synthesis and subsequent reduced nuclear accumulation and transcriptional activity. Microtubule stabilizing agents may interfere with a regulated HIF-1α mRNA-microtubule association and guided nuclear import of the HIF-1α subunit into the nucleus [3,5]. However these experiments were performed at concentrations of the respective compounds that strongly induced microtubule stabilization and destabilization, respectively and treatment-dependent cell cycle redistribution into G2-M phase. Here we demonstrate that low-dose concentrations of patupilone (epothilone B) strongly reduce HIF-1α protein levels and subsequent downregulation of the major downstream target VEGF at up to 100-fold lower concentrations, which do not result in microtubule interference-related G2-M cell cycle redistribution, and that patupilone counteracts a potential pro-angiogenic stress response [23]. Furthermore these low concentrations of patupilone are still β-tubulin-specific, without any effect in the A549-mutated cell line and are suf-

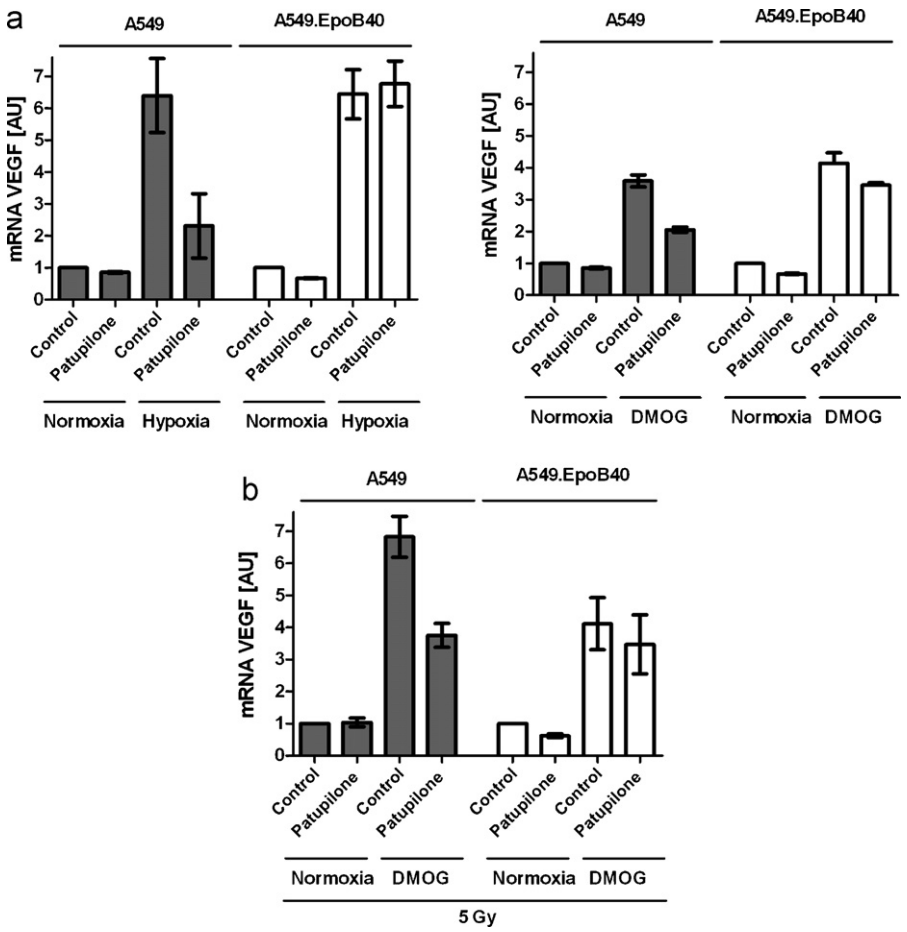

Fig. 3. Regulation of hypoxia-driven VEGF-mRNA-expression by patupilone and IR. (a) A549 wildtype and A549.EpoB40 cells were treated for 24 h with patupilone (0.5 nM) and subjected to hypoxia or hypoxia mimicking conditions (0.2% pO_2 or DMOG, respectively) for 24 h. (b) A549 wildtype and A549.EpoB40 cells were treated for 24 h with patupilone (0.5 nM), subjected to hypoxia mimicking conditions and irradiated after 4 h. VEGF mRNA was determined 24 h after start of DMOG incubation by real time PCR and normalized to β-action mRNA expression. Data were pooled from three independent experiments, columns: mean; bars: ±SE.

ficient to sensitize for ionizing radiation ([2,4], and data not shown).

Despite direct *in vitro* cytotoxicity against endothelial cells [11], our prior results allocate part of the anti-angiogenic effect of patupilone to interference with the tumor cellular stress response. *In vitro* experiments performed with a hypoxia-regulated reporter gene assay demonstrated that patupilone reduces the expression of the HIF-1 "transcriptome" but only in patupilone sensitive tumor cells, thereby abrogating the paracrine, tumor cell-mediated protection of the tumor endothelium [2]. Here we specifically determine downregulation of VEGF expression and subsequent secretion of the HIF-1α downstream target and major endothelial growth and survival factor VEGF on cellular treatment with patupilone. Similar to patupilone in this study, the MSA paclitaxel also downregulates VEGF-gene expression and VEGF-protein secretion, however only at high cytotoxic doses of paclitaxel as demonstrated in MKN45 and HT29 gastrointestinal carcinoma cell lines (≥0.1 μM) [24,25].

Regulation of HIF-1α in response to irradiation is complex and dependent on multiple factors including hypoxia and reoxygenation-enhanced generation of reactive oxygen species [14,15]. Furthermore the treatment response *in vitro* might not reflect the *in vivo* situation with its dynamic adaptation to microenvironmental changes in response to radiotherapy. Here we determined multiple endpoints in response to IR alone and in combination with patupilone in the two related adenocarcinoma cell lines (HIF-1α protein levels, VEGF expression and secretion). In part they are difficult to be reconciled. For example IR enhanced VEGF expression under hypoxic condition, but no enhanced HIF-1α protein levels could be detected in irradiated cells. This might be due to undetected posttranslational modifications, which increases the transcriptional activity of HIF-1α, but might also be due to incomplete analysis of HIF-1α due to technical limitations. In this study, patupilone-reduced VEGF-mRNA expression was normalized to β-actin-housekeeping gene expression and is therefore not affected by a small reduction of cell viability at patupilone-concentrations used (20% at 0.5 nM, data not shown). However we cannot exclude that patupilone-reduced VEGF-secretion might in part derive from patupilone-affected cell viability at a later time point. On the other hand MSA may also interfere with the secretion of vesicles and proteases required for VEGF-release along a dynamic microtubular system [26], which is currently investigated as part of ongoing studies.

However and more important a strong dominant counteracting effect was always observed when IR was combined with patupilone, on the level of HIF-1 protein stability, VEGF-expression and VEGF-secretion.

Overall, we demonstrate that low dose, subnanomolar treatment of lung carcinoma cells with the clinically relevant microtubule stabilizing agent patupilone interferes with the major hypoxic signaling axes. This effect is most probably linked to microtubules interference, as indicated by the negative results in the β-tubulin-mutated drug-resistant A549.EpoB40 cell line. Patupilone treatment results in reduced VEGF expression and secretion under hypoxic conditions and subsequent lack of paracrine protection of the tumor vasculature. Thus besides its direct cytotoxic

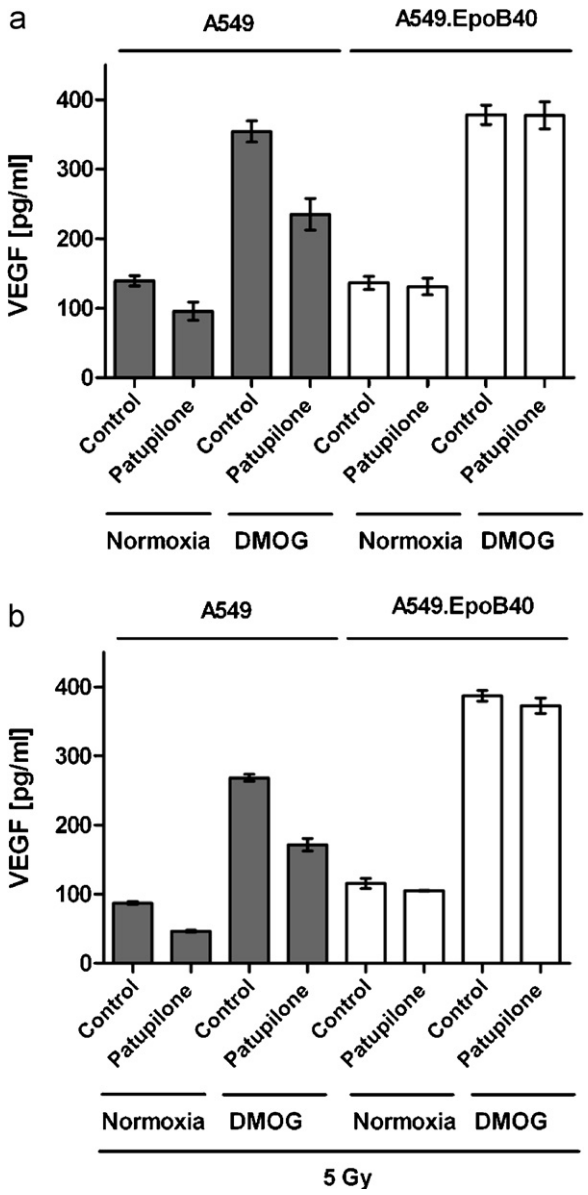

Fig. 4. Regulation of hypoxia-driven VEGF-secretion by patupilone and IR. A549 wildtype and A549.EpoB40 cells were treated for 24 h with patupilone (0.5 nM), subjected to hypoxia mimicking conditions for 30 h (a) and irradiated at the 4 h time point following DMOG-addition (b). Supernatants were collected during a 12 h interval of incubation under hypoxia-mimicking conditions (18–30 h time period) and analyzed for VEGF protein levels by ELISA. Data presented are derived from three independent experiments, columns: mean; bars: ±SE.

and radiosensitizing effect on the tumor cell level, patupilone might concomitantly render endothelial cells more vulnerable to ionizing radiation. This eventually contributes to the strong supra-additive treatment response observed *in vivo* in response to the combined treatment modality of IR with patupilone [2,4] and will also be of future clinical interest [27]. Thus a pharmacological approach which interferes with the hypoxic signaling of neoplastic cells renders these cells more radiosensitive and subsequently enhances the tumor response to ionizing radiation.

Conflict of interest statement

No actual or potential conflict of interest in relation to this article exists for any author.

Funding

We acknowledge the following sources of funding: Oncosuisse, the Sassella, the Novartis and Swiss National Foundations (to M.P.).

Acknowledgements

We thank Dr. Malgorzata Roos from of the Section of Biostatistics, ISPM, University of Zurich for statistical assistance and Susan Band Horwitz for the A549 and A549.EpoB40 cells.

References

[1] Altmann KH, Gertsch J. Anticancer drugs from nature – natural products as a unique source of new microtubule-stabilizing agents. Nat Prod Rep 2007;24:327–57.
[2] Bley CR, Jochum W, Orlowski K, Furmanova P, Vuong V, McSheehy PM, et al. Role of the microenvironment for radiosensitization by patupilone. Clin Cancer Res 2009;15:1335–42.
[3] Escuin D, Kline ER, Giannakakou P. Both microtubule-stabilizing and microtubule-destabilizing drugs inhibit hypoxia-inducible factor-1alpha accumulation and activity by disrupting microtubule function. Cancer Res 2005;65:9021–8.
[4] Hofstetter B, Vuong V, Broggini-Tenzer A, Bodis S, Ciernik IF, Fabbro D, et al. Patupilone acts as radiosensitizing agent in multidrug-resistant cancer cells in vitro and in vivo. Clin Cancer Res 2005;11:1588–96.
[5] Mabjeesh NJ, Escuin D, LaVallee TM, Pribluda VS, Swartz GM, Johnson MS, et al. 2ME2 inhibits tumor growth and angiogenesis by disrupting microtubules and dysregulating HIF. Cancer Cell 2003;3:363–75.
[6] Altmann KH, Wartmann M, O'Reilly T. Epothilones and related structures – a new class of microtubule inhibitors with potent in vivo antitumor activity. Biochim Biophys Acta 2000;1470:M79–91.
[7] Kong Z, Raghavan P, Xie D, Boike T, Burma S, Chen D, et al. Epothilone B confers radiation dose enhancement in DAB2IP gene knock-down radioresistant prostate cancer cells. Int J Radiat Oncol Biol Phys 2010;78:1210–8.
[8] Pawlik TM, Keyomarsi K. Role of cell cycle in mediating sensitivity to radiotherapy. Int J Radiat Oncol Biol Phys 2004;59:928–42.
[9] Sinclair WK. Cyclic X-ray responses in mammalian cells in vitro. Radiat Res 1968;33:620–43.
[10] Thorpe PE. Vascular targeting agents as cancer therapeutics. Clin Cancer Res 2004;10:415–27.
[11] Bocci G, Nicolaou KC, Kerbel RS. Protracted low-dose effects on human endothelial cell proliferation and survival in vitro reveal a selective antiangiogenic window for various chemotherapeutic drugs. Cancer Res 2002;62:6938–43.
[12] Ferretti S, Allegrini PR, O'Reilly T, Schnell C, Stumm M, Wartmann M, et al. Patupilone induced vascular disruption in orthotopic rodent tumor models detected by magnetic resonance imaging and interstitial fluid pressure. Clin Cancer Res 2005;11:7773–84.
[13] Pasquier E, Honore S, Braguer D. Microtubule-targeting agents in angiogenesis: where do we stand? Drug Resist Updat 2006;9:74–86.
[14] Dewhirst MW, Cao Y, Li CY, Moeller B. Exploring the role of HIF-1 in early angiogenesis and response to radiotherapy. Radiother Oncol 2007;83:249–55.
[15] Moeller BJ, Cao Y, Li CY, Dewhirst MW. Radiation activates HIF-1 to regulate vascular radiosensitivity in tumors: role of reoxygenation, free radicals, and stress granules. Cancer Cell 2004;5:429–41.
[16] Galmarini CM. Sagopilone a microtubule stabilizer for the potential treatment of cancer. Curr Opin Investig Drugs 2009;10:1359–71.
[17] Hanna N, Shepherd FA, Fossella FV, Pereira JR, De Marinis F, von Pawel J, et al. Jr. Randomized phase III trial of pemetrexed versus docetaxel in patients with non-small-cell lung cancer previously treated with chemotherapy. J Clin Oncol 2004;22:1589–97.
[18] Saloustros E, Mavroudis D, Georgoulias V. Paclitaxel and docetaxel in the treatment of breast cancer. Expert Opin Pharmacother 2008;9:2603–16.
[19] Giannakakou P, Gussio R, Nogales E, Downing KH, Zaharevitz D, Bollbuck B, et al. A common pharmacophore for epothilone and taxanes: molecular basis for drug resistance conferred by tubulin mutations in human cancer cells. Proc Natl Acad Sci USA 2000;97:2904–9.
[20] He L, Yang CP, Horwitz SB. Mutations in beta-tubulin map to domains involved in regulation of microtubule stability in epothilone-resistant cell lines. Mol Cancer Ther 2001;1:3–10.
[21] Wang Y, O'Brate A, Zhou W, Giannakakou P. Resistance to microtubule-stabilizing drugs involves two events: beta-tubulin mutation in one allele followed by loss of the second allele. Cell Cycle 2005;4:1847–53.
[22] Stimpfl M, Tong D, Fasching B, Schuster E, Obermair A, Leodolter S, et al. Vascular endothelial growth factor splice variants and their prognostic value in breast and ovarian cancer. Clin Cancer Res 2002;8:2253–9.
[23] Gorski DH, Beckett MA, Jaskowiak NT, Calvin DP, Mauceri HJ, Salloum RM, et al. Blockage of the vascular endothelial growth factor stress response increases the antitumor effects of ionizing radiation. Cancer Res 1999;59:3374–8.
[24] Toiyama Y, Inoue Y, Hiro J, Ojima E, Watanabe H, Narita Y, et al. The range of optimal concentration and mechanisms of paclitaxel in

radio-enhancement in gastrointestinal cancer cell lines. Cancer Chemother Pharmacol 2007;59:733–42.
[25] Toiyama Y, Inoue Y, Hiro J, Ojima E, Watanabe H, Narita Y, et al. Paclitaxel inhibits radiation induced VEGF secretion and enhances radiosensitizing effects in human colon cancer cell HT29. Cancer Ther 2009;7:123–32.
[26] Schnaeker EM, Ossig R, Ludwig T, Dreier R, Oberleithner H, Wilhelmi M, et al. Microtubule-dependent matrix metalloproteinase-2/matrix metalloproteinase-9 exocytosis: prerequisite in human melanoma cell invasion. Cancer Res 2004;64:8924–31.
[27] Fogh S, Machtay M, Werner-Wasik M, Curran Jr WJ, Bonanni R, Axelrod R, et al. Phase I trial using patupilone (epothilone B) and concurrent radiotherapy for central nervous system malignancies. Int J Radiat Oncol Biol Phys 2010;77:1009–16.

3.4. The microtubule stabilizer Patupilone (Epothilone B) is a potent radiosensitizer in medulloblastoma cells

Christoph. Oehler[#], André O. von Bueren[#], Polina Furmanova[#], Angela Broggini-Tenzer[#], Katrin Orlowski, Stefan Rutkowski, Karl Frei, Michael A. Grotzer, and Martin Pruschy

Dept. Radiation Oncology, University Hospital Zurich, CH-8091 Zurich, Switzerland (C.O.,P.F.,K.O.,A.B-T.,M.P.). Dept. Pediatric Oncology, University Children's Hospital, CH-8032 Zurich, Switzerland (A.O.vB.,M.A.G). Dept. Neurosurgery, University Hospital Zurich, CH-8091 Zurich, Switzerland (K.F.). Dept. Pediatric Haemotology and Oncology, University Medical Center Hamburg-Eppendorf, D-20246 Hamburg, Germany (A.O.vB.,S.R.)

[#]These authors contributed equally

Status of the manuscript: Neuro-Oncology 13(9):1000-1010, 2011

Author contribution K. Orlowski:
Seeding and treatment of medulloblastoma cell lines with patupilone for further analysis of the cell cycle leading to figure 2. Involved in proof-reading of the manuscript.

Neuro-Oncology 13(9):1000–1010, 2011.
doi:10.1093/neuonc/nor069
Advance Access publication July 9, 2011

The microtubule stabilizer patupilone (epothilone B) is a potent radiosensitizer in medulloblastoma cells

Christoph Oehler[a], André O. von Bueren[a], Polina Furmanova[a], Angela Broggini-Tenzer[a], Katrin Orlowski, Stefan Rutkowski, Karl Frei, Michael A. Grotzer, and Martin Pruschy

Department of Radiation Oncology, University Hospital Zurich (C.O., P.F., K.O., A.B-T., M.P.), Department of Pediatric Oncology, University Children's Hospital (A.O.vB., M.A.G), Department of Neurosurgery, University Hospital Zurich (K.F.), Zurich, Switzerland; Department of Pediatric Haemotology and Oncology, University Medical Center Hamburg-Eppendorf, Hamburg, Germany (A.O.vB., S.R.).

Concurrent radiochemotherapy for medulloblastoma includes the microtubule disrupting agent vincristine; however, vincristine alone or as part of a combined treatment regimen is highly toxic. A major goal is therefore to replace vincristine with novel potent chemotherapeutic agents—in particular, with microtubule stabilizing and destabilizing compounds—with a larger therapeutic window. Here, we investigated the antiproliferative, cytotoxic and radiosensitizing effect of patupilone (epothilone B [EPO906]), a novel, non–taxane-related and nonneurotoxic microtubule-stabilizing agent in human medulloblastoma cell lines. The antiproliferative and cytotoxic effects of patupilone alone and in combination with ionizing radiation was determined in the 3 representative human medulloblastoma cell lines D341Med, D425Med, and DAOY. Patupilone alone effectively reduced the proliferative activity and clonogenicity of all medulloblastoma cell lines tested at picomolar concentrations (50–200 pM) and resulted in an at least additive anticlonogenic effect in combination with clinically relevant doses of ionizing radiation (2 or 5 Gy). Cell-cycle analysis revealed a sequential G2-M arrest and sub-G1 accumulation in a dose- and treatment-dependent manner after exposure to patupilone. In tumor xenografts derived from D425Med cells, a minimal treatment regimen with patupilone and fractionated irradiation (1 × 2 mg/kg plus 3 × 3 Gy) resulted in an extended tumor growth delay for the 2 single treatment modalities alone and a supra-additive treatment response for the combined treatment modality, with complete tumor regressions. These results demonstrate the potent efficacy of patupilone against medulloblastoma cell lines and indicate that patupilone represents a promising candidate to replace vincristine as part of a combined treatment strategy with ionizing radiation.

Keywords: apoptosis, autophagy, ionizing radiation, medulloblastoma, patupilone.

Medulloblastoma is the most common malignant brain tumor of childhood.[1] Standard therapy for medulloblastoma comprises neurosurgical resection, radiotherapy, and chemotherapy. However, nearly one-half of all patients die of progressive disease, and survivors experience considerable adverse effects,[2–4] including radiation-dependent reduction of neurocognitive performance.[5–8] Medulloblastoma is a relatively radiation sensitive tumor entity. Concurrent radiochemotherapy for medulloblastoma often includes the microtubule-disrupting agent vincristine. However, use of vincristine alone or as part of a combined treatment regimen is highly toxic;[3,9] therefore, treatment modifications have been reported frequently.[10–12] Of note, excellent outcomes were reported in a multi-institution phase II trial in which patients with average- and high-risk medulloblastoma were treated with risk-adapted craniospinal radiotherapy without concurrent vincristine therapy. In this trial, vincristine was only part of the dose-intensive postirradiation treatment (cyclophosphamide, cisplatin, and vincristine), challenging the value of concomitant vincristine treatment during radiotherapy.[13] Therefore, a major goal is to replace vincristine,

Received July 13, 2010; accepted March 18, 2011.

[a]These authors contributed equally to the study.

Corresponding Author: Prof. Dr. Martin Pruschy, Laboratory for Molecular Radiobiology, Department of Radiation Oncology, University Hospital Zurich, CH-8091 Zürich, Switzerland (martin.pruschy@usz.ch).

as part of multimodality treatment regimens, with novel potent chemotherapeutic agents, such as carboplatin, which is under clinical investigation, either a) together with vincristine during craniospinal radiotherapy—as in the COG 99701 trial (ClinicalTrials.gov number NCT00003203) for patients with metastatic medulloblastoma[14]— b) with the aim of substituting vincristine during craniospinal radiotherapy—as in the future SIOP-Europe PNET 6 medulloblastoma study for "standard-risk" patients with medulloblastoma—or c) with other promising microtubule-stabilizing and -destabilizing agents, which have been investigated thoroughly in the preclinical setting and which show promising activity against a panel of xenograft-derived embryonal tumors.[15]

Patupilone (epothilone B [EPO906]), which is currently being tested in phase III clinical trials,[16] is a novel microtubule-targeting cytotoxic agent that is structurally unrelated to paclitaxel and docetaxel. Patupilone is 3–20 times more potent than the taxanes in vitro and has shown a safe toxicity profile in adults.[17] Patupilone stabilizes preformed microtubules and leads to aberrant spindle formation during mitosis. Patupilone has been shown to induce regression of various types of human tumors in vivo, including glioma, lung, colon, breast, prostate, and ovarian carcinomas. Of note and in contrast to paclitaxel, patupilone is equally cytotoxic to paclitaxel-susceptible and paclitaxel-resistant cells that display a multidrug-resistance phenotype due to overexpression of the P-glycoprotein (P-gp) efflux pump.[17] The combined treatment with patupilone and ionizing irradiation showed a supra-additive effect in vitro and in vivo in lung and colon carcinoma models.[18,19] Combination of ionizing radiation and patupilone has also been tested in a phase I trial involving brain tumors.[20]

We investigated the efficacy of patupilone alone and in combination with ionizing radiation in different human medulloblastoma cell lines. We showed that patupilone alone is extremely potent at picomolar concentrations in medulloblastoma cell lines, and combined treatment with clinically relevant doses of ionizing radiation results in an at least additive anticlonogenic effect in vitro and induces a strong supra-additive treatment response in vivo.

Materials and Methods

Cell Cultures, Reagents, and Irradiation

Patupilone was kindly provided by Novartis Pharma. D425Med human medulloblastoma cells were purchased from the American Type Culture Collection. D341Med and D425Med human medulloblastoma cells were the kind gift of Dr Henry Friedman (Duke University). All medulloblastoma cells were cultured in Richter's zinc option medium supplemented with 10% fetal bovine serum (nonessential amino acids were added to the medium of D341Med and D425Med cells to a final concentration of 1%). All cell cultures were maintained at 37°C in a humidified atmosphere with 5% CO_2.

For in vitro assays, a stock solution (1 mM) of patupilone was prepared in DMSO and further diluted with water/DMSO- and serum-containing media. Irradiation was performed at room temperature, using a Pantak Therapax 300 kV X-ray unit at 0.7 Gy/min. 3-Methyladenine (Sigma) was prepared in water at a stock solution of 100 mM and further diluted in serum-containing media. Bafilomycin-1 (Sigma) was prepared in DMSO at a stock solution of 100 μM and further diluted in serum-containing media. The broad-range caspase inhibitor z-VAD-FMK (Calbiochem; Merck Chemicals) was prepared in DMSO at a concentration of 10 μM and further diluted in serum-containing media.

Cell Proliferation, Clonogenic Cell Survival, and Cell Viability Assay

Proliferative activity was assessed in 96-well F-plates using the Alamar Blue (Biosource International) and MTS assays (Promega). Absorption was measured at 570 and 630 nm (Alamar blue) using a GenTec spectrophotometer or at 490 nm (MTS) using a microplate spectrophotometer (Molecular Devices).[19,30,31] The half-maximal inhibitory concentration (IC_{50}) values were calculated from the regression curve using GraphPad Prism software, version 4 (GraphPad Software).[30] Each experiment was performed at least in triplicate. For the cell viability assay, 400 000 or 500 000 cells were seeded and treated 24 h thereafter. Cell viability was determined 72 h after treatment began using the trypan blue exclusion assay. Each experiment was performed at least in duplicate. To determine clonogenic cell survival, the number of single-seeded cells was adjusted to obtain 100 colonies per cell culture dish with a given treatment. After treatment with different regimens, cells were maintained at 37°C in a humidified atmosphere containing 5% CO_2 and allowed to grow for 14 days before fixation in methanol/acetic acid (ratio, 75%:25%) and staining with crystal violet. Only colonies with >50 cells/colony were counted. For combined treatment, cells were pre-incubated with patupilone or control solution 1 h before irradiation. Clonogenic cell survival assays were repeated as independent experiments at least twice.

Cell-Cycle Analysis

For cell-cycle analysis, medulloblastoma cells were treated with patupilone for 6, 12, and 24 h, respectively. Both floating and adherent cells were collected. After washing twice in phosphate-buffered saline (PBS), cells were stained with propidium iodide (50 μg/mL) (Becton-Dickinson) in PBS containing 100 U/mL RNase A (Qiagen) for 30 min at room temperature. The percentage of cells in the different phases of the cell cycle was determined by evaluating DNA content, as described elsewhere.[30,31]

Caspase-3 Activity Assay

Asp-Glu-Val-Asp (DEVD)ase activity was determined in cytosolic cell extracts. Cells were treated with increasing concentrations of patupilone for 6, 12, 24, and 48 h. Cells were harvested thereafter by trypsin/EDTA, centrifuged, and washed with precooled PBS. The cell pellet was suspended in 5 volumes of precooled buffer A (20 mM HEPES-KOH [pH 7.5], 10 mM KCl, 1.5 mM MgCl2, 1 mM sodium EDTA, 1 mM sodium EGTA, 1 mM dithiothreitol [DDT], 250 mM sucrose, and 0.1 mM phenylmethylsulfonyl fluoride [PMSF] supplemented with protease inhibitors [5 mg/mL pepstatin A, 10 mg/mL leupeptin, 2 mg/mL aprotinin, 2 mg/mL DTT, and 1 mM of PMSF]). After incubation on ice for 15 min, the cells were disrupted by freezing and thawing. Cell lysates were centrifuged at 1000 *g* for 10 min at 4°C, and the supernatant was further centrifuged at 100 000 *g* for 30 min. The resulting supernatant (S-100 fraction) was stored at −80°C. To determine caspase 3-like activity, 75 μg of protein from the S-100 fraction was incubated at 37°C with the colorimetric caspase 3 substrate N-acetyl-Asp-Glu-Val-Asp p-nitroanilide (100 mM; Ac-DEVD-pNA; Calbiochem) and 1 mM dATP in a final volume of 120 μL. Cleavage of the caspase substrate was monitored at 405 nm using a GenTec spectrophotometer.

Detection and Quantification of Acidic Vesicular Organelles (AVOs) with Acridine Orange

To detect and quantify AVOs, cellular vital staining with acridine orange was performed. In acridine orange-stained cells, the cytoplasm and nucleolus fluoresce bright green and dim red, whereas the acidic compartments fluoresce bright red.[32] The intensity of the red fluorescence isproportional to the degree of acidity and/or the volume of the cellular acidic compartment and was measured 6, 12, 24, and 48 hafter exposure to patupilone alone or 48 h after treatment with patupilone combined with ionizing radiation. After treatment with patupilone alone or in combination with irradiation, both adherent and suspended cells were stained at the indicated time points with acridine orange (1 mg/mL) for a period of 15 min, harvested by trypsin/EDTA, and collected in PBS. As a negative control, 0.5 μM bafilomycin A1 (Sigma) was added 30 min before acridine orange staining. Green (510–530 nm) and red (465 nm) fluorescence emission from 5×10^5 cells illuminated with blue (488 nm) excitation light was measured with a FACS Calibur from Becton Dickinson using CellQuest software. The ratio of red to green fluorescence was determined in control and treated cells and normalized in relation to untreated cells.

Tumor Xenograft in Nude Mice and Application of Treatment Regimes

D425Med cells (6×10^6) were injected subcutaneously on the backs of 4–6-week-old athymic nude mice. Tumor volumes were determined from caliper measurements of tumor length (L) and width (l) according to the formula $(L \times l^2)/2$. Tumors were allowed to expand to a volume of 200 mm^3 (±10%) before treatment start. With the use of a customized shielding device, mice were given strictly loco regional radiotherapy of 3 × 3 Gy on 3 consecutive days using a Gulmay 200 kV X-ray unit at 100 cGy/min at room temperature. Patupilone (2 mg/kg; dissolved in 30% PEG-300/70% saline) was applied intravenously 24 h before the first treatment with ionizing radiation (at day 0 of the treatment; $n = 5$ per group). Tumor growth was monitored daily.

Results

Patupilone Strongly Reduces Proliferation and Viability in Human p53wt and p53mt Medulloblastoma Cell Lines

The antiproliferative effect of the microtubule-stabilizing agent patupilone was tested in the 3 representative human medulloblastoma cell lines D341Med, D425Med, and DAOY. Patupilone reduced the proliferative activity in the D341 cell line, with an IC_{50} of 0.53 nM (95% confidence interval [CI], 0.45–0.62) (Fig. 1A); in the D425Med cell line, with an IC_{50} of 0.37 nM (95% CI, 0.14–0.96) (Fig. 1B); and in the DAOY cell line, with an IC_{50} of 0.19 nM (95% CI, 0.12–0.29) (Fig. 1C). Likewise, cell viability, as detected by trypan blue exclusion, was reduced to 50% when treated with subnanomolar concentrations of patupilone (D341Med, 0.25 nM; D425Med and DAOY, 0.1 nM) (Fig. 1D–F). Of note, up to 10-fold higher IC_{50} values were obtained when the different cell lines were treated with the microtubule-destabilizing agent vincristine (Supplement 1).

Next, clonogenic cell survival was determined in the 3 cell lines after treatment with increasing concentrations of patupilone. In the D341Med cell line, the effect of patupilone on clonogenic survival was at dose range of patupilone similar to the level of proliferative activity and viability (IC_{50}, 0.50–0.75 nM). However, the clonogenicity of D425Med and DAOY cells was already strongly reduced at a 10-fold lower concentration of patupilone (IC_{50}, 30 pM) (Fig. 1G, H). These results overall demonstrate that patupilone is highly potent against different medulloblastoma cell lines. These medulloblastoma cell lines differ in the expression of and mutations in specific genes (eg, p53, c-myc). However, a differential treatment sensitivity so far cannot be attributed to a specific genetic background.[21]

Patupilone Sequentially Induces a G2-M-Phase Arrest and Apoptosis in Medulloblastoma Cell Lines

To investigate patupilone-induced alterations of cell cycle progression, we determined the cell-cycle distribution over time in the 3 medulloblastoma cell lines following treatment with low and high concentrations of patupilone (0.1–1 nM). Low-dose treatment with patupilone

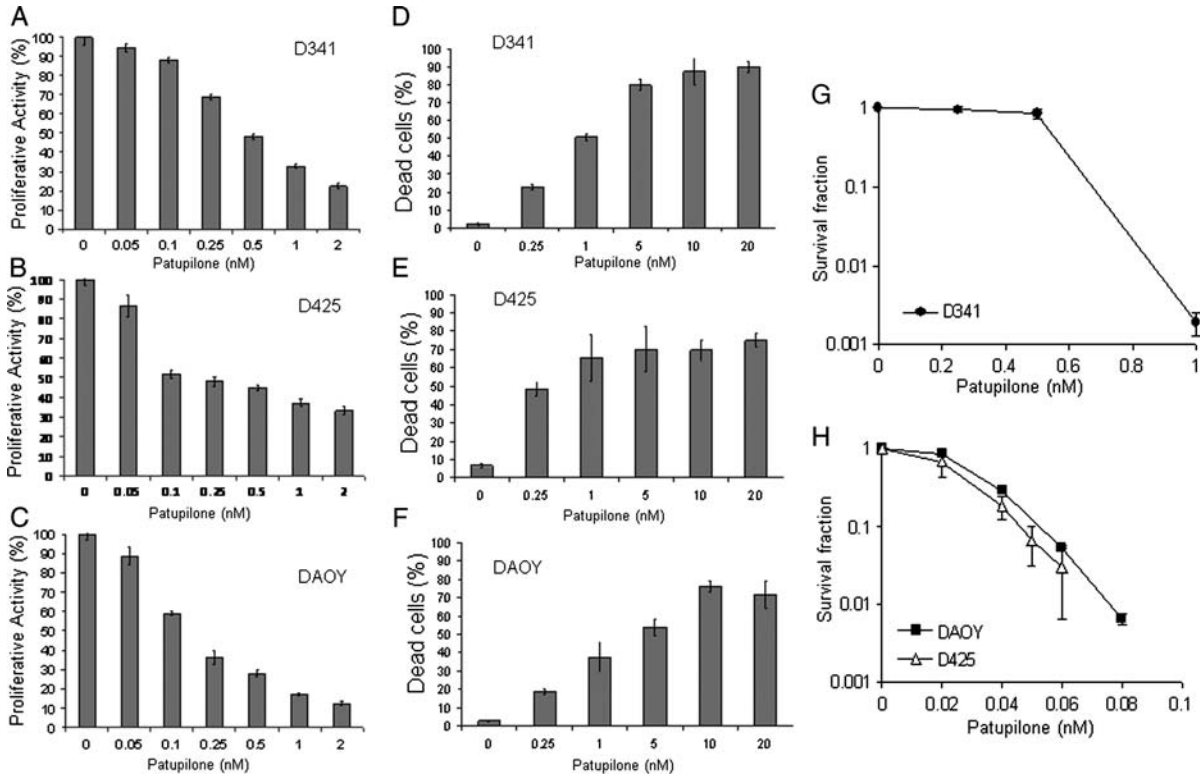

Fig. 1. Antiproliferative and cytotoxic effects of patupilone in human medulloblastoma cell lines. A–C, D341Med (A), D425Med (B), and DAOY (C) human medulloblastoma cells were treated with increasing doses of patupilone, and the antiproliferative activity was determined after 72 h of exposure. D–F, D341Med (D), D425Med (E), and DAOY (F) human medulloblastoma cells were treated with increasing doses of patupilone, and cell viability was determined by trypan blue exclusion after 72 h of exposure. (G) Clonogenicity of the D341Med cells after treatment with increasing doses of patupilone. (H) Clonogenicity of the D425Med and DAOY cells after treatment with increasing doses of patupilone. Results of a representative experiment are shown ($n = 3$).

resulted in minor changes in cell-cycle distribution in all 3 cell lines but also in a small accumulation of cells in a sub-G1-peak in the D341Med and D425Med cell population, which is indicative of apoptosis. On the other hand, exposure to increased concentrations of patupilone resulted in extended G2-M-phase accumulation in all 3 medullobastoma cell lines (D341Med and DAOY cell lines, 1 nM; D425Med cell line, 0.5 nM patupilone) (Fig. 2). Twelve hours after patupilone exposure, 33.3% (D341Med), 40.6% (D425Med), and 46.2% (DAOY) of cells were accumulated in the G2-M phase, compared with 16.5% (D341Med), 26.3% (D425Med), and 17.5% (DAOY) of the untreated cell populations (see Table I). Accumulation of cells in the G2-M phase was most prominent in the DAOY cell line, probably because of an inactive G1 checkpoint. After the patupilone-induced G2-M-phase redistribution, extended accumulation of cells in a subG1-peak was observed in the D341Med and DAOY cells after treatment with 1 nM patupilone and in the D425Med cells after treatment with 0.5 nM of patupilone, again indicative of patupilone-induced, late apoptosis. These results demonstrate a dose-dependent sequential antiproliferative and cytotoxic effect of patupilone in the medulloblastoma cell lines.

Patupilone Induces Apoptosis and Autophagy in Medulloblastoma Cell Lines

To further investigate patupilone-induced apoptosis, caspase-3 activity was assessed in the 3 medulloblastoma cell lines treated with the same concentrations as used for FACS analysis (see above). Caspase-3 activity was increased over time in the D425Med and the DAOY cell lines (Fig. 3B and 3C) and, to a smaller extent, in

Table 1. Cell-cycle analysis following treatment with high doses of patupilone.

Cell line		0 h (%)	12 h (%)	24 h (%)
D341	G0-1	53	30.22	42.53
	G2-M	17	33.26	12.55
	S	30	36.52	44.92
	sub-G1	0.6	16.85	26.03
D425	G0-1	39.7	15.36	21.52
	G2-M	26	40.65	21.74
	S	34	44	56
	sub-G1	2	22.47	38.32
DAOY	G0-1	35	25.2	44.87
	G2-M	17.5	46.21	25.05
	S	47	28.6	30.08
	sub-G1	1	16.6	14.79

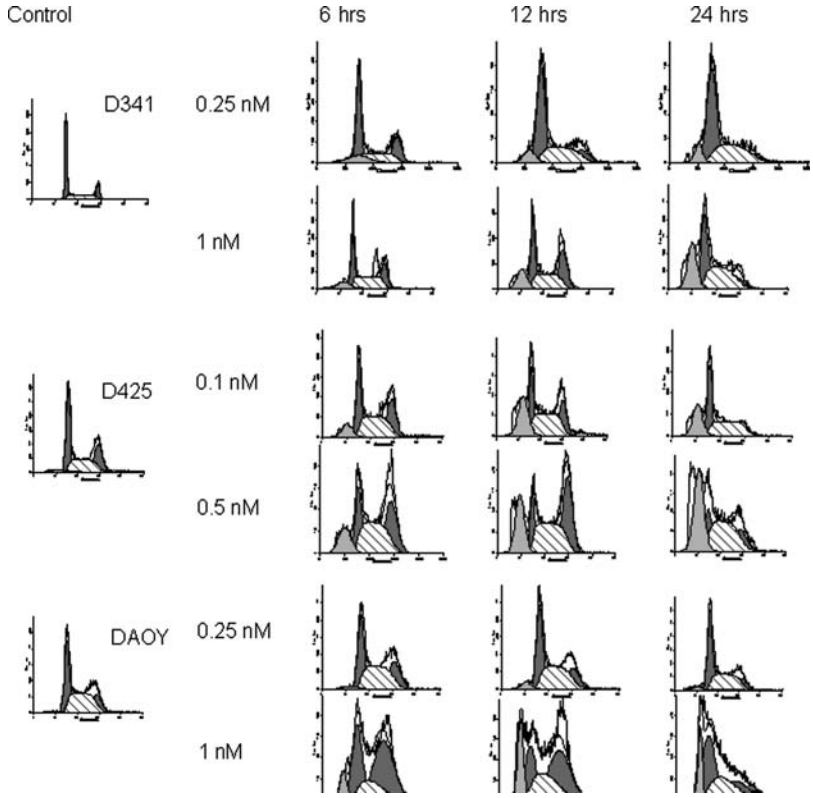

Fig. 2. Cell-cycle analysis after treatment with patupilone. Human medulloblastoma cell lines D341Med (top row), D425Med (middle row), and DAOY (bottom row) were treated with patupilone at low concentrations (D425Med and DAOY, 0.1 nM; D341Med, 0.25 nM) or high concentrations (D425Med, 0.5 nM; D341Med and DAOY, 1 nM) and subjected to cell-cycle determination by propidium iodide staining and FACS analysis at the indicated time points.

the D341Med cell line, reflecting the outcome of subG1-accumulation, as obtained by FACS analysis (Fig. 3A). Of note, pretreatment with the broad-range caspase inhibitor z-VAD-FMK did not rescue D425Med or DAOY cell lines from undergoing cell death, as assessed by the trypan blue viability assay (data not shown).

Comparable treatment sensitivity but a reduced amount of apoptosis in the D341Med cell line suggested another form of cell death induced by patupilone in this cell line. As a marker for autophagy, the fractional volume of acidic vesicular organelles (AVO) in control and patupilone-treated cells was quantified. A time-dependent increase in the amount of AVOs was exclusively observed in the D341Med (Fig. 3D) but not in the D425Med and DAOY medulloblastoma cell lines (Fig. 3E and 3F). To inhibit the autophagic process induced by patupilone, cells were pretreated with bafilomycin A1, which prevents the fusion of autophagosomes with lysosomes. High concentrations of bafilomycin A1 alone (100 nM) were not toxic to the D341Med cells, but interestingly, pretreatment with bafilomycin A1 strongly sensitized D341Med cells to patupilone (0.5 nM), resulting in nearly 100% dead cells (Supplementary Fig. S1). To determine a putative switch to apoptotic cell death after inhibition of autophagy, caspase-3 activity was assessed in cells pretreated with bafilomycin A1. No additional increase in caspase-3 activity could be detected after patupilone treatment (data not shown). These results suggest that after a G2-M-phase arrest, patupilone induces late apoptosis in the medulloblastoma cell lines D425Med and DAOY. On the other hand, D341Med cells are apoptosis resistant, and patupilone-induced autophagy might initially protect these cells from undergoing cell death not related to apoptosis.

Patupilone Sensitizes Medulloblastoma Cell Lines to Ionizing Radiation

Patupilone is a promising agent for combined treatment with ionizing radiation. We therefore investigated its antitumor effect in these 3 medulloblastoma cell lines in combination with increasing doses of ionizing radiation. The D341Med cell line was clearly more radiosensitive than the D425Med and DAOY cell lines with regard to the level of proliferative activity, viability, and clonogenic survival (Fig. 4A–C). On the level of the short-term end points (ie, proliferative capacity and viability), the combined treatment modality induced an additive effect in the D341Med cell line but not in the D425Med and DAOY cell lines (Fig. 4A–F). More

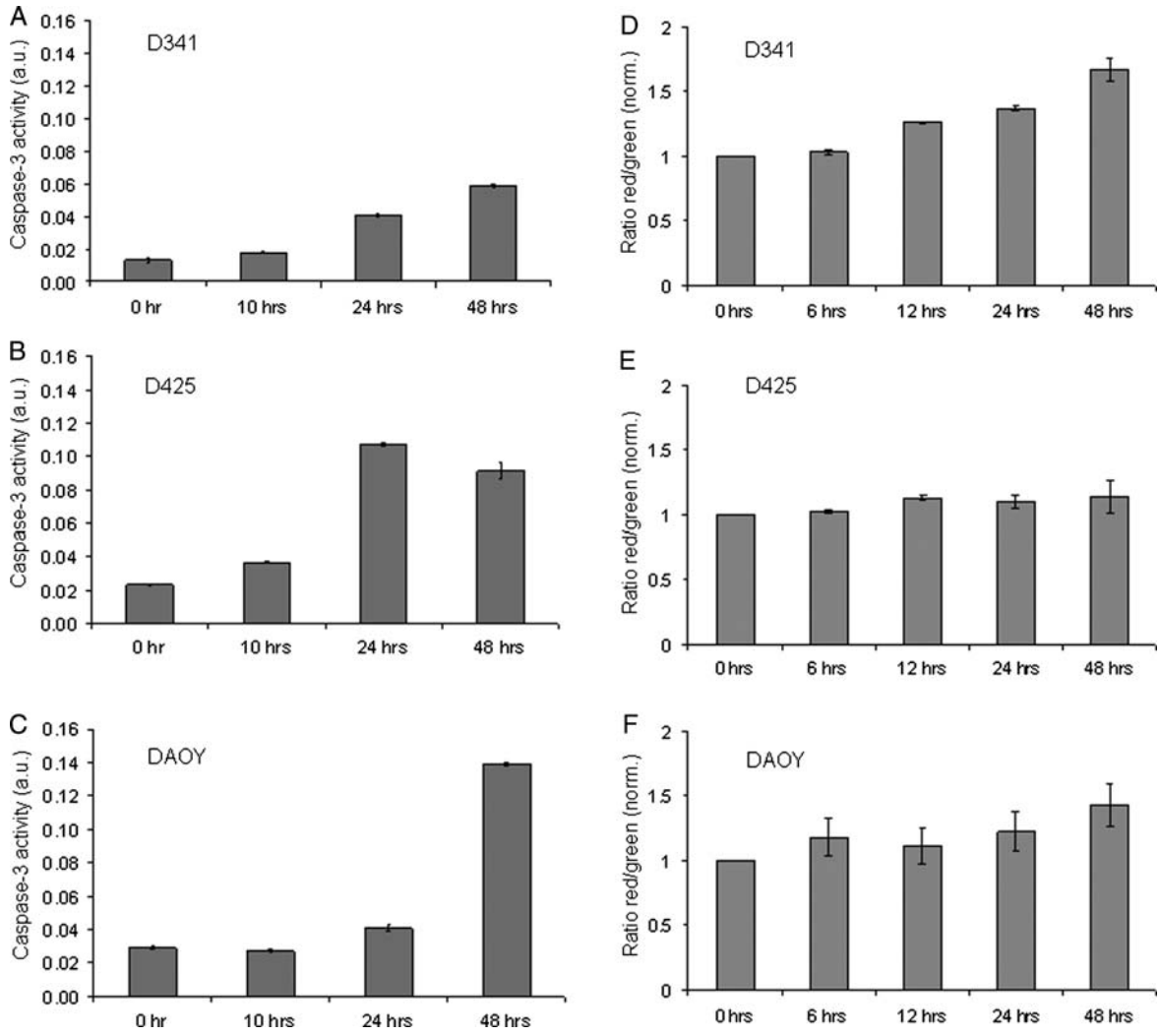

Fig. 3. Caspase-3 activity and formation of acidic vesicular organelles (AVOs) after treatment with patupilone. Caspase-3 activity in patupilone-treated medulloblastoma cells (D341Med [A], D425Med [B], and DAOY [C]) was determined at the indicated time points. (D–F) AVO formation was determined in patupilone-treated medulloblastoma cells ([D] D341Med, 1 nM; [E] D425Med, 0.5 nM; [F] DAOY, 1 nM). Green (510–530 nm) and red (465 nm) fluorescence emission from 5×10^5 cells illuminated with blue (488 nm) excitation light was measured with a FACSCalibur at the indicated time points.

important, combined treatment reduced clonogenicity in all cell lines in an at least additive and comparable extent. As expected from the response to patupilone alone (see above), the D425Med and DAOY cell lines were sensitized to ionizing radiation at a 10-fold lower concentration of patupilone, compared with the D341Med cells (Fig. 4G–I). On the basis of the additive effects of combined treatment on the level of cell viability and clonogenicity, caspase-3 activity and the fractional volume of acidic vesicular organelles were determined in response to treatment. Caspase-3 activity in response to irradiation was least induced in the DAOY cells; however, no additive caspase-3 activation could be observed in all 3 cell lines in response to combined treatment with ionizing radiation (Fig. 5A–C). The autophagy-related end point was most prominently induced in the D341Med cell line in response to irradiation (Fig. 5D–F); however, a minor additive effect could only be detected in the D425Med cell line in response to the combined treatment modality. Overall, these data demonstrate that patupilone enhances the effect of ionizing radiation in human medulloblastoma cell lines with regard to viability and clonogenicity. However, combined treatment of these meduloblastoma cell lines does not result in enhanced amounts of apoptosis or autophagy in these cell lines.

Radiosensitizing Effect of Patupilone on Tumor Xenografts

To determine an at least additive effect of the combined treatment modality in vivo, a combined treatment regimen with patupilone and ionizing radiation

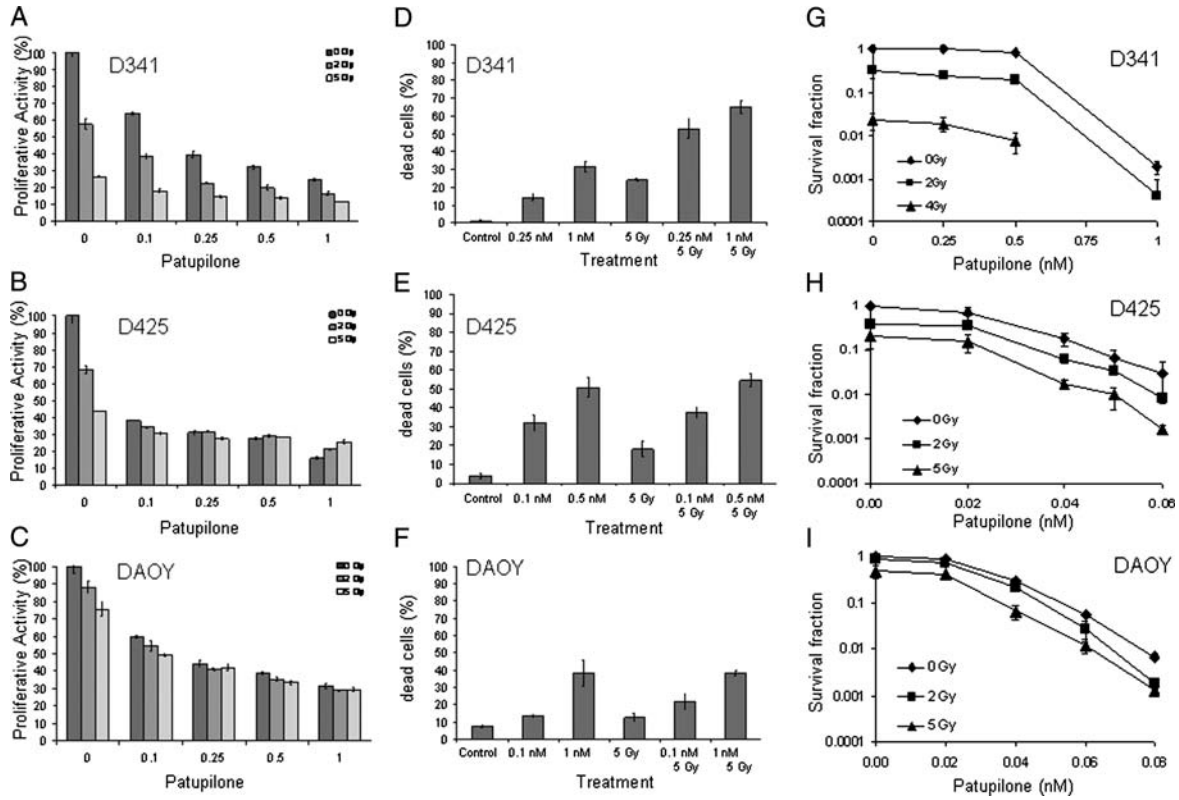

Fig. 4. Antiproliferative and cytotoxic effect of patupilone in combination with ionizing radiation. (A–C) Human medulloblastoma cell lines D341Med (A), D425Med (B), and DAOY (C) were treated with patupilone alone or in combination with clinically relevant doses of ionizing radiation (2–5 Gy). Patupilone was added 30–60 min before irradiation. The antiproliferative activity was determined after 72 h of exposure. (D–F) Human medulloblastoma cell lines D341Med (D), D425Med (E) and DAOY (F) were treated with patupilone at low (D425Med and DAOY, 0.1 nM; D341Med, 0.25 nM) or high (D425Med, 0.5 nM; D341Med and DAOY, 1 nM) concentrations, alone or in combination with ionizing radiation (5 Gy), and cell viability was determined by trypan blue exclusion after 72 h of exposure. (G–H) Clonogenicity of human medulloblastoma cells after treatment with increasing doses of patupilone or in combination with ionizing radiation.

was tested against xenografts derived from human D425Med medulloblastoma cells, which were subcutaneously injected into the backs of nude mice. Treatment was started when tumors reached a minimal size of 200 $mm^3 \pm 10\%$ (on days 20–27 after cell injection). In vivo studies were performed with loco regional application of ionizing radiation using a shielding device and a minimal fractionated treatment regimen of 3 Gy on 3 consecutive days. This daily dose is applied when fractionated radiotherapy is used for the treatment of human malignancies. For practical reasons only 3 fractions were chosen as the treatment regimen, but the response to such a regimen was previously found to be useful for treatment evaluation.[19] Fig. 6 summarizes the effect of tumor treatment with patupilone alone (2 mg/kg patupilone once), ionizing radiation alone (vehicle combined with 3×3 Gy), and patupilone and ionizing radiation in combination (2 mg/kg once combined with 3×3 Gy), compared with a vehicle alone–treated control group. Patupilone was applied 24 h before the first of 3 fractions of irradiation applied on 3 consecutive days. Determination of treatment-related body weight changes did not reveal a patupilone-dependent transient weight loss after patupilone application (data not shown), and no skin changes or tissue damage were observed in the co-irradiated healthy tissue area around the tumor during the follow-up period of tumor growth. Treatment with patupilone or ionizing radiation alone resulted in a partial tumor growth suppression over 10 days, whereas combined treatment exerted a strong supra-additive tumor growth control, with complete tumor regression in the follow-up period ($P < .005$, for ionizing radiation or patupilone alone vs combined treatment) (Fig. 6). Interestingly, tumors only slowly regressed after the end of treatment, coinciding with the in vitro results that treatment-induced apoptosis might only play a minor role for the treatment response of these medulloblastoma cells to ionizing radiation and patupilone. Complete visible tumor regression was observed in all mice treated with the combined treatment modality. In 2 of 5 mice, slow-growing tumor recurrences could be observed 25–30 days after the start of treatment. No recurrences at all occurred in the remaining cohort of mice treated with the combined treatment modality (data not shown). Overall, these results demonstrate that patupilone might be a promising alternative for a combined treatment regimen using microtubule inhibitors and ionizing radiation.

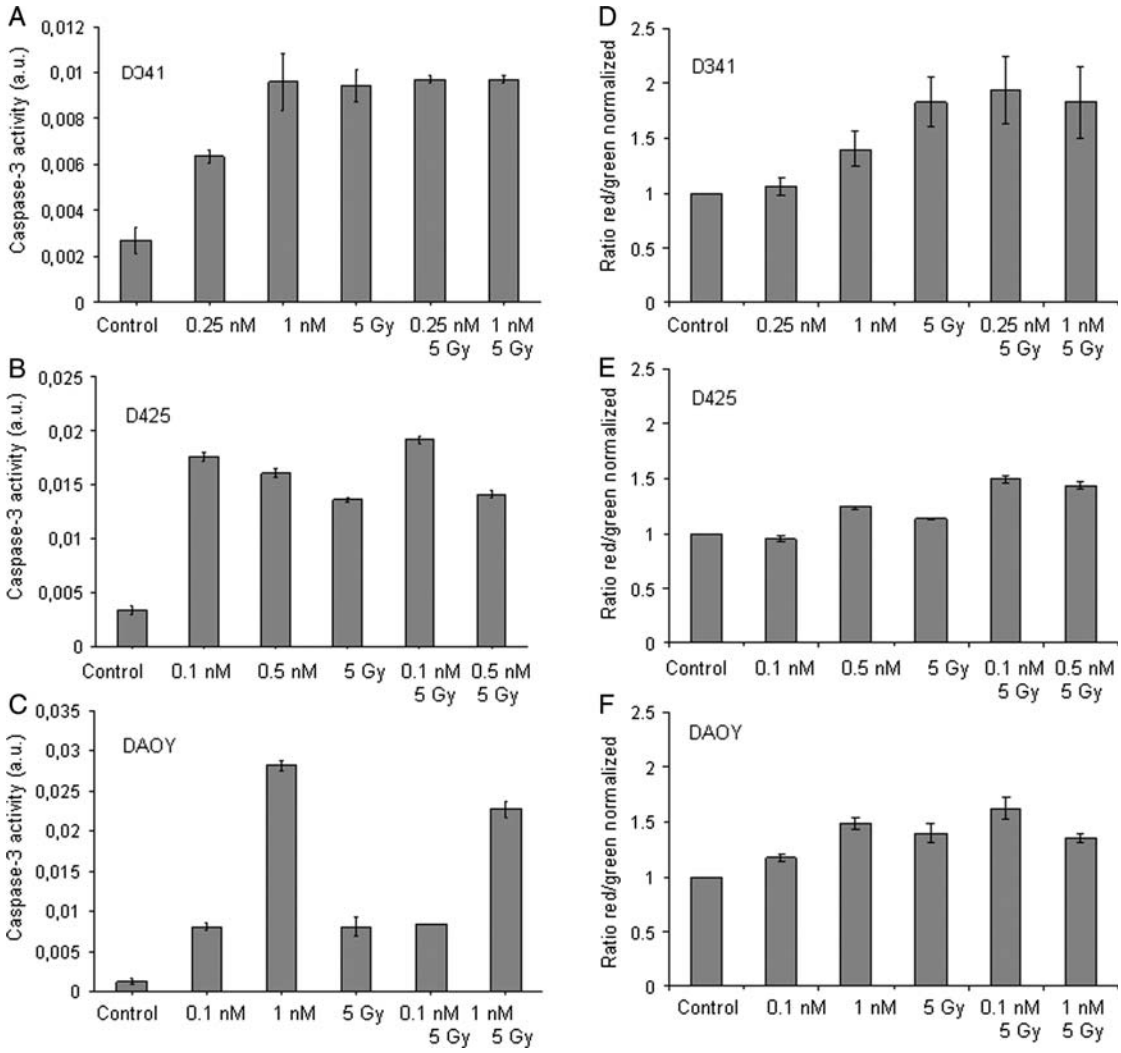

Fig. 5. Apoptosis and autophagy after combined treatment with patupilone and ionizing radiation. (A–C) Human medulloblastoma cell lines D341Med (A), D425Med (B), and DAOY (C) were treated with patupilone at low (D425Med and DAOY, 0.1 nM; D341Med, 0.25 nM) or high (D425, 0.5 nM; D341Med and DAOY, 1 nM) concentrations, alone or in combination with ionizing radiation. Caspase-3 activity was determined after 48 h. (D–F) Human medulloblastoma cell lines D341Med (D), D425Med (E), and DAOY (F) were treated with patupilone at low (D425Med and DAOY, 0.1 nM; D341Med, 0.25 nM) or high (D425Med, 0.5 nM; D341Med and DAOY, 1 nM) concentrations, alone or in combination with ionizing radiation. Green (510–530 nm) and red (465 nm) fluorescence emission from 5×10^5 cells illuminated with blue (488 nm) excitation light was measured with a FACSCalibur at the indicated time points or after 48 h.

Discussion

Vincristine-associated side effects in medulloblastoma have led to an intense search for novel microtubule-interfering agents with radiosensitizing potential and devoid of toxicities. Here, we investigated the effect of the novel clinically relevant microtubule inhibitor patupilone alone and in combination with ionizing radiation on 3 human medulloblastoma cell lines and determined a strong cytotoxic potency of patupilone at picomolar concentrations. Importantly, patupilone was 10-fold more potent than vincristine at inhibiting proliferation at subnanomolar concentrations (IC_{50} for patupilone, 0.1–0.25 nM; IC_{50} for vincristine, 1–1.4 nM) in all medulloblastoma cell lines tested. Cell-cycle analysis revealed that patupilone sequentially induced a strong G2-M-phase arrest in all cell lines, followed by signs of apoptosis in the 2 medulloblastoma cell lines D425Med and DAOY. In combination with ionizing radiation, an at least additive cytotoxic effect against both radiation-susceptible and radiation-resistant medulloblastoma tumor cell lines was observed. These results demonstrate a potent cytotoxic effect of patupilone alone and in combination with ionizing radiation, and they suggest that such a combined treatment modality qualifies for additional preclinical and clinical testing in medulloblastoma. Patupilone and other epothilone-derivatives are currently being tested in clinical phase II/III trials in adults, and there is an ongoing phase

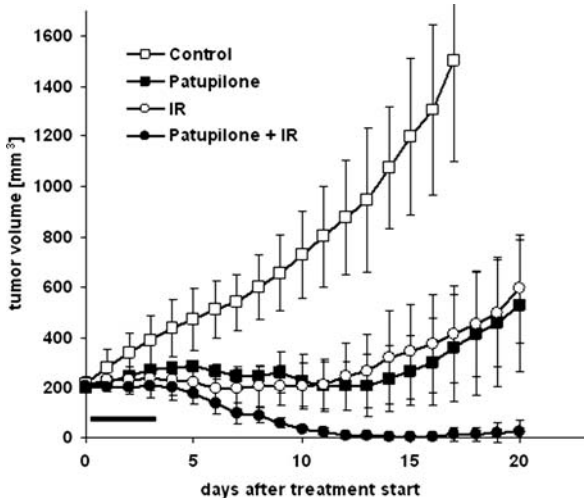

Fig. 6. The effect of patupilone and ionizing radiation alone or in combination on the growth of D425Med-derived xenografts in nude mice. Mice were treated with patupilone (2 mg/kg once) and ionizing radiation (3 × 3 Gy on consecutive days), alone and in combination, with administration of patupilone or the vehicle 24 h prior to the first fraction of ionizing radiation. The horizontal bar indicates days of treatment. Each curve represents the mean tumor volume per group ± standard error.

I/II trial of combined treatment with patupilone and radiotherapy in brain tumors.

We previously investigated the cytotoxic effect of patupilone alone or as part of a combined treatment modality with ionizing radiation against tumor cells derived from different tumor entities. Interestingly, the combination of patupilone with ionizing radiation resulted only in an additive cytotoxic effect against various cancer cell types only in vitro, but it resulted in a supra-additive tumor growth delay when tested against tumor xenografts derived from the same tumor cells as those tested in vitro.[18,19] To the same extent, we could also now demonstrate an at least additive effect on combined treatment in the medulloblastoma cell lines in vitro and, more important, a strong supra-additive treatment response, including complete tumor regressions in tumor xenografts treated with a minimal combined treatment regimen in vivo. The accumulation of tumor cells in the most radiosensitive G2-M phase of the cell cycle represents the major rational for the sensitization to ionizing radiation,[22–24] although other, S-phase progression-related mechanisms have also been observed.[19] Additional anti-vascular and anti-angiogenic effects might contribute to the supra-additive tumor growth delay observed in vivo, and in fact, direct targeting of endothelial cells[25–27] and indirect, anti-angiogenic interference with the secretion of pro-angiogenic factors from tumor cells have been proposed.

Interestingly, the semisynthetic epithilone B derivative ixabepilone has previously been investigated against several pediatric cancer models and revealed broad-spectrum activity.[15] To our knowledge, this is the first report to have investigated the potency of patupilone alone and in combination with ionizing radiation in medulloblastoma cell lines and tumor xenografts, and we observed a differential cell line–dependent response with regard to the patupilone-induced mode of cell death. A strong G2-M-phase arrest was induced in all cell lines by patupilone 6 and 12 h after the commencement of treatment with low subnanomolar concentrations (0.1–1 nM). However, we also observed an initial longer-lasting accumulation of cells in the radioresistant S-phase in D425Med and D341 cell lines (data not shown), as previously manifested in other tumor cells in response to low-dose treatment with patupilone.[19] The combined treatment with ionizing radiation in all cell lines resulted in an at least additive cytotoxic effect. After G2-M-phase arrest, patupilone potently induced apoptosis in the D425Med and the DAOY medulloblastoma cell lines, as indicated by caspase-3 activation and the occurrence of a subG1-peak cell population by flow cytometry. The D341Med medulloblastoma cell line was less susceptible to patupilone in terms of proliferation, clonogenic cell survival, and the apoptosis level, with an IC_{50} of patupilone 10-fold higher than the IC_{50} for the 2 other medulloblastoma cell lines. Interestingly, the fractional volume of patupilone-induced acidic vesicular organelles was increased in this cell line versus the other 2 cell lines, indicating an enhanced patupilone-dependent autophagic process. These medulloblastoma cell lines differ in their expression level and mutations of specific genes; however, a differential treatment sensitivity thus far could not be attributed to a specific genetic background.[21]

In addition to apoptosis, several additional cell death pathways exist, such as autophagy, necrosis, senescence, and mitotic catastrophe. Autophagy, which is also called self-cannibalism, includes the degradation and recycling of intracellular proteins and small organelles. Autophagy may protect cells under the condition of environmental stress but may also lead to cell death. Patupilone only induced autophagy-related acidic vacuolar organelles in the D341Med cells, which were also less susceptible to patupilone, compared with the 2 other medulloblastoma cell lines. Interestingly, interference with autophagy sensitized cells to patupilone-induced cell death, indicating that autophagy acts as a cell-protective rather than a cell death–related response to patupilone in these cells. However, how microtubule-stabilizing agents promote autophagy on the molecular level is far from clear. Only recently, a novel functional link has been suggested between autophagy and microtubules that is relevant for the cellular redistribution of the autophagy related LC3-protein and coordinated fusion of lysosomes and autophagosomes.[28]

Microtubule inhibitors and ionizing radiation also induce mitotic catastrophe as a mode of cell death,[29] because they result in aberrant chromosomal segregation and failed mitosis. Treatment with patupilone led to a strong accumulation of cells in G2-M and multinucleation, as indicators for mitotic catastrophe, which has been identified in all 3 medulloblastoma cell lines (data

not shown). Treatment-induced mitotic catastrophe can also trigger other late cell death end points, including apoptosis and independent of the original cytotoxic insult. Thus, we cannot exclude that patupilone-induced apoptosis in the medulloblastoma cells is a secondary end point and that the cells have already undergone mitotic catastrophe. Because pretreatment of cells with the broad-range caspase inhibitor did not reduce patupilone-induced cell viability, activation of apoptosis-related end points might indeed represent a secondary mode of cell death.

Overall, we demonstrated that patupilone is a very potent cytotoxic agent against several medulloblastoma cells lines, strongly reduces clonogenic survival alone and in combination with ionizing radiation, and induces different modes of cell death in a cell-line-dependent way. The strong treatment response also determined in vivo against tumor xenografts suggests that patupilone is a promising agent for combined treatment modality instead of vincristine and merits further preclinical investigation and eventually clinical evaluation.

Supplementary Material

Supplementary material is available online at *Neuro-Oncology* (http://neuro-oncology.oxfordjournals.org/).

Acknowledgments

Patupilone was kindly provided by Novartis Pharma (Basel, Switzerland). We thank Paul McSheehy for his continuous support of our patupilone-related research program and Oralea Buechi for her technical support with the flow cytometry experiments.

Conflict of interest. The authors declare no conflict of interest.

Funding

We acknowledge the following sources of funding: Oncosuisse, the Radiumfonds, the Swiss National Foundations (to C.O. and M.P.); the Swiss National Fonds, the Swiss Research Foundation Child and Cancer (to A.O.v.B., M.A.G.); German Children's Cancer Foundation/Deutsche Kinderkrebsstiftung (to A.O.v.B., S.R.); and Fonds für Medizinische Forschung UZH (to A.B.-T.)

References

1. Louis DN, Ohgaki H, Wiestler OD, et al. The 2007 WHO classification of tumours of the central nervous system. *Acta Neuropathol (Berl)*. 2007;114(2):97–109.
2. Kuhl J. Modern treatment strategies in medulloblastoma. *Childs Nerv Syst*. 1998;14(1-2):2–5.
3. Packer RJ, Goldwein J, Nicholson HS, et al. Treatment of children with medulloblastomas with reduced-dose craniospinal radiation therapy and adjuvant chemotherapy: a Children's Cancer Group Study. *J Clin Oncol*. 1999;17(7):2127–2136.
4. Reeves CB, Palmer SL, Reddick WE, et al. Attention and memory functioning among pediatric patients with medulloblastoma. *J Pediatr Psychol*. 2006;31(3):272–280.
5. Radcliffe J, Packer RJ, Atkins TE, et al. Three- and four-year cognitive outcome in children with noncortical brain tumors treated with whole-brain radiotherapy. *Ann Neurol*. 1992;32(4):551–554.
6. Silber JH, Radcliffe J, Peckham V, et al. Whole-brain irradiation and decline in intelligence: the influence of dose and age on IQ score. *J Clin Oncol*. 1992;10(9):1390–1396.
7. Chapman CA, Waber DP, Bernstein JH, et al. Neurobehavioral and neurologic outcome in long-term survivors of posterior fossa brain tumors: role of age and perioperative factors. *J Child Neurol*. 1995;10(3):209–212.
8. Dennis M, Spiegler BJ, Hetherington CR, Greenberg ML. Neuropsychological sequelae of the treatment of children with medulloblastoma. *J Neurooncol*. 1996;29(1):91–101.
9. Packer RJ, Sutton LN, Goldwein JW, et al. Improved survival with the use of adjuvant chemotherapy in the treatment of medulloblastoma. *J Neurosurg*. 1991;74(3):433–440.
10. Greenberg HS, Chamberlain MC, Glantz MJ, Wang S. Adult medulloblastoma: multiagent chemotherapy. *Neuro Oncol*. 2001;3(1):29–34.
11. von Bueren AO, von Hoff K, Benesch M, Rutkowski S. Dose reductions of vincristine in children with medulloblastoma treated in the maintenance arm of the prospective multicenter trial HIT'91. *Klin Padiatr*. 2009;221(6):396–397.
12. Zeltzer PM, Boyett JM, Finlay JL, et al. Metastasis stage, adjuvant treatment, and residual tumor are prognostic factors for medulloblastoma in children: conclusions from the Children's Cancer Group 921 randomized phase III study. *J Clin Oncol*. 1999;17(3):832–845.
13. Gajjar A, Chintagumpala M, Ashley D, et al. Risk-adapted craniospinal radiotherapy followed by high-dose chemotherapy and stem-cell rescue in children with newly diagnosed medulloblastoma (St Jude Medulloblastoma-96): long-term results from a prospective, multicentre trial. *Lancet Oncol*. 2006;7(10):813–820.
14. Jakacki RBP, Zhou T, Holmes E, Packer RJ, Goldwein J, et al. Outcome for metastatic (M+) medulloblastoma (MB) treated with carboplatin during craniospinal radiotherapy (CSRT) followed by cyclophosphamide (CPM) and vincristine (VCR): Preliminary results of COG 99701. ASCO Annual Meeting Proceedings Part I, Journal of Clinical Oncology 2007.
15. Peterson JK, Tucker C, Favours E, et al. In vivo evaluation of ixabepilone (BMS247550), a novel epothilone B derivative, against pediatric cancer models. *Clin Cancer Res*. 2005;11(19 Pt 1):6950–6958.
16. Ten Bokkel Huinink WW, Sufliarsky J, Smit WM, et al. Safety and efficacy of patupilone in patients with advanced ovarian, primary fallopian, or primary peritoneal cancer: a phase I, open-label, dose-escalation study. *J Clin Oncol*. 2009;27(19):3097–3103.
17. Rothermel J, Wartmann M, Chen T, Hohneker J. EPO906 (epothilone B): a promising novel microtubule stabilizer. *Semin Oncol*. 2003;30(3 Suppl 6):51–55.

18. Bley CR, Jochum W, Orlowski K, et al. Role of the microenvironment for radiosensitization by patupilone. *Clin Cancer Res*. 2009;15(4):1335–1342.
19. Hofstetter B, Vuong V, Broggini-Tenzer A, et al. Patupilone acts as radiosensitizing agent in multidrug-resistant cancer cells in vitro and in vivo. *Clin Cancer Res*. 2005;11(4):1588–1596.
20. Fogh S, Machtay M, Werner-Wasik M, et al. Phase I Trial Using Patupilone (Epothilone B) and Concurrent Radiotherapy for Central Nervous System Malignancies. *Int J Radiat Oncol Biol Phys*. 2010;77(4):1009–1016.
21. Saylors RL, 3rd, Sidransky D, Friedman HS, et al. Infrequent p53 gene mutations in medulloblastomas. *Cancer Res*. 1991;51(17):4721–4723.
22. Altmann KH, Wartmann M, O'Reilly T. Epothilones and related structures–a new class of microtubule inhibitors with potent in vivo antitumor activity. *Biochim Biophys Acta*. 2000;1470(3):M79–91.
23. Pawlik TM, Keyomarsi K. Role of cell cycle in mediating sensitivity to radiotherapy. *Int J Radiat Oncol Biol Phys*. 2004;59(4):928–942.
24. Sinclair WK. Cyclic x-ray responses in mammalian cells in vitro. *Radiat Res*. 1968;33(3):620–643.
25. Bocci G, Nicolaou KC, Kerbel RS. Protracted low-dose effects on human endothelial cell proliferation and survival in vitro reveal a selective anti-angiogenic window for various chemotherapeutic drugs. *Cancer Res*. 2002;62(23):6938–6943.
26. Ferretti S, Allegrini PR, O'Reilly T, et al. Patupilone induced vascular disruption in orthotopic rodent tumor models detected by magnetic resonance imaging and interstitial fluid pressure. *Clin Cancer Res*. 2005;11(21):7773–7784.
27. Thorpe PE. Vascular targeting agents as cancer therapeutics. *Clin Cancer Res*. 2004;10(2):415–427.
28. Shen S, Kepp O, Martins I, et al. Defective autophagy associated with LC3 puncta in epothilone-resistant cancer cells. *Cell Cycle*. 2010;9(2):377–383.
29. Demidenko ZN, Kalurupalle S, Hanko C, Lim CU, Broude E, Blagosklonny MV. Mechanism of G1-like arrest by low concentrations of paclitaxel: next cell cycle p53-dependent arrest with sub G1 DNA content mediated by prolonged mitosis. *Oncogene*. 2008;27(32):4402–4410.
30. von Bueren AO, Shalaby T, Oehler-Janne C, et al. RNA interference-mediated c-MYC inhibition prevents cell growth and decreases sensitivity to radio- and chemotherapy in childhood medulloblastoma cells. *BMC Cancer*. 2009;9:10.
31. von Bueren AO, Shalaby T, Rajtarova J, et al. Anti-proliferative activity of the quassinoid NBT-272 in childhood medulloblastoma cells. *BMC Cancer*. 2007;7:19.
32. Kanzawa T, Germano IM, Komata T, Ito H, Kondo Y, Kondo S. Role of autophagy in temozolomide-induced cytotoxicity for malignant glioma cells. *Cell Death Differ*. 2004;11(4):448–457.

3.5. Microtubule Stabilizing Agents and Ionizing Radiation: Multiple Exploitable Mechanisms for Combined Treatment

Carla Rohrer Bley[a,b;], Polina Furmanova[a], Katrin Orlowski[a], Nicole Grosse[a], Angela Broggini-Tenzer[a], Paul MJ. McSheehy[c], Martin Pruschy[a]

[a]Department of Radiation Oncology, University Hospital Zurich, Zurich, Switzerland

[b]Division of Radiation Oncology, Vetsuisse Faculty, University of Zurich, Zurich, Switzerland

[c]Novartis Institutes for BioMedical Research, Novartis Pharma AG, Basel, Switzerland

Status of the manuscript: Accepted for publication in the European Journal of Cancer

Author contribution K. Orlowski:

Concepts and data of this PhD thesis were also recapitulated in this review.

Short title: Microtubule Stabilizing Agents and Ionizing Radiation

Conflict of interest statement: No potential conflicts of interest were disclosed.

Grant Support: Swiss Cancer League, Vontobel-Stiftung, Swiss National Science Foundation

Abstract

Combined radiochemotherapy treatment modalities are in use for many indications and therefore of high interest. Even though a combined modality in clinical use is often driven by pragmatic aspects, mechanistic preclinical-based concepts of interaction are of importance in order to translate and implement an optimal combination and scheduling of two modalities into the clinics. The use of microtubule stabilizing agents is a promising strategy for anti-cancer therapy as a part of combined treatment modality with ionizing radiation. Traditionally, microtubule targeting agents are classified as cytotoxic chemotherapeutics and are mostly used in a maximally tolerated dose regimen. Apart from direct cytotoxicity and similar to mechanisms of molecular targeting agents, microtubule stabilizing agents interfere with multiple cellular processes, which can be exploited as part of combined treatment modalities. Recent preclinical investigations on the combination of ionizing radiation and microtubule stabilizing agents reveal new mechanistic interactions on the cellular and tumor level and elucidate the supra-additive tumor response observed particularly *in vivo*. The major focus on the mechanism of interaction was primarily based on radiosensitization due to cell cycle arrest in the most radiosensitive G2/M-phase of the cell cycle. However, other mechanisms of interaction such as reoxygenation and direct as well as indirect endothelial damage have also been identified. In this review we summarize and allocate additive and synergistic effects induced by the combined treatment of clinically relevant microtubule stabilizing agents and ionizing radiation along a described radiobiological framework encompassing distinct mechanisms relevant for exploiting the combination of drugs and ionizing radiation.

Keywords: Ionizing Radiation, Microtubule Stabilizing Agents, Radiochemotherapy, Epothilones, Taxanes

Introduction: Microtubule Stabilizing Agents

Microtubule targeting agents belong to the most important classes of anti-cancer agents and are subdivided in two groups, according to their mode of action. While microtubule destabilizers prevent the assembly of tubulin heterodimers, microtubule stabilizing agents (MSA) prevent the shortening of microtubules resulting in the accumulation of polymerized microtubule bundles and the interference of the mitotic spindle function.(1-4) Experimental evidence concerning the kinetics and mechanism of tubulin-binding as well as the ability to actively promote microtubule function by paclitaxel mimetics has been recently provided using biochemical and NMR techniques.(5) Eventually both classes of microtubule targeting agents alter spindle-microtubule dynamics, which results in a transient or permanent M-phase arrest and the induction of apoptotic cell death or mitotic catastrophe (Figure 1).(6) In this review we will specifically focus on the mode of interaction between MSA and ionizing radiation as part of a combined treatment modality.

Taxanes and epothilones are the clinically most relevant microtubule stabilizing agents. The *taxanes* (paclitaxel and docetaxel) have been approved for a broad range of indications, including advanced breast cancer after failure of combination chemotherapy or at early relapse,(7) high grade ovarian cancer in combination with platinum compounds, and primary treatment of non-small cell lung cancer in combination with cisplatin.(8) Furthermore paclitaxel is used in an “off-label manner” for other tumor types, such as cancer of unknown origin, bladder, esophagus, gastric, head and neck, and cervical cancers (reviewed in (9)). Paclitaxel has also been evaluated clinically for its radiosensitizing properties for various tumors(10-14) and drug plasma concentrations in patients. Low concentrations with prolonged exposure during long parts of the course of radiation therapy have been found feasible and tolerated in patients.(12-18) Docetaxel is used as first-line chemotherapy for locally advanced or metastatic breast cancer,(19) nonresectable, advanced or metastatic non-small cell lung cancer after failure of cisplatin-based therapy, hormone-refractory metastatic prostate cancer in combination with prednisone,(20) gastric adenocarcinoma in combination with cisplatin and 5-fluorouracil,(21) and inoperable advanced squamous cell cancer of the head and neck in combination with cisplatin and 5-fluorouracil. Both of the approved taxane derivates are hydrophobic and require organic solvents for administration (cremophor EL / ethanol, polysorbate / ethanol), which by themselves can cause unwanted side effects.(22) The *epothilones* are nontaxoid macrolide MSA of bacterial origin, which share the same binding site on beta-tubulin (in close proximity to residue Thr274) with taxanes,(23) albeit

with different affinities.(1, 24-26) Clinically different epothilone derivatives are currently in various stages of development as antitumor compounds. Several properties like increased water solubility, low susceptibility to common mechanisms of resistance and the more tolerable toxicity profile, favor their development. Ixabepilone (Ixempra®) is the first approved compound in this class and indicated as monotherapy or in combination with capecitabine for the treatment of patients with metastatic breast cancer. Apart from a manageable safety profile, ixabepilone demonstrates activity after failure and resistance towards anthracycline and taxane standard therapy.(27) Epothilone B (patupilone) was tested as a phase III monotherapy agent against ovarian cancer and other epothilones are undergoing a wide spectrum of single and combined treatment modality in phase II studies (e.g. for recurrent glioblastoma, CNS metastases from breast cancer, prostate, cervical, renal cell, gastric and lung tumor, as well as non-Hodgkin's Lymphoma (www.cancer.gov).(15, 28-31)

Both, taxanes and epothilones, have been extensively tested at the preclinical level in combination with ionizing radiation, demonstrating a strong supra-additive treatment response. Here, we will outline classic rationales for the combined treatment modality of ionizing radiation with microtubule stabilizing agents and discuss novel mechanistic preclinical-based concepts of interaction between these two modalities.

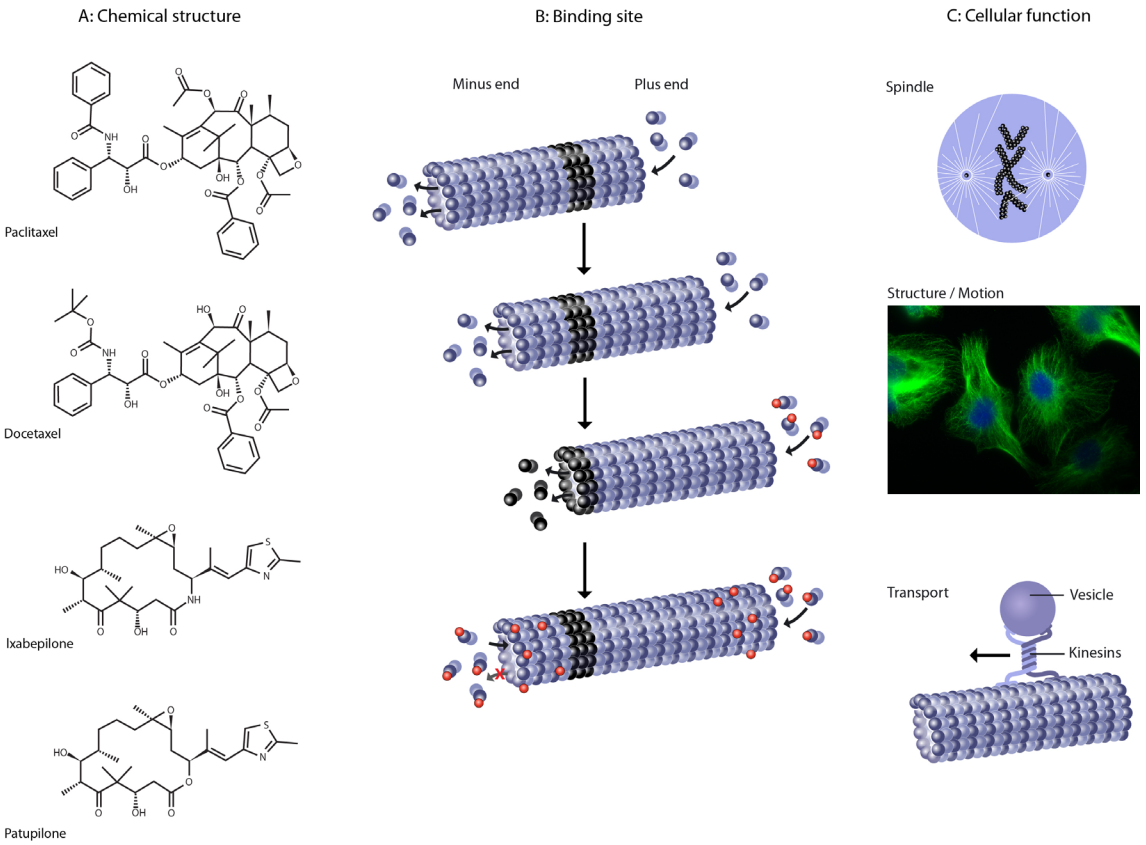

Fig. 1. A: Chemical structure: The MSA compounds are of complex structure and high chemical diversity. The complex structure of these compounds explains the difficulty for chemical synthesis.

B: Binding site: Microtubules are dynamic structures of α- and β-tubulin molecules arranged in tubular form. The microtubule-stabilizing agents of the taxane and epothilone groups bind along the interior surface of the microtubules to the same or an overlapping taxoid-binding site on β-tubulin. Thereby microtubular polymerization is enhanced and microtubular dynamics reduced.

C: Microtubules interact with various intracellular organelles: In the mitotic spindle, proper alignment and separation of the chromosomes during cellular division is provided by the normal microtubular function. Furthermore cellular structure and motion as well as vesicular transport take place by and along tubular structures.

Rationale for the Combined Use of Irradiation and Cytotoxic Agents

The rationale for a combined treatment with ionizing radiation (IR) and chemotherapy is to increase survival by improving locoregional tumor control and decrease the probability of distant disease, with concurrent organ and function preservation.(32, 33) Recently, a new framework encompassing five distinct mechanisms relevant for exploiting the combination of drugs and ionizing radiation has been proposed.(34) While for some of the mechanisms direct drug-radiation interactions at the tumor-cellular level is not required (e.g. *in spatial*

cooperation, normal tissue protection), other mechanisms are fundamentally based on their mutual interaction (e.g. *cytotoxic enhancement, biological cooperation, temporal modulation*). With regard to microtubule stabilizing agents, IR-MSA interactions can be allocated to several of these mechanisms. Interestingly these mechanisms even complement each other on several levels thereby further enhancing the potency of this promising combined treatment modality.

The main rationale to exploit *spatial cooperation*, combining a drug with efficacy against systemic disease with radiotherapy against locoregional disease, is to achieve local *and* systemic control by full doses of both treatment modalities, often applied in sequence.(20) For the mechanisms involving a direct drug-radiation interaction at the cellular level (*cytotoxic enhancement, biological cooperation and temporal modulation*), the strategies aim mainly at enhancing cell killing, interfering with repair mechanisms, targeting distinct cell populations (e.g. hypoxic cells) and microenvironmental structures within the tumor.

Interactions between Ionizing Radiation and MSA (Figure 2)

Cell cycle specific enhancement (cytotoxic enhancement). MSAs induce mitotic arrest in most tumor cells. Depending on the dose applied and/or the genetic background and inherent cellular sensitivity of the tumor cells, MSA-induced mitotic arrest will lead to transient cell cycle arrest or apoptosis. Therefore only a poor correlation exists between MSA-induced mitotic arrest and tumor control, as mitotically arrested cells in some tumors are capable of continued survival (35, 36). In paclitaxel- and docetaxel-resistant tumors, the radioenhancing mechanism is primarily based on the transient accumulation of cells in this cell cycle phase.(36, 37)

The cell cycle phases of late G2 and mitosis are most sensitive to ionizing radiation.(38, 39) Ionizing radiation produces different types and quantities of chromosomal aberrations at various stages of the cell cycle. The frequency of IR-induced chromosomal aberrations is higher for cells in G2- and M-phase than for cells irradiated in the G1- and S-phase of the cell cycle.(40) In addition, cells in late G2/M-phase already passed the G2-checkpoint to repair their DNA damage, and thus the frequency of residual, detrimental chromosomal aberrations in cells entering mitosis is also increased. As mitotic cells with double strand breaks will lose genetic material following cell division, irradiation of MSA-treated, transiently arrested late G2-/M-phase-cells will result in genomic instability and eventually mitotic catastrophe.(35, 41-45)

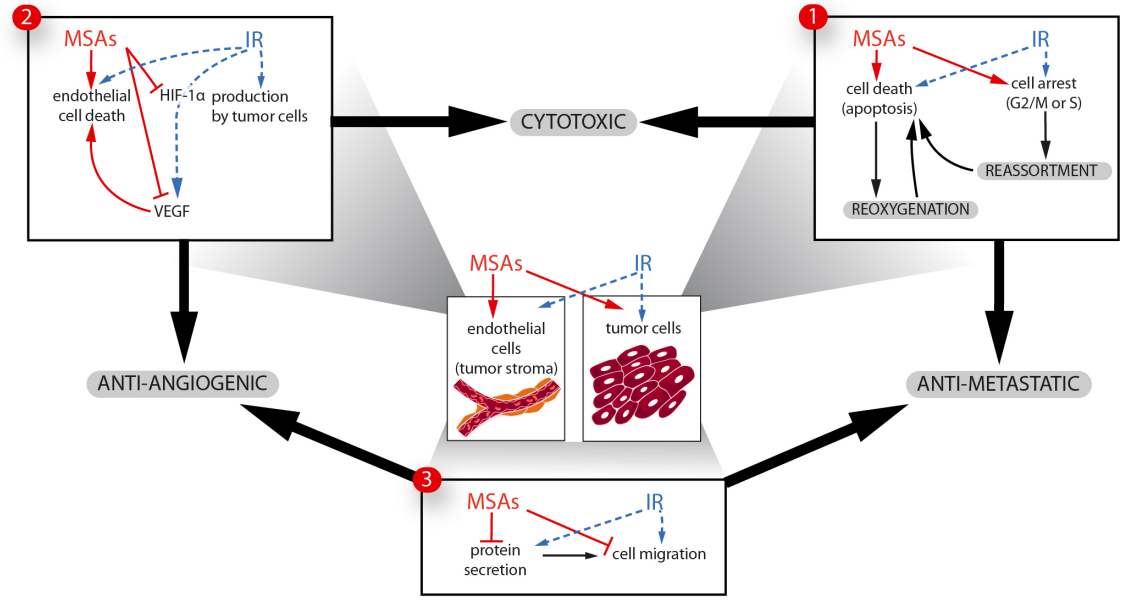

Fig. 2. Multifaceted interaction of MSA and ionizing radiation on the tumor and endothelial cell level: 1. High doses of MSA and IR lead to reassortment of cells in the cell cycle, cell loss and subsequent tumor reoxygenation. Massive tumoral cell loss will directly decrease the metastatic potential. 2. MSAs counteract the pro-angiogenic IR-induced stress response. 3. MSAs counteract IR-induced secretion of survival and pro-metastatic factors thereby sensitizing the tumor to the combined treatment modality.

This implies that the therapeutic efficacy of the combined treatment modality strongly depends on the innate cellular drug sensitivity and in particular on the combination scheduling. Indeed, effects ranging from supra-additive interactions (Figure 3), to additive, and even sub-additive effects are documented.(43, 46-50) The radiosensitizing effect of MSA is most prominent between 8-12 hours after start of drug exposure at the time of accumulation of cells in G2/M-phase (Figure 4).(42, 43, 49, 50) In contrary, the cytotoxic M-phase-related potency of paclitaxel added *after* irradiation was lost and did not increase IR-induced cell death due to the strong IR- induced G1- and G2- cell cycle arrest and subsequent sublethal damage repair.(49, 51) *In vivo*, multiple doses of taxanes given during the course of fractionated irradiation maximized the exposure for cells to ionizing radiation even in drug resistant tumors.(52) However, with intermittent multiple high doses of taxanes, the therapeutic gain was in part limited by side effects in acutely responding tissues such as jejunal mucosa, skin and connective tissues as observed in murine tumor models.(52-54)

Moderate concentrations of MSA, which are sufficient to induce a G2-M cell cycle arrest are optimal for radioenhancement.(43, 47-50) Interestingly, low dose MSA-treatment may also induce an additional G2/M-phase independent mode of radiosensitization. Low doses of patupilone induced a transient accumulation of cells in S phase, but only on combined treatment with ionizing radiation.(55) Combined treatment did not result in the accumulation of cells in the radiosensitive G2/M-phase and radiosensitization was rather due to an S-phase-related process. A similar effect has also been described for synchronized HeLa cells, in which docetaxel resulted in a S-phase specific (and hence radioresistant) cell killing.(56, 57)

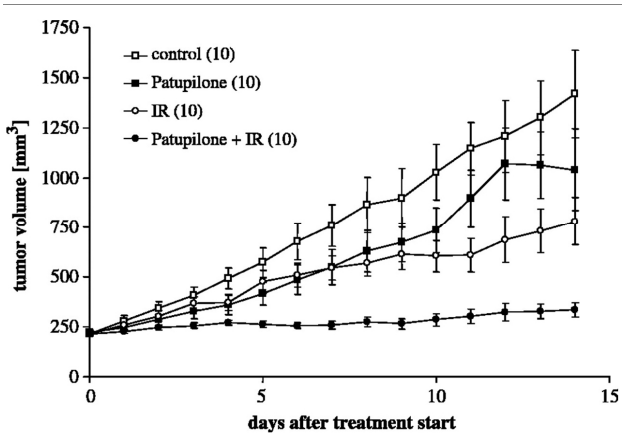

Fig. 3. (Adapted from Hofstetter et al.,(55)). Effect of Patupilone and IR alone or in combination on the growth of SW480-derived xenografts in nude mice: Mice were treated with Patupilone (2 mg/kg, once) and IR (4 × 3 Gy, on 4 consecutive days), alone and in combination. Patupilone or the vehicle was administered 24 hours before the first fraction of IR. Combined treatment exerted a strong, supra-additive tumor growth control during treatment and the follow-up period. The human colon adenocarcinoma cell line SW480 is a p-glycoprotein (*MDR1*)-overexpressing tumor. Patupilone is a promising alternative in multidrug-resistant tumors for a combined treatment regimen using microtubule inhibitors and IR.

Reoxygenation theory (biological cooperation, temporal modulation). The enhanced radiation response of combined treatment with microtubule stabilizing agents and ionizing radiation has also been attributed to "tumor cell reoxygenation". Massive cell loss due to MSA-induced apoptosis or necrosis might lead to a shortening of the tumor cell-vascular distance and a decrease of the intratumoral fluid pressure (IFP) with a subsequently increased blood delivery to hypoxic tumor regions as well as a decreased overall oxygen consumption rate. Eventually this results in increased tumor oxygenation, and subsequently increased radiation sensitivity (Figure 4).(35, 37, 52, 54, 58, 59) For example, paclitaxel in combination with ionizing radiation significantly reduced tumor hypoxia in MCA-4 xenograft tumors, especially in a

drug-radiation interval of 3 days.(59) Due to the high concentration of the administered drug, this effect was mostly attributed to extensive cytotoxicity caused by paclitaxel.

Endothelial theory (biological cooperation, temporal modulation). As the radiosensitivity of the tumor vascular network codetermines the tumor response to IR, enhanced tumor radiosensitivity can be attributed to the effect of microtubule agents on the tumor endothelial system.(60) Microtubule stabilizing agents have anti-angiogenic properties at high and at low, non-tumor cytotoxic doses.(61) These properties are on one hand based on *direct* anti-endothelial cell activity, but also on the *indirect* tumor-cell mediated anti-angiogenic effect, by inhibition and subsequent down-regulation of proteins and genes involved in angiogenesis and hypoxic adaptation.(62, 63) High doses of microtubule stabilizing agents act in a cytotoxic manner via mitotic block and activation of the mitochondrial apoptotic pathway, while on the other hand, low doses decelerate overall cell cycle progression and inhibit migration and proliferation,(64, 65) which results in reduced capillary-like tube formation.(61, 66) Similar to the radiosensitizing effect on the tumor cell level, prolonged metaphase-to-anaphase transition in endothelial cells can also provoke an increase of the radiation response on the tumor vasculature level by temporal modulation in the classic radiobiological framework of cell cycle redistribution (see above).(34) In addition to the anti-angiogenic effects, MSA such as epothilone B also exert vascular disruptive effects. Drug administration led to a rapid destruction of blood vessels (observable at day two) associated with a decrease in tumor IFP.(67) This direct destruction of blood vessels and decrease of IFP might also lead to a subsequent reorganization of the vasculature, thereby temporarily decreasing the hostility of tumor microenvironment by also changing oxygenation and pH-status of the tumor.(67, 68) Enhanced tumor oxygenation could also be attributed to the proposed concept of tumor vasculature normalization, caused by a transient decrease of VEGF signaling and thereby reduction of vessel abnormalities such as tortuosity and leakage of the impaired tumor vasculature. Addition of radiation therapy during this “window of normalization” would in principle enhance radiation response.(68, 69)

However, reduction of tumor hypoxia on MSA-treatment is not a prerequisite for a supra-additive anti-tumor effect when combined with ionizing radiation. Early results indicated that paclitaxel suppresses the expression of VEGF in murine breast cancer cells *in vivo* and *in vitro*.(70) Our own experiments performed with patupilone in a genetically defined MSA-sensitive and MSA-resistant tumor model revealed that the anti-angiogenic and

radiosensitizing effect on the level of the tumor vasculature of MSA is strongly promoted in an indirect tumor-cell mediated way. A significant reduction in microvessel density and initial increase of tumor hypoxia on treatment with epothilone B (patupilone) alone was only detected in tumors derived from the MSA-sensitive A549 wild-type cells but not in the MSA-resistant cell line. These results indicate that the anti-angiogenic effect of patupilone *in vivo* is *indirectly* induced by interference at the level of the tumor cellular stress response.(62, 71) MSA interfere with the expression and transcriptional activity of the hypoxia-inducible factor 1α (HIF-1α) and subsequent reduction of the downstream pro-angiogenic HIF-transcriptome, including VEGF and other genes involved in angiogenesis, endothelial cell survival and hypoxic adaptation.(62, 63, 71) Vascular disruption as well as a decrease of the radioprotective effect of endothelial cells by VEGF and other survival factors will thereby enhance the radiation response, which is attributed to biological cooperation.(34, 60, 72)

Antimetastatic properties of MSAs (spatial cooperation). There is currently an ongoing discussion on the impact of ionizing radiation on tumor cell dissemination. Enhanced cell invasion and metastatic spread was observed in selected preclinical experiments in response to irradiation.(73-77) This effect is most probably due to IR-induced expression and secretion of matrix metalloproteinases (MMPs) required for cell invasion.(78-81) Interestingly the secretion of MMPs and related tissue inhibitors of metalloproteinases are also regulated by MSAs, as they are at least partially dependent on the dynamic functional MT system.(82, 83) At low doses, paclitaxel impairs the secretion of MMP-2 and MMP-9 by human melanoma and prostate cancer cells, thereby inhibiting cell invasion(84, 85) and this may be relevant mechanistically for the promising anti-metastatic effect of MSA. Furthermore, taxanes and epothilones can reduce migration of non-neoplastic smooth muscle and endothelial cells,(86-88) as well as neoplastic tumor cells (e.g. ovarian and colon carcinoma).(89, 90) The anti-metastatic properties of paclitaxel and epothilones were also demonstrated in tumor-bearing mice (for lung, prostate and breast tumors).(91-94)

Our own studies are currently investigating the combined treatment modality of epothilones and IR on MMP function. Interestingly, epothilones specifically counteract IR-induced MMP activity and IR-induced cell invasion of human fibrosarcoma and glioma cell lines.(95) This might represent an additional cause for the supra-additive tumor growth delay observed on combined treatment in preclinical *in vivo* experiments and is an interesting rational for a combined treatment modality in the clinical setting.

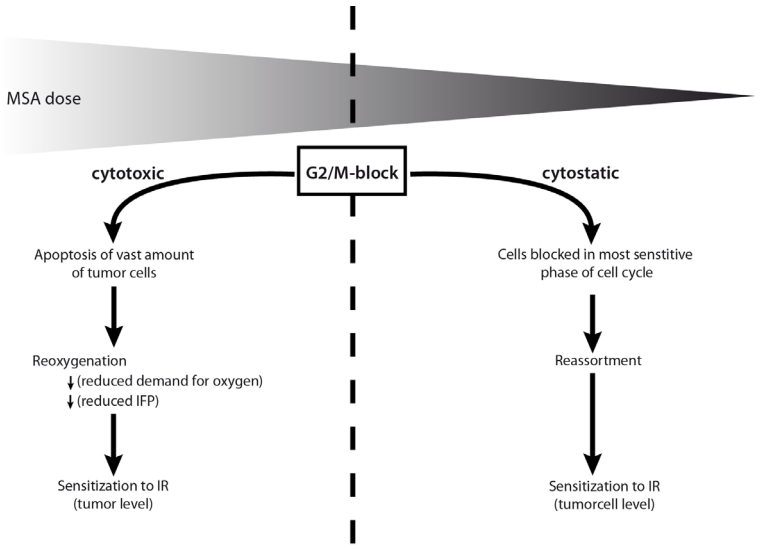

Fig. 4. Dose dependent consequences of MSA via initial G2/M-phase block: cytostatic, low doses of MSA lead to cellular reassortment into the most radiosensitive phase of the cell cycle, while cytotoxic high doses of MSA radiosensitize the tumor by tumor reoxygenation.

The combined treatment modality of ionizing radiation with microtubule stabilizing agents fulfill the classic rationales of cell cycle specific enhancement, biological cooperation, temporal modulation and, in part, spatial cooperation. By causing cell cycle arrest in the most radiosensitive phase of the cell cycle, reducing the hypoxic fraction within the cellular population and thereby redistributing and reoxygenating the remaining tumor cells, and by interference with angiogenic signaling and endothelial cells, the interaction between microtubule stabilizing agents and ionizing radiation has a promising potential to increase the potency of this treatment combination. It is not only the additive effect of each of these mechanisms, which contribute to radiosensitization by MSAs, interestingly these mechanisms even complement each other on several levels thereby further enhancing the potency of this promising combined treatment modality.

References

1. Bollag DM, McQueney PA, Zhu J, Hensens O, Koupal L, Liesch J, et al. Epothilones, a new class of microtubule-stabilizing agents with a taxol-like mechanism of action. Cancer Res 1995;55(11):2325-33.

2. Kowalski RJ, Giannakakou P, Hamel E. Activities of the microtubule-stabilizing agents epothilones A and B with purified tubulin and in cells resistant to paclitaxel (Taxol(R)). J Biol Chem 1997;272(4):2534-41.

3. Manfredi JJ, Parness J, Horwitz SB. Taxol binds to cellular microtubules. J Cell Biol 1982;94(3):688-96.

4. Schiff PB, Horwitz SB. Taxol stabilizes microtubules in mouse fibroblast cells. Proc Natl Acad Sci U S A 1980;77(3):1561-5.

5. Canales A, Rodriguez-Salarichs J, Trigili C, Nieto L, Coderch C, Andreu JM, et al. Insights into the interaction of discodermolide and docetaxel with tubulin. Mapping the binding sites of microtubule-stabilizing agents by using an integrated NMR and computational approach. ACS Chem Biol 2011;6(8):789-99.

6. Jordan MA, Wilson L. Microtubules as a target for anticancer drugs. Nat Rev Cancer 2004;4(4):253-65.

7. Sparano JA. Taxanes for breast cancer: an evidence-based review of randomized phase II and phase III trials. Clin Breast Cancer 2000;1(1):32-40; discussion 41-2.

8. Bonomi P, Kim K, Fairclough D, Cella D, Kugler J, Rowinsky E, et al. Comparison of survival and quality of life in advanced non-small-cell lung cancer patients treated with two dose levels of paclitaxel combined with cisplatin versus etoposide with cisplatin: results of an Eastern Cooperative Oncology Group trial. J Clin Oncol 2000;18(3):623-31.

9. Lee JJ, Harris LN. Antimicrotubule Agents. In: De Vita VT, Lawrence TS, Rosenberg SA, editors. Cancer, Priniples & Practice of Oncology. 8th ed. Philadelphia: Lippincott Williams & Wilkins; 2008. p. 447-456.

10. Klautke G, Foitzik T, Ludwig K, Ketterer P, Klar E, Fietkau R. Neoadjuvant radiochemotherapy in locally advanced gastric carcinoma. Strahlenther Onkol 2004;180(11):695-700.

11. Leibl BJ, Vitz S, Schafer W, Alfrink M, Gschwendtner A, Grabenbauer GG. Adenocarcinoma of the esophagogastric junction: neoadjuvant radiochemotherapy and radical surgery : early results and toxicity. Strahlenther Onkol 2011;187(4):231-7.

12. Liu L, Vapiwala N, Munoz LK, Winick NJ, Weitman S, Strauss LC, et al. A phase I study of cranial radiation therapy with concomitant continuous infusion paclitaxel in children with brain tumors. Med Pediatr Oncol 2001;37(4):390-2.

13. Rosenthal DI, Fuller CD, Machtay M, Algazy KM, Meyer DM, Kaiser LR, et al. Phase I study of Paclitaxel given by seven-week continuous infusion concurrent with radiation therapy for locally advanced non-small cell lung cancer. J Thorac Oncol 2006;1(1):38-45.

14. Rosenthal DI, Lee JH, Sinard R, Yardley DA, Machtay M, Rosen DM, et al. Phase I study of paclitaxel given by seven-week continuous infusion concurrent with radiation therapy for locally advanced squamous cell carcinoma of the head and neck. J Clin Oncol 2001;19(5):1363-73.

15. Fogh S, Machtay M, Werner-Wasik M, Curran WJ, Jr., Bonanni R, Axelrod R, et al. Phase I trial using patupilone (epothilone B) and concurrent radiotherapy for central nervous

system malignancies. Int J Radiat Oncol Biol Phys;77(4):1009-16.

16. Rosenthal DI, Close LG, Lucci JA, 3rd, Schold SC, Truelson J, Fathallah-Skaykh H, et al. Phase I studies of continuous-infusion paclitaxel given with standard aggressive radiation therapy for locally advanced solid tumors. Semin Oncol 1995;22(4 Suppl 9):13-7.

17. Wiernik PH, Schwartz EL, Einzig A, Strauman JJ, Lipton RB, Dutcher JP. Phase I trial of taxol given as a 24-hour infusion every 21 days: responses observed in metastatic melanoma. J Clin Oncol 1987;5(8):1232-9.

18. Wiernik PH, Schwartz EL, Strauman JJ, Dutcher JP, Lipton RB, Paietta E. Phase I clinical and pharmacokinetic study of taxol. Cancer Res 1987;47(9):2486-93.

19. Jones SE, Erban J, Overmoyer B, Budd GT, Hutchins L, Lower E, et al. Randomized phase III study of docetaxel compared with paclitaxel in metastatic breast cancer. J Clin Oncol 2005;23(24):5542-51.

20. Tannock IF, de Wit R, Berry WR, Horti J, Pluzanska A, Chi KN, et al. Docetaxel plus prednisone or mitoxantrone plus prednisone for advanced prostate cancer. N Engl J Med 2004;351(15):1502-12.

21. Van Cutsem E, Moiseyenko VM, Tjulandin S, Majlis A, Constenla M, Boni C, et al. Phase III study of docetaxel and cisplatin plus fluorouracil compared with cisplatin and fluorouracil as first-line therapy for advanced gastric cancer: a report of the V325 Study Group. J Clin Oncol 2006;24(31):4991-7.

22. Edelman MJ. Novel taxane formulations and microtubule-binding agents in non-small-cell lung cancer. Clin Lung Cancer 2009;10 Suppl 1:S30-4.

23. Nettles JH, Li H, Cornett B, Krahn JM, Snyder JP, Downing KH. The binding mode of epothilone A on alpha,beta-tubulin by electron crystallography. Science 2004;305(5685):866-9.

24. Altmann KH, Gertsch J. Anticancer drugs from nature--natural products as a unique source of new microtubule-stabilizing agents. Nat Prod Rep 2007;24(2):327-57.

25. Altmann KH, Pfeiffer B, Arseniyadis S, Pratt BA, Nicolaou KC. The Chemistry and Biology of Epothilones-The Wheel Keeps Turning. ChemMedChem 2007;2(4):396-423.

26. Altmann KH, Wartmann M, O'Reilly T. Epothilones and related structures--a new class of microtubule inhibitors with potent in vivo antitumor activity. Biochim Biophys Acta 2000;1470(3):M79-91.

27. Gradishar W. Management of advanced breast cancer with the epothilone B analog, ixabepilone. Drug Des Devel Ther 2009;3:163-71.

28. Dumontet C, Jordan MA. Microtubule-binding agents: a dynamic field of cancer therapeutics. Nat Rev Drug Discov;9(10):790-803.

29. Freedman RA, Bullitt E, Sun L, Gelman R, Harris G, Ligibel JA, et al. A Phase II Study of Sagopilone (ZK 219477; ZK-EPO) in Patients With Breast Cancer and Brain Metastases. Clin Breast Cancer.

30. Rustin G, Reed N, Jayson GC, Ledermann JA, Adams M, Perren T, et al. A phase II trial evaluating two schedules of sagopilone (ZK-EPO), a novel epothilone, in patients with platinum-resistant ovarian cancer. Ann Oncol.

31. Stupp R, Tosoni A, Bromberg JE, Hau P, Campone M, Gijtenbeek J, et al. Sagopilone (ZK-EPO, ZK 219477) for recurrent glioblastoma. A phase II multicenter trial by the European Organisation for Research and Treatment of Cancer (EORTC) Brain Tumor Group.

Ann Oncol.

32. Steel GG. Terminology in the description of drug-radiation interactions. Int J Radiat Oncol Biol Phys 1979;5(8):1145-50.

33. Steel GG, Peckham MJ. Exploitable mechanisms in combined radiotherapy-chemotherapy: the concept of additivity. Int J Radiat Oncol Biol Phys 1979;5(1):85-91.

34. Bentzen SM, Harari PM, Bernier J. Exploitable mechanisms for combining drugs with radiation: concepts, achievements and future directions. Nat Clin Pract Oncol 2007;4(3):172-80.

35. Milas L, Milas MM, Mason KA. Combination of taxanes with radiation: preclinical studies. Semin Radiat Oncol 1999;9(2 Suppl 1):12-26.

36. Milross CG, Mason KA, Hunter NR, Chung WK, Peters LJ, Milas L. Relationship of mitotic arrest and apoptosis to antitumor effect of paclitaxel. J Natl Cancer Inst 1996;88(18):1308-14.

37. Milross CG, Mason KA, Hunter NR, Terry NH, Patel N, Harada S, et al. Enhanced radioresponse of paclitaxel-sensitive and -resistant tumours in vivo. Eur J Cancer 1997;33(8):1299-308.

38. Sinclair WK, Morton RA. X-ray sensitivity during the cell generation cycle of cultured Chinese hamster cells. Radiat Res 1966;29(3):450-74.

39. Terasima T, Tolmach LJ. Variations in several responses of HeLa cells to x-irradiation during the division cycle. Biophys J 1963;3:11-33.

40. Pawlik TM, Keyomarsi K. Role of cell cycle in mediating sensitivity to radiotherapy. Int J Radiat Oncol Biol Phys 2004;59(4):928-42.

41. Geard CR, Jones JM, Schiff PB. Taxol and radiation. J Natl Cancer Inst Monogr 1993(15):89-94.

42. Kim JS, Amorino GP, Pyo H, Cao Q, Price JO, Choy H. The novel taxane analogs, BMS-184476 and BMS-188797, potentiate the effects of radiation therapy in vitro and in vivo against human lung cancer cells. Int J Radiat Oncol Biol Phys 2001;51(2):525-34.

43. Liebmann J, Cook JA, Fisher J, Teague D, Mitchell JB. In vitro studies of Taxol as a radiation sensitizer in human tumor cells. J Natl Cancer Inst 1994;86(6):441-6.

44. Lobrich M, Jeggo PA. The impact of a negligent G2/M checkpoint on genomic instability and cancer induction. Nat Rev Cancer 2007;7(11):861-9.

45. Steren A, Sevin BU, Perras J, Angioli R, Nguyen H, Guerra L, et al. Taxol sensitizes human ovarian cancer cells to radiation. Gynecol Oncol 1993;48(2):252-8.

46. Baumgart T, Klautke G, Kriesen S, Kuznetsov SA, Weiss DG, Fietkau R, et al. Radiosensitizing effect of epothilone B on human epithelial cancer cells. Strahlenther Onkol 2012;188(2):177-84.

47. Gupta N, Hu LJ, Deen DF. Cytotoxicity and cell-cycle effects of paclitaxel when used as a single agent and in combination with ionizing radiation. Int J Radiat Oncol Biol Phys 1997;37(4):885-95.

48. Leonard CE, Chan DC, Chou TC, Kumar R, Bunn PA. Paclitaxel enhances in vitro radiosensitivity of squamous carcinoma cell lines of the head and neck. Cancer Res 1996;56(22):5198-204.

49. Liebmann J, Cook JA, Fisher J, Teague D, Mitchell JB. Changes in radiation survival

curve parameters in human tumor and rodent cells exposed to paclitaxel (Taxol). Int J Radiat Oncol Biol Phys 1994;29(3):559-64.

50. Tishler RB, Geard CR, Hall EJ, Schiff PB. Taxol sensitizes human astrocytoma cells to radiation. Cancer Res 1992;52(12):3495-7.

51. Zanelli GD, Quaia M, Robieux I, Bujor L, Santarosa M, Favaro D, et al. Paclitaxel as a radiosensitiser: a proposed schedule of administration based on in vitro data and pharmacokinetic calculations. Eur J Cancer 1997;33(3):486-92.

52. Mason KA, Hunter NR, Milas M, Abbruzzese JL, Milas L. Docetaxel enhances tumor radioresponse in vivo. Clin Cancer Res 1997;3(12 Pt 1):2431-8.

53. Mason KA, Milas L, Peters LJ. Effect of paclitaxel (taxol) alone and in combination with radiation on the gastrointestinal mucosa. Int J Radiat Oncol Biol Phys 1995;32(5):1381-9.

54. Milas L, Saito Y, Hunter N, Milross CG, Mason KA. Therapeutic potential of paclitaxel-radiation treatment of a murine ovarian carcinoma. Radiother Oncol 1996;40(2):163-70.

55. Hofstetter B, Vuong V, Broggini-Tenzer A, Bodis S, Ciernik IF, Fabbro D, et al. Patupilone acts as radiosensitizing agent in multidrug-resistant cancer cells in vitro and in vivo. Clin Cancer Res 2005;11(4):1588-96.

56. Hennequin C, Giocanti N, Favaudon V. S-phase specificity of cell killing by docetaxel (Taxotere) in synchronised HeLa cells. Br J Cancer 1995;71(6):1194-8.

57. Hennequin C, Giocanti N, Favaudon V. Interaction of ionizing radiation with paclitaxel (Taxol) and docetaxel (Taxotere) in HeLa and SQ20B cells. Cancer Res 1996;56(8):1842-50.

58. Milas L, Hunter NR, Mason KA, Kurdoglu B, Peters LJ. Enhancement of tumor radioresponse of a murine mammary carcinoma by paclitaxel. Cancer Res 1994;54(13):3506-10.

59. Milas L, Hunter NR, Mason KA, Milross CG, Saito Y, Peters LJ. Role of reoxygenation in induction of enhancement of tumor radioresponse by paclitaxel. Cancer Res 1995;55(16):3564-8.

60. Garcia-Barros M, Paris F, Cordon-Cardo C, Lyden D, Rafii S, Haimovitz-Friedman A, et al. Tumor response to radiotherapy regulated by endothelial cell apoptosis. Science 2003;300(5622):1155-9.

61. Honore S, Pasquier E, Braguer D. Understanding microtubule dynamics for improved cancer therapy. Cell Mol Life Sci 2005;62(24):3039-56.

62. Bley CR, Jochum W, Orlowski K, Furmanova P, Vuong V, McSheehy PM, et al. Role of the microenvironment for radiosensitization by patupilone. Clin Cancer Res 2009;15(4):1335-42.

63. Escuin D, Kline ER, Giannakakou P. Both microtubule-stabilizing and microtubule-destabilizing drugs inhibit hypoxia-inducible factor-1alpha accumulation and activity by disrupting microtubule function. Cancer Res 2005;65(19):9021-8.

64. Bocci G, Nicolaou KC, Kerbel RS. Protracted low-dose effects on human endothelial cell proliferation and survival in vitro reveal a selective antiangiogenic window for various chemotherapeutic drugs. Cancer Res 2002;62(23):6938-43.

65. Stalder MW, Anthony CT, Woltering EA. Metronomic dosing enhances the anti-angiogenic effect of epothilone B. J Surg Res;169(2):247-56.

66. Pasquier E, Carre M, Pourroy B, Camoin L, Rebai O, Briand C, et al. Antiangiogenic activity of paclitaxel is associated with its cytostatic effect, mediated by the initiation but not

completion of a mitochondrial apoptotic signaling pathway. Mol Cancer Ther 2004;3(10):1301-10.

67. Ferretti S, Allegrini PR, O'Reilly T, Schnell C, Stumm M, Wartmann M, et al. Patupilone induced vascular disruption in orthotopic rodent tumor models detected by magnetic resonance imaging and interstitial fluid pressure. Clin Cancer Res 2005;11(21):7773-84.

68. Jain RK. Normalization of tumor vasculature: an emerging concept in antiangiogenic therapy. Science 2005;307(5706):58-62.

69. Carmeliet P, Jain RK. Principles and mechanisms of vessel normalization for cancer and other angiogenic diseases. Nat Rev Drug Discov;10(6):417-27.

70. Lau DH, Xue L, Young LJ, Burke PA, Cheung AT. Paclitaxel (Taxol): an inhibitor of angiogenesis in a highly vascularized transgenic breast cancer. Cancer Biother Radiopharm 1999;14(1):31-6.

71. Rohrer Bley C, Orlowski K, Furmanova P, McSheehy PM, Pruschy M. Regulation of VEGF-expression by patupilone and ionizing radiation in lung adenocarcinoma cells. Lung Cancer 2011;73(3):294-301.

72. Borghaei RC, Gorski G, Javadi M. NF-kappaB and ZBP-89 regulate MMP-3 expression via a polymorphic site in the promoter. Biochem Biophys Res Commun 2009;382(2):269-73.

73. Agemy L, Harmelin A, Waks T, Leibovitch I, Rabin T, Pfeffer MR, et al. Irradiation enhances the metastatic potential of prostatic small cell carcinoma xenografts. Prostate 2008;68(5):530-9.

74. Camphausen K, Moses MA, Beecken WD, Khan MK, Folkman J, O'Reilly MS. Radiation therapy to a primary tumor accelerates metastatic growth in mice. Cancer Res 2001;61(5):2207-11.

75. Jadhav U, Mohanam S. Response of neuroblastoma cells to ionizing radiation: modulation of in vitro invasiveness and angiogenesis of human microvascular endothelial cells. Int J Oncol 2006;29(6):1525-31.

76. Qian LW, Mizumoto K, Urashima T, Nagai E, Maehara N, Sato N, et al. Radiation-induced increase in invasive potential of human pancreatic cancer cells and its blockade by a matrix metalloproteinase inhibitor, CGS27023. Clin Cancer Res 2002;8(4):1223-7.

77. Speake WJ, Dean RA, Kumar A, Morris TM, Scholefield JH, Watson SA. Radiation induced MMP expression from rectal cancer is short lived but contributes to in vitro invasion. Eur J Surg Oncol 2005;31(8):869-74.

78. Cheng JC, Chou CH, Kuo ML, Hsieh CY. Radiation-enhanced hepatocellular carcinoma cell invasion with MMP-9 expression through PI3K/Akt/NF-kappaB signal transduction pathway. Oncogene 2006;25(53):7009-18.

79. Park CM, Park MJ, Kwak HJ, Lee HC, Kim MS, Lee SH, et al. Ionizing radiation enhances matrix metalloproteinase-2 secretion and invasion of glioma cells through Src/epidermal growth factor receptor-mediated p38/Akt and phosphatidylinositol 3-kinase/Akt signaling pathways. Cancer Res 2006;66(17):8511-9.

80. Strup-Perrot C, Vozenin-Brotons MC, Vandamme M, Linard C, Mathe D. Expression of matrix metalloproteinases and tissue inhibitor metalloproteinases increases in X-irradiated rat ileum despite the disappearance of CD8a T cells. World J Gastroenterol 2005;11(40):6312-21.

81. Susskind H, Hymowitz MH, Lau YH, Atkins HL, Hurewitz AN, Valentine ES, et al. Increased plasma levels of matrix metalloproteinase-9 and tissue inhibitor of

metalloproteinase-1 in lung and breast cancer are altered during chest radiotherapy. Int J Radiat Oncol Biol Phys 2003;56(4):1161-9.

82. Remacle AG, Rozanov DV, Baciu PC, Chekanov AV, Golubkov VS, Strongin AY. The transmembrane domain is essential for the microtubular trafficking of membrane type-1 matrix metalloproteinase (MT1-MMP). J Cell Sci 2005;118(Pt 21):4975-84.

83. Sbai O, Ferhat L, Bernard A, Gueye Y, Ould-Yahoui A, Thiolloy S, et al. Vesicular trafficking and secretion of matrix metalloproteinases-2, -9 and tissue inhibitor of metalloproteinases-1 in neuronal cells. Mol Cell Neurosci 2008;39(4):549-68.

84. Schnaeker EM, Ossig R, Ludwig T, Dreier R, Oberleithner H, Wilhelmi M, et al. Microtubule-dependent matrix metalloproteinase-2/matrix metalloproteinase-9 exocytosis: prerequisite in human melanoma cell invasion. Cancer Res 2004;64:8924-31.

85. Stearns ME, Wang M. Taxol blocks processes essential for prostate tumor cell (PC-3 ML) invasion and metastases. Cancer Res 1992;52(13):3776-81.

86. Bijman MN, van Nieuw Amerongen GP, Laurens N, van Hinsbergh VW, Boven E. Microtubule-targeting agents inhibit angiogenesis at subtoxic concentrations, a process associated with inhibition of Rac1 and Cdc42 activity and changes in the endothelial cytoskeleton. Mol Cancer Ther 2006;5(9):2348-57.

87. Hu YL, Li S, Miao H, Tsou TC, del Pozo MA, Chien S. Roles of microtubule dynamics and small GTPase Rac in endothelial cell migration and lamellipodium formation under flow. J Vasc Res 2002;39(6):465-76.

88. Wiskirchen J, Schober W, Schart N, Kehlbach R, Wersebe A, Tepe G, et al. The effects of paclitaxel on the three phases of restenosis: smooth muscle cell proliferation, migration, and matrix formation: an in vitro study. Invest Radiol 2004;39(9):565-71.

89. Ogasawara M, Matsubara T, Suzuki H. Screening of natural compounds for inhibitory activity on colon cancer cell migration. Biol Pharm Bull 2001;24(6):720-3.

90. Westerlund A, Hujanen E, Hoyhtya M, Puistola U, Turpeenniemi-Hujanen T. Ovarian cancer cell invasion is inhibited by paclitaxel. Clin Exp Metastasis 1997;15(3):318-28.

91. Jiang H, Tao W, Zhang M, Pan S, Kanwar JR, Sun X. Low-dose metronomic paclitaxel chemotherapy suppresses breast tumors and metastases in mice. Cancer Invest 2010;28(1):74-84.

92. O'Reilly T, Wartmann M, Brueggen J, Allegrini PR, Floersheimer A, Maira M, et al. Pharmacokinetic profile of the microtubule stabilizer patupilone in tumor-bearing rodents and comparison of anti-cancer activity with other MTS in vitro and in vivo. Cancer Chemother Pharmacol 2008;62(6):1045-54.

93. Strube A, Hoffmann J, Stepina E, Hauff P, Klar U, Kakonen SM. Sagopilone inhibits breast cancer bone metastasis and bone destruction due to simultaneous inhibition of both tumor growth and bone resorption. Clin Cancer Res 2009;15(11):3751-9.

94. Zhang AL, Russell PJ. Paclitaxel suppresses the growth of primary prostate tumours (RM-1) and metastases in the lung in C57BL/6 mice. Cancer Lett 2006;233(1):185-91.

95. Furmanova P, Eggel M, Millard A, Pruschy M. The Microtubule Stabilizer Patupilone Counteracts Ionizing Radiation-Induced Matrix Metalloproteinase Activity and Tumor Cell Invasion. Manuscript submitted.

4. Discussion

4.1. Combined treatment modality of patupilone and ionizing irradiation

Cancer therapy using the MSA patupilone has been extensively studied *in vitro* and *in vivo* using several different preclinical models [1,2]. Patupilone acts through several mechanisms to serve as an anti-cancer agent: by stabilizing microtubules it impairs mitosis, which results in an accumulation of cells in the G2/M-phase of the cell cycle and inhibition of proliferation. However, microtubule dynamics not only play an important role in cell division but also in intracellular trafficking of cell organelles, vesicles and proteins as well as in cell motility. Treatment with patupilone leads to inhibition of invasion, vascular disruption, and deregulation of the HIF-1 protein [2-4]. Clinical trials using patupilone (EPO906) demonstrated promising results for metastatic castration-resistant prostate cancer in a phase II trial [5] and for previously treated advanced metastatic colon carcinoma in a phase I trial [6]. Patupilone was also evaluated in phase I and II trials for small cell lung carcinoma; its strongest indications are for breast, lung and prostate cancer [7]. Patupilone has also been studied as part of combined treatment modalities: a phase Ib clinical trial in combination with carboplatin [8] and a phase I trial in combination with gemcitabine [9] revealed anti-tumor activity and tolerable toxicity. Despite the radiosensitizing properties of patupilone, so far only one phase I clinical trial has been reported for the combination with concurrent IR, applied to central nervous system malignancies [10], with another trial combining patupilone with IR for head and neck cancer currently ongoing (clinicaltrials.gov). However, the future of patupilone as a clinical anti-cancer agent is uncertain. While combined treatments with IR seemed promising, a phase III trial investigating single agent patupilone for ovarian cancer in 2010 failed to show an increase in overall survival in comparison to doxorubicin. Therefore, Novartis International AG decided not to proceed with regulatory filings for patupilone (www.novartis.com). Nevertheless, characterizing and analyzing the radiosensitizing properties of epothilones - with patupilone as a model compound - is of high clinical relevance.

In this study we demonstrated a very strong radiosensitizing effect of patupilone in a concurrent treatment scheme with IR *in vitro* and especially *in vivo* (Bley et al, 2009). Tumor xenografts derived from A549 cells revealed an at least additive tumor growth delay in response to the combined treatment regimen, whereas tumors derived from the patupilone-resistant tumor cell line A549.EpoB40 did not exhibit an enhanced response to combined

treatment. Therefore, we concluded that the radiosensitizing effect of patupilone on the A549-derived xenografts must result from the cytotoxic effect on the tumor cell compartment.

However, combined treatment modalities are often effective because they simultaneously target both the tumor cell compartment and the tumor microenvironment. Here we showed that the tumor growth delay caused by the combined treatment modality of patupilone and IR on the A549-derived xenografts was further enhanced by interference with tumor VEGF secretion (Rohrer Bley et al., 2011). As VEGF secreted from tumor cells protects endothelial cells from treatment with IR [11], this resulted in sensitization of the endothelial cells supporting the tumor, as shown by a reduction in microvessel density. We demonstrated a decrease of both VEGF mRNA and VEGF secretion levels under patupilone treatment in the patupilone-sensitive cell line, whereas no difference was detected in the resistant A549.EpoB40 cell line *in vitro*. Reduced VEGF mRNA and secretion most probably resulted from interference of patupilone with HIF-1α protein functions. We and others have shown that microtubule interfering agents lead to a reduction of the HIF-1α protein level [12]; moreover, Carbonaro and colleagues demonstrated an accumulation of HIF-1α mRNA in cytoplasmic P-bodies under taxol treatment [13]. However, an additional mechanism leading to reduced VEGF secretion could be impaired microtubule trafficking of vesicles containing VEGF as a result of patupilone interference with microtubule stability.

The additive tumor growth inhibition of the combined treatment modality might therefore derive from two complementary mechanisms: first, from the accumulation of tumor cells in the radiosensitive G2/M-phase of the cell cycle, and second, from reduced secretion of growth factors leading to decreased protection of endothelial cells. This work focused primarily on the secretion of the pro-angiogenic cytokine VEGF and the general HIF-1 “transcriptome” by the luciferase assay in the A549 cell line in response to the different treatment modalities. To extend this work, it would be of interest to determine whether patupilone also impairs VEGF secretion in other cell lines. This paracrine regulatory mechanism could be tested in a co-cultivation assay analyzing radiosensitivity of endothelial cells when co-cultivated with patupilone-treated versus untreated A549 cells. Furthermore, altered levels of other cytokines besides VEGF could also be responsible for the decrease in microvessel density and consequent increase in tumor hypoxia after patupilone treatment. We aimed to identify cytokines differentially regulated under hypoxic conditions upon patupilone treatment using a human angiogenesis array. This analysis demonstrated small but statistically insignificant

differences in angiogenin, interleukin 8 (IL-8), monocyte chemotactic protein 1 (MCP-1) and placental growth factor (PIGF) (data not shown). Surprisingly, the patupilone-resistant A549.EpoB40 cells exhibited a generally increased secretion profile: nearly all cytokines analyzed in the array were considerably elevated in comparison to A549 secretion levels. The higher amount of microvessels in the A549.EpoB40 xenografts may thus result from the overall higher amount of pro-angiogenic factors secreted, inducing new blood vessel formation and protecting the existing tumor vasculature.

We also analyzed the medulloblastoma cell line response to patupilone as compared to the microtubule destabilizing agent vincristine, part of the standard treatment regimen for medulloblastoma. We observed equal inhibition of cell proliferation by both agents, however by a 10-fold lower dose of patupilone than vincristine. This finding is significant, as vincristine, used in a concomitant treatment schedule with IR, leads to severe side effects like neurocognitive sequelae. At nanomolar concentrations, patupilone led to an accumulation of cells in the radiosensitive G2/M-phase of the cell cycle, and at sub-nanomolar concentrations, to minor changes in cell cycle distribution with some accumulation in a sub-G1 phase. The sub-G1 population represented cells undergoing apoptosis, as confirmed by caspase 3 cleavage. Patupilone also induced autophagy in one of the three medulloblastoma cell lines. Regardless of the mode of induced cell death and genetic differences between cell lines, patupilone led to radiosensitization of all medulloblastoma cell lines studied. Most importantly, the combination of patupilone and IR resulted in strong supra-additive tumor growth delay with complete tumor remission in 3 out of 5 xenografts. The ability of patupilone to cross the blood brain barrier and to sensitize cancer cells to IR makes it a very promising compound in combined treatments with IR for CNS malignancies.

In conclusion, the data provided in this work indicate that the combined treatment of patupilone and IR has a strong antitumoral effect on different tumor xenograft models. Patupilone exerts its effect through multiple complementary mechanisms: first, the accumulation of tumor cells in the radiosensitive G2/M phase of the cell cycle, and second, alteration of the HIF-1α protein level, with a resulting decrease of secreted VEGF and consequently more radiosensitive microvessels. Additionally, the overexpression of HIF-1α is often accompanied by a more aggressive phenotype. Especially for those cancers, the combination of patupilone with IR may emerge as a promising anti-cancer treatment strategy.

4.2. The importance of monitoring tumor hypoxia in anti-cancer treatment

Hypoxia is one of the most undesired features of tumors for anti-cancer therapy, leading to an increase in aggressiveness and general treatment resistance. Hypoxia results from insufficient vascularization of the tumor, which can also reduce the potency of chemotherapeutics that have difficulty reaching all tumor cells. Furthermore, hypoxia leads to radioresistance due to decreased ROS-mediated damage in irradiated cells. In general, tumors with an oxygen pressure below 10 mmHg are considered hypoxic. It has been shown that a partial oxygen pressure below 2.5 mmHg, determined by the pO_2 electrode, is prognostic for poor loco-regional control after radiotherapy in head and neck cancer [14,15]. Tumor hypoxia below 5 mmHg corresponds to a poor prognosis in both non-small cell lung carcinoma [16] and uterine cervix carcinoma [17]. These data indicate that even small differences in low oxygen tension are of clinical relevance.

Within this work (Orlowski et al.), we established a non-invasive bioluminescence system to probe tumor hypoxia over a prolonged treatment and follow-up period in an *in vivo* tumor model. For this purpose, a vector construct in which a part of the ODD-domain of HIF-1α was fused to the luciferase gene was designed. The vector construct is constitutively expressed due to a SV40 promoter 5' of the luciferase gene. The ODD-luciferase protein is degraded under normoxia, which is initiated by the hydroxylation of proline564 within the ODD-domain by PHDs, leading to recognition by VHL followed by ubiquitination. Therefore, this construct depends on the proper functions of PHDs and VHL in transfected cells and has limited use in certain renal cell carcinoma cell lines in which VHL is mutated, as well as in tumors with altered PHD expression [18]. The advantage of this vector construct compared to other luciferase constructs reporting hypoxia in tumors is the stable activity of luciferase even under treatment conditions altering the protein level of the HIF-1 transcription factor. We therefore could accurately monitor the course of hypoxia under treatment with patupilone. We further monitored the course of tumor hypoxia after treatment with the epidermal growth factor receptor (EGFR) tyrosine kinase inhibitor PKI166 in A549 xenografts expressing the ODD-luciferase construct. In these mice, treatment with PKI166 decreased luciferase activity and therefore tumor hypoxia (data not shown), which is in line with results of Cerniglia and colleagues demonstrating decreased hypoxia after treatment with the EGFR inhibitor erlotinib [19].

Luciferase measurements of two different xenograft models revealed a prolonged transient increase of luciferase activity after patupilone treatment. This increase occurred only in tumors that responded to patupilone with a delay in tumor growth. No substantial patupilone-induced tumor growth delay was observed in three patupilone-treated xenografted mice, and luciferase activity likewise did not increase in these tumor xenografts. Nonetheless, as we are confident that the injection of the drug was performed correctly, we cannot explain the lack of tumor response in these mice. A possibility might be that patupilone did not reach the bulk of the tumor due to abnormalities in tumor vasculature in these mice or rapid absorption in other tissues. An acquired resistance of the tumor cells to patupilone without previous exposure to the drug is rather unlikely. Nevertheless, these data illustrate the correlation between the anti-tumoral effect of patupilone and the increase in intratumoral hypoxia in response to patupilone treatment. The specific increase of tumor hypoxia after patupilone treatment as observed in our work is further supported by data of Ferretti and colleagues in which they demonstrated destruction of blood vessels and a decrease in tumor blood volume with patupilone treatment. As the destruction of blood vessels and decreased blood volume can be correlated with a decrease of interstitial fluid pressure, they suggest that the decrease in interstitial fluid pressure after patupilone treatment can be used as a surrogate biomarker for patupilone efficacy [3].

Our data (Bley et al., 2009) revealed a decrease in microvessel density at day 4 after patupilone treatment, accompanied by an increase in pimonidazole positive areas. Another group demonstrated a reduction in blood volume at day 2 and a reduction in microvessel density at day 7 after patupilone treatment in a rat tumor model [3]. Both sets of data support the specific increase in tumor hypoxia after patupilone treatment as observed by our luciferase-based reporter gene approach (Orlowski et al.). We analyzed microvessel density and pimonidazole staining in tumors expressing ODD-luciferase at day 10 after patupilone treatment. At this time point, luciferase activity was increased in all animals treated with patupilone compared to the control animals. Surprisingly, we could not detect any significant changes in microvessel density or pimonidazole staining in patupilone-treated versus control mice at this time point. One explanation might be that microvessel density 10 days after patupilone treatment already readjusted to control levels. Analyses of microvessel density and pimonidazole staining of the tumors at an earlier time point after treatment might reveal greater differences between patupilone-treated versus control tumors. Another possibility for the discrepancy between the luciferase and pimonidazole data could be that a tumor section,

as used for pimonidazole staining, cannot be used to quantify tumor hypoxia over a whole tumor as analyzed by bioimaging using luciferase. To test this possibility, we also analyzed luciferase activity in tumor sections derived from patupilone and control tumors at day 10 after patupilone treatment. Consecutive frozen tumor sections were stained for pimonidazole and analyzed for luciferase activity using bioimaging. Some samples revealed areas of strong correlation between pimonidazole staining and luciferase signal, e.g. in tissue surrounding necrotic islets. However, we could also detect areas in which the two hypoxia analyses differed from each other. Therefore, we conclude that hypoxia determined by pimonidazole and ODD-luciferase activity measurements are not directly comparable.

One reason for incompatible hypoxia measurements between the two methods could be a difference in sensitivity towards varying levels of hypoxia. Indeed, we observed that pimonidazole staining allowed only the detection of differences in oxygen levels ranging from normoxia to 1% pO_2, but not below. The ODD-luciferase reporter, in contrast, exhibited a much higher sensitivity for low oxygen tensions, as we could detect a 2.8-fold difference in luciferase signal between 1% and 0.2% pO_2. The differences in sensitivity could explain the observed discrepancy between the pimonidazole staining and luciferase measurement data. Evans at al. demonstrated that binding intensity of the hypoxic marker EF5 correlated to different oxygen levels ranging from anoxia to 10% pO_2 [20]. It would be of interest to determine whether EF5 staining and luciferase measurements correlate in their ability to detect hypoxia. A very reliable method to measure exact partial pressures within the tumor is the use of a pO_2 electrode. However, applying this technique requires larger tumors than we used in our study, in order to obtain more than one data set of partial pressures within one tumor.

Our luciferase measurements in the context of pimonidazole staining results suggest that the hypoxic fractions of the tumors have a pO_2 less than 1%. However, only collective luminescence derived from the luciferase activity of the whole tumor can be determined with the IVIS apparatus, representing the mean tumor oxygenation status of the whole tumor. The highly sensitive camera within the IVIS apparatus detects emitted light from the surface of the tumor, generating a 2-dimensional picture of a 3-dimensional structure. The system does not, therefore, distinguish between areas within the tumors with high or low tumor hypoxia. Another disadvantage of the IVIS apparatus is the generation of low resolution images when light emitted from the luciferase-expressing tumor cells is low. Cells expressing a higher

amount of luciferase would lead to a higher luciferase signal and therefore a slightly better resolution. However, scattered light emitted from the luciferase-expressing tumor cells would again decrease the resolution. Future *in vivo* bioimaging approaches with improved resolution are required to overcome these drawbacks.

One key conclusion from our studies is that patupilone treatment does not affect sensitivity towards IR, despite increasing tumor hypoxia. Several explanations could account for this result. First, tumors might contain only small areas with very high tumor hypoxia and consequently high overall luciferase activity, not reflective of the majority of the tumor. Wouters and Brown determined that tumor cells at intermediate hypoxia (0.5 – 20 mmHg) are the cells most susceptible to fractionated irradiation with doses of 2 Gy, and not hypoxic cells below 0.5 mmHg [21]. Therefore, small areas of highly hypoxic cells might not interfere with radiosensitivity in our tumor model. Hypoxic tumor cells below a partial pressure of 0.5 mmHg, however, are highly important for tumor regrowth after treatment, or for radiation resistance at high dose irradiation. An experimental set-up analyzing long-term tumor control, or the influence of higher doses of irradiation, would be indicated if this scenario of small areas of highly hypoxic cells were indeed the case. A second explanation for the equal sensitivity towards IR of patupilone pre-teated and control mice is that a low, radiosensitizing level of patupilone is still present at the time point of irradiation and therefore counteracts the negative influence of hypoxia on sensitivity to IR.

Hypoxia in tumors can also increase the aggressiveness of a tumor by promoting invasion and dissemination. Therefore, induction of hypoxia caused by patupilone treatment would be counterproductive as anti-cancer treatment. Despite the poor premise, unpublished data from our group demonstrated that patupilone instead reduces invasiveness and migration *in vitro*. Matrix metalloproteinases (MMPs) are responsible for the degradation of extracellular matrix and therefore promote invasiveness and migration. Patupilone treatment led to a reduction in the secretion of these pro-invasive proteins. These data underline the very complex nature of this MSA in inhibiting tumor progression.

In this work (Orlowski et al.), we demonstrated the feasibility of the developed *in vivo* bioluminescence system to successfully monitor tumor hypoxia over a whole treatment period in single animals. We demonstrated a transient increase in tumor hypoxia after treatment with patupilone, which seems to be a specific feature of the compound and could be used as a surrogate marker for treatment response. Patupilone-induced tumor hypoxia does not reduce

radiation sensitivity, which substantiates the feasibility of patupilone as part of both concomitant and neo-adjuvant treatments with IR. Nevertheless, concomitant treatment leads to a stronger tumor growth delay than the neo-adjuvant treatment schedule. Unpublished data from our group further demonstrated a patupilone-specific inhibition of the secretion of pro-invasive proteins normally induced by hypoxia. Another very interesting feature of patupilone is that its activity remains unchanged regardless of the oxygenation level of the tumor. The developed *in vivo* bioluminescence system can be used to study additional treatment set-ups, e.g. anti-angiogenic agents like Avastin as part of a combined treatment modality with IR, to probe tumor hypoxia and treatment outcome. The disadvantage of the technique, however, is that it is only applicable in preclinical models.

4.3. Translational importance

This work describes a novel method to accurately report tumor oxygenation *in vivo*. Traditionally, non-invasive tumor hypoxia measurements are performed by using PET imaging with different hypoxia tracers. The most common tracer used in the clinics is F-MISO. Different studies were performed to predict treatment response towards IR based on the hypoxic status of the tumor using F-MISO. Evidence demonstrates that hypoxia analysis during fractionated irradiation rather than before treatment correlates with treatment outcome [22,23]. However, measurements acquired by PET with the hypoxic tracer F-MISO did not correspond with measurements from the pO_2 electrode, the gold standard, in a virtual voxel model. Tumors were in general more hypoxic based on the pO_2 electrode measurements as compared to F-MISO PET [24]. Another hypoxic tracer, EF5, has been evaluated for its feasibility in the clinic and has demonstrated good pharmacological characteristics, biodistribution and safety profile [25]. Jenkins and colleagues compared binding of EF5 with hypoxia measurements using the pO_2 electrode. In general, the amount of bound EF5 correlated well with the level of tissue oxygen, even at very low oxygen levels down to anoxia. There were still a few discrepancies, however, as the pO_2 electrode overestimated hypoxia especially in necrotic tissues, whereas EF5 did not accumulate in these areas [26]. Evans and colleagues then applied EF5 binding to measure hypoxia in the clinical setting, first with the use of specific antibodies on tumor biopsies [27] and afterwards in a study with 18 patients using PET scan [20]. In the PET scan study, higher EF5 binding correlated with high-grade tumors, and patients with moderate to severe hypoxia were more likely to develop metastases.

While PET tracers have proven to be fairly accurate, non-invasive indicators of tumor hypoxia, our data obtained from luciferase measurements indicate that pimonidazole-related tracers might not allow detection of the exact hypoxic level of a tumor. This might explain the poor ability in some studies to predict treatment outcome based on the initial hypoxic level of the tumor measured by pimonidazole-related tracers. These studies also had difficulty predicting the outcome of individual patients depending on the hypoxic level of the tumors. Most of the studies used the mean hypoxic status of the tumors to predict general aggressiveness or treatment response. In another approach, Toustrup as well as Marotta and colleagues identified sets of genes that allow the identification of hypoxic tumors. The specific hypoxia gene expression classifier predicted responsiveness towards radiosensitizers when given to patients with hypoxic tumors. This very interesting technique is, however, also dependent on tumor biopsies and does not represent the tumor oxygenation level of the whole tumor [28,29]. Therefore, there is a strong need for a new non-invasive method of determining the tumor oxygenation level that can be applied uniformly in the clinics.

Using our luciferase technique, we were able to probe longitudinal tumor oxygen levels throughout the course of treatment with IR or patupilone alone, or as part of a combined treatment modality. While it is generally accepted that hypoxia impairs sensitivity to radiation, we showed that hypoxia induced by patupilone treatment did not appear to affect the response to IR. Thus, combined treatment modalities of IR with compounds that could induce tumor hypoxia should not be prematurely rejected and should be evaluated.

This work demonstrates that the combination of patupilone and IR is a very potent treatment modality in xenografts derived from different cancer cell lines. The concomitant treatment schedule with one dose of patupilone and 3 fractions of IR led in all cases to an at least additive tumor growth delay. The ability of patupilone to pass the blood brain barrier and to inhibit proliferation to the same extent as the microtubule-destabilizing agent vincristine, though at a 10 times lower dosage, makes it a very compelling compound for treatment of brain malignancies. The phase I study on patupilone with concurrent IR in central nervous system malignancies demonstrated promising results [10], however no phase II trial was initiated. Due to the fact that Novartis International AG is not continuing research on patupilone, other epothilones should be used for further studies of the promising combined treatment modality with IR.

Ixabepilone is a very promising epothilone B derivative already approved by the FDA for treatment of breast cancer. Ixabepilone is in various clinical trials in combination with other chemotherapeutics; however, no clinical or preclinical trials are being performed in combination with radiotherapy. Despite data from Kim and colleagues demonstrating a radio-sensitizing effect of Ixabepilone on human NCI-H460 lung cancer cells *in vitro* and *in vivo*, no further research has been initiated in combination with IR [30]. Using the luciferase approach developed here, the combined treatment modality of Ixabepilone and IR could be analyzed in various experimental set-ups. In this way, treatment efficacy and tumor hypoxia could be monitored at the same time, and various scheduling possibilities could be analyzed. If preclinical data demonstrate promising results, clinical trials with already approved agents could be initiated more readily. Based on the data presented in this work, further preclinical and clinical trials should be initiated analyzing the very potent combined treatment modality of microtubule stabilizing agents and ionizing radiation.

5. Outlook

Here we demonstrated that the concomitant combination of patupilone and IR leads to an at least additive tumor growth delay in different tumor xenografts. However, the tested treatment schedule consisted only of one single dose of patupilone followed by 3 low-dose fractions of IR. Since we demonstrated that the neo-adjuvant treatment did not improve nor impair radiation response, it would be of interest to analyze the effect of further treatment combinations on tumor growth. A combined treatment schedule of repetitive cycles of patupilone followed by IR over several weeks would allow us to analyze long-term local tumor control instead of tumor growth delay.

Another promising strategy to analyze tumor growth delay could consist of a different compound in combination with patupilone, IR or both. Tumor cells that are resistant to treatment with one of the compounds like patupilone could still be sensitized for the consecutive treatment with IR. One radiosensitizing agent that acts on a completely different level than patupilone and can be used in such a combination is the mTOR inhibitor RAD001. An interesting approach would be to combine the three treatment modalities and analyze the tumor growth of A549-derived xenografts and patupilone-resistant A549.EpoB40 xenografts. In this manner, development of treatment resistance to one of the compounds could be

attenuated, and the dosage of the individual compounds could be reduced. To further investigate this question, tumor xenografts derived from a mixture of patupilone-sensitive and patupilone-resistant cells could be analyzed for the growth advantage of the single cell lines under the various treatments. The addition of RAD001 to these tumors should sensitize tumor cells derived from both cell lines towards IR. Interestingly, a phase I clinical trial is currently analyzing the combined treatment modality of RAD001 and patupilone in a dose-escalation study on advanced cancer (clinicaltrials.gov).

Having in hand a highly sensitive bioluminescence system to monitor tumor hypoxia *in vivo,* it would be of interest to analyze other combinations of treatment modalities for their effect on tumor hypoxia. The combination of anti-angiogenic agents like Avastin or DC101 with IR could be used to investigate the still-unanswered questions about tumor vasculature normalization after treatment with anti-angiogenic agents. Furthermore, optimal treatment scheduling for these combinations could be determined to help adapt already existing therapies. Most importantly, the use of the hypoxic tracer EF5 to replace the luciferase system for clinical use should be validated and analyzed in our *in vivo* model. If EF5-based hypoxia measurements correlate with luciferase measurements, the preclinical data obtained from scheduling experiments with the luciferase system could be validated and translated into clinical trials.

In conclusion, this work illustrates the promise of combined MSA and IR treatments for cancer therapy and introduces a highly sensitive system for monitoring tumor hypoxia *in vivo*. It opens the door to countless future studies focusing on multi-compound treatment regimens for radiosensitization, as well as on optimal treatment scheduling, which can now be validated by measurements of tumor oxygenation throughout the treatment course using the novel bioimaging method. Together with a complementary non-invasive method for oxygen measurement feasible for clinical use, these results could ultimately be translated into clinical trials.

References

1. O'Reilly T, Wartmann M, Brueggen J, Allegrini PR, Floersheimer A, et al. (2008) Pharmacokinetic profile of the microtubule stabilizer patupilone in tumor-bearing rodents and comparison of anti-cancer activity with other MTS in vitro and in vivo. Cancer Chemother Pharmacol 62: 1045-1054.
2. Hofstetter B, Vuong V, Broggini-Tenzer A, Bodis S, Ciernik IF, et al. (2005) Patupilone acts as radiosensitizing agent in multidrug-resistant cancer cells in vitro and in vivo. Clin Cancer Res 11: 1588-1596.
3. Ferretti S, Allegrini PR, O'Reilly T, Schnell C, Stumm M, et al. (2005) Patupilone induced vascular disruption in orthotopic rodent tumor models detected by magnetic resonance imaging and interstitial fluid pressure. Clin Cancer Res 11: 7773-7784.
4. Mabjeesh NJ, Escuin D, LaVallee TM, Pribluda VS, Swartz GM, et al. (2003) 2ME2 inhibits tumor growth and angiogenesis by disrupting microtubules and dysregulating HIF. Cancer Cell 3: 363-375.
5. Chi KN, Beardsley E, Eigl BJ, Venner P, Hotte SJ, et al. (2012) A phase 2 study of patupilone in patients with metastatic castration-resistant prostate cancer previously treated with docetaxel: Canadian Urologic Oncology Group study P07a. Ann Oncol 23: 53-58.
6. Melichar B, Casado E, Bridgewater J, Bennouna J, Campone M, et al. (2011) Clinical activity of patupilone in patients with pretreated advanced/metastatic colon cancer: results of a phase I dose escalation trial. Br J Cancer 105: 1646-1653.
7. Bystricky B, Chau I (2011) Patupilone in cancer treatment. Expert Opin Investig Drugs 20: 107-117.
8. Forster M, Kaye S, Oza A, Sklenar I, Johri A, et al. (2007) A phase Ib and pharmacokinetic trial of patupilone combined with carboplatin in patients with advanced cancer. Clin Cancer Res 13: 4178-4184.
9. Schelman W, Morgan-Meadows S, Bailey H, Holen K, Thomas JP, et al. (2008) A phase I trial of gemcitabine in combination with patupilone in patients with advanced solid tumors. Cancer Chemother Pharmacol 62: 727-733.
10. Fogh S, Machtay M, Werner-Wasik M, Curran WJ, Jr., Bonanni R, et al. (2010) Phase I trial using patupilone (epothilone B) and concurrent radiotherapy for central nervous system malignancies. Int J Radiat Oncol Biol Phys 77: 1009-1016.
11. Moeller BJ, Cao Y, Li CY, Dewhirst MW (2004) Radiation activates HIF-1 to regulate vascular radiosensitivity in tumors: role of reoxygenation, free radicals, and stress granules. Cancer Cell 5: 429-441.
12. Escuin D, Kline ER, Giannakakou P (2005) Both microtubule-stabilizing and microtubule-destabilizing drugs inhibit hypoxia-inducible factor-1alpha accumulation and activity by disrupting microtubule function. Cancer Res 65: 9021-9028.
13. Carbonaro M, O'Brate A, Giannakakou P (2011) Microtubule disruption targets HIF-1alpha mRNA to cytoplasmic P-bodies for translational repression. J Cell Biol 192: 83-99.
14. Nordsmark M, Overgaard J (2000) A confirmatory prognostic study on oxygenation status and loco-regional control in advanced head and neck squamous cell carcinoma treated by radiation therapy. Radiother Oncol 57: 39-43.
15. Nordsmark M, Overgaard J (2004) Tumor hypoxia is independent of hemoglobin and prognostic for loco-regional tumor control after primary radiotherapy in advanced head and neck cancer. Acta Oncol 43: 396-403.

16. Le QT, Chen E, Salim A, Cao H, Kong CS, et al. (2006) An evaluation of tumor oxygenation and gene expression in patients with early stage non-small cell lung cancers. Clin Cancer Res 12: 1507-1514.
17. Knocke TH, Weitmann HD, Feldmann HJ, Selzer E, Potter R (1999) Intratumoral pO2-measurements as predictive assay in the treatment of carcinoma of the uterine cervix. Radiother Oncol 53: 99-104.
18. Bordoli MR, Stiehl DP, Borsig L, Kristiansen G, Hausladen S, et al. (2011) Prolyl-4-hydroxylase PHD2- and hypoxia-inducible factor 2-dependent regulation of amphiregulin contributes to breast tumorigenesis. Oncogene 30: 548-560.
19. Cerniglia GJ, Pore N, Tsai JH, Schultz S, Mick R, et al. (2009) Epidermal growth factor receptor inhibition modulates the microenvironment by vascular normalization to improve chemotherapy and radiotherapy efficacy. PLoS One 4: e6539.
20. Evans SM, Judy KD, Dunphy I, Jenkins WT, Hwang WT, et al. (2004) Hypoxia is important in the biology and aggression of human glial brain tumors. Clin Cancer Res 10: 8177-8184.
21. Wouters BG, Brown JM (1997) Cells at intermediate oxygen levels can be more important than the "hypoxic fraction" in determining tumor response to fractionated radiotherapy. Radiat Res 147: 541-550.
22. Thorwarth D, Eschmann SM, Paulsen F, Alber M (2007) A model of reoxygenation dynamics of head-and-neck tumors based on serial 18F-fluoromisonidazole positron emission tomography investigations. Int J Radiat Oncol Biol Phys 68: 515-521.
23. Yaromina A, Kroeber T, Meinzer A, Boeke S, Thames H, et al. (2011) Exploratory study of the prognostic value of microenvironmental parameters during fractionated irradiation in human squamous cell carcinoma xenografts. Int J Radiat Oncol Biol Phys 80: 1205-1213.
24. Mortensen LS, Buus S, Nordsmark M, Bentzen L, Munk OL, et al. (2010) Identifying hypoxia in human tumors: A correlation study between 18F-FMISO PET and the Eppendorf oxygen-sensitive electrode. Acta Oncol 49: 934-940.
25. Koch CJ, Scheuermann JS, Divgi C, Judy KD, Kachur AV, et al. (2010) Biodistribution and dosimetry of (18)F-EF5 in cancer patients with preliminary comparison of (18)F-EF5 uptake versus EF5 binding in human glioblastoma. Eur J Nucl Med Mol Imaging 37: 2048-2059.
26. Jenkins WT, Evans SM, Koch CJ (2000) Hypoxia and necrosis in rat 9L glioma and Morris 7777 hepatoma tumors: comparative measurements using EF5 binding and the Eppendorf needle electrode. Int J Radiat Oncol Biol Phys 46: 1005-1017.
27. Evans SM, Fraker D, Hahn SM, Gleason K, Jenkins WT, et al. (2006) EF5 binding and clinical outcome in human soft tissue sarcomas. Int J Radiat Oncol Biol Phys 64: 922-927.
28. Toustrup K, Sorensen BS, Nordsmark M, Busk M, Wiuf C, et al. (2011) Development of a hypoxia gene expression classifier with predictive impact for hypoxic modification of radiotherapy in head and neck cancer. Cancer Res 71: 5923-5931.
29. Marotta D, Karar J, Jenkins WT, Kumanova M, Jenkins KW, et al. (2011) In vivo profiling of hypoxic gene expression in gliomas using the hypoxia marker EF5 and laser-capture microdissection. Cancer Res 71: 779-789.
30. Kim JC, Kim JS, Saha D, Cao Q, Shyr Y, et al. (2003) Potential radiation-sensitizing effect of semisynthetic epothilone B in human lung cancer cells. Radiother Oncol 68: 305-313.

Curriculum Vitae

Personal Information

Name:	Katrin Orlowski
Born on:	January 24th, 1981
Citizenship:	German

Academic Education

since 2007 PhD student in Molecular Biology
University of Zurich, Zurich, Switzerland
Department of Radiation Oncology, Lab. for Molecular Radiobiology, University Hospital Zurich, Zurich, Switzerland
Participant of cancer Biology PhD Program, Cancer Network Zurich

2001 – 2007 Diploma in Technical Biology, University of Stuttgart, Germany,
Diploma Thesis: "Activation of the lipid kinase PI4KIIIβ by protein kinase D and neuronal calcium sensor 1", University Stuttgart

Bachelor-thesis: "A screen for CFTR trafficking correctors in Yeast", performed at the McGill University, Montreal, Canada

2000 – 2001 Courses in Process Engineering at the University Stuttgart, Germany

1991 – 2000 Grammar school „Oscar-Paret-Schule" in Freiberg, Germany

Publications

Bley, C.R., W. Jochum, **K. Orlowski,** P. Furmanova, V. Vuong, P.M. McSheehy, and M. Pruschy. 2009. Role of the microenvironment for radiosensitization by patupilone. *Clin Cancer Res*. 15:1335-42.

Rohrer Bley C, **Orlowski K**, Furmanova P, McSheehy PM, Pruschy M. 2011. Regulation of VEGF-expression by patupilone and ionizing radiation in lung adenocarcinoma cells. *Lung Cancer* 73(3):294-301

Oehler C, von Bueren AO, Furmanova P, Broggini-Tenzer A, **Orlowski K**, Rutkowski S, Frei K, Grotzer MA, Pruschy M. 2011. The microtubule stabilizer patupilone (epothilone B) is a potent radiosensitizer in medulloblastoma cells.
Neuro Oncol. Sep;13(9):1000-10

Rohrer Bley C., Furmanova P., **Orlowski K**., Grosse N., Broggini-Tenzer A., McSheehy PM., Pruschy M. 2012. Microtubule Stabilizing Agents and Ionizing Radiation: Multiple Exploitable Mechanisms for Combined Treatment**.** Accepted for publication in the European Journal of Cancer

Conferences/Meetings

11th Day of Clinical Research, April 19, 2012, Zurich, Switzerland
Abstract: "Dynamic Changes of the Tumor Micromilieu under Treatment";
Oral Presentation
Orlowski K, Broggini-Tenzer A, Rohrer Bley C, Zimmermann M, Soltermann A, Vuong V, Pruschy M

Keystone Symposia Cancer and Metabolism
February 12-17, 2012, Banff, Alberta, Canada
Abstract: "Dynamic Changes of the Tumor Micromilieu under Treatment";
Poster presentation
Orlowski K, Broggini-Tenzer A, Rohrer Bley C, Zimmermann M, Soltermann A, Vuong V, Pruschy M

12th International Wolfsberg Meeting on Molecular Radiation Biology/Oncology
June 25-27, 2011, Wolfsberg, Switzerland
Abstract: "Longitudinal *in vivo* measurement of tumor hypoxia under treatment"; Poster presentation
Orlowski K, Rohrer Bley C, Zimmermann M, Soltermann A, Vuong V, Pruschy M

11th International Wolfsberg Meeting on Molecular Radiation Biology/Oncology
June 27-29, 2009, Wolfsberg, Switzerland
Abstract: "Probing the tumor response under treatment"; Poster presentation
Orlowski K, Rohrer Bley C, Zimmermann M, Jochum W, Furmanova P, Vuong V, Pruschy M

SASRO 2009, March 19-21, 2009, Baden, Switzerland
Abstract: "Probing the tumor response under treatment"; Oral presentation
Orlowski K, Zimmermann M, Vuong V, Rohrer Bley C, Pruschy M

ICTR 2009 (Fourth International Conference on Translational Research and Pre-Clinical Strategies in Radiation Oncology), March 11-13, 2009, Geneva, Switzerland
Abstract: "Probing the tumor response under treatment"; Oral presentation
Orlowski K, Zimmermann M, Vuong V, Rohrer Bley C, Pruschy M.

Acknowledgements

I would like to express my sincere gratitude to the many people I have come across during the PhD period here in Zurich.
I would like to express my gratitude to Prof. Dr. Martin Pruschy for giving me the possibility to work in his group and for supervising my thesis. I am thankful for his continuous support of my PhD study and research, for his encouragement, motivation and enthusiasm. Furthermore, I would like to thank him for giving me the chance to visit several interesting conferences and broaden my knowledge.

I would like to thank Prof. Dr. Roland Wenger and Prof. Dr. Stephan Bodis for being Co-examinators in my thesis, for their support and interest in my project.
I would like to thank the Department of Radiation Oncology and especially Prof. Dr. Urs Lütolf for his interest in scientific projects and support of our research activities.

My sincere thanks goes to all current and former members of the Laboratory for Molecular Radiobiology: Angela Broggini-Tenzer, Matthias Eggel, Andreas Hollenstein, Polina Furmanova Hollenstein, Daniel Hug, Colette Shen, Carla Rohrer Bley, Nicole Grosse, Van Vuong, Tamara Codilupi, Andrea Fontana, Ashish Sharma, Martina Zimmermann. Thank you all for your big support and for caring. I especially would like to thank Martina Zimmermann, Nadia Sanchez and Andreas Hollenstein, my lab colleagues in the F-Lab for scientific discussions, good talks and for cheering me up during these years.

Special thanks goes to Colette Shen for the fast proof-reading of this thesis and the English corrections. Thank you for finding time in your busy time schedule.

I would like to thank Carla Rohrer Bley and Van Vuong for introducing me so patiently to the work with laboratory animals. The calm and respectful handling of the mice and the detailed instructions from Carla enabled me to perform animal experiments accurately. I would like to acknowledge Mirzet Delic for his kind support in the animal facility.

I would like to thank Sinan Hanic and Marc Bovet from the informatics support for their immediate help with computer problems especially during the writing up phase.

I would like to acknowledge several people from the Institute of Pathology: Alex Soltermann and Matteo Montani for their collaboration and professional help, Silvia Behnke for the excellent support and suggestions for the immunohistological analysis, as well as Monika Bieri and Norbert Wey for their help with the evaluation.

Big thanks goes to Martina Zimmermann and Evi Waiblinger for proof-reading parts of my thesis and Evi Waiblinger for her interest and help with the statistical analysis.

I would like to acknowledge the Cancer Network Zurich for accepting me in the PhD program. I would like to specifically thank the coordinators Dr. Denise Hengartner, Dr. Cornelia Schauz and Dr. Eveline Bergmüller for their great administrative support.

I would like to thank my friends Beate, Cristina, Nadia, Daniela N., Daniela E., Martina, Novella, Ola, Colette, Mauro, Marc and Nicole for the big support during these years.

Ein besonderer Dank geht an meine Familie. Mama, Papa und Oma, ihr habt immer an mich geglaubt und mich bei allen meinen Entscheidungen unterstützt. Vielen Dank für eure konstante moralische Unterstützung, das Zuhören und die Ratschläge.
Ein grosser Dank geht an meinen Bruder Sven und meine Schwester Maren, sowie Gerd und Inge, Thekla und meine Zweitfamilie in Italien für ihre Unterstützung und Interesse.

Zum Schluss möchte ich mich besonders bei meinem Freund Dario bedanken. Vielen Dank für deine immerwährende moralische Unterstützung, deinen Glauben an mich und meine Fähigkeiten und den Ausgleich zum Laboralltag.